PLR-1, a putative E3 ubiquitin ligase and AEX-3, the GDP/GTP exchange factor homologue for RAB-3, respectively regulate cell polarity and axon navigation of the ventral nerve cord pioneer AVG in *Caenorhabditis elegans*

by

Jaffar M. Bhat

M.Sc. Botany, University of Kashmir, 2005

Thesis Submitted in Partial Fulfillment of the
Requirements for the Degree of
Doctor of Philosophy

in the
Department of Biological Sciences
Faculty of Science

SIMON FRASER UNIVERSITY

Fall 2015

Approval

Name: **Jaffar M. Bhat**

Degree: **Doctor of Philosophy**

Title: ***PLR-1, a putative E3 ubiquitin ligase and AEX-3, the GDP/GTP exchange factor homologue for RAB-3, respectively regulate cell polarity and axon navigation of the ventral nerve cord pioneer AVG in Caenorhabditis elegans***

Examining Committee: **Chair:** Dr. Michael Silverman
Associate Professor

Dr. Harald Hutter
Senior Supervisor
Professor

Dr. Nancy Hawkins
Supervisor
Associate Professor

Dr. Gordon Rintoul
Supervisor
Associate Professor

Dr. Jim Mattsson
Internal Examiner
Associate Professor

Dr. Timothy O'Connor
External Examiner
Professor
Department of Cellular and
Physiological Sciences
University of British Columbia

Date Defended/Approved: October 27, 2015

Abstract

Accurate and precise neuronal circuit formation is the hallmark of a functional nervous system. During development neurons extend axons and dendrites that have to reach their appropriate targets. This process is highly regulated and is achieved by using a set of conserved guidance cues and receptors. 'Pioneer' neurons extend axons first and are closely followed by the late outgrowing axons called 'followers' to extend upon. In *Caenorhabditis elegans*, the AVG axon pioneers the right axon tract of the ventral nerve cord (VNC). The molecular basis for the navigation of the AVG axon is largely unknown. The aim of this study was to identify novel regulators of AVG axon navigation.

In genetic screens for AVG axon outgrowth and guidance defects we identified alleles of *plr-1* that reversed the polarity of AVG neuron and also caused outgrowth and navigation defects in the AVG axon and several other neuronal and non-neuronal cells. *plr-1* is predicted to encode a putative transmembrane E3 ligase, widely expressed during the development including in the AVG neuron. *plr-1* and its vertebrate homologues control Wnt signalling by removing the frizzled receptors from the cell surface. We have shown that mutations in a gene reducing Wnt-signalling as well as mutations in *unc-53* and *unc-73* suppress the AVG polarity reversal defects, but not the other defects seen in *plr-1* mutants. This suggests that *plr-1* has Wnt dependent and Wnt independent functions.

Simple genetic screens have not yielded mutants with penetrant AVG axon navigation defects except *plr-1*. In enhancer screens for AVG axon navigation defects in a *nid-1* mutant background we isolated several candidate mutants including an allele of *aex-3*. *aex-3* mutant animals show penetrant AVG axon navigation defects as well as follower axon navigation defects in the VNC, which are *nid-1* dependent. AEX-3 is a GDP/GTP exchange factor for RAB-3 and RAB-27 GTPases. Our genetic interaction data suggests that AEX-3 regulates RAB-3 and not RAB-27. We also show that *aex-3* acts along with *unc-31*/CAPS, *ida-1*/IA-2 and *unc-64*/Syntaxin in the same genetic pathway for AVG navigation. Moreover, our genetic interaction data suggests that AEX-3 might regulate the transport of the Netrin receptor UNC-5 in the growth cone.

Keywords: AVG pioneer, axon navigation, Wnt signalling, growth cone, endomembrane trafficking, *C. elegans*

Dedicated to my parents, my brother and sisters, my wife and son, my grandparents, friends, teachers and well-wishers

Acknowledgements

First of all I would like to thank my supervisor Dr. Harald Hutter for giving me the opportunity to complete my Ph.D. in his laboratory. Your guidance and generous support through all these years was overwhelming. I know the freedom I got while working with you was such a great comfort. I was fortunate enough to knock on your door any time and get my answers. Credit also goes to you for encouraging and supporting me to attend several scientific conferences.

I am highly thankful to my committee members Dr. Nancy Hawkins and Dr. Gordon Rintoul for their guidance, valuable feedback and suggestions. Thanks to Dr. Jim Mattsson and Dr. Timothy O'Connor for agreeing to be my Internal and External examiners respectively. Furthermore, I would like to thank Dr. Michael Silverman for chairing my defence exmanination.

Before moving to Canada, I was initially introduced to worms by Dr. Sandhya P Koushika in her laboratory at NCBS Bangalore, which helped me. Thanks to her, Dr. Zaffar Reshi, Dr. Firdous Khanday and Dr. Aijaz Parray who encouraged me to pursue Ph.D. abroad.

Special thanks to present Hutter Lab. members: Dr. Jie Pan without whom part of my thesis would have been incomplete, Jesse Taylor a great colleague and friend, Abigail Feresten, Zeena Aburegeba, Rick Zapf, Wendy Zhang and past Lab. members: Dr. Andreas Steimel, Dr. Thomas Unsöld, Robert Greenland, Dr. Jinkyo Suh and Keri Ozsumanogiu who worked with me as an undergrad summer student. I had a wonderful experience with working you all and thanks for providing such a cordial environment.

Thanks to the Biology Department staff for being cooperative and helpful. Marlene Nguyen deserves big thanks for her tremendous support in all the department paper work.

Friends from all over the world especially in Vancouver have made my life smooth and delightful. Thank you all for being with me and special gratitude to my late friend Imtiyaz Bhat.

Lastly, I would like to thank my parents who supported me in every walk of life. Without your support my quest for seeking knowledge would have never been fulfilled. My brother and sisters equally supported me whenever it was needed. Thanks to my late grandfather who always encouraged me to pursue higher studies. Special thanks to my wife who sacrificed her precious time so that I was able to complete my Ph.D. I know staying away from me for most of the time is such a pain. My son was born while I was doing my Ph.D., so I consider him a part of it. I am looking forward to enjoy rest of my life with my wonderful family.

Table of Contents

List of Tables

List of Figures

List of Acronyms

A:T	adenine: thymine
aa	amino acid
ABI-1	Abelson kinase interactor
abLIM	Actin-binding LIM protein
ABP	actin binding protein
AEX-3	ABoc, EXpulsion (defecation) defective
AL region	antennal lobe region
ALPS	Agrin-Laminin-Perlecan-Slit
A-P	anterior-posterior
aPKC	atypical Protein Kinase C
Arp2/3	Actin related proteins 2/3
AVG	Anterior Ventral Ganglion
BMP	bone morphogenetic protein
BN	Bolwing's nerve
Boc	biregional Cdon-binding protein
C. elegans	*caenorhabditis elegans*
cAMP	cyclic adenosylmonophosphate
CC	corpus callosum
Cdc42	Cell division control protein 42 homolog
cdh	CaDHerin family
ced	CEll Death abnormality
CELSR	Cadherin-EGF-Laminin G-domain-containing serpentine receptor
CFP	cyane fluorescent protein
cfz-2	Caenorhabditis FriZzled homolog
cGMP	cyclic guanosine monophosphate
CHC	Clathrin Heavy Chain
CHL-1	Neural cell adhesion molecule L1-like protein (close homolog of L1)
CNS	Central nervous system
CO	cross-over
comm	commissureless

CST	corticospinal tract
cwn	C. elegans WNT family
D/V	dorso-ventral
Dbl	diffuse B-cell lymphoma
DCC	deleted in colorectal cancer
DNA	desoxy-ribonucleic acid
*D*N-cadherin	*Drosophila* neuronal cadherin
DOCK180	Dedicator of cytokinesis
Drl	Derailed
Dscam	Down's syndrome cell adhesion molecule
DsRed	Discosoma sp. red fluorescent protein
EC	cadherin domains
ECM	extracellular matrix
EFN	Eph(F)riN
EGF	Epidermal growth factor
egl	EGg Laying defective
EHS	Engelberth-Holm-Swarm
emb	abnormal EMBroygenesis
EMS	ethyl methanesulphonate
ena	Enabled
EPI	abnormal EPIthelia
ER	endoplasmic reticulum
eva	Enhancer of unc-40 Ventral Axon guidance defects
exc	EXCretory canal abnormal
F2	second filial generation
flp	FMRF-Like Peptide
fmi-1	FlaMIngo (cadherin plus 7TM domain) homolog
Fz	frizzled
FZD5	Frizzled class receptor 5
G:C	Guanine: Cytosine
GABA	γ-aminobutyric acid
GAP	GTPase activating protein

GCPs	growth cone particles
GDF	Growth differentiation factor
GDP	Guanosine diphosphate
GEF	guanine nucleotide exchange factor
GFP	green fluorescent protein
GLO	Gut granule LOss
glr	GLutamate Receptor family (AMPA)
GMC	Ganglion mother cell
GPI	Glycosyl phosphatidylinositol
GRIP	Glutamate Receptor-Interacting Protein
GTP	Guanosine triphosphate
GTPase	Guanosine triphosphatase
HGPPS	Horizontal Gaze Palsy with Progressive Scoliosis
Hh	Hedgehog
Hh-r	hedgehog related
Hip	Hedgehog interacting protein
hmr	HaMmeRhead embryonic lethal
Hspg2	heparan sulfate proteoglycan 2
Ig	immunoglobulin
IgCAMs	Immunoglobulin domain cell adhesion molecule
ina	INtegrin Alpha
inx	INneXin
kb	Kilobase
LAD	L1 CAM Adhesion molecule homolog
LAM	LAMinin related
let	LEThal
lin	abnormal cell LINeage
LRP6	low density lipoprotein receptor protein 6
LRR	leucine-rich repeats
Ly-6	leukocyte antigen-6
mab	Male ABnormal
MAG	myelin associated glycoprotein

mig	abnormal cell MIGration
M-L	medial to lateral
mm	millimetre
mM	milliMolar
mom	More Of MS
MuSK	muscle-specific receptor tyrosine kinase
NAV	Neuron Navigator
N-cadherin	neuronal cadherin
nid	NIDogen (basement membrane protein)
nuc PC	nuclear post commissure
N-WASP	Neural Wiskott-Aldrich syndrome protein
odr	ODoRant response abnormal
ORF	open reading frame
ORN	olfactory receptor neuron
pac	parachute
PAG	pre-anal ganglion
PAK	p21 activated kinase
pat	Paralysed Arrest at Two- fold
pceh	C. Elegans Homeobox
PCP	planar cell polarity
PCR	polymerase chain reaction
pgp	P-GlycoProtein related
PI3K	phosphatidylinositol 3-kinase
PLM	Posterior lateral mechanosensory
PLR-1	cell PoLaRity defective
PLX	PLeXin
PNS	Peripheral nervous system
PPVs	plasmalemal precursor vesicles
Ptc	Patched
PTR	Patched related proteins
R1-R8	photoreceptor neurons 1-8
RAB	RAB family

Rac	Ras-related C3 botulinum toxin substrate
RB	Rohon-Beard
RGC	Retinal ganglion cell
Rho	Ras Homolog Family Member
RING	Really interesting gene
RME	Receptor Mediated Endocytosis
RNAi	RNA interference
RNF43	Ring Finger Protein 43
Robo	Roundabout
ROCK	Rho-associated, Coiled-Coil Containing protein kinase
Ror1/2	Receptor Tyrosine Kinase-Like Orphan Receptor 1/2
RTK	receptor tyrosine kinases
RVG	retrovesicular ganglion
sax	Sensory AXon guidance
SC	superior colliculus
Sema	Semaphorin
SGO	sensory neurons of the subgenual organ
SLT	SLiT (*Drosophila*) homolog
SMART	Simple Modular Architecture Research Tool
Smo	Smoothened
smp	SeMaPhorin related
SNAPs	soluble N-ethylmaleimide-sensitive factor attachment proteins
SNARE	Soluble NSF Attachment Protein REceptor
SNB	SyNaptoBrevin related
snip-SNP	single nucleotide polymorphism that creates a restriction fragment linked polymorphism
SNP	single nucleotide polymorphism
SNT	SyNapTotagmin
SOS	son of sevenless
SS	signal sequence
SYG-2	SYnaptoGenesis abnormal
TGF-β	Transforming Growth factor-β

TM	transmembrane
tph	TryPtophan Hydroxylase
TPOC	tract of the postoptic commissure
TRIM9	Tripartite Motif Containing 9
TUBB3	Tubulin, Beta 3 Class III
unc	uncoordinated
vab	Variable ABnormal morphology
VAMPs	vesicle associated membrane proteins
VGCCS	voltage gated calcium channels
VNC	ventral nerve cord
Wnt	wingless
WRK	Wrapper/Rega-1/Klingon homolog
ZIG	(Zwei) IG domain protein
ZNRF3	Zinc And Ring Finger 3

Chapter 1.

The role of axon guidance families and endomembrane trafficking in the axon navigation

1.1. The Development of the Nervous System

The nervous system is one of the most complex and least understood organs present in all animals from invertebrates to vertebrates. Central to the nervous system is the brain, which has the ability to receive, process and send information to other parts of the body. This leads to the coordinated and controlled outputs which are important for the proper functioning of the whole body.

The development of the nervous system is a highly regulated process which has been extensively studied in both invertebrate (e.g. *Caenorhabditis elegans* and *Drosophila melanogaster)* and vertebrate (zebrafish, frogs, chicken and mouse) model organisms. The vertebrate nervous system develops from the ectoderm, which gives rise to the neural plate and neural crest cells to from the central nervous system (CNS), peripheral nervous system (PNS) and other sensory ganglia after neurulation (Squire et al., 2008). Within the ectoderm, neuroblasts in CNS arise from the neuroectoderm which divides and forms neurons. In *Drosophila*, neuroblasts divide asymmetrically in a stem cell fashion giving rise to a large neuroblast and a small ganglion mother cell (GMC) at each division. The ganglion mother cell further divides and gives rise to two post-mitotic neurons. In vertebrates, the neuroepithelial cells first divide symmetrically to generate two dividing progenitor cells but as neurogenesis proceeds they tend to divide asymmetrically and give rise to a neuroepithelial progenitor cell and a differentiated neuron. The two main cell types in the nervous system are neurons which process information and glial cells which provide general support to the neurons (Squire et al., 2008).

The generation of functional neuronal circuits has long fascinated developmental neurobiologists and is under intense investigation. Once the neurons are born, they begin to extend processes (axons and dendrites) which migrate over long distances and eventually make contacts with the appropriate target cells. The axons are tipped by a highly motile amoeboid structure called the growth cone. The growth cone extends finger-like protrusions called filopodia which scan the microenvironment for extracellular guidance cues. The guidance cues bind to the transmembrane receptors which are linked to the actin cytoskeleton through downstream effectors and modulate actin dynamics which results in collapse, turning or straight movement of the growth cone. This whole process helps the axons to navigate and make contacts with the appropriate target. These contacts are either between axon-dendrite (synapses) or axon-muscle (neuromuscular junctions) and are important for communication between neurons and the target tissue. The axon navigation and target selection is so precise and accurate as minor miswiring can have the devastating consequences on the overall health of the animal. There are numerous pathologies and diseases which are associated with improper axon guidance and navigation (Engle, 2010). In humans and mouse, defects in the outgrowth and guidance of axons in the corpus callosum (CC) which normally connects the left and the right cerebral hemispheres, is one of the factors leading to the CC dysgenesis (Kamnasaran, 2005; Paul et al., 2007). The failure of motor and sensory projections to cross the midline in the human brain with a mutation in the *ROBO3* gene is the underlying cause of Horizontal Gaze Palsy with Progressive Scoliosis (HGPPS) (Jen et al., 2004). Mutations in the L1 cell adhesion molecule cause the neurological disorder known as L1 syndrome with a primary defects in axon navigation (Demyanenko et al., 1999; Buhusi et al., 2008; Engle, 2010).

1.2. Pioneers

The nervous system is interconnected by an intricate network of axon tracts. The building of initial axon scaffold which comprises of longitudinal and commissural axon tracts is ancient and evolutionary conserved (Ware et al., 2015; Reichert & Boyan, 1997). The neurons which send out the processes first when there are no other axons are called ‘pioneer’ neurons. The pioneer neurons extend the processes in the embryo

when the distances are short and the environment is simpler than in adults and lay down the tracts which are used by the latter outgrowing axons called ‘follower’ neurons. The pioneer-follower relationship is important as the former provides tracts and guidance cues used by the latter outgrowing neurons to extend along.

Pioneer axons have been extensively studied in the simple nervous systems of invertebrate organisms, particularly insects. This is in part because the pioneer neurons in insects are identifiable on the basis of size, location and morphology. In grasshopper, the path from the periphery to the central nervous system is pioneered by the axons of peripheral neurons in both limbs and antennae. A pair of neurons arises at the distal tip of antennae which extend axons to the base of the antenna and enters the embryonic deuterocerebrum. These neurons initiate the development of the antennal nerve at a developmental stage when there are no other axons in the antenna. Subsequently in the development, these pioneer axons are followed and joined by axons of differentiating receptors to form two bundles of nerves in the lumen of the antenna (Bate, 1976). Similarly, a pair of transient (Ti) neurons arises at the base of each of the three thoracic limb buds which extend axons through the limb towards the central nervous system and are followed by the axons of the sensory neurons of the subgenual organ (SGO). The ablation of Ti pioneer neurons early during the development leads to failure of SGO sensory neurons to extend suggesting that the pioneers are important for the extension of the follower axons (Bate, 1976; Klose and Bentley, 1989). In the house cricket *Acheta domesticus* pioneer fibers form tracts first in the cercus which is required for the proper organisation of the cercal sensory nerve. Laser ablation of the “cercal tip” before the differentiation of pioneer fibers resulted in multiple nerve bundles rather than the normal two pairs of tightly fasciculated bundles. However, if the cercal tip was laser ablated after the formation of fiber tracts and associated glia, the cercal nerve was normal suggesting that pioneer fibers are important for the correct organisation of the cercal nerve (Edwards, 1981). The ventral nerve cord of the *Drosophila* central nervous system is H shaped and is pioneered by a group of four neurons. The longitudinal tracts are missing with thickened commissures if all the four pioneer neurons are ablated. However there is no effect on the longitudinal tracts if the individual pioneers are removed. This suggests that all the four pioneers collectively pioneer the longitudinal tracts (Hidalgo & Brand, 1997). In *C. elegans* AVG is the first neuron which arises at the anterior end of the

animal and sends out a posterior process that pioneers the right side of ventral nerve cord (Durbin, 1987). This is later on followed by the axons of DD/VD motor neurons, interneurons and many other neurons which extend axons into the right side of the ventral nerve cord. The ablation or removal of AVG leads to the formation of a disorganised ventral nerve cord with misguided axons, suggesting that it is important for the proper organisation of the ventral nerve cord (Durbin, 1987; Hutter, 2003). The left axon tract is pioneered by the PVPR axon which crosses the left side from the posterior end. This is followed by the axons of PVQL and HSNL from the posterior side. The pioneer follower relationship is strict here. The ablation of PVPR pioneer leads to the failure of PVQL follower to extend into the left axon tract. Instead the PVQL axon crosses and extends into the right axon tract, suggesting that PVQL needs PVPR for pioneering function. The ablation of PVPL has no effect on the PVQR follower axon possibly because there are other axons present in the right axon tract of the VNC which PVQR can use to extend upon. Similarly the ablation of PVQL follower axons has no effect on the PVPR axon, suggesting that PVPR is the pioneer and has the ability to navigate without the support of other axons (Durbin, 1987).

The vertebrate nervous system is more complex than that of the invertebrate, with a large number of neurons and associated glia. Therefore, the role of pioneers in vertebrates is difficult to study. However, zebrafish which is transparent with a simple embryonic nervous system organisation has been used to study the importance of pioneer neurons. In zebrafish, the 1 day post fertilization nervous system is simple with few axon tracts and commissures with well defined positions. By day 2 the axon tracts are populated by the addition of axons to the pre-existing ones suggesting that the early axons can mediate the pioneering function (Wilson et al., 1990). The growth cones of the nuclear post commissure (nuc PC) axons exit and turn posteriorly and follow the tract of the postoptic commissure (TPOC) towards the hindbrain in a stereotyped fashion. The surgical removal of TPOC results in both aberrant and normal paths taken by nuc PC axons emphasizing the role of TPOC as pioneers for the nuc PC followers (Chitnis & Kuwada, 1991). The role of pioneers in Zebrafish is further supported by the experiments where the pioneer Rohon-Beard (RB) neurons were laser ablated which lead to the failure of normal extension of DLF follower axons (Kuwada, 1986). In mouse the subplate neurons pioneer the path towards the thalamus and superior colliculus

(SC). Most of these neurons are short lived and disappear in the postnatal life when the adult pattern of axon projections is established (McConnell et al., 1989). In conclusion, the pioneers lay down the earlier axon tracts which are used by the late outgrowing neurons and thus play a critical role during the nervous system development.

1.3. Axon guidance cue families

Over the past 25 years by using biochemical, molecular and genetic approaches, many guidance cues and their receptors have been discovered in both invertebrates and vertebrates, which have advanced our knowledge of axon guidance. These include Netrins, Slits, Semaphorins, Ephrins and morphogens which are conserved in invertebrates and vertebrates (Tessier-lavigne and Goodman, 1996) (Figure 1.1). These extra-cellular guidance cues are either secreted or membrane bound, and can also form gradients thus acting as long or short range cues and can either attract (chemo-attractant) or repel (chemo-repellent) the growth cone. Most of the time it is the combined action of these cues and mechanisms which guides the growing axon. In the coming sections I will discuss the role of various axon guidance cues and their receptors in nervous system development. This will be followed by the role of basement membrane components with special emphasis on nidogen. In later sections I will discuss the cross talk between endomembrane trafficking and axon guidance. Lastly, I will introduce the development of *C. elegans* nervous system as a useful model to study axon guidance.

1.3.1. Netrins

Netrins are a class of guidance cues that structurally resemble the extracellular matrix protein laminin. Netrins are conserved in both vertebrates and invertebrates with *C. elegans* having only one Netrin (UNC-6), *Drosophila* with two (Netrin-A and Netrin-B), and mammals with five Netrin homologs (reviewed in Lai Wing Sun et al., 2011) (Figure 1.1). The Netrin homolog UNC-6 was first identified and characterised in the nematode *C. elegans*. *unc-6* mutant animals have severely disrupted dorsal and ventral directed axonal and mesodermal migrations (Hedgecock et al., 1990; Ishii et al., 1992) which lead to the idea that UNC-6 might act as global guidance cue for dorso-ventral

migrations. In the same study, two other mutants, *unc-40* with mostly ventral guidance and few dorsal guidance defects and *unc-5* with only dorsal guidance defects were also reported (Hedgecock et al., 1990). UNC-6 is an extracellular secreted guidance cue which is expressed in the neuroglia and neurons along the ventral nerve cord and likely forms a ventral to dorsal gradient (Ishii et al., 1992; Wadsworth et al., 1996) (Figure 1.2). UNC-6 acts through the receptors UNC-5 and UNC-40/DCC (deleted in colorectal cancer) which are type I transmembrane receptors of the immunoglobulin (Ig) super family (Leung-Hagesteijn et al., 1992; Chan et al., 1996). Cells and axons expressing UNC-40 are attracted towards the ventral source of UNC-6 whereas those expressing both UNC-5 and UNC-40 are repelled away towards the dorsal side (Leung-Hagesteijn et al., 1992; Chan et al., 1996) (Figure 1.2). Thus UNC-6 acts as a bifunctional guidance cue and mediates both attraction towards and repulsion away from the ventral side.

Vertebrate homologs Netrin-1 and Netrin-2 were first purified from chick brain as substances with growth promoting activity for commissural neurons (Serafini et al., 1994). Like UNC-6 in *C. elegans*, Netrins in vertebrates also mediate the dorsal-ventral guidance of commissural axons (Serafini et al., 1994; Kennedy et al., 1994). Netrin-1 is expressed by the floor plate of the spinal cord and coincides with the timing of commissural axon outgrowth whereas Netrin-2 is excluded from the floor plate but is expressed in the lower two thirds of spinal cord (Kennedy et al., 1994). Netrins are secreted and can diffuse over long range distance and can reorient commissural axons when expressed in COS cells, suggesting that Netrins likely form a gradient (Kennedy et al., 1994). Like UNC-6 in *C. elegans*, Netrin-1 acts through receptor UNC-40 homologue DCC (deleted in colorectal cancer), a single transmembrane protein of immunoglobin (Ig) superfamily expressed in commissural axons (Keino-Masu et al., 1996) (Figure 1.1). In *Drosophila Netrin-A* and *Netrin-B* are expressed in the ventral midline and guide the commissural axons. Either of these two genes is sufficient to rescue the mutant phenotype (Harris et al., 1996; Mitchell et al., 1996). Both *Netrin-A* and *Netrin-B* mutants have a similar phenotype to that of *frazzled* mutants related to vertebrate DCC. Frazzled is an Ig superfamily member, which is expressed and required for the guidance of Netrin responsive axons (Kolodziej et al., 1996), suggesting that frazzled is the receptor for Netrin in *Drosophila* (Figure 1.1).

In summary, Netrins are highly conserved guidance cues present in both vertebrates and invertebrates. Netrins act as bifunctional guidance cues and can either attract or repel growth cones depending on the type of Netrin receptor on their surface.

1.3.2. Slit-Robo system

Slits are secreted glycoproteins and are highly conserved in vertebrates and invertebrates. Vertebrates have three Slit members (Slit1, Slit2 and Slit3) and both *Drosophila* (dSlit) and *C. elegans* (SLT-1) have only one Slit member (Figure 1.1). Domain structure for all these Slit proteins is similar with each member containing a signal peptide (SS), four tandem leucine-rich repeats (LRR), EGF repeats, a conserved ALPS spacer and a cysteine knot (Brose et al., 1999) (Figure 1.1). Slit was first identified and characterised in *Drosophila* where it is secreted by the midline glia and is associated with commissural and longitudinal axons. The lack of Slit here causes the axons to stall and collapse within the midline, indicating that Slit is a repellent for axons which normally do not cross the midline (Rothberg et al., 1988; Rothberg et al., 1990). Slit binds to its receptor roundabout (Robo) (Kidd et al., 1998; Brose et al., 1999) (Fig 1.1), which was isolated in genetic screens aimed for commissural axon guidance defects in *Drosophila*. In Robo mutants, the axons which never cross the ventral midline, cross repeatedly (Seeger et al., 1993). Another mutant, commissureless (*comm*), which was isolated in the same genetic screen has the opposite phenotype to that of Robo. In *comm* mutants the commissural axons which normally cross, fail to cross the ventral midline (Seeger et al., 1993; Tear et al., 1996). It turns out that in *Drosophila* the ipsilateral axons express the Robo receptor which binds to the midline Slit and this Slit-Robo signalling keeps these axons away from the ventral midline (Kidd et al., 1998). For the commissural axons which cross the ventral midline, the Robo receptor is sorted internally to endosomes by Comm to prevent Robo from reaching the growth cone surface (Keleman et al., 2002; Keleman et al., 2005). This allows the commissural axons to overcome the midline Slit repulsion which are then attracted by the Netrin signalling (Mitchell et al., 1996; Harris et al., 1996) (Figure 1.3). After crossing the ventral midline, the Comm in commissural axons is down regulated by frazzled. While the detailed mechanism is unknown frazzled is thought to control the transcription of *comm* in a Netrin independent manner (Yang et al., 2009). This allows the Robo receptor to reach the growth cones of

commissural axons which are again then repelled by midline Slit (Kidd et al., 1998; Keleman et al., 2002) (Figure 1.3). After crossing the midline commissural axons turn anteriorly and grow longitudinally along specific fascicles. The combinatorial expression of three Robo genes within the commissural axons determines the fascicle these axons choose. The commissural axons with only Robo, with Robo + Robo3 and with Robo + Robo2 + Robo3 are accordingly repelled by the midline Slit and join medial, intermediate and lateral fascicles respectively (Rajagopalan et al., 2000; Simpson et al., 2000).

Like *Drosophila*, commissural axons also cross the ventral midline in vertebrates, more or less in a similar way. Vertebrates have each three Slits (Slit1, Slit2 and Slit3) expressed by floor plate and three Robos (Robo1, Robo2 and Robo3) expressed by the commissural axons (Long et al., 2004; Sabatier et al., 2004) (Figure 1.1). Despite the fact that Comm regulates the midline crossing in *Drosophila*, it is not present in vertebrates and nematodes. Instead in vertebrates the function of Comm has been taken by Robo3. The switch to cross first and to keep away from the midline after crossing is mediated here by splice variants of Robo3 (Robo3.1 and Robo3.2). Pre-crossing commissural axons express Robo3.1, which interferes with Robo1-mediated Slit signalling and allows the axons to cross (Figure 1.3). After crossing the ventral midline, commissural axons express Robo3.2 which along with Robo1 and Robo2 mediates Slit repulsion and keeps these axons away from the midline (Chen et al., 2008) (Figure 1.3).

The *C. elegans* genome codes for one Slit gene (*slt-1*) and one Robo receptor gene (*sax-3*) (Figure 1.1). SLT-1 is expressed in the anterior region in the embryo, dorsal and ventral muscles in the larvae and adults with higher levels in dorsal and lower levels in the ventral muscle. However, SLT-1 expression was not detected in the ventral midline (Hao et al., 2001). SAX-3 is expressed in most of the neurons transiently during the time of axon outgrowth (Zallen et al., 1998). Both *slt-1* and *sax-3* mutant animals display midline crossing defects (Zallen et al., 1998; Hao et al., 2001). In contrast to *Drosophila* and vertebrates axons normally do not cross the ventral midline in *C. elegans* and very few axons grow towards the midline (Zallen et al., 1998). In *C. elegans* SLT-1 signalling repels ventrally directed axons from the dorsal side and acts in parallel with the UNC-6/Netrin: UNC-40/DCC signalling pathway which attracts these axons towards the ventral side (Hao et al., 2001). *sax-3* has both *slt-1* dependent and independent

defects (Hao et al., 2001), and SLT-1 binds to another receptor known as EVA-1 which is required for SAX-3 signalling (Fujisawa, 2007). It has been also proposed that the unbound SAX-3 near the ventral midline where SLT-1 levels are low could dampen the UNC-40 signalling. This allows the growth cones to counter the higher concentration of ventral UNC-6/Netrin (Fujisawa, 2007). In summary, Slit is a repellent guidance cue which binds to its receptor Robo and this signalling system is conserved in both invertebrates and vertebrates.

1.3.3. Semaphorins and plexins

Semaphorins are a large family of signalling molecules consisting of both transmembrane and secreted glycoproteins characterised by the presence of a conserved 500 aa sema domain and are conserved from invertebrates to mammals (Kolodkin, 1996; Puschel, 1996; Kolodkin et al., 1997) (Figure. 1.1). Semaphorins are classified into eight groups on the basis of structural elements and amino acid sequence similarity. Class 1 and 2 are invertebrate specific, class 3-7 are vertebrate specific (Figure 1.1) and the final group is viral specific. Most of the semaphorins are membrane bound except class 2, 3 and viral coded ones which are secreted (Kruger et al., 2005). Several members of the Semaphorins are implicated in axon guidance (Raper, 2000). Fasciclin IV/Sema I which is expressed in the central nervous system of grasshopper and Collapsin/Sema III from the chicken were the first semaphorins to be identified as repulsive axon guidance molecules (Kolodkin et al., 1992; Luo et al., 1993). However, later studies have shown that Sema I can also act as a permissive/ attractive cue for the guidance of SGO axons (Wong et al., 1997). Sema 2a is a secreted repulsive cue which forms a gradient in the limb bud and guides pioneer Ti axons towards the central nervous system (Isbister et al., 1999). Antibody blocking experiments have suggested that Sema I and Sema 2a function independently as well as in combination for the guidance of Ti axons (Isbister et al., 1999). The *Drosophila* Sema 1 which is closely related to the grasshopper Sema 1 acts as a repulsive guidance cue and guides the motor axons to the pheripheral targets and also controls CNS pathfinding (Yu et al., 1998). In vertebrates the members of the class III semaphorins (SEMA-3A, SEMA-3B, SEMA-3C, SEMA-3D, SEMA-3E and SEMA-3F) have been shown to guide variety of axons predominantly by acting as repulsive cues (Raper, 2000). The principal receptors

for Semaphorins are Plexins which also have a sema domain like that of Semaphorins (Winberg et al., 1998; Tamagnone et al., 1999) (Figure 1.1). Plexins comprise a large family of transmembrane proteins which on the basis of sequence similarity are divided into four (A-D) groups (Tamagnone et al., 1999). *Drosophila* PlexinA and vertebrate PlexinAs are functional receptors for the transmembrane Sema 1a and secreted class 3 semaphorins respectively (Winberg et al., 1998; Tamagnone et al., 1999; Cheng et al., 2001). Neuropilin, a type I transmembrane glycoprotein (Figure 1.1) is the co-receptor for vertebrate Sema III which repels the sensory axons during the neuronal development (He and Tessier-Lavigne, 1997; Kolodkin et al., 1997). Genetic analysis of Semaphorins in different organisms have lead to the conclusion that Semaphorins mostly act as short range repulsive guidance cues that keep axons away from the wrong target regions (Raper, 2000; Cheng et al., 2001). In *C. elegans* Semaphorins are not involved in axon guidance but regulate epidermal morphogenesis by discouraging improper cell contacts. The *C. elegans* genome codes for three Semaphorins (*mab-20*, *smp-1*, *smp-2*) and two Plexin (*plx-1 and plx-2*) genes (Figure 1.1). Except for sema-2a (*mab-20*), the mutant animals of which have low penetrant dorsal defasciculation defects, the Semaphorins are mainly involved in the epidermal morphogenesis and establish proper cell-cell contacts (Roy et al., 2000; Ginzburg et al., 2002; Fujii et al., 2002). In conclusion, Semaphorins represent a class of both secreted and transmembrane proteins, with several members acting as axon guidance cues and keep axons away from the wrong target regions by binding to the Plexin receptors.

1.3.4. Ephrins and Eph receptors

Ephrins are a class of proteins which are either anchored to the membrane by glycosylphosphatidylinositol (GPI) linkage (ephrin-A class) or have a transmembrane domain (ephrin-B class) (Figure 1.1). The receptors for ephrins are Eph receptor tyrosine kinases (RTK) and both are functionally divided in two major subclasses. Consequently, ephrin As bind and activate Eph A receptors whereas ephrin Bs bind and activate Eph B receptors. During the nervous system development Eph receptors and ephrins act as repellents and prevent cells and axons form entering the wrong territories and thus establish the correct boundaries (Gale et al., 1996; reviewed in Wilkinson DG, 2001). Eph-ephrin interactions in adjacent cells have the potential to lead to bidirectional

signalling. That means ephrin and Eph can act both as ligands as well as receptors. For example, the binding of transmembrane (TM) ligand (ephrin B) to the Nuk (Eph B type receptor) promotes the aggregation and autophosphorylation of the receptor. The interaction of the Nuk to the TM ligand can also cause the aggregation of the latter which is phosphorylated by the associated cytoplasmic tyrosine kinase, thus leading the signalling in both directions (Holland et al., 1996; Brückner et al., 1997). The most widely used example of ephrin-Eph signalling is the topographic mapping of retinal axons in the visual system. Axons from the temporal retina project to the anterior tectum/superior colliculus, whereas axons from the nasal parts of the retina project to posterior parts of the tectum. This topographic mapping along the anterior-posterior axis is mediated by the graded expression of ephrin-A ligand in the tectum and Eph A receptor in the retina respectively. Retinal axons with successively higher levels of Eph A receptor map successively to the lower points on the tectum and vice-versa (Drescher et al., 1995; Cheng et al., 1995; reviewed in Wilkinson DG, 2001 and Dickson, 2002).

Ephrins and Eph receptors are expanded in vertebrates with at least 14 Eph receptors, 5 ephrin-A ligands and 3 ephrin-B ligands present (reviewed in Wilkinson DG, 2001). Invertebrates have few ephrins with *Drosophila* having only one ephrin ligand and Ephrin receptor (Figure 1.1), and this signalling is required for the axon guidance in the mushroom body (reviewed in Wilkinson DG, 2001; Boyle et al., 2006). The *C. elegans* genome codes for four ephrin ligands (VAB-2/EFN-1, EFN-2, EFN-3 and EFN-4) and a sole Eph receptor (VAB-1) (Figure 1.1), mainly involved in epidermal morphogenesis with limited role in axon guidance (George et al., 1998; Chin-Sang et al., 1999; reviewed in Wilkinson DG, 2001). VAB-2 ephrin signals through its receptor VAB-1 in the adjacent neuron to regulate epidermal morphogenesis (George et al., 1998; Chin-Sang et al., 1999). *vab-1* mutant animals also have sensory axon guidance and touch receptor axon extension defects, suggesting a role in axon guidance (Zallen et al., 1999; Mohamed and Chin-Sang, 2006).

In summary, ephrins are either GPI anchored or membrane bound repulsive guidance cues which bind to Eph receptors and have the potential to mediate signalling in both directions. Their cell-cell communication role is ancient but they have gained an important role in the axon guidance during vertebrate evolution.

1.4. Morphogens

Morphogens were initially identified as graded positional cues determining cell fate and tissue patterning during embryogenesis. However, recent findings have also implicated morphogens in axon guidance during nervous system development. Members of three families of morphogens are involved in axon guidance: Hedgehog (Hh), Wingless/Wnt and Bone Morphogenetic protein/Transforming Growth factor-β (BMP/TGF-β). I will discuss briefly Hedgehogs and BMPs here. Wnts which are more relevant to my thesis will be discussed under separate heading.

Sonic hedgehog (Shh) plays an important role in vertebrate development. In mouse, Shh expressed in the floor plate collaborates with the Netrin-1 signalling and attracts commissural axons towards the ventral midline. The Shh here binds to the receptor Boc expressed by the commissural axons which interacts with Smo directly or indirectly. This is also evident from the *in vitro* studies where *Boc*$^{-}$ commissural axons fail to turn towards the Shh source (Charron et al., 2003; Okada et al., 2006). Shh can also act as repellent cue. The chick commissural axons grow anteriorly along the floor plate after crossing the ventral midline. This anterior turn of post-commissural axons is mediated by Shh through receptor Hip, which is transiently expressed by the commissural axons (Domanitskaya et al., 2010). Shh also regulates the progression of Retinal ganglion cell (RGC) axons through the optic chiasm and the signalling here is dependent on Patched (Ptc) and Smoothened (Smo) receptors (Trousse et al., 2001). In *C. elegans* the key components of the hedgehog signalling including the Hh and Smo homologs are absent. However, over 60 hedgehog related (Hh-r) proteins, 3 Patched proteins and 24 Patched related proteins (PTR) are present in *C. elegans* which are involved in number of functions including roles in molting. The roles of Hh-r, Patched proteins and PTRs in nervous system development remain to be identified (reviewed in Bürglin and Kuwabara, 2006).

While the floor plate derived cues attract the commissural axon towards the ventral midline, the roof plate derived cues initially push these axons from the dorsal side. It turned out that the members of the TGF-β family/BMP are secreted from the dorsal side and guide the commissural axons through the first dorsal half trajectory.

Furthermore, genetic and biochemical evidence in mice has suggested that BMP7 and GDF7 (a member of growth/differentiation factor and a subfamily of BMPs) form heterodimers which mediates the floor plate chemorepellent activity (Augsburger et al., 1999; Butler and Dodd, 2003). In *C elegans*, UNC-129, which was identified in axon guidance screens, belongs to the TGF-β superfamily (Colavita and Culotti, 1998; Colavita et al., 1998). In *C. elegans*, the motor axons expressing UNC-40/DCC and UNC-5 together are repelled by UNC-6/Netrin towards the dorsal side. UNC-129 promotes this long rage (UNC-40 + UNC-5) signalling and thus indirectly attracts motor axons towards the dorsal side. UNC-129 is expressed by the dorsal body wall muscles and likely forms a dorsal to ventral gradient opposite to that of UNC-6/Netrin. This increases the sensitivity of the growth cones to UNC-6/Netrin which are migrating up the UNC-129 gradient and down the UNC-6/Netrin gradient (Colavita et al., 1998; MacNeil et al., 2009). Unlike vertebrate TGF-βs, UNC-129 does not require DAF-4, the only known type II TGF-β receptor in *C. elegans* for this function. In conclusion, both hedgehogs and BMPs apart from controlling early morphogenetic events are involved in axon guidance.

1.4.1. Wnt Signalling in axon guidance

Wnts are a large family of secreted glycoproteins that regulate many developmental processes including cell specification, proliferation, differentiation and polarity largely by binding to frizzled (Fz) receptors (Cadigan & Nusse, 1997). Wnts activate different signalling pathways upon binding to their receptors. These include canonical Wnt/β-catenin, the planar cell polarity (PCP) and the Wnt/Ca^{2+} pathways (Figure 1.4). For axon guidance Wnts bind Fz, a seven-pass transmembrane protein and many other divergent receptors such as Derailed Drl/Ryk, Ror1/2 and the MuSK and are thought to activate both canonical as well non-canonical pathways (reviewed in Sánchez-Camacho and Bovolenta, 2009). Wnts form gradients and can both attract and repel axons. In mouse, the spinal cord commissural axons after crossing the ventral midline turn anteriorly and extend along the anterior-posterior (A-P) axis. Wnt4 forms a gradient along the A-P direction and likely binds to the receptor Fz3 to guide these post-crossing commissural axons ascending along the A-P axis of the neural tube by an attractive mechanism (Lyuksyutova et al., 2003). Biochemical studies have further confirmed that this interaction activates an atypical Protein Kinase C (aPKC) and also

requires the p110γ catalytic subunit of the phosphatidylinositol 3-kinase (PI3K) upstream of aPKC. As these are the components of PCP pathway which suggests that Wnt4/Fz3 activates PCP signalling pathway for the guidance of post-crossing commissural axons (Karner et al., 2006; Wolf et al., 2008). In *Drosophila*, the commissural axons before crossing the ventral midline make a choice to join either anterior or posterior commissure. This is mediated by Wnt5 which is expressed at the posterior commissure and repels the anterior commissural axons which express Derailed (Drl) receptor (Yoshikawa et al., 2003). The vertebrate homolog of Drl known as Ryk similarly repels the CST axon in opposite direction to that of ascending axons (mentioned above). Wnt1 and Wnt5a form the A-P gradient and repel the CST axons down the spinal cord which express Ryk receptor (Liu et al., 2005). Drl/Ryk is an atypical tyrosine kinase and likely lacks the catalytic activity, therefore, downstream signalling in unknown here (reviewed in Sánchez-Camacho and Bovolenta, 2009). Wnts along with ephrins also regulate topographic mapping in the brain. In chicken, Wnt3 forms a medial to lateral (M-L) gradient and repels retinoganglion cell (RGC) axons laterally through the Ryk receptor expressed ventral-dorsally in a decreasing gradient by these axons (Schmitt et al., 2006).

The *C. elegans* genome codes for five Wnt genes (*lin-44, egl-20, mom-2, cwn-1* and *cwn-2*) and four Wnt receptor (frizzled) genes (*lin-17, mom-5, mig-1, cfz-2*) and one atypical tyrosine kinase (aPKC) gene *lin-18* (Ryk/Drl), which control a variety of developmental processes (Goldstein et al., 2006; Gleason et al., 2006; Green et al., 2008; Gleason and Eisenmann, 2010; Song et al., 2010; Harterink et al., 2011). In *C. elegans*, migrations happen along two body axes, anterior-posterior (A/P) and dorso-ventral (D/V). While migrations along the D/V axis are well characterized, the migrations along the A/P axis are poorly understood. However, a few key players including the Wnts are known to mediate migrations along the A/P axis (Wightman et al., 1996; Wolf et al., 1998; Stringham et al., 2002; Pan et al., 2006). Wnts influence several neuronal cell migrations and also control polarity of certain neurons. EGL-20/Wnt is expressed in the posterior part of the embryo and repels HSN neurons from the posterior side. The growth cones of anterior touch receptor neurons ALMs and AVM are also repelled by EGL-20/Wnt. The EGL-20/Wnt here acts redundantly through MIG-1 and MOM-5 which are frizzled receptors and also possibly by LIN-18/Ryk which is a non-frizzled receptor

(Pan et al., 2006). EGL-20/Wnt also regulates the migration of the decedents of Q-neuroblasts QL and QR. EGL-20 induces the expression of *mab-5*, a Hox gene in the QL neuroblast which specifies the cell fate and regulates the migration towards the posterior side. The anterior migration of the decedents of the QR regulated by EGL-20 does not involve *mab-5* expression (Harris et al., 1996; Maloof et al., 1999; Whangbo and Kenyon, 1999). In *C. elegans* touch receptor neurons (ALM and PLM) are polar with a longer anterior process (axon) and much shorter posterior process (dendrite). LIN-44/Wnt and LIN-17 frizzled which are expressed in the tail region regulate the anterior-posterior polarity of the PLM. In both *lin-44* and *lin-17* mutant animals the polarity of PLM is disrupted. The polarity of ALM neurons is regulated redundantly by EGL-20 and CWN-1 (Hilliard & Bargmann, 2006).

In summary, Wnts are a large family of secreted glycoproteins which regulate different developmental processes including axon guidance. Their role in axon guidance along anterior-posterior axis is conserved in *C. elegans*, *Drosophila* and mammals.

1.5. Growth cone signalling and cytoskeleton dynamics

The growing axons are tipped by a highly motile and specialized structure named ‘growth cone’ in 1890 by Raymon Y. Cajal (Cajal, 1890). The growth cone generally consists of two regions which are the peripheral (P) and central (C) domains. It forms two kinds of protrusions: filopodia, which are the finger like extensions and lamellipodia, which are the flat sheet like protrusions. The growth cone continuously advances and searches for the cues in the environment. This behaviour of the growth cone depends on the dynamic assembly, turnover, organisation and protein associations of the actin filaments in the P domain. Polymerisation and recycling of actin filaments are important in the sense that they provide the protrusive forces for the exploratory filopodia and lamellipodia. Actin filaments in the P-domain also interact with myosin II motor protein which moves the growth cone forward by generating traction forces against adhesions (reviewed in Gomez and Letourneau, 2014). The drugs which block actin polymerisation and myosin II activity do not inhibit axon outgrowth. This suggests that actin polymerisation and myosin II activity is not essential for the elongation of the axon. The axon elongation can still occur by microtubule advance and membrane expansion.

However, this whole process of axon elongation slows down and is unresponsive to the guidance cues (Marsh and Letourneau, 1984; Turney and Bridgman, 2005). Microtubules which are usually present in the axon shaft and the central C domain can occasionally invade the P domain as well as filopodia (reviewed in Liu and Dwyer, 2014). The inhibitors of the microtubules dynamics have suggested that it is important for continuous axonal growth rather than the dynamic growth (Yamada et al., 1971). However, recent studies have suggested that microtubules can also play an instructive role. Netrin-1 has been shown to directly regulate microtubule dynamics through the coupling of its receptor DCC to TUBB3, which steers the growth cone towards Netrin-1 source (Qu et al., 2013; also reviewed in Liu and Dwyer, 2014).

The binding of guidance cues to the corresponding receptor triggers local intracellular signals that modulate actin filament dynamics during growth cone navigation (Quinn & Wadsworth, 2008) (Figure 1.5). The key signalling intermediates activated by the guidance receptors are the members of Rho family GTPases: RhoA, Rac and Cdc42 (Hall & Lalli, 2010). These Rho GTPases act as molecular switches and are activated by guanine nucleotide exchange factors (GEFs) and inactivated by GTPase activating protein (GAPs) (Kaibuchi et al., 1999) (Figure 1.5). The Rho GTPases coordinate the downstream effects by modifying various cytoskeleton effectors resulting in the responses such as actomyosin contraction, actin disassembly and polymerisation (Figure 1.5), steps required for growth cone steering (Lowery & Van Vactor, 2009). The major guidance cues like Netrin, Slit, Semaphorin and ephrins all regulate the activity of Rho family GTPases for both chemoattraction as well chemorepulsion (reviewed in Bashaw and Klein, 2010). The *C. elegans* genome codes for three Rac like genes (*ced-10*, *mig-2* and *rac-2*), which act redundantly for axon guidance (Lundquist et al., 2001). The UNC-73 Rac-GEF related to mammalian Trio activates these Rac like proteins and mutations in *unc-73* cause axon outgrowth and guidance defects (Steven et al., 1998). Similarly mutations in *Drosophila* Trio leads to axon guidance defects and Trio also acts as a GEF for Racs. Trio activated Rac binds to pak which is required for the regulation of photoreceptor axon guidance (Newsome et al., 2000). Ephexin which is a Dbl family GEF is involved in the ephrin mediated repulsion by activating RhoA and inhibiting Cdc42 and Rac1(Shamah et al., 2001). In addition to this many other Rho GEFs (DOCK180 and SOS) (Côté and Vuori, 2002; Brugnera et al., 2002; Yang and Bashaw,

2006) and Rho GAPs (Vilse) (Hu et al., 2005) have been implicated in axon guidance. This indicates that the Rho GTPase signalling which modulates the actin dynamics for growth cone guidance is complicated.

Although Rho GEFs are the downstream signalling components, an additional role in the receptor localisation cannot be ruled out. In *C. elegans* UNC-73/Trio GEF along with VAB-8L, a cytoplasmic kinesin regulates the localisation of many guidance receptors for directed cell and growth cone migrations (Levy-Strumpf and Culotti, 2007; Watari-Goshima et al., 2007). Several downstream targets of Rho family GTPases have been identified (Figure 1.5). RhoA kinase ROCK is activated by RhoA to control the growth cone repulsion. Activities of several actin binding proteins (ABPs) are increased by Rac1 and Cdc42 signalling. This in turn promotes the polymerisation of actin filaments which leads to growth cone protrusion and turning towards the guidance cues (reviewed in Gomez and Letourneau, 2014). Rac1 and Cdc42 also activate WAVE and N-WASP respectively which results in the Arp2/3 mediated polymerisation of dendritic actin rays (Hall & Lalli, 2010). The other downstream targets include UNC-115/abLIM actin binding protein (Lundquist et al., 1998; Struckhoff and Lundquist, 2003), slingshot phosphatase, a depolymerising cofilin factor (Ng & Luo, 2004), p21 activated kinase (PAK1-3) (Santiago-Medina et al., 2013), ena/Vasp anti capping factors, actin nucleating formins, and F-bar-containing membrane curving proteins (reviewed in Hall and Lalli, 2010).

Growth cone cytoskeleton is also modulated by Rac independent regulators for axon guidance. UNC-34/Enabled is the mediator of SLT-1 dependent SAX-3 repulsive guidance signalling which is potentiated by the Netrin independent UNC-40 signalling (Yu et al., 2002). Ena also mediates Robo's repulsive signalling at *Drosophila* ventral midline (Bashaw et al., 2000). However, UNC-34/Enabled can also attract axons along with UNC-40 and in parallel with Rac and UNC-115/abLIM (Gitai et al., 2003). The ligand for Ena/WASP which is Lamellipodin regulates the lamellipodial dynamics (Krause et al., 2004). The *C. elegans* lamellipodin homolog MIG-10 cooperates with Ena/WASP homolog UNC-34 and guides axons towards Netrin (UNC-6) and away from Slit (SLT-1) sources (Chang et al., 2006).

Calcium ($Ca^{2+)}$ is also one of the crucial downstream signal transducer in axon guidance. Ca^{2+} enters into growth cone either through voltage gated calcium channels (VGCCS) or is released from intracellular calcium stores. Among VGCCs, the L-type Ca^{2+} channels are the most important for growth cone turning (reviewed in Sutherland et al., 2014). Netrin-1 leads to the elevation of Ca^{2+} through these channels which mediates the growth cone attraction. However, blocking of these L-type channels can turn attractive response into repulsive response (Hong et al., 2000). Downstream of Ca^{2+} the activities of these L-type channels are regulated by cAMP and cGMP. The high levels of cAMP and cGMP promote attraction and repulsion respectively in response to Netrin-1 (Movshon et al., 2003). This Ca^{2+} elevation also occurs in response to other guidance receptors. For example, the binding of Wnt5a to Ryk and frizzled receptors invokes the Ca^{2+} transients inside the cortical axons which mediates the cortical axon outgrowth and guidance through distinct pathways (Li et al., 2010). In conclusion, the growth cone navigation is highly dependent on the cytoskeleton remodelling especially actin dynamics which is achieved by the guidance cue signalling mainly through Rho GTPase and other downstream effectors.

1.6. Role of cell adhesion molecules in axon guidance

1.6.1. Cadherins

Cadherins are membrane bound glycoproteins and constitute a diverse family with common structural domains. Cadherins are grouped into classical cadherins, desmosomal cadherins, protocadherins, Flamingo/CELSRs and FAT (Nollet et al., 2000). The best characterised and understood are the classical Cadherins. They are single-pass transmembrane proteins characterised by an ectodomain with five cadherin domains (EC1-EC5) and a highly conserved cytoplasmic region (reviewed in Ranscht, 2000). Cadherin molecules are linked to actin-based cytoskeleton by a group of cytoplasmic proteins called catenins which associate with the intracellular region of cadherin (Ozawa et al., 1990; reviewed in Ranscht, 2000). Cadherin interactions are either homophilic where same sub-type of cadherins interact or heterophilic where

different sub-types of cadherins interact. The homophilic interactions are generally stronger than heterophilic interactions.

Over 100 members of cadherin superfamily have been identified in the vertebrate nervous system including the classical cadherins (reviewed in Takeichi, 2007). Cadherins play an important role during the development of the vertebrate eye. The zebrafish N-cadherin mutant *parachute* (*pac*) displays several developmental defects including defects in retinal lamination, amacrine axonal outgrowth, and RGC axon guidance. This suggests that N-cadherin is involved in the proper retinal lamination, amacrine axon outgrowth and RGC axon guidance (Masai et al., 2003). The expression of a dominant negative form of cadherins in retinal cells leads to axonal outgrowth and denritic morphology defects, further supporting the role of cadherins in the development of retina (Riehl et al., 1996; Tanabe et al., 2006). The cadherin-catenin interaction regulates the proper axon tract formation in mouse. In catenin knockout mouse, the axons at the olfactory region fail to cross the midline and consequently, the anterior commissure is not formed (Uemura & Takeichi, 2006). Cadherins can also act as repulsive cues and preclude axons from invading wrong target regions. In chicken, the projection of motor axons into hindlimb muscles is controlled by repulsive action of T-cadherins. During the early growth phase T-cadherin is expressed in all the motor axons of the trajectory which innervate the limb muscles but this expression is restricted to certain motor axons at the terminal phase. Thus T-cadherin guides and extends these motor axons in the early phase and only targets certain motors axons among the pool to the muscles (Fredette & Ranscht, 1994).

Like vertebrates, cadherins are also involved in the development of the nervous system in invertebrates. In *Drosophila*, among the classical cadherins, neuronal cadherin (*D*N-cadherin) is abundantly expressed in the nervous system. In *D*N-cadherin mutant flies, the initial tracts laid down by pioneers are fine but as soon as the followers join, the ventral nerve cord looks disorganised with discontinuous axon bundles due to stalling or misrouting of growth cones. This suggests that the proper navigation of follower axons is regulated by cadherin dependent contacts with pioneer axons (Iwai et al., 1997). Like in the vertebrate retina, cadherins also control the axon navigation and innervations in the fly visual system. Ommatidia, the single units of the *Drosophila* eye consist of eight cells

(R1-R8) which express *D*N-cadherin. The axons of these neurons travel and project to specific targets in the lamina and medulla which is mediated by the attraction of *D*N-cadherin from photoreceptor axons as well target neurons (Prakash et al., 2005). *D*N-cadherin also controls the ORN (olfactory receptor neuron) targeting in the fly olfactory system. In mutant flies lacking *D*N-cadherin, although the ORNs are able to innervate the AL region but fail to establish AL dendritic field (Hummel & Zipursky, 2004).

C. elegans genome codes for only one classical cadherin which exists in two isoforms *hmr-1a* and *hmr-1b*. *hmr-1b* is expressed in the nervous system and is the functional homologue of *D*N-cadherin. *hmr-1b* mutant animals show axon guidance and fasciculation defects in a subset of motor neurons in the ventral nerve cord (Broadbent & Pettitt, 2002). This suggests that like *D*N-cadherin, *hmr-1b* is also involved in the nervous system development and hence cadherin function is conserved in metazoans. The *C. elegans* genome also codes for a Fat-like cadherin *cdh-4* and a Flamingo ortholog *fmi-1*, which mediate the fasciculation of axons (Schmitz et al., 2008; Steimel et al., 2010). *cdh-4* mutant animals display variety of developmental defects including ventral and dorsal nerve cord fasciculation defects. These fasciculation defects in the major longitudinal axon tracts suggest that CDH-4 acts as an adhesion molecule and keeps these axons together in specific bundles (Schmitz et al., 2008). In *fmi-1* mutant animals the follower axon guidance is disrupted. FMI-1 plays distinct roles for pioneer and follower axons. For pioneer axons FMI-1 acts a receptor and likely activates downstream signalling pathway. For followers, FMI-1 mediates their adhesion with the pre-existing pioneer axons (Steimel et al., 2010). The *Drosophila* flamingo is involved in many aspects of nervous system development including the dendritic outgrowth and navigation (Gao et al., 1999), formation of proper dendritic fields (Gao et al., 2000), targeting of photoreceptor axons (Chen & Clandinin, 2008) and synaptic development (Bao et al., 2007).

In summary, cadherins are cell adhesion molecules which act as cell surface receptors and mediate adhesion between axons. Their interaction can be either homophilic or heterophilic and have conserved roles in both vertebrates and invertebrates.

1.6.2. IgCAMs

The IgCAMs are a diverse and large family of adhesion molecules present in the nervous system which are characterised by the presence of one or more 100 aa long Ig (Immunoglobulin domains) in the extracellular region. IgCAMs are important regulators of the cell-cell recognition and adhesion (Harpaz & Chothia, 1994). They can either mediate homophilic or heterophilic adhesions and numerous interactions with other family members (Brummendorf and Rathjen, 1998). The canonical axon guidance receptors UNC-40/DCC, UNC-5 and SAX-3/Robo (discussed above) also belong to the IgCAM family. Apart from these canonical axon guidance receptors, the best characterised members of this family are the neural cell adhesion molecule NCAM and members of the L1 subfamily (Maness & Schachner, 2007). The absence of both NCAM and the members of the L1 subfamily leads to variety of defects in the nervous system development in vertebrates. NCAM deficiency in mice results in the reduced size of olfactory bulb and deficits in spatial learning (Cremer et al., 1994). The absence of NCAM in mice also leads to fasciculation and pathfinding defects in mossy fibers of hippocampus (Cremer, 1997). Both NCAM and L1 mutant mice shows guidance defects in the axons of the corticospinal tract (CST), where a portion of axons fail to cross the midline to the opposite dorsal column which causes the hypoplasia of CST (Cohen et al., 1998; Rolf et al., 2002). The deficiency of another member of L1 subfamily, CHL-1 in mice results in the disorganisation of mossy fibers in the hippocampus and guidance defects in the axons of olfactory neurons (Montag-Sallaz et al., 2002).

The IgCAMs are conserved and are also required in the development of the invertebrate nervous system. In *Drosophila D*own's *s*yndrome *c*ell *a*dhesion *m*olecule (*Dscam*) which has 10 Ig domains potentially generates 38016 splice variants by alternative splicing which form 19008 distinct homophilic Dscam pairs to exhibit isoform specific homophilic binding (Schmucker et al., 2000; Wojtowicz et al., 2004; Wojtowicz et al., 2007; Schmucker and Chen, 2009). This diversity within the Dscam is required for shaping the denritic field, more specifically avoiding sister dendrite branches (Hughes et al., 2007), accurate wiring in the brain and mushroom body development (Hattori et al., 2007; Hattori et al., 2009). The Dscam also acts as guidance receptor for the proper

guidance of the axons of the Bolwing's nerve (BN) in the *Drosophila* embryo (Schmucker et al., 2000).

In *C. elegans* the L1 homolog LAD-1/SAX-7 regulates the maintenance of neuronal positions in the head (nerve ring) and ventral nerve cord and also regulates the organisation of the head ganglia (Zallen et al., 1999; Wang et al., 2005; Sasakura et al., 2005; Pocock et al., 2008). Another homolog of L1 in *C. elegans* known as LAD-2 acts as a co-receptor for the secreted MAB-20/Sema2 along with plexin receptor PLX-2 to repel the SDQL neuron for proper navigation (Wang et al., 2008). The proper placement of synapses of the HSNL neuron is regulated by the IgCAMs SYG-2 along with its receptor SYG-1 through heterophilic interaction (Shen and Bargmann, 2003; Shen et al., 2004; Chao and Shen, 2008). Recently another IgCAM, WRK-1, a guidance cue present in the motor neuron cell bodies has been shown to act through Eph receptor VAB-1 to prevent axons from inappropriately crossing the ventral midline (Boulin et al., 2006). Apart from this ZIG (1-5) and ZIG-8 proteins which are secreted IgCAMs with two Ig domains and co-expressed by the PVT neuron stabilize the two axon tracts of the ventral nerve cord (Aurelio et al., 2002). The other IgCAMs present in *C. elegans* display limited neuronal defects most notably axon guidance defects in some single mutants (Schwarz et al., 2009). In conclusion, IgCAMs are diverse group of cell adhesion molecules which can also act as receptors for axon navigation, synapses formation and maintenance in the nervous system.

1.7. Extracellular matrix and basement membrane

The extracellular matrix (ECM) is comprised of several distinct molecules which include laminins, collagens, proteoglycans, fibronectin, perlecan and many others. The ECM plays important roles in embryogenesis as well in adult tissues. These include providing adhesive substrate, mechanical strength, presenting growth factor to their receptors, sequestering and storing of growth factors and transduction of mechanical signals (Rozario & DeSimone, 2010). In multicellular animals, most of the tissues are surrounded by thin specialized extracellular matrices called basement membrane which demarks a boundary between tissues and the extracellular space. The major

components of the basement membrane are laminin, nidogen and heparin sulphate proteoglycans such as perlecan and type IV collagens (Yurchenco, 2011) (Figure 1.6).

Laminins, which are major structural components, are large heterotrimeric glycoproteins with α, β and γ chain joined through a long coiled-coil domain. Vertebrates have multiple α, β and γ chains and as a consequence form many laminin isoforms (Parsons et al., 2002; Aumailley et al., 2005). In contrast to vertebrates, *C. elegans* have only two α (LAM-3 and EPI-1) and single β (LAM-1) and γ (LAM-2) chains which result in two laminin isoforms (Kramer, 2005). Cell surface adhesion and receptor interaction are largely mediated by the α subunit, but it can also contribute to self assembly. The structural roles like polymerisation and nidogen binding are mediated by β and γ subunits (Yurchenco, 2011).

Laminins interact with basement membrane receptors integrins connecting them to the inside cytoskeleton. Integrins are transmembrane α/β heterodimers capable of binding to many ECM molecules and are critical for cell adhesion to laminins (Nishiuchi et al., 2006). Vertebrates have around 24 different integrins which are generated from 18 α and 8 β genes. The *C. elegans* genome codes for two α (*ina-1* and *pat-2*) chain genes and single β (*pat-3*) chain genes which generate two integrins (Kramer, 2005). INA-1 regulates neuronal cell migration and axonal fasciculation and also has been shown to associate with PAT-3, the only integrin β subunit in *C. elagans* (Baum & Garriga, 1997).

Collagens are the structural molecules in the ECM with a characteristic triple helix domain (Figure 1.6). Vertebrates have many collagen subtypes with humans alone having 27 distinct types of collagen (Myllyharju & Kivirikko, 2001). Type IV collagens, which form networks are the most abundant basement membrane collagens. They exist in heterotrimeric form comprising of two α1-like and one α2-like chain. Vertebrates have three each α1 and α2-like genes. The macromolecular network formed by collagen IV gives proper organisation and biochemical stability to basement membranes (Kühn, 1995). Collagen IV interacts with cells by binding to the integrin receptors α1β1 and α2β1 (Vandenberg et al., 1991; Golbik et al., 2000). The *C. elegans* genome codes for two type IV collagens with one each α1 (*emb-9*) and α2 (*let-2*) genes. Both *emb-9* and *let-2* are homologous to mammalian α1(IV) and α2(IV) collagen genes and are involved

in embryogenesis. *let-2* exists in two alternately splice forms, one is predominant in the embryo and the other during larval and adult stages, suggesting isoform specific roles in development (Guo and Kramers, 1989; Sibley et al., 1993; Sibley et al., 1994). EMB-9 and LET-2 colocalize *in vivo* but unlike mammalian type IV collagens they are not associated with basement membrane in certain regions (Graham et al., 1997).

Perlecans are large, multidomain and most abundant heparin sulphate proteoglycans of ECM expressed in early stages of development. They were originally identified in basement membranes. Perlecans influence intracellular signalling by interacting with other components of the ECM, growth factors and cell surface receptors. In mouse the mutation in the perlecan (*Hspg2*) gene is mostly embryonic lethal with severe defects in cartilage and cephalic development (Arikawa-Hirasawa et al., 1999; Costell et al., 1999), indicating their critical role in development. The nematode ortholog of perlecan is UNC-52, which is associated with muscle basement membranes. UNC-52 generates many isoforms by altenative splicing including the major isoforms which are short (S), medium (M) and long (L). This classification is based on the basis of presence or absence of domains IV and/or V at the carboxyl end of the molecule. The *unc-52* mutant animals have severe musculature defects and arrest at the two fold stage of embryogenesis (Rogalski et al., 1993; Rogalski et al., 1995).

In summary, ECM and basement membranes are involved in many developmental processes including cell migrations and axon guidance. Although the composition of ECM varies in different families of animals, their role seems to be conserved in vertebrates and invertebrates. The nidogen which is more relevant to my thesis is discussed separately in the following section.

1.7.1. Nidogen

Nidogens (entactin) are monomeric sulphated glycoproteins which are ubiquitously present in the basement membrane (Ho et al., 2008). Nidogen was first isolated from mouse EHS (Engelberth-Holm-Swarm) sarcoma basement membranes (Timpl et al., 1983). Mammals have two nidogen family members, nidogen-1 (entactin-1) and nidogen-2 (entactin-2). These are elongated molecules comprised of three globular

domains (G1, G2 and G3). The G1 domain is linked to G2 by a flexible protease sensitive link and the G2 domain is linked to G3 by a rod like domain (Fox et al., 1991; Kohfeldt et al., 1998; Kimura et al., 1998) (Figure 1.7). While the globular domains are structurally similar in both nidogen-1 and nidogen-2, the differences occur mainly between the linker and the rod domain (Ho et al., 2008). Nidogens are thought to connect laminin and collagen IV networks to form a scaffold and integrate other proteins, therefore, stabilizing the basement membrane (Figure 1.6). *In vitro* studies have shown that both nidogen-1 and nidogen-2 bind and interact with laminins, collagen IV and perlecans with high affinity. Nidogen-1 can also bind to fibulins (Fox et al., 1991; Mayer and Timpl., 1994; Kohfeldt et al., 1998). However, the *in vivo* studies have suggested that nidogens do not have a structural role in the basement membrane. In nidogen-1 and nidogen-2 mutant mouse lines the basement membrane is formed and maintained properly with some alteration in selected regions (Murshed et al., 2000; Dong et al., 2002; Schymeinsky et al., 2002). Moreover, the absence of nidogen-1 or nidogen-2 or both did not have any impact on the occurrence and localization of basement membrane components in the murine kidney (Gersdorff et al., 2007). Nidogens have been shown to play an important role in peripheral neuronal regeneration. In the rat nervous system nidogen -1, through β1 integrin, regulates the migration and survival of Schwann cells which is important for the peripheral nerve regeneration (Lee et al., 2007).

The *C. elegans* genome codes for one nidogen gene *nid-1* which generates three alternately spliced isoforms (NID-1A, NID-1B and NID-1C) differing with each other with respect to the number of EGF repeats in the rod domain (Figure 1.7). NID-1 is present in all the basement membranes and is highly expressed in the nerve ring, distal tip cells of the gonad, spermatheca and ventral nerve cord region. In *nid-1* mutant animals which are viable and fertile, the type IV collagen was normally localized into the basement membrane (Kang & Kramer, 2000) and the basement membrane was normal (Kang and Kramer, 2000; Kim and Wadsworth, 2000). This suggests that like mammalian nidogens, *nid-1* in *C. elegans* is not required for the assembly of basement membranes. However, the guidance and positioning of many axons most notably in the ventral and dorsal nerve cords were affected, which in general is unlikely due to the abnormal basement membrane per se, as many other axons are not affected in the *nid-1* mutant animals (Kim and Wadsworth, 2000). The ventral nerve cord which is a highly asymmetric

structure with more axons in the right axon tract in the wild type, displays symmetric ventral nerve cord where many axons over populate the left axon tract. This is mainly due to the failure of motor neuron processes to extend into the right axon tract, which instead extend into the left axon tract. Moreover, the interneuron axons cross the ventral midline from the left side inappropriately in small bundles as compared to the one fascicle in wild type. The axons approaching the ventral midline from the left side (PVQL and HSNL) which normally extend in the left axon tract cross the ventral midline and extend into the right axon tract. The axons that reach the dorsal side from the right side have guidance problems whereas those reaching from the left side are normal, which results in the splitting of dorsal nerve cord (Kim and Wadsworth, 2000). As mentioned above, NID-1 is enriched along the longitudinal axon tracts between the muscles edges and nerve cords in close proximity to the synapse-rich regions. In *nid-1* mutant animals the localisation of SNT-1 (synaptotagmin) and SNB-1 (synaptobrevin) is affected, suggesting that NID-1 regulates the organisation of the presynaptic zone. The synapses along the ventral and dorsal cords are elongated and closely spaced as compared to the wild type (Ackley et al., 2003).

In conclusion, nidogen is ubiquitously present in basement membranes and is conserved in mammals and nematodes. However, nidogen is not required for the basement membrane assembly in both mammals and nematodes.

1.8. Endomembrane trafficking and axon guidance

The growth cone acts as a navigation centre by sensing and integrating the guidance cues encountered during navigation. In response to these guidance cues, the growth cone makes different choices like to grow straight or to make a turn or to retract (collapse). This entirely depends on the nature of the guidance cue, e.g. on encountering the attractive or repulsive cue, the growth cone moves towards or away respectively from the source of the cue. The binding of guidance cues to the growth cone surface receptors evokes an asymmetric Ca^{2+} elevation in the leading edge facing the guidance cue. Whether a growth cone is attracted or repelled highly depends on the source of Ca^{2+}. The attractive cues evoke a Ca^{2+} release from the endoplasmic reticulum (ER) whereas a repulsive cue evokes Ca^{2+} from the plasma membrane channels (Hong et al.,

2000; Ooashi et al., 2005). Downstream of these attractive or repulsive Ca^{2+} is the endomembrane trafficking which instructs the guidance of growth cone (Tojima et al., 2011; Tojima, 2012; Tojima et al., 2014) (Figure 1.8).

Trafficking of different molecules both by exocytosis and endocytosis at the growth cone surface are highly involved in its guidance (Tojima & Kamiguchi, 2015). To continuously advance and navigate, the migrating growth cones need a supply of materials including the plasmamembrane for expansion (Pfenninger, 2009). The trafficking of the plasmamembrane components which are supplied by the intracellular organelles is regulated by the SNARE proteins. SNARE family proteins which include vesicle associated membrane proteins (VAMPs) also called v-SNAREs, soluble N-ethylmaleimide-sensitive factor attachment proteins (SNAPs), and syntaxins also called t-SNAREs mediate the fusion of exocytic vesicles (Kasai et al., 2012). During the development of an axon much before the synaptic vesicles precursors start appearing, the growth cones contain membranous vesicles of about 150nm called plasmalemal precursor vesicles (PPVs) (Pfenninger, 2009) or growth cone particles (GCPs) (Igarashi et al., 1997). Further subcellular fractionation has shown that these GCPs also contain SNARE components suggesting that these GCPs also go through SNARE mediated fusion (Igarashi et al., 1997). Axon guidance by extracellular cues also involves SNARE mediated machinery. The Netrin dependent interaction between UNC-40/DCC and SNARE components Syntaxin-1 and T1-VAMP likely triggers the exocytosis in the selected regions of growth cone which is required for the attraction of the commissural axons (Cotrufo et al., 2011; Cotrufo et al., 2012; Ros et al., 2015). Furthermore, VAMP2 (also a SNARE component) mediated exocytosis is required for growth cone attraction but not repulsion (Tojima et al., 2007). The attractive cue leads to asymmetric Ca^{2+} elevations on the side facing the cue and subsequent VAMP2 mediated exocytosis on that side (Tojima et al., 2007) (Figure 1.8). In contrast to this, Sema3A mediates repulsion of DRG axons by inhibiting Syb2 (VAMP2) mediated exocytosis asymmetrically on the side facing the cue. This suggests that axon repulsion by Sema3A mediated signalling requires Syb2 dependent vesicular traffic (Zylbersztejn et al., 2012). The imbalance between exocytosis and endocytosis leads to the turning of growth towards the side with more net exocytosis and less net endocytosis and vice versa (Figure 1.8). Growth cones turn even in absence of guidance cues by direct

manipulation of local exocytosis or endocytosis. The balance between exocytosis and endocytosis abolishes the turning and leads to straight growth (Tojima et al., 2010; Tojima, 2012; Tojima et al., 2014). Netrin-1 dependent SNARE mediated exocytosis is also required for axon branching in murine cortical neurons. Binding of TRIM9, an E3 ligase releases SNAP25 from cortical neurons upon Netrin-1 stimulation which promotes exocytosis and axon branching (Winkle et al., 2014).

Like exocytosis, guidance cues also evoke endocytosis which is critical for growth cone repulsion (Figure 1.8). The repellent cue Sema3A upregulates clathrin mediated endocytosis asymmetrically in the leading edge of growth cone facing the cue. This Sema3A mediated repulsion is abolished if the clathrin mediated endocytosis is pharmacologically blocked (Tojima et al., 2010). Similarly the myelin associated glycoprotein-MAG repels growth cones by inducing the asymmetric clathrin mediated endocytosis of β1 integrin in the leading edge of the growth cone facing the MAG. Loss of β1 integrin asymmetric function or induction of repulsive Ca^{2+} was sufficient for chemorepulsion (Hines et al., 2010). Macropinocytosis, a less characterised form of endocytosis involving large vesicles usually accompanied by cell surface ruffling (Swanson & Watts, 1995), also mediates the repulsive action of guidance cues. Sonic hedgehog (Shh) at higher concentrations repels the RGC axons by inducing the macropinocytosis in the growth cone. Although this is clathrin independent it depends also on dynamin and also activates Rho GTPase and non-muscle myosin-II signalling. This Shh induced repulsion of axons and growth cone collapse is abolished by inhibiters of macropincytosis. Similar dynamin dependent macropinocytosis was also induced by another repulsive cue ephrin-2A. This indicates that endomembrane trafficking mediated by macropinocytosis is important for repulsive axon guidance (Kolpak et al., 2009).

Newly synthesised proteins are packed into vesicles which bud off from the golgi and are sorted into the developing neuronal processes such as axons and dendrites. Different members of the Rab family of small GTPases are inolved in the sorting and trafficking of these vesicles (Villarroel-Campos et al., 2014). Rab GTPases are activated by guanine nucleotide exchange factors (GEFs) which promote the exchange of GDP with GTP (Wada et al., 1997). Once activated Rab GTPases bind with the vesicles and also recruit other effectors including motor proteins and thus target these vesicles to the

target membranes where they exocytose. The Rabs which mediate the exocytosis are known as exocytic Rab GTPases. In contrast the entry of cell surface molecules into the cell via endocytosis is mediated by endocytic Rabs. Members of both exocytic as well endocytic Rabs are involved in different aspects of axonal development including promotion and inhibition of axonal outgrowth (Tojima & Kamiguchi, 2015). Several different molecules act as the cargoes for these secretory as well as endocytic vesicles. These include trophic factors, guidance cues and receptors, cell adhesion molecules and cytoplamic proteins (Tojima & Kamiguchi, 2015). This suggests that membrane trafficking undoubtedly has an instructive role in the guidance of growth cone.

In summary, endomembrane trafficking is crucial for the regulation of axon guidance. The attractive cues induce exocytosis in the region of the growth cone facing the cue whereas the repulsive cues induce endocytosis in the region of the growth cone facing the cue. More exocytosis leads to the attraction towards the cue and more endocytosis leads to repulsion away from the source of the cue.

1.9. Development of the *C. elegans* ventral and dorsal nerve cords

The nematode *Caenorhabditis elegans* was introduced as a model organism to study nervous system development by S. Brenner in 1974. The characteristic features like short generation time, hermaphroditic mode of life cycle, transparent body, amenable to genetic analysis and small number of cells makes it an excellent model organism (Brenner, 1974). *C. elegans* is a small (1 mm long) nematode. The adult hermaphrodite has 959 somatic cells including 302 neurons and 56 glial cells with the lineage of each individual cell known (Sulston et al., 1983; Sulston, 1983). The structure and connectivity of the nervous system has been deduced from serial electron microscopic reconstructions. These 302 neurons are divided into 118 different classes based on their morphology, position and connectivity which make around 5000 chemical synapses, 2000 neuromuscular junctions and 600 gap junctions. This shows that, although the nervous system is simple, the complexity in function is still maintained. Neurons are mostly simple, unbranched and bipolar with a longer process (axon) and a much shorter process (dendrite) that run in defined positions. The axons are mostly

bundled together in axon tracts with en pasant synaptic contacts made between the adjacent neurons (White et al., 1986).

In *C. elegans* the major areas of neuropil are the nerve ring which is present in the head, and the ventral and dorsal nerve cords running longitudinally along the body (Figure 1.9). The ventral nerve cord (VNC) is the major longitudinal axon bundle and is highly asymmetric structure with all the axons running in right axon tract except four axons which form the left axon tract (Durbin, 1987) (Figure 1.10C). At the anterior front of VNC is the AVG neuron, whose cell body is present in the retrovesicular ganglion (RVG), close to the posterior pharyngeal bulb (Figure 1.10A). The other neurons present in RVG are RIF, RIG and SABV and among these RIF neurons pioneer the path towards the nerve ring (Durbin, 1987). The AVG is single bipolar neuron with a longer posterior process present in the right axon tract of VNC and much sorter anterior process which grows towards the head. Neuronal outgrowth starts around 480 minutes in the two fold stage embryo after the fertilization. AVG is the first neuron to extend an axon into the right axon tract of the ventral nerve cord from the anterior side. Therefore, AVG is the pioneer for the right axon tract of the VNC (Figure 1.10A), which is followed by the later outgrowing axons (Durbin, 1987) (Figure 1.10B). The AVG neuron makes large gap junctions with the closely located two RIF interneurons in the RVG (Figure 1.9A) and also receives a small input from the PHA phasmid neurons (White et al., 1986). However, its physiological aspects have not been studied in great detail and it is most popular for its pioneering function. The ablation of AVG leads to the formation of a disorganised VNC with axons frequently crossing the midline. The most affected ones are the interneurons and DD/VD motor neurons. This suggests that AVG is required for the correct organisation of the ventral nerve cord (Durbin, 1987; Hutter, 2003).

After AVG, the next neurons to extend processes in the VNC are the six inhibitory DD motor neurons. DD motor neuron cell bodies are located along the ventral midline and each cell body extends a process into the right axon tract of the VNC (Figure 1.10B). DD and another class of motor neurons (DA/DB) whose cell bodies are also located along the ventral midline send out commissures at the same time. The DA/DB motor neurons send out commissures directly from the cell bodies along the right and left side of VNC (Figure 1.10B). In case of DD motor neurons the commissures branch

from the anterior processes and extend only on the right side of VNC towards the dorsal side (Figure 1.10B). The only exception being DD1, which extends commissure on the left side. On reaching the dorsal side these commissures link and form the dorsal cord with DA commissures turning anteriorly, DB posteriorly and DD in both directions. Once the dorsal cord processes have grown some distance, the dendrites of DA/DB motor neurons start appearing in the right axon tract of the VNC (Durbin, 1987) (Figure 1.9B). The DA/DB motor axons form neuromuscular junctions and also synapse with DD processes jointly on the dorsal side. However, DD processes do not form neuromuscular junctions on the ventral side. DA motor neurons receive the synaptic input from the AVA, AVD and AVE interneurons whereas the DB motor neurons receive the synaptic input from AVB and PVC interneurons (White et al., 1986). The DA/DB motor neurons are excitatory and contain acetylcholine as a neurotransmitter. Forward and backward movement of the animals is controlled by DB and DA motor neurons respectively along with their associated interneurons (Chalfie et al., 1985). On the other hand DD motor neurons do not receive synaptic input from interneurons but from other classes of motor neurons (VA, VB and VC) from the ventral side (White et al., 1986). DD motor neurons are inhibitory and contain γ-aminobutyric acid (GABA) as neurotransmitter. They form synapses with and innervate dorsal cord muscle arms and help in coordinating the forward and backward movement (Chalfie et al., 1985; White et al., 1986).

While the motor neuron commissural outgrowth is in progress, the PVP and PVQ neurons present in the pre-anal ganglion (PAG) at the posterior side start extending axons into the ventral nerve cord. The PVPs are a pair of bilaterally symmetrical interneurons and their axons cross the ventral midline immediately after the exit from PAG. The PVPR which is present on the right side crosses and extends into the left axon tract of the VNC. The PVPL crosses from the left side and extends into the right axon tract of the VNC (Figure 1.10A). PVPs are closely followed by PVQs which do not cross and extend on their own side, PVQR into the right and PVQL into the left axon tract (Figure 1.10B). Thus PVPR is the first axon to extend into and thereby, pioneers the left axon tract of the VNC (Durbin, 1987). PVP interneurons make chemical synapses with AVA, AVB and AVD interneurons and gap junctions with AQR motor neurons. PVQ interneuron receives input from the amphid channel receptor ASJ and phasmid receptor neuron PHA (White et al., 1986).

At the time when DA/DB motor neurons extend dendrites into the ventral nerve cord, the command interneurons exit the nerve ring in two fascicles one on each right and left side of the VNC. The left side fascicle crosses infront of the RVG and joins the right fascicle and both extend into the right axon tact and terminate in the tail region (Figure 1.10B). The only exception being AVK, which extends an axon on both sides, AVKR into the left axon tarct and AVKL into the right axon tract (Durbin, 1987). Among the command interneurons, the five pairs (AVA, AVB, PVC, AVD and AVE) with all having cell bodies at the anterior side in the lateral ganglia except PVC whose cell body is located at the posterior side in the lumbar ganglia, from synapses with DA/DB motor neurons. In the first larval stage, VD motor neurons whose cell bodies are also located in the ventral midline extend commissures towards the dorsal side (Durbin, 1987). VD motor neurons receive their synaptic input from the DA, DB and AS motor neurons on the dorsal side and innervate the ventral body muscles. Postembryonically, at the fourth larval stage HSN neurons extend axons into the either side of ventral midline, HSNL extends into the left whereas HSNR extends into the right axon tract (Durbin, 1987). In the embryo these neurons are born in the tail region and migrate towards the center and are located around the vulva (Sulston et al., 1983; Garriga et al., 1993). HSNs are serotogenic motor neurons and innervate vulval muscles and stimulate egg laying (Trent et al., 1983; White et al., 1986; Desai et al., 1988).

In conclusion, the axon tracts in the ventral and dorsal nerve cords are simple with sequential outgrowth. Hence provides an excellent model within model system to study axon guidance, in particular pioneer-follower navigation.

1.10. Goals and the content of this thesis

In *C. elegans* AVG pioneers the right axon tract of the ventral nerve cord. The molecular mechanism of AVG navigation is largely unknown. The major goal of this thesis was to identify novel regulators of AVG axon navigation. In the first part of this thesis I have characterised the *plr-1* mutants which were isolated in EMS forward genetic screens for AVG axon guidance defects. The detailed phenotypic characterisation of three alleles of *plr-1*(*hd128*, *hd129* and *tm2957*) was carried out with respect to AVG defects. *plr-1* mutant animals display polarity reversal defects in the AVG

neuron, outgrowth and navigation defects in the AVG axon. Further phenotypic characterisation of the strongest allele *hd129* was carried out for other neuronal and non-neuronal defects. Detailed genetic interactions and expression pattern of *plr-1* are also provided. We also provide genetic interaction data where the polarity reversal defects are suppressed by the mutations in the *mig-14*/Wntless, *unc-53*/NAV2 and *unc-73*/Trio. These results are discussed in the chapter 2.

For the second part of this thesis I have carried out an enhancer screen for AVG axon guidance defects in a *nid-1* mutant background. By mutagenising 2400 hapliod genomes I was able to isolate 21 mutants with penetrant AVG axon guidance defects. The methods and results of the screen are discussed in the chapter 3. One of the candidate mutants which I choose to further characterise turned out to be an allele of *aex-3*. The detailed phenotypic characterisation of *aex-3* mutants in *nid-1* background was carried out for AVG and other neurons of the VNC. AEX-3 is a GDP/GTP exchange factor for RAB-3 and AEX-6/Rab-27. We provide genetic interaction data which suggests that AEX-3 regulates RAB-3 but not AEX-6/Rab27 for the AVG axon navigation. We also provide genetic interaction data which suggests that *aex-3* acts along with the components of the vesicle release and fusion (*ida-1*/IA-2, *unc-31*/CAPS, *unc-64*/Syntaxin) in the same genetic pathway. Lastly, we also provide genetic evidence which suggests that AEX-3 might regulate the trafficking of the Netrin receptor UNC-5 to the growth cone surface for the proper navigation of AVG axon. This is the first study which implicates AEX-3 in axon guidance. The results are discussed in the chapter 4. Chapter 5 summarizes the overall results and outlines the general conclusions.

1.11. Figures

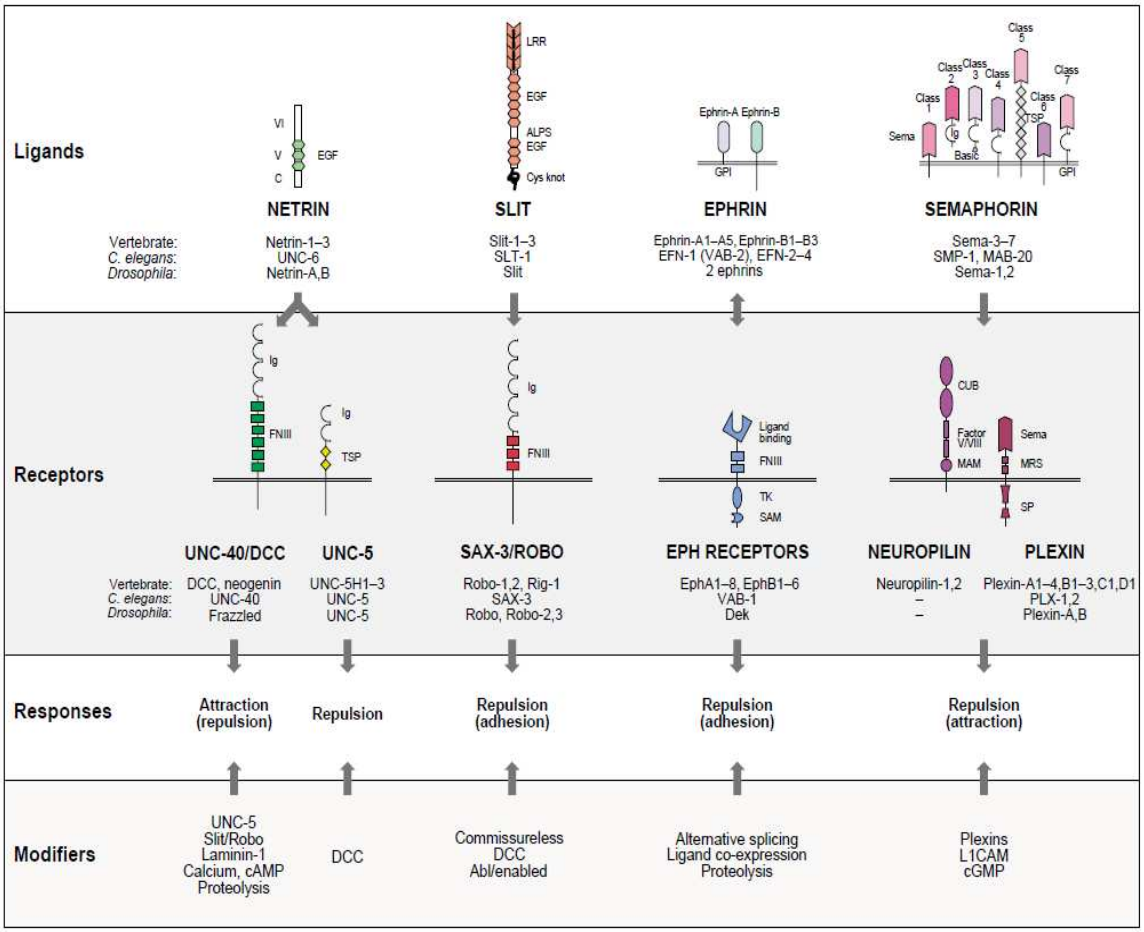

Figure 1.1 Major axon guidance families

Overview of the major axon guidance cues and their receptors: The guidance response and the modifiers for each ligand receptor pair are also indicated. ALPS, agrin–laminin–perlecan–Slit domain; C, netrin C terminus; CUB, C1/Uegf/BMP-1 domain; DCC, deleted in colorectal cancer; EGF, epidermal growth factor; FNIII, fibronectin type III domain; GPI, glycosylphosphatidyl–inositol anchor; Ig, immunoglobulin domain; LRR, leucine-rich repeat; MAM, meprin/A5 antigen motif; MRS, Mettyrosine kinase–related sequence; RK, arginine/lysine-rich basic domain; SAM, sterile alpha motif; SP, 'sex and plexins' domain; TK, tyrosine kinase domain; TSP, thrombospondin domain; VI and V, homology to laminin domains VI and V, respectively. Reprinted with permission from Nature Publishing Group: Nature Neuroscience Vol. 4, pp 1169-1176, 'Dynamic regulation of axon guidance', Timothy W. Yu and Cornelia I. Bargmann, © 2001

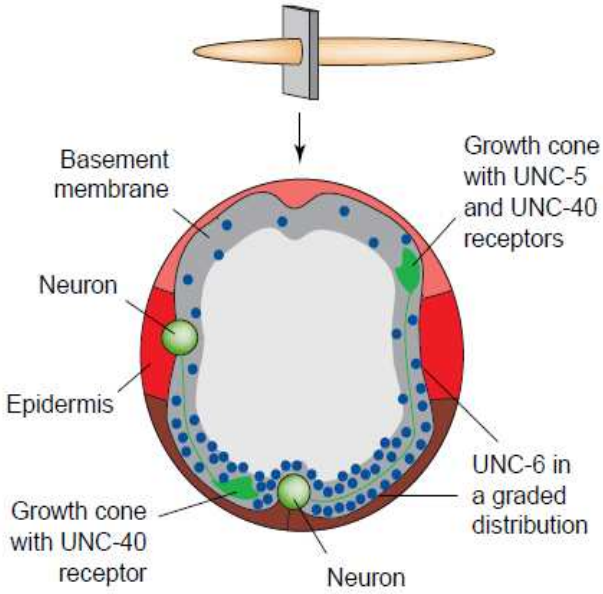

Figure 1.2 Dorsal-ventral migrations by UNC-6 in *C. elegans*

The UNC-6/Netrin (blue) forms a ventral to dorsal gradient. Growth cones migrate between body wall muscles and basement membrane along the dorso-ventral axis. Growth cones expressing both UNC-5 and UNC-40/DCC (green) Netrin receptors are repelled by the ventral UNC-6/Netrin source and migrate towards the dorsal side. Growth cones expressing only UNC-40/DCC (green) are attracted towards the ventral source of UNC-6/netrin and thus migrate to the ventral side. A transverse section of the *C. elegans* body wall is shown. Reprinted with permission from Elsevier: Trends in Neuroscience, Vol. 25, pp 423-429, 'Moving around in a worm: netrin UNC-6 and circumferential axon guidance in *C. elegans'*, William G.Wadsworth, © 2002

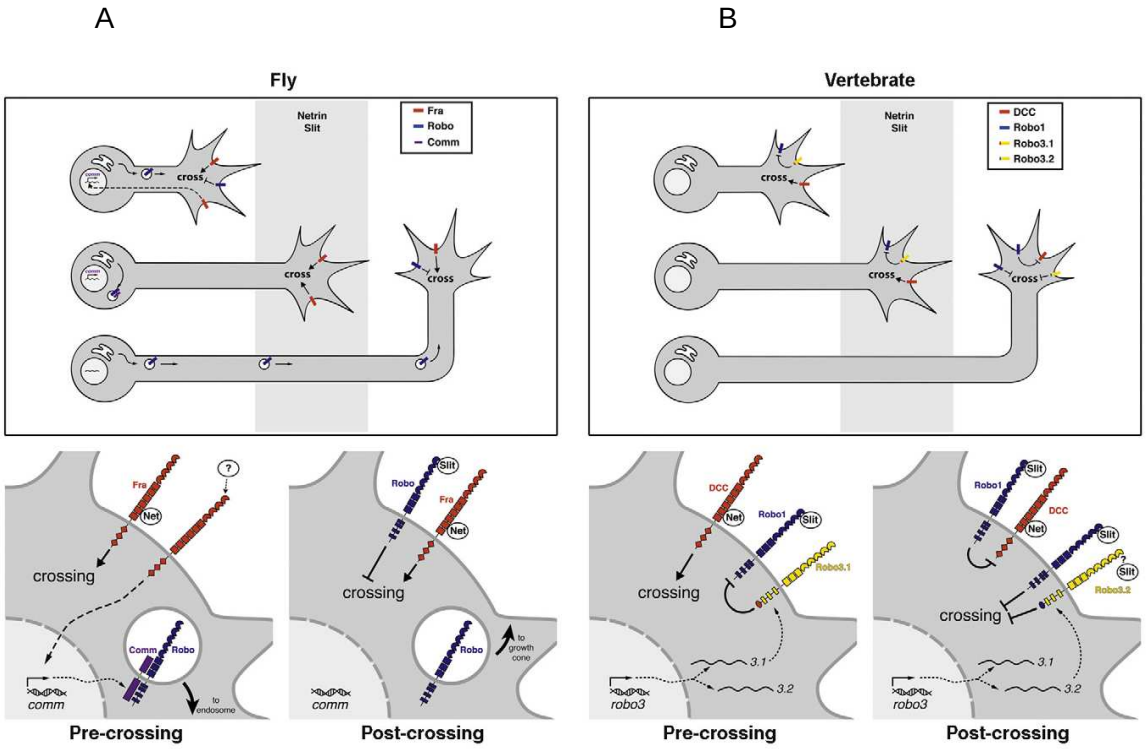

Figure 1.3 Midline crossing in *Drosophila* and Vertebrates

(A) In Drosophila, the precrossing (Bottom left) commissural axons express Comm (purple) which sorts Robo (blue) internally to endosomes and prevent it from reaching the growth cone surface and are thus attracted towards the midline by Netrin-Frazzled (red) signalling. In postcrossing (Bottom right) commissural axons, the Comm is downregulated and Robo reaches the growth cone surface. The Slit-Robo signalling repels and prevents these axons from re-crossing the midline. (B) In vertebrates, the precrossing (bottom left) commissural axons express Robo 3.1 (yellow) which interferes with the Slit-Robo signalling and allows these axons to cross. The post-crossing (bottom right) commissural axons express Robo3.2 which along with Robo1 (blue) and Robo2 (not shown) mediates Slit repulsion and keeps these axons away from the midline. Reprinted with permission from Elsevier: Current Opinion in Neurobiology, Vol. 20, pp 79-85, Timothy A. Evans and Greg J. Bashaw, 'Axon guidance at the midline: of mice and flies', © 2010

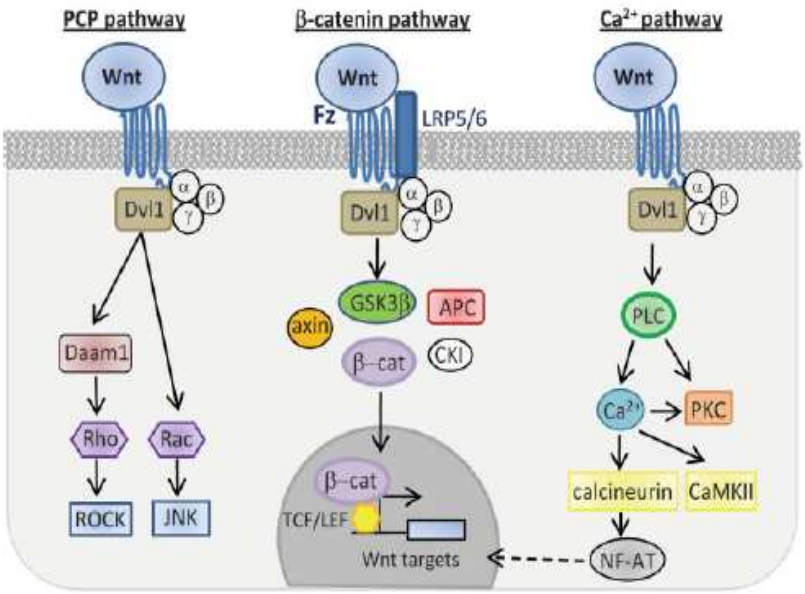

Figure 1.4 Classical Wnt signalling pathways

Wnt ligans upon binding to their receptors activate three different signalling pathways: The canonical β-catenin, the plannar cell polarity (PCP) and the Wnt/Ca^{2+} pathway. The common step in all the three pathways is the Fz-mediated recruitment of Dvl, a cytoplasmic scaffolding protein. In the canonical pathway (middle), the activation of Dvl results in the inhibition of glycogen synthase kinase-3β (GSK3β), a serine threonine kinase with multiple substrates including β-catenin. In the absence of Wnt ligand, GSK3β forms complex with other proteins which recruits β-catenin for degradation. Wnt-Fz interaction leads to the disintegration of this complex and the accumulation of β-catenine (transcription factor) which translocates to the nucleus and activates the transcription of target genes. In the PCP pathway (left), Wnt-Fz interaction leads to Dvl-mediated activation of the small GTPases Rho and Rac, which activate the Rho kinase (ROCK) and c-JNK, respectively, affecting the dynamics of the cytoskeleton. The Wnt/Ca^{2+} pathway (right) involves G proteins, phospholipase C (PLC), phosphodiesterase (PDE) and the activation of the Ca^{2+}/calmodulin dependent protein kinase II (CaMKII), protein kinase C (PKC), calcineurin and nuclear factor of activated T cells (NF-AT). Reprinted with permission from John Willey and sons: BioEssays, Vol. 31, pp 1013-1025, 'Emerging mechanisms in morphogen-mediated axon guidance', Cristina Sánchez-Camacho and Paola Bovolenta, © 2009

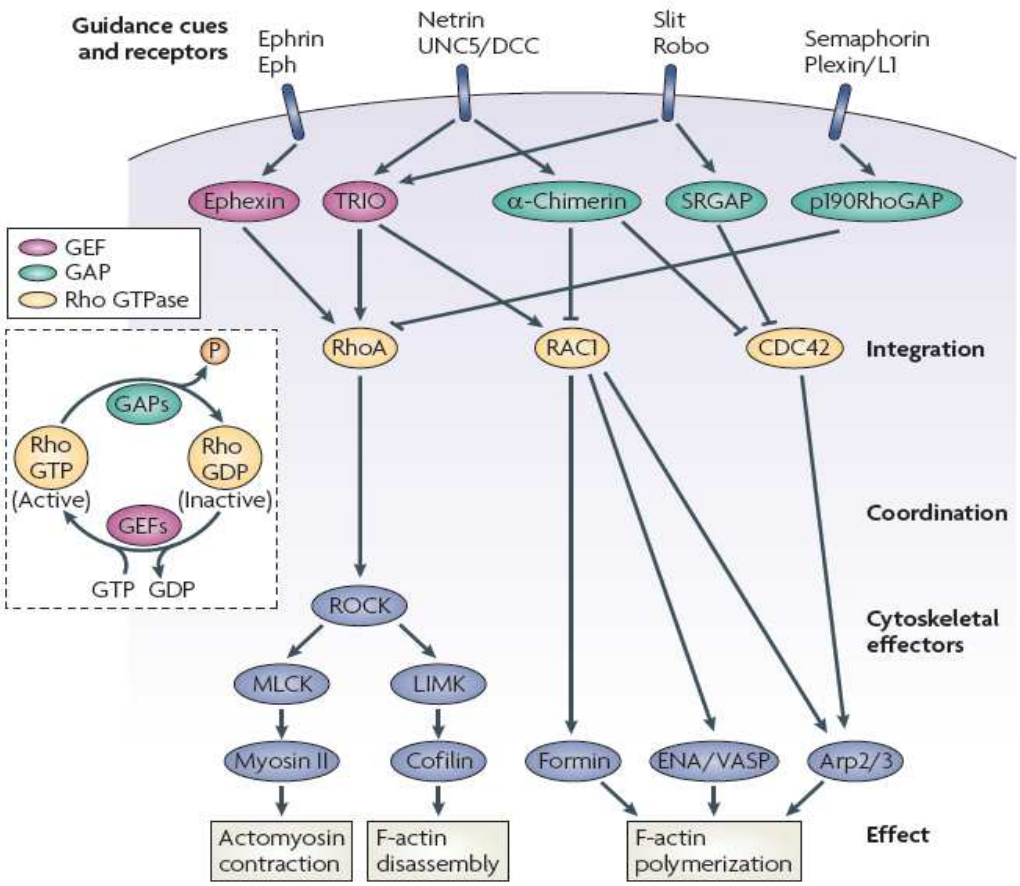

Figure 1.5 Growth cone signalling

The binding of guidance cues to their corresponding receptors leads to the activation of the Rho GTPase regulators including guanine nucleotide exchange factors (GFFs) and GTPase activating proteins (GAPs), which activate and inactivate Rho GTPases respectively. The Rho GTPases inturn coordinate the downstream effects by modifying the function of cytoskeleton effectors. The activation or inactivation of the cytoskeleton effectors leads to responses such as actomyosin contraction, filamentous (F) actin disassembly or polymerisation. Only some of the known examples of guidance cues and receptors, GEFs, GAPs and cytoskeletal effectors that are downstream of Rho GTPases are shown in the figure. Arrows do not necessarily denote direct interaction. The boxed inset shows the Rho GTPase activation–inactivation cycle, in which GAPs lead to the hydrolysis of GTP to GDP, whereas GEFs catalyse the exchange of GDP for GTP. Arp2/3, actin-related protein2/3; ENA/VASP, enabled/vasolidator-stimulated phosphoprotein; LIMK, LIM domain kinase; MLCK, myosin light chain kinase; ROCK, Rho kinase; SRGAP, slit–robo GAP; UNC5, uncoordinated protein 5. Reprinted with permission from Nature Publishing Group: Nature Reviews Molecular Cell Biology, Vol. 10, pp 332-343, 'The trip of the tip: understanding the growth cone machinery', Laura Anne Lowery and David Van Vactor, © 2009

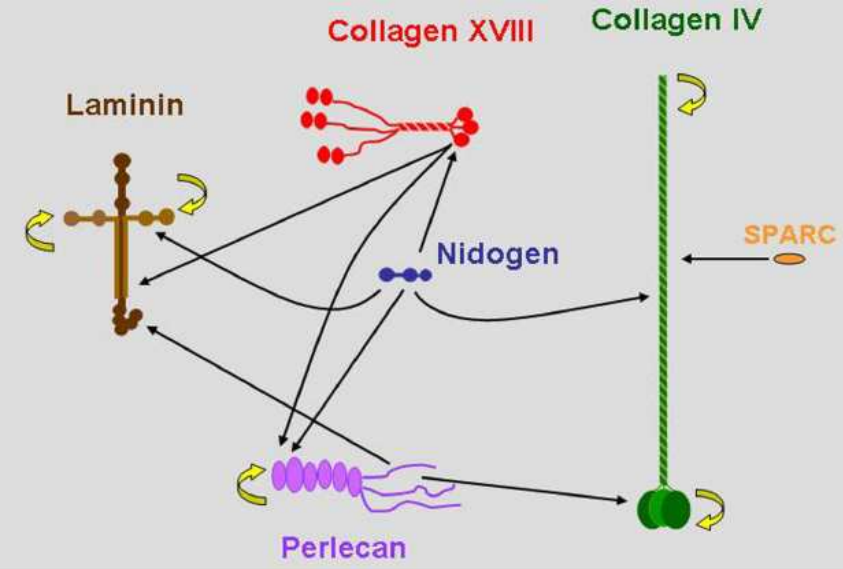

Figure 1.6 Basement membrane components in *C. elegans*

The major basement membrane molecules are represented in approximately appropriate relative sizes. Arrows represent biochemically defined interactions, mostly derived from the studies of vertebrate molecules. The abilities of the collagen IV and laminin to polymerise and perlecan to oligomerise are indicated by the curved yellow arrows. Reprinted from Kramer, J.M. 'Basement membranes' (September 1, 2005), WormBook, © 2005 James M. Kramer under the terms of the Creative Commons Attribution License

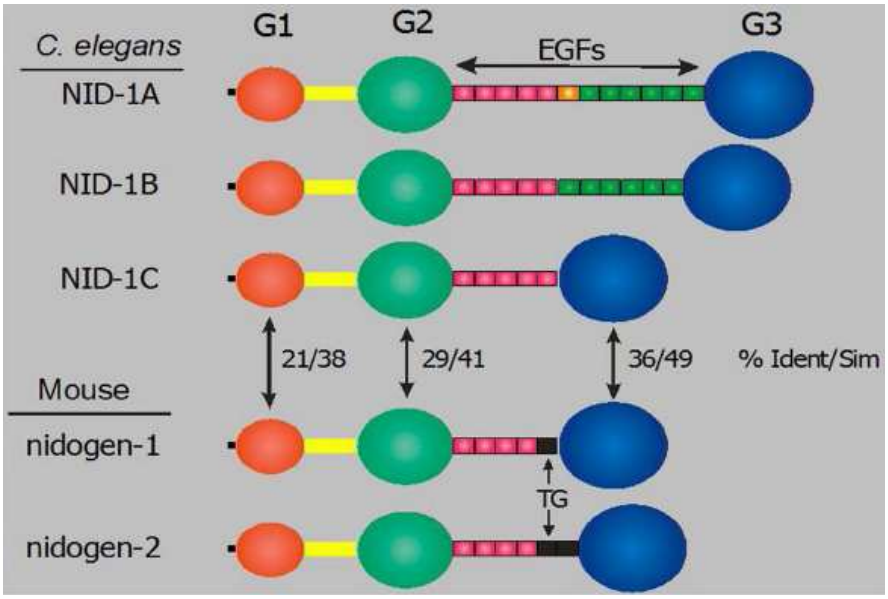

Figure 1.7 Domain structure of *C. elegans* and mouse Nidogens

Nidogen has three globular domains G1, G2 and G3. G1 and G1 are connected by a linker whereas G2 and G3 are connected by EGF repeats. *C. elegans* NID-1 exists in three alternately spliced isoforms (NID-1A, NID-1B and NID-1C) whereas mouse has two nidogens (nidogen-1 and nidogen-2). The percentage of amino acid similarity between *C. elegans* and mouse is also shown. TG indicates thyroglobulin modules in mouse. Reprinted from Kramer, J.M. 'Basement membranes' (September 1, 2005), WormBook, © 2005 James M. Kramer under the terms of the Creative Commons Attribution License

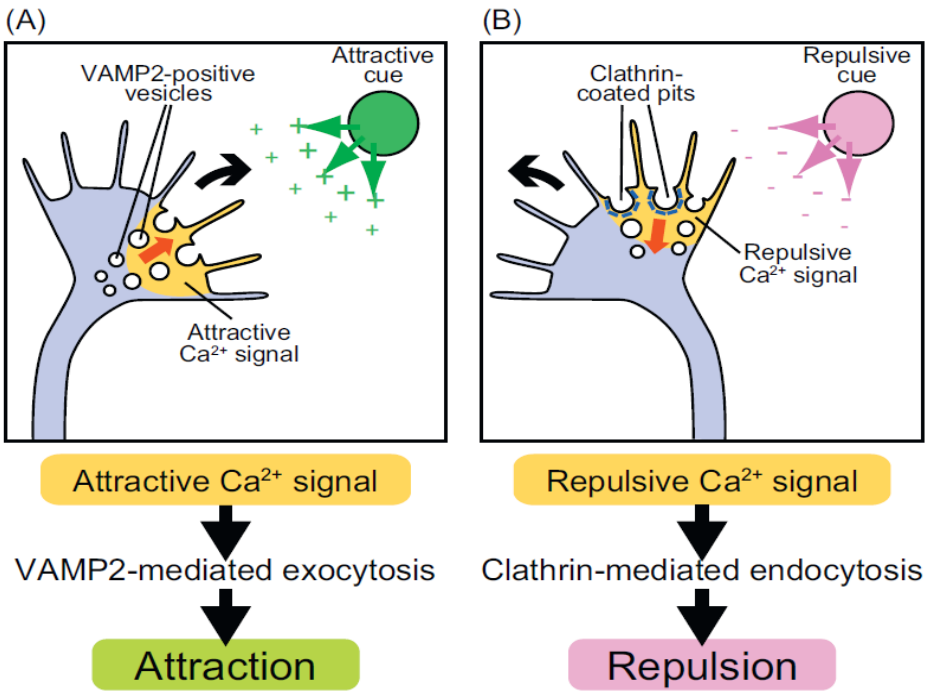

Figure 1.8 Membrane trafficking in growth cone

(A) The attractive cue evokes the Ca^{2+} release from the endoplasmic reticulum (ER) which behaves as attractive Ca^{2+} signal and somehow leads to the increase in net exocytosis of the growth cone region facing the cue. This asymmetric insertion of membrane components results in the turning of growth cone towards the source of the cue. (B) On the other hand, the repulsive cue evokes the Ca^{2+} release form the plasmamembrane channels which behaves as repulsive Ca^{2+} signal and leads to the increase in net endocytosis at the growth cone region facing the source of cue. This asymmetric removal of membrane components results in the turning of growth cone away from the source of the cue. The black arrows indicate the direction of the growth cone turning. The red arrow indicates the movement of the vesicles. Reprinted with permission from Elsevier: Neuroscience Research, Vol. 73, pp 269-274, 'Intracellular signaling and membrane trafficking control bidirectional growth cone guidance', Takuro Tojima, © 2012

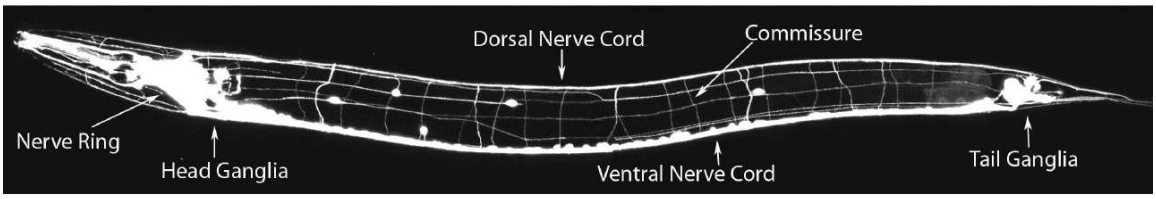

Figure 1.9 The *C. elegans* nervous system

Image showing the whole nervous system of *C. elegans* labelled by Pan-neuronal GFP. Lateral view, anterior to left. Major regions of the nervous system are also indicated. Reprinted with permission from Dr. Harald Hutter

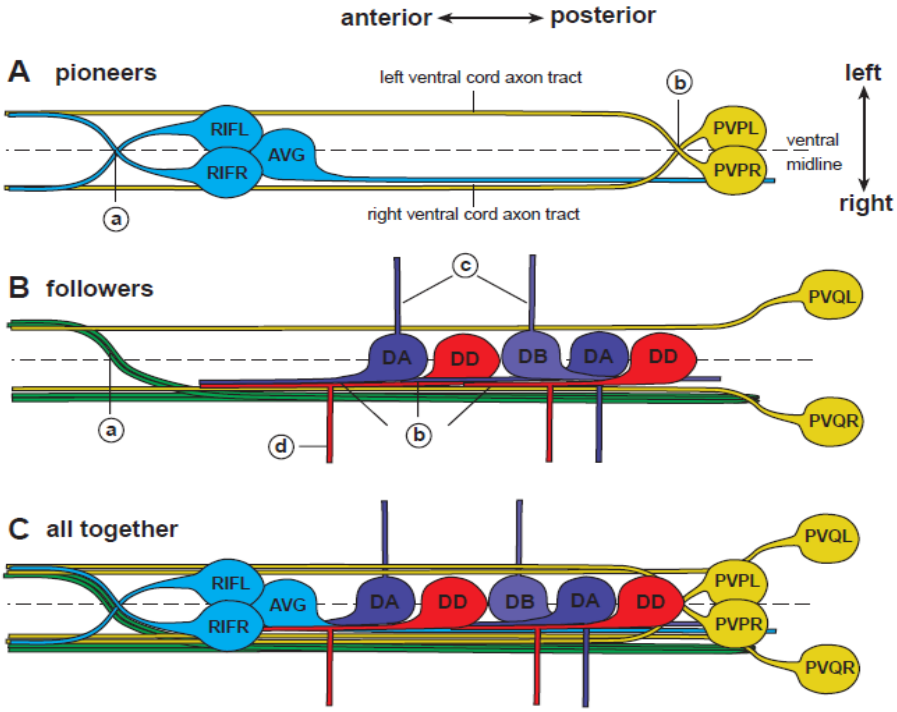

Figure 1.10 Development of the *C. elegans* ventral nerve cord

(A-C) Trajectories of different axons in the ventral nerve cord. (A) Showing pioneers only except PVPL. AVG cell body is present in the RVG at the anterior side and extends the axon into the right axon tract. The PVPR neuron extends an axon which crosses (b) from right side and joins the left axon tract from the posterior side. The PVPL axon crosses (b) from the left side and extends into the right axon tract. The RIF neuron cell bodies which are also present in the RVG extend axons which cross (a) and pioneer the path towards the nerve ring. (B) Showing followers only. The interneurons (green) initially exit the nerve ring in two fascicles, immediately after the exit the left side fascicle crosses (a) and both fascicles follow the AVG pioneer in the right axon tract. The DD motor neurons extend a process into the right axon tract (b) which branches and sends out a commissure (d) on the right side towards the dorsal side. DA/DB motor neurons extend a commissure (c) directly from the cell body on both right and left side towards the dorsal side and a denrite into the right axon tract. PVQR extends an axon into the right axon tract whereas PVQL extends an axon into the left axon tract. (C) Overlay of (A) and (B). Reprinted with permission from Development: Vol. 130, pp 5307-18, 'Extracellular cues and pioneers act together to guide axons in the ventral cord of *C. elegans'*, Harald Hutter, © 2003

1.12. References

Ackley, B.D., Kang, S.H., Crew, J.R., Suh, C., Jin, Y., Kramer, J.M., 2003. The basement membrane components nidogen and type XVIII collagen regulate organization of neuromuscular junctions in *Caenorhabditis elegans*. J. Neurosci. 23, 3577–3587.

Arikawa-Hirasawa, E., Watanabe, H., Takami, H., Hassell, J.R., Yamada, Y., 1999. Perlecan is essential for cartilage and cephalic development. Nat. Genet. 23, 354–358.

Augsburger, A., Schuchardt, A., Hoskins, S., Dodd, J., Butler, S., 1999. Bmps as mediators of roof plate repulsion of commissural neurons. Neuron 24, 127–141.

Aumailley, M., Bruckner-Tuderman, L., Carter, W.G., Deutzmann, R., Edgar, D., Ekblom, P., Engel, J., Engvall, E., Hohenester, E., Jones, J.C.R., Kleinman, H.K., Marinkovich, M.P., Martin, G.R., Mayer, U., Meneguzzi, G., Miner, J.H., Miyazaki, K., Patarroyo, M., Paulsson, M., Quaranta, V., Sanes, J.R., Sasaki, T., Sekiguchi, K., Sorokin, L.M., Talts, J.F., Tryggvason, K., Uitto, J., Virtanen, I., Von Der Mark, K., Wewer, U.M., Yamada, Y., Yurchenco, P.D., 2005. A simplified laminin nomenclature. Matrix Biol. 24, 326–332.

Aurelio, O., Hall, D.H., Hobert, O., 2002. Immunoglobulin-domain proteins required for maintenance of ventral nerve cord organization. Science 295, 686–690.

Bao, H., Berlanga, M.L., Xue, M., Hapip, S.M., Daniels, R.W., Mendenhall, J.M., Alcantara, A. a., Zhang, B., 2007. The atypical cadherin flamingo regulates synaptogenesis and helps prevent axonal and synaptic degeneration in Drosophila. Mol. Cell. Neurosci. 34, 662–678.

Bashaw, G.J., Kidd, T., Murray, D., Pawson, T., Goodman, C.S., 2000. Repulsive axon guidance: Abelson and Enabled play opposing roles downstream of the roundabout receptor. Cell 101, 703–715.

Bashaw, G.J., Klein, R., 2010. Signaling from axon guidance receptors. Cold Spring Harb. Perspect. Biol. 2, 1–16.

Bate, C.M., 1976. Pioneer neurons in an insect embryo. Nature 260, 54-56.

Baum, P.D., Garriga, G., 1997. Neuronal migrations and axon fasciculation are disrupted in ina-1 integrin mutants. Neuron 19, 51–62.

Boulin, T., Pocock, R. & Hobert, O., 2006. A Novel Eph Receptor-Interacting IgSF Protein Provides *C. elegans* Motoneurons with Midline Guidepost Function. *Current Biology*, 16(19), pp.1871–1883.

Boyle, M., Nighorn, A., Thomas, J.B., 2006. *Drosophila* Eph receptor guides specific axon branches of mushroom body neurons. Development 133, 1845–1854.

Brenner, S., 1974. The genetics of *Caenorhabditis elegans*. *Genetics*, 77(1), pp.71–94.

Broadbent, I.D., Pettitt, J., 2002. The *C. elegans hmr-1* gene can encode a neuronal classic cadherin involved in the regulation of axon fasciculation. Curr. Biol. 12, 59–63.

Brose, K., Bland, K.S., Wang, K.H., Arnott, D., Henzel, W., Goodman, C.S., Tessier-Lavigne, M., Kidd, T., 1999. Slit proteins bind Robo receptors and have an evolutionarily conserved role in repulsive axon guidance. Cell 96, 795–806.

Brückner, K., Pasquale, E.B., Klein, R., 1997. Tyrosine phosphorylation of transmembrane ligands for Eph receptors. Science 275, 1640–1643.

Brugnera, E., Haney, L., Grimsley, C., Lu, M., Walk, S.F., Tosello-Trampont, A.-C., Macara, I.G., Madhani, H., Fink, G.R., Ravichandran, K.S., 2002. Unconventional Rac-GEF activity is mediated through the Dock180-ELMO complex. Nat. Cell Biol. 4, 574–582.

Brummendorf, T., Rathjen, F.G., 1998. Molecular interactions involving immunoglobulin superfamily adhesion molecules. In Ig Superfamily Molecules in the Nervous System Edited by: Sonderegger P. Amsterdam: Harwood academic publishers, 23-56.

Buhusi, M., Schlatter, M.C., Demyanenko, G.P., Thresher, R., Maness, P.F., 2008. L1 interaction with ankyrin regulates mediolateral topography in the retinocollicular projection. J. Neurosci. 28, 177–188.

Bürglin, T.R., Kuwabara, P.E., 2006. Homologs of the Hh signalling network in *C. elegans*. WormBook 1–14.

Butler, S.J., Dodd, J., 2003. A role for BMP heterodimers in roof plate-mediated repulsion of commissural axons. Neuron 38, 389–401.

Cadigan, K.M., Nusse, R., 1997. Wnt signalling: a common theme in animal development. Genes Dev. 11, 3286–3305.

Cajal S. R. Y. (1890) A quelle epoque apparaissent les expansions des cellules nerveuses de la moelle epiniere du poulet. Anat Anz 5: 609-613,631-639.

Chalfie, M., Sulston, J.E., White, J.G., Southgate, E., Thomson, J.N., Brenner, S., 1985. The neural circuit for touch sensitivity in *Caenorhabditis elegans*. J. Neurosci. 5, 956–964.

Chan, S.S.Y., Zheng, H., Su, M.W., Wilk, R., Killeen, M.T., Hedgecock, E.M., Culotti, J.G., 1996. UNC-40, a *C. elegans* homolog of DCC (Deleted in Colorectal Cancer), is required in motile cells responding to UNC-6 netrin cues. Cell 87, 187–195.

Chang, C., Adler, C.E., Krause, M., Clark, S.G., Gertler, F.B., Tessier-Lavigne, M., Bargmann, C.I., 2006. MIG-10/Lamellipodin and AGE-1/PI3K Promote Axon Guidance and Outgrowth in Response to Slit and Netrin. Curr. Biol. 16, 854–862.

Chao, D.L., Shen, K., 2008. Functional dissection of SYG-1 and SYG-2, cell adhesion molecules required for selective synaptogenesis in *C. elegans*. Mol. Cell. Neurosci. 39, 248–257.

Charron, F., Stein, E., Jeong, J., McMahon, A.P., Tessier-Lavigne, M., 2003. The morphogen sonic hedgehog is an axonal chemoattractant that collaborates with Netrin-1 in midline axon guidance. Cell 113, 11–23.

Chen, P.L., Clandinin, T.R., 2008. The Cadherin Flamingo Mediates Level-Dependent Interactions that Guide Photoreceptor Target Choice in Drosophila. Neuron 58, 26–33.

Chen, Z., Gore, B.B., Long, H., Ma, L., Tessier-Lavigne, M., 2008. Alternative Splicing of the Robo3 Axon Guidance Receptor Governs the Midline Switch from Attraction to Repulsion. Neuron 58, 325–332.

Cheng, H.J., Nakamoto, M., Bergemann, a D., Flanagan, J.G., 1995. Complementary gradients in expression and binding of ELF-1 and Mek4 in development of the topographic retinotectal projection map. Cell 82, 371–381.

Cheng, H.J., Bagri, A., Yaron, A., Stein, E., Pleasure, S.J., Tessier-Lavigne, M., 2001. Plexin-A3 mediates semaphorin signaling and regulates the development of hippocampal axonal projections. Neuron 32, 249–263.

Chin-Sang, I.D., George, S.E., Ding, M., Moseley, S.L., Lynch, a S., Chisholm, a D., 1999. The ephrin VAB-2/EFN-1 functions in neuronal signaling to regulate epidermal morphogenesis in *C. elegans*. Cell 99, 781–790.

Chitnis, a. B., Kuwada, J.Y., 1991. Elimination of a brain tract increases errors in pathfinding by follower growth cones in the zebrafish embryo. Neuron 7, 277–285.

Cohen, N.R., Taylor, J.S., Scott, L.B., Guillery, R.W., Soriano, P., Furley, a J., 1998. Errors in corticospinal axon guidance in mice lacking the neural cell adhesion molecule L1. Curr. Biol. 8, 26–33.

Colavita, a, Culotti, J.G., 1998. Suppressors of ectopic UNC-5 growth cone steering identify eight genes involved in axon guidance in *Caenorhabditis elegans*. Dev. Biol. 194, 72–85.

Colavita, a, Krishna, S., Zheng, H., Padgett, R.W., Culotti, J.G., 1998. Pioneer axon guidance by UNC-129, a *C. elegans* TGF-beta. Science 281, 706–709.

Cornel, E. & Holt, C., 1992. Precocious pathfinding: Retinal axons can navigate in an axonless brain. *Neuron*, 9(6), pp.1001–1011.

Costell, M., Gustafsson, E., Aszódi, A., Mörgelin, M., Bloch, W., Hunziker, E., Addicks, K., Timpl, R., Fässler, R., 1999. Perlecan maintains the integrity of cartilage and some basement membranes. J. Cell Biol. 147, 1109–1122.

Côté, J.-F., Vuori, K., 2002. Identification of an evolutionarily conserved superfamily of DOCK180-related proteins with guanine nucleotide exchange activity. J. Cell Sci. 115, 4901–4913.

Cotrufo, T., Perez-Branguli, F., Muhaisen, a., Ros, O., Andres, R., Baeriswyl, T., Fuschini, G., Tarrago, T., Pascual, M., Urena, J., Blasi, J., Giralt, E., Stoeckli, E.T., Soriano, E., 2011. A Signaling Mechanism Coupling Netrin-1/Deleted in Colorectal Cancer Chemoattraction to SNARE-Mediated Exocytosis in Axonal Growth Cones. J. Neurosci. 31, 14463–14480.

Cotrufo, T., Andrés, R.M., Ros, O., Pérez-Brangulí, F., Muhaisen, A., Fuschini, G., Martínez, R., Pascual, M., Comella, J.X., Soriano, E., 2012. Syntaxin 1 is required for DCC/Netrin-1-dependent chemoattraction of migrating neurons from the lower rhombic lip. Eur. J. Neurosci. 36, 3152–3164.

Cremer, H., Lange, R., Christoph, a, Plomann, M., Vopper, G., Roes, J., Brown, R., Baldwin, S., Kraemer, P., Scheff, S., 1994. Inactivation of the N-CAM gene in mice results in size reduction of the olfactory bulb and deficits in spatial learning. Nature 367, 455–459.

Cremer, H., Chazal, G., Goridis, C., Represa, A. 1997. NCAM Is Essential for Axonal Growth and Fasciculation in the Hippocampus. *Molecular and Neuroscience*, 8 pp.323–335.

Demyanenko, G.P., Tsai, a Y., Maness, P.F., 1999. Abnormalities in neuronal process extension, hippocampal development, and the ventricular system of L1 knockout mice. J. Neurosci. 19, 4907–4920.

Desai, C., Garriga, G., McIntire, S.L., Horvitz, H.R., 1988. A genetic pathway for the development of the *Caenorhabditis elegans* HSN motor neurons. Nature 336, 638–646.

Dickson, B.J., 2002. Molecular mechanisms of axon guidance. Science 298, 1959–1964.

Domanitskaya, E., Wacker, A., Mauti, O., Baeriswyl, T., Esteve, P., Bovolenta, P., Stoeckli, E.T., 2010. Sonic hedgehog guides post-crossing commissural axons both directly and indirectly by regulating Wnt activity. J. Neurosci. 30, 11167–11176.

Dong, L., Chen, Y., Lewis, M., Hsieh, J.-C., Reing, J., Chaillet, J.R., Howell, C.Y., Melhem, M., Inoue, S., Kuszak, J.R., DeGeest, K., Chung, A.E., 2002. Neurologic defects and selective disruption of basement membranes in mice lacking *entactin-1/nidogen-1*. Lab. Invest. 82, 1617–1630.

Drescher, U., Kremoser, C., Handwerker, C., Löschinger, J., Noda, M., Bonhoeffer, F., 1995. In vitro guidance of retinal ganglion cell axons by RAGS, a 25 kDa tectal protein related to ligands for Eph receptor tyrosine kinases. Cell 82, 359–370.

Durbin, R.M., 1987. Studies on the Development and Organisation of the Nervous System of *Caenorhabditis elegans*. Ph.D.dissertation,University of Cambridge, England.

Edwards, S., 1981. Cercal sensory development following laser microlesions of embryonic apical cells in Acheta domesticus. J Neurosci. 1 (3), pp. 250-8.

Engle, E.C., 2010. Human genetic disorders of axon guidance. Cold Spring Harb. Perspect. Biol. 2, 1–18.

Fox, J.W., Mayer, U., Nischt, R., Aumailley, M., Reinhardt, D., Wiedemann, H., Mann, K., Timpl, R., Krieg, T., Engel, J., 1991. Recombinant nidogen consists of three globular domains and mediates binding of laminin to collagen type IV. EMBO J. 10, 3137–3146.

Fredette, B.J., Ranscht, B., 1994. T-cadherin expression delineates specific regions of the developing motor axon-hindlimb projection pathway. J. Neurosci. 14, 7331–7346.

Fujii, T., Nakao, F., Shibata, Y., Shioi, G., Kodama, E., Fujisawa, H., Takagi, S., 2002. *Caenorhabditis elegans* PlexinA, PLX-1, interacts with transmembrane semaphorins and regulates epidermal morphogenesis. Development 129, 2053–2063.

Fujisawa, K., Jeffrey, L. W., Culotti, J. G. 2007. The Slit Receptor EVA-1 Coactivates a SAX-3/Robo–Mediated Guidance Signal in *C. elegans*. *Science*, 317(5846) 1934-1938.

Gale, N.W., Holland, S.J., Valenzuela, D.M., Flenniken, A., Pan, L., Ryan, T.E., Henkemeyer, M., Strebhardt, K., Hirai, H., Wilkinson, D.G., Pawson, T., Davis, S., Yancopoulos, G.D., 1996. Eph receptors and ligands comprise two major specificity subclasses and are reciprocally compartmentalized during embryogenesis. Neuron 17, 9–19.

Gao, F.B., Brenman, J.E., Jan, L.Y., Jan, Y.N., 1999. Genes regulating dendritic outgrowth, branching, and routing in *Drosophila*. Genes Dev. 13, 2549–2561.

Gao, F.B., Kohwi, M., Brenman, J.E., Jan, L.Y., Jan, Y.N., 2000. Control of dendritic field formation in *Drosophila*: the roles of flamingo and competition between homologous neurons. Neuron 28, 91–101.

Garriga, G., Guenther, C., Horvitz, H.R., 1993. Migrations of the *Caenorhabditis elegans* HSNs are regulated by egl-43, a gene encoding two zinc finger proteins. Genes Dev. 7, 2097–2109.

George, S.E., Simokat, K., Hardin, J., Chisholm, A.D., 1998. The VAB-1 Eph receptor tyrosine kinase functions in neural and epithelial morphogenesis in *C. elegans*. Cell 92, 633–643.

Gersdorff, N., Otto, S., Roediger, M., Kruegel, J., Miosge, N., 2007. The absence of one or both nidogens dose not alter basement membrane composition in adult murine kidney. Histol. Histopathol. 22, 1077–1084.

Ginzburg, V.E., Roy, P.J., Culotti, J.G., 2002. Semaphorin 1a and semaphorin 1b are required for correct epidermal cell positioning and adhesion during morphogenesis in *C. elegans*. Development 129, 2065–2078.

Gitai, Z., Yu, T.W., Lundquist, E. a., Tessier-Lavigne, M., Bargmann, C.I., 2003. The netrin receptor UNC-40/DCC stimulates axon attraction and outgrowth through enabled and, in parallel, Rac and UNC-115/abLIM. Neuron 37, 53–65.

Gleason, J.E., Eisenmann, D.M., 2010. Wnt signaling controls the stem cell-like asymmetric division of the epithelial seam cells during *C. elegans* larval development. Dev. Biol. 348, 58–66.

Gleason, J.E., Szyleyko, E. a., Eisenmann, D.M., 2006. Multiple redundant Wnt signaling components function in two processes during *C. elegans* vulval development. Dev. Biol. 298, 442–457.

Golbik, R., Eble, J. a, Ries, a, Kühn, K., 2000. The spatial orientation of the essential amino acid residues arginine and aspartate within the alpha1beta1 integrin recognition site of collagen IV has been resolved using fluorescence resonance energy transfer. J. Mol. Biol. 297, 501–509.

Goldstein, B., Takeshita, H., Mizumoto, K., Sawa, H., 2006. Wnt signals can function as positional cues in establishing cell polarity. Dev. Cell 10, 391–396.

Gomez, T.M., Letourneau, P.C., 2014. Actin dynamics in growth cone motility and navigation. J. Neurochem. 129, 221–234.

Graham, P.L., Johnson, J.J., Wang, S., Sibley, M.H., Gupta, M.C., Kramer, J.M., 1997. Type IV Collagen Is Detectable in Most, but Not All, Basement Membranes of 137, 1171–1183.

Green, J.L., Inoue, T., Sternberg, P.W., 2008. Opposing Wnt Pathways Orient Cell Polarity during Organogenesis. Cell 134, 646–656.

Guo, X. D., & Kramers, J. M., 1989. The two *Caenorhabditis elegans* basement membrane (Type IV) collagen genes are located on separate chromosomes. J Biol Chem. 264(29), pp.17574–17582.

Hall, A. & Lalli, G., 2010. Rho and Ras GTPases in Axon Growth, Guidance, and Branching. *Cold Spring Harb Perspect Biol*, pp.1–18.

Hao, J.C., Yu, T.W., Fujisawa, K., Culotti, J.G., Gengyo-Ando, K., Mitani, S., Moulder, G., Barstead, R., Tessier-Lavigne, M., Bargmann, C.I., 2001. *C. elegans* slit acts in midline, dorsal-ventral, and anterior-posterior guidance via the SAX-3/Robo receptor. Neuron 32, 25–38.

Harpaz, Y. & Chothia, C., 1994. Many of the immunoglobulin superfamily domains in cell adhesion molecules and surface receptors belong to a new structural set which is close to that containing variable domains. *Journal of molecular biology*, 238(4), pp.528–539.

Harris, J., Honigberg, L., Robinson, N., Kenyon, C., 1996. Neuronal cell migration in *C. elegans*: regulation of Hox gene expression and cell position. Development 122, 3117–3131.

Harris, R., Sabatelli, L.M., Seeger, M. A., 1996. Guidance cues at the *Drosophila* CNS midline: Identification and characterization of two *Drosophila* Netrin/UNC-6 homologs. Neuron 17, 217–228.

Harterink, M., Kim, D.H., Middelkoop, T.C., Doan, T.D., van Oudenaarden, A., Korswagen, H.C., 2011. Neuroblast migration along the anteroposterior axis of *C. elegans* is controlled by opposing gradients of Wnts and a secreted Frizzled-related protein. Development 138, 2915–2924.

Hattori, D., Chen, Y., Matthews, B.J., Salwinski, L., Sabatti, C., Grueber, W.B., Zipursky, S.L., 2009. Robust discrimination between self and non-self neurites requires thousands of Dscam1 isoforms. Nature 461, 644–648.

Hattori, D., Demir, E., Kim, H.W., Viragh, E., Zipursky, S.L., Dickson, B.J., 2007. Dscam diversity is essential for neuronal wiring and self-recognition. Nature 449, 223–227.

He, Z., Tessier-Lavigne, M., 1997. Neuropilin is a receptor for the axonal chemorepellent semaphorin III. Cell 90, 739–751.

Hedgecock, E.M., Culotti, J.G., Hall, D.H., 1990. The *unc-5*, *unc-6*, and *unc-40* genes guide circumferential migrations of pioneer axons and mesodermal cells on the epidermis in *C. elegans*. Neuron 4, 61–85.

Hidalgo, A., Brand, A. H., 1997. Targeted neuronal ablation: the role of pioneer neurons in guidance and fasciculation in the CNS of *Drosophila*. Development 124, 3253–3262.

Hilliard, M. A., Bargmann, C.I., 2006. Wnt signals and Frizzled activity orient anterior-posterior axon outgrowth in *C. elegans*. Dev. Cell 10, 379–390.

Hines, J.H., Abu-Rub, M., Henley, J.R., 2010. Asymmetric endocytosis and remodeling of beta1-integrin adhesions during growth cone chemorepulsion by MAG. Nat. Neurosci. 13, 829–837.

Ho, M.S.P., Böse, K., Mokkapati, S., Nischt, R., Smyth, N., 2008. Nidogens-extracellular matrix linker molecules. Microsc. Res. Tech. 71, 387–395.

Holland, S.J., Nicholas, W.G., Mbamalu, G., Yancopoulos, M.H., Henkemeyer, M., Tony, Pawson., 1996. Bidirectional signalling through the EPH-family receptor Nuk and its transmembrane ligands. Nature 383, 722-725.

Hong, K., Nishiyama, M., Henley, J., Tessier-Lavigne, M., Poo, M., 2000. Calcium signalling in the guidance of nerve growth by netrin-1. Nature 403, 93–98.

Hu, H., Li, M., Labrador, J. P., McEwen, J., Lai, E.C., Goodman, C.S., Bashaw, G.J., 2005. Cross GTPase-activating protein (CrossGAP)/Vilse links the Roundabout receptor to Rac to regulate midline repulsion. Proc. Natl. Acad. Sci. U. S. A. 102, 4613–4618.

Hughes, M.E., Bortnick, R., Tsubouchi, A., Bäumer, P., Kondo, M., Uemura, T., Schmucker, D., 2007. Homophilic Dscam Interactions Control Complex Dendrite Morphogenesis. Neuron 54, 417–427.

Hummel, T., Zipursky, S.L., 2004. Afferent induction of olfactory glomeruli requires N-cadherin. Neuron 42, 77–88.

Hutter, H., 2003. Extracellular cues and pioneers act together to guide axons in the ventral cord of *C. elegans*. *Development*, 130(22), pp.5307–5318.

Igarashi, M., Tagaya, M., Komiya, Y., 1997. The soluble N-ethylmaleimide-sensitive factor attached protein receptor complex in growth cones: molecular aspects of the axon terminal development. J. Neurosci. 17, 1460–1470.

Isbister, C.M., Tsai, A., Wong, S.T., Kolodkin, a L., O'Connor, T.P., 1999. Discrete roles for secreted and transmembrane semaphorins in neuronal growth cone guidance in vivo. Development 126, 2007–2019.

Ishii, N., Wadsworth, W.G., Stern, B.D., Culotti, J.G., Hedgecock, E.M., 1992. UNC-6, a laminin-related protein, guides cell and pioneer axon migrations in *C. elegans*. Neuron 9, 873–881.

Iwai, Y., Usui, T., Hirano, S., Steward, R., Takeichi, M., Uemura, T., 1997. Axon patterning requires DN-cadherin, a novel neuronal adhesion receptor, in the *Drosophila* embryonic CNS. Neuron 19, 77–89.

Jen, J.C., Chan, W.-M., Bosley, T.M., Wan, J., Carr, J.R., Rüb, U., Shattuck, D., Salamon, G., Kudo, L.C., Ou, J., Lin, D.D.M., Salih, M. a M., Kansu, T., Al Dhalaan, H., Al Zayed, Z., MacDonald, D.B., Stigsby, B., Plaitakis, A., Dretakis, E.K., Gottlob, I., Pieh, C., Traboulsi, E.I., Wang, Q., Wang, L., Andrews, C., Yamada, K., Demer, J.L., Karim, S., Alger, J.R., Geschwind, D.H., Deller, T., Sicotte, N.L., Nelson, S.F., Baloh, R.W., Engle, E.C., 2004. Mutations in a human ROBO gene disrupt hindbrain axon pathway crossing and morphogenesis. Science 304, 1509–1513.

Kaibuchi, K., Kuroda, S. & Amano, M. 1999. Regulation of the cytoskeleton and cell adhesion by the Rho family GTPases in mammalian cells. *Annual review of biochemistry*, 68 pp.459–486.

Kamnasaran, D., 2005. Agenesis of the corpus callosum: lessons from humans and mice. Clin. Invest. Med. 28, 267–282.

Kang, S.H., Kramer, J.M., 2000. Nidogen is nonessential and not required for normal type IV collagen localization in *Caenorhabditis elegans*. Mol. Biol. Cell 11, 3911–3923.

Karner, C., Wharton, K. a., Carroll, T.J., 2006. Planar cell polarity and vertebrate organogenesis. Semin. Cell Dev. Biol. 17, 194–203.

Kasai, H., Takahashi, N., Tokumaru, H., 2012. Distinct Initial SNARE Configurations Underlying the Diversity of Exocytosis. Physiol. Rev. 92, 1915–1964.

Keino-Masu, K., Masu, M., Hinck, L., Leonardo, E.D., Chan, S.S.Y., Culotti, J.G., Tessier-Lavigne, M., 1996. Deleted in Colorectal Cancer (DCC) encodes a netrin receptor. Cell 87, 175–185.

Keleman, K., Rajagopalan, S., Cleppien, D., Teis, D., Paiha, K., Huber, L. a., Technau, G.M., Dickson, B.J., 2002. Comm sorts Robo to control axon guidance at the *Drosophila* midline. Cell 110, 415–427.

Keleman, K., Ribeiro, C., Dickson, B.J., 2005. Comm function in commissural axon guidance: cell-autonomous sorting of Robo in vivo. Nat. Neurosci. 8, 156–163.

Kennedy, T.E., Serafini, T., de la Torre, J.R., Tessier-Lavigne, M., 1994. Netrins are diffusible chemotropic factors for commissural axons in the embryonic spinal cord. Cell 78, 425–435.

Kidd, T., Brose, K., Mitchell, K.J., Fetter, R.D., Tessier-Lavigne, M., Goodman, C.S., Tear, G., 1998. Roundabout controls axon crossing of the CNS midline and defines a novel subfamily of evolutionarily conserved guidance receptors. Cell 92, 205–215.

Kim, S., Wadsworth, W.G., 2000. Positioning of longitudinal nerves in *C. elegans* by nidogen. Science 288, 150–154.

Kimura, N., Toyoshima, T., Kojima, T., Shimane, M., 1998. Entactin-2: a new member of basement membrane protein with high homology to entactin/nidogen. Exp. Cell Res. 241, 36–45.

Klose, M., Bentley, D., 1989. Transient pioneer neurons are essential for formation of an embryonic peripheral nerve. Science 245, 982–984.

Kohfeldt, E., Sasaki, T., Göhring, W., Timpl, R., 1998. Nidogen-2: a new basement membrane protein with diverse binding properties. J. Mol. Biol. 282, 99–109.

Kolodkin, a L., Matthes, D.J., O'Connor, T.P., Patel, N.H., Admon, a, Bentley, D., Goodman, C.S., 1992. Fasciclin IV: sequence, expression, and function during growth cone guidance in the grasshopper embryo. Neuron 9, 831–845.

Kolodkin, A.L., 1996. Semaphorins: mediators of repulsive growth cone guidance. Trends Cell Biol. 6, 15–22.

Kolodkin, A.L., Levengood, D. V., Rowe, E.G., Tai, Y.T., Giger, R.J., Ginty, D.D., 1997. Neuropilin is a semaphorin III receptor. Cell 90, 753–762.

Kolodziej, P. a., Timpe, L.C., Mitchell, K.J., Fried, S.R., Goodman, C.S., Jan, L.Y., Jan, Y.N., 1996. frazzled Encodes a *Drosophila* member of the DCC immunoglobulin subfamily and is required for CNS and motor axon guidance. Cell 87, 197–204.

Kolpak, A.L., Jiang, J., Guo, D., Standley, C., Bellve, K., Fogarty, K., Bao, Z.-Z., 2009. Negative guidance factor-induced macropinocytosis in the growth cone plays a critical role in repulsive axon turning. J. Neurosci. 29, 10488–10498.

Kramer, J.M., 2005. Basement membranes. WormBook 1–15.

Krause, M., Leslie, J.D., Stewart, M., Lafuente, E.M., Valderrama, F., Jagannathan, R., Strasser, G. a., Rubinson, D. a., Liu, H., Way, M., Yaffe, M.B., Boussiotis, V. a., Gertler, F.B., 2004. Lamellipodin, an Ena/VASP ligand, is implicated in the regulation of lamellipodial Dynamics. Developmental Cell 7, 571–583.

Kruger, R.P., Aurandt, J., Guan, K. L., 2005. Semaphorins command cells to move. Nat. Rev. Mol. Cell Biol. 6, 789–800.

Kuwada, J.Y., 1986. Cell recognition by neuronal growth cones in a simple vertebrate embryo. Sciecne, 233(4765), pp.740–746.

Kühn, K., 1995. Basement membrane (type IV) collagen. *Matrix biology : journal of the International Society for Matrix Biology*, 14(6), pp.439–445.

Lai Wing Sun, K., Correia, J.P., Kennedy, T.E., 2011. Netrins: versatile extracellular cues with diverse functions. Development 138, 2153–2169.

Lee, H.K., Seo, I.A., Park, H.K., Park, Y.M., Ahn, K.J., Yoo, Y.H., Park, H.T., 2007. Nidogen is a prosurvival and promigratory factor for adult Schwann cells. J. Neurochem. 102, 686–698.

Leung-Hagesteijn, C., Spence, A. M., Stern, B.D., Zhou, Y., Su, M.W., Hedgecock, E.M., Culotti, J.G., 1992. UNC-5, a transmembrane protein with immunoglobulin and thrombospondin type 1 domains, guides cell and pioneer axon migrations in *C. elegans*. Cell 71, 289–299.

Levy-Strumpf, N., Culotti, J.G., 2007. VAB-8, UNC-73 and MIG-2 regulate axon polarity and cell migration functions of UNC-40 in *C. elegans*. Nat. Neurosci. 10, 161–168.

Li, L., Hutchins, B.I., Kalil, K., 2010. Wnt5a induces simultaneous cortical axon outgrowth and repulsive turning through distinct signaling mechanisms. Sci. Signal. 3, pt2.

Liu, G., Dwyer, T., 2014. Microtubule dynamics in axon guidance. Neurosci. Bull. 30, 569–583.

Liu, Y., Shi, J., Lu, C.-C., Wang, Z.-B., Lyuksyutova, A.I., Song, X.-J., Zou, Y., 2005. Ryk-mediated Wnt repulsion regulates posterior-directed growth of corticospinal tract. Nat. Neurosci. 8, 1151–1159.

Long, H., Sabatier, C., Ma, L., Plump, A., Yuan, W., Ornitz, D.M., Tamada, A., Murakami, F., Goodman, C.S., Tessier-Lavigne, M., 2004. Conserved roles for Slit and Robo proteins in midline commissural axon guidance. Neuron 42, 213–223.

Lowery, L.A., Van Vactor, D., 2009. The trip of the tip: understanding the growth cone machinery. Nat. Rev. Mol. Cell Biol. 10, 332–343.

Lundquist, E. a, Herman, R.K., Shaw, J.E., Bargmann, C.I., 1998. UNC-115, a conserved protein with predicted LIM and actin-binding domains, mediates axon guidance in *C. elegans*. Neuron 21, 385–392.

Lundquist, E. a, Reddien, P.W., Hartwieg, E., Horvitz, H.R., Bargmann, C.I., 2001. Three *C. elegans* Rac proteins and several alternative Rac regulators control axon guidance, cell migration and apoptotic cell phagocytosis. Development 128, 4475–4488.

Luo, Y., Raible, D., Raper, J. a, 1993. Collapsin: a protein in brain that induces the collapse and paralysis of neuronal growth cones. Cell 75, 217–227.

Lyuksyutova, A.I., Lu, C.-C., Milanesio, N., King, L. a, Guo, N., Wang, Y., Nathans, J., Tessier-Lavigne, M., Zou, Y., 2003. Anterior-posterior guidance of commissural axons by Wnt-frizzled signaling. Science 302, 1984–1988.

MacNeil, L.T., Hardy, W.R., Pawson, T., Wrana, J.L., Culotti, J.G., 2009. UNC-129 regulates the balance between UNC-40 dependent and independent UNC-5 signaling pathways. Nat. Neurosci. 12, 150–155.

Maloof, J.N., Whangbo, J., Harris, J.M., Jongeward, G.D., Kenyon, C., 1999. A Wnt signaling pathway controls hox gene expression and neuroblast migration in *C. elegans*. Development 126, 37–49.

Maness, P.F., Schachner, M., 2007. Neural recognition molecules of the immunoglobulin superfamily: signaling transducers of axon guidance and neuronal migration. Nat. Neurosci. 10, 19–26.

Marsh, L., Letourneau, P.C., 1984. Growth of neurites without filopodial or lamellipodial activity in the presence of cytochalasin B. J. Cell Biol. 99, 2041–2047.

Mayer, U., Timpl, R., 1994. Nidogen, a versatile binding protein of basement membranes. In Extracellular Matrix Assembly and Structure (Yurchenco, P. D., Birk, D. & Mecham, R. P., eds), pp. 389-416,Academic Press, Orlando, FL.

Masai, I., Lele, Z., Yamaguchi, M., Komori, A., Nakata, A., Nishiwaki, Y., Wada, H., Tanaka, H., Nojima, Y., Hammerschmidt, M., Wilson, S.W., Okamoto, H., 2003. N-cadherin mediates retinal lamination, maintenance of forebrain compartments and patterning of retinal neurites. Development 130, 2479–2494.

McConnell, S.K., Ghosh, a, Shatz, C.J., 1989. Subplate neurons pioneer the first axon pathway from the cerebral cortex. Science 245, 978–982.

Mitchell, K.J., Doyle L., J.L., Serafini, T., Kennedy, T.E., Tessier-Lavigne, M., Goodman, C.S., Dickson, B.J., 1996. Genetic analysis of Netrin genes in *Drosophila*: Netrins guide CNS commissural axons and peripheral motor axons. Neuron 17, 203–215.

Mohamed, A.M., Chin-Sang, I.D., 2006. Characterization of loss-of-function and gain-of-function Eph receptor tyrosine kinase signaling in *C. elegans* axon targeting and cell migration. Dev. Biol. 290, 164–176.

Montag-Sallaz, M., Schachner, M., Montag, D., 2002. Misguided axonal projections, neural cell adhesion molecule 180 mRNA upregulation, and altered behavior in mice deficient for the close homolog of L1. Mol. Cell. Biol. 22, 7967–7981.

Movshon, J. a, Nundy, S. & Crowley, J.C., 2003. Cyclic AMP/GMP-dependent modulation of Ca 21 channels sets the polarity of nerve growth-cone turning. *Nature*, 423(6943), pp.990–995.

Murshed, M., Smyth, N., Miosge, N., Karolat, J., Krieg, T., Paulsson, M., Nischt, R., 2000. The absence of nidogen 1 does not affect murine basement membrane formation. Mol. Cell. Biol. 20, 7007–7012.

Myllyharju, J., Kivirikko, K.I., 2001. Collagens and collagen-related diseases. Ann. Med. 33, 7–21.

Newsome, T.P., Schmidt, S., Dietzl, G., Keleman, K., Asling, B., Debant, a, Dickson, B.J., 2000. Trio combines with dock to regulate Pak activity during photoreceptor axon pathfinding in *Drosophila*. Cell 101, 283–294.

Ng, J., Luo, L., 2004. Rho GTPases regulate axon growth through convergent and divergent signaling pathways. Neuron 44, 779–793.

Nishiuchi, R., Takagi, J., Hayashi, M., Ido, H., Yagi, Y.,Sanzen, N., Tsuji, T., Yamada, M., Sekiguchi, K. 2006. Ligand-binding specificities of laminin-binding integrins: A comprehensive survey of laminin-integrin interactions using recombinant α3β1, α6β1, α7β1 and α6β4 integrins. Matrix Biology, 25(3), pp.189–197.

Nollet, F., Kools, P., van Roy, F., 2000. Phylogenetic analysis of the cadherin superfamily allows identification of six major subfamilies besides several solitary members. J. Mol. Biol. 299, 551–572.

Okada, A., Charron, F., Morin, S., Shin, D.S., Wong, K., Fabre, P.J., Tessier-Lavigne, M., McConnell, S.K., 2006. Boc is a receptor for sonic hedgehog in the guidance of commissural axons. Nature 444, 369–373.

Ooashi, N., Futatsugi, A., Yoshihara, F., Mikoshiba, K., Kamiguchi, H., 2005. Cell adhesion molecules regulate Ca2+-mediated steering of growth cones via cyclic AMP and ryanodine receptor type 3. J. Cell Biol. 170, 1159–1167.

Ozawa, M., Ringwald, M., Kemler, R., 1990. Uvomorulin-catenin complex formation is regulated by a specific domain in the cytoplasmic region of the cell adhesion molecule. Proc. Natl. Acad. Sci. U. S. A. 87, 4246–4250.

Pan, C.L., Howell, J.E., Clark, S.G., Hilliard, M., Cordes, S., Bargmann, C.I., Garriga, G., 2006. Multiple Wnts and Frizzled receptors regulate anteriorly directed cell and growth cone migrations in *Caenorhabditis elegans*. Dev. Cell 10, 367–377.

Parsons, M.J., Campos, I., Hirst, E.M. a, Stemple, D.L., 2002. Removal of dystroglycan causes severe muscular dystrophy in zebrafish embryos. Development 129, 3505–3512.

Paul, L.K., Brown, W.S., Adolphs, R., Tyszka, J.M., Richards, L.J., Mukherjee, P., Sherr, E.H., 2007. Agenesis of the corpus callosum: genetic, developmental and functional aspects of connectivity. Nat. Rev. Neurosci. 8, 287–299.

Pfenninger, K.H., 2009. Plasma membrane expansion: a neuron's Herculean task. Nat. Rev. Neurosci. 10, 251–261.

Pocock, R., Bénard, C.Y., Shapiro, L., Hobert, O., 2008. Functional dissection of the *C. elegans* cell adhesion molecule SAX-7, a homologue of human L1. Mol. Cell. Neurosci. 37, 56–68.

Prakash, S., Caldwell, J.C., Eberl, D.F., Clandinin, T.R., 2005. *Drosophila* N-cadherin mediates an attractive interaction between photoreceptor axons and their targets. Nat. Neurosci. 8, 443–450.

Püschel, A.W., 1996. The semaphorins: a family of axonal guidance molecules? Eur. J. Neurosci. 8, 1317–21.

Qu, C., Dwyer, T., Shao, Q., Yang, T., Huang, H., Liu, G., 2013. Direct binding of TUBB3 with DCC couples netrin-1 signaling to intracellular microtubule dynamics in axon outgrowth and guidance. J. Cell Sci. 126, 3070–81.

Quinn, C.C., Wadsworth, W.G., 2008. Axon guidance: asymmetric signaling orients polarized outgrowth. Trends Cell Biol. 18, 597–603.

Rajagopalan, S., Vivancos, V., Nicolas, E., Dickson, B.J., 2000. Selecting a longitudinal pathway: Robo receptors specify the lateral position of axons in the *Drosophila* CNS. Cell 103, 1033–1045.

Ranscht, B., 2000. Cadherins: Molecular codes for axon guidance and synapse formation. *International Journal of Developmental Neuroscience*, 18(7), pp.643–651.

Raper, J.A., 2000. Semaphorins and their receptors in vertebrates and invertebrates. Curr. Opin. Neurobiol. 10, 88–94.

Reichert, H., Boyan, G., 1997. Building a brain: Developmental insights in insects. Trends Neurosci. 20, 258–264.

Riehl, R., Johnson, K., Bradley, R., Grunwald, G.B., Cornel, E., Lilienbaum, A., Holt, C.E., 1996. Cadherin function is required for axon outgrowth in retinal ganglion cells in vivo. Neuron 17, 837–848.

Rogalski, T.M., Gilchrist, E.J., Mullen, G.P., Moerman, D.G., 1995. Mutations in the *unc-52* gene responsible for body wall muscle defects in adult *Caenorhabditis elegans* are located in alternatively spliced exons. Genetics 139, 159–169.

Rogalski, T.M., Williams, B.D., Mullen, G.P., Moerman, D.G., 1993. Products of the *unc-52* gene in *Caenorhabditis elegans* are homologous to the core protein of the mammalian basement membrane heparan sulfate proteoglycan. Genes Dev. 7, 1471–1484.

Rolf, B., Bastmeyer, M., Schachner, M., Bartsch, U., 2002. Pathfinding errors of corticospinal axons in neural cell adhesion molecule-deficient mice. J. Neurosci. 22, 8357–8362.

Ros, O., Cotrufo, T., Martinez-Marmol, R., Soriano, E., 2015. Regulation of Patterned Dynamics of Local Exocytosis in Growth Cones by Netrin-1. J. Neurosci. 35, 5156–5170.

Rothberg, J.M., Hartley, D. a, Walther, Z., Artavanis-Tsakonas, S., 1988. slit: an EGF-homologous locus of *D. melanogaster* involved in the development of the embryonic central nervous system. Cell 55, 1047–1059.

Rothberg, J.M., Roger Jacobs, J., Goodman, C.S., Artavanis-Tsakonas, S., 1990. Slit: An extracellular protein necessary for development of midline glia and commissural axon pathways contains both EGF and LRR domains. Genes Dev. 4, 2169–2187.

Roy, P.J., Zheng, H., Warren, C.E., Culotti, J.G., 2000. mab-20 encodes Semaphorin-2a and is required to prevent ectopic cell contacts during epidermal morphogenesis in *Caenorhabditis elegans*. Development 127, 755–767.

Rozario, T., DeSimone, D.W., 2010. The extracellular matrix in development and morphogenesis: A dynamic view. Dev. Biol. 341, 126–140.

Sabatier, C., Plump, A.S., Ma, L., Brose, K., Tamada, A., Murakami, F., Lee, E.Y.H.P., Tessier-Lavigne, M., 2004. The divergent robo family protein Rig-1/Robo3 is a negative regulator of slit responsiveness required for midline crossing by commissural axons. Cell 117, 157–169.

Sánchez-Camacho, C., Bovolenta, P., 2009. Emerging mechanisms in morphogen-mediated axon guidance. BioEssays 31, 1013–1025.

Santiago-Medina, M., Gregus, K. a, Gomez, T.M., 2013. PAK-PIX interactions regulate adhesion dynamics and membrane protrusion to control neurite outgrowth. J. Cell Sci. 126, 1122–33.

Sasakura, H., Inada, H., Kuhara, A., Fusaoka, E., Takemoto, D., Takeuchi, K., Mori, I., 2005. Maintenance of neuronal positions in organized ganglia by SAX-7, a *Caenorhabditis elegans* homologue of L1. EMBO J. 24, 1477–1488.

Schmitt, A.M., Shi, J., Wolf, A.M., Lu, C.-C., King, L. a, Zou, Y., 2006. Wnt-Ryk signalling mediates medial-lateral retinotectal topographic mapping. Nature 439, 31–37.

Schmitz, C., Wacker, I., Hutter, H., 2008. The Fat-like cadherin CDH-4 controls axon fasciculation, cell migration and hypodermis and pharynx development in *Caenorhabditis elegans*. Dev. Biol. 316, 249–259.

Schmucker, D., Chen, B., 2009. Dscam and DSCAM: Complex genes in simple animals, complex animals yet simple genes. Genes Dev. 23, 147–156.

Schmucker, D., Clemens, J.C., Shu, H., Worby, C. a, Xiao, J., Muda, M., Dixon, J.E., Zipursky, S.L., 2000. *Drosophila* Dscam is an axon guidance receptor exhibiting extraordinary molecular diversity. Cell 101, 671–684.

Schwarz, V., Pan, J., Voltmer-Irsch, S., Hutter, H., 2009. IgCAMs redundantly control axon navigation in *Caenorhabditis elegans*. Neural Dev. 4, 13.

Schymeinsky, J., Nedbal, S., Miosge, N., Poschl, E., Rao, C., Beier, D.R., Skarnes, W.C., Timpl, R., Bader, B.L., 2002. Gene structure and functional analysis of the mouse *nidogen-2* gene: *nidogen-2* is not essential for basement membrane formation in mice. Mol Cell Biol 22, 6820–6830.

Seeger, M., Tear, G., Ferres-Marco, D., Goodman, C.S., 1993. Mutations affecting growth cone guidance in *Drosophila*: genes necessary for guidance toward or away from the midline. Neuron 10, 409–426.

Serafini, T., Kennedy, T.E., Galko, M.J., Mirzayan, C., Jessell, T.M., Tessier-Lavigne, M., 1994. The netrins define a family of axon outgrowth-promoting proteins homologous to *C. elegans* UNC-6. Cell 78, 409–424.

Shamah, S.M., Lin, M.Z., Goldberg, J.L., Estrach, S., Sahin, M., Hu, L., Bazalakova, M., Neve, R.L., Corfas, G., Debant, A., Greenberg, M.E., 2001. EphA receptors regulate growth cone dynamics through the novel guanine nucleotide exchange factor ephexin. Cell 105, 233–244.

Shen, K., Bargmann, C.I., 2003. The immunoglobulin superfamily protein SYG-1 determines the location of specific synapses in *C. elegans*. Cell 112, 619–630.

Shen, K., Fetter, R.D., Bargmann, C.I., 2004. Synaptic specificity is generated by the synaptic guidepost protein SYG-2 and its receptor, SYG-1. Cell 116, 869–881.

Sibley, M.H., Graham, P.L., von Mende, N., Kramer, J.M., 1994. Mutations in the alpha 2(IV) basement membrane collagen gene of *Caenorhabditis elegans* produce phenotypes of differing severities. EMBO J. 13, 3278–3285.

Sibley, M.H., Johnson, J.J., Mello, C.C., Kramer, J.M., 1993. Genetic identification, sequence, and alternative splicing of the *Caenorhabditis elegans* alpha 2(IV) collagen gene. J. Cell Biol. 123, 255–264.

Simpson, J.H., Bland, K.S., Fetter, R.D., Goodman, C.S., 2000. Short-range and long-range guidance by Slit and its Robo receptors: A combinatorial code of Robo receptors controls lateral position. Cell 103, 1019–1032.

Song, S., Zhang, B., Sun, H., Li, X., Xiang, Y., Liu, Z., Huang, X., Ding, M., 2010. A wnt-frz/ror-dsh pathway regulates neurite outgrowth in *caenorhabditis elegans*. PLoS Genet. 6 (8). pii: e1001056

Squire, L., Berg, D., Floyd, B., Du-Lac, S., Ghosh, a, Spitzer, N., 2008. Fundamental neuroscience,.Amsterdam ; Boston: Academic Press/Elsevier.

Steimel, A., Wong, L., Najarro, E.H., Ackley, B.D., Garriga, G., Hutter, H., 2010. The Flamingo ortholog FMI-1 controls pioneer-dependent navigation of follower axons in *C. elegans*. Development 137, 3663–3673.

Steven, R., Kubiseski, T.J., Zheng, H., Kulkarni, S., Mancillas, J., Morales, A.R., Hogue, C.W. V, Pawson, T., Culotti, J., 1998. UNC-73 activates the Rac GTPase and is required for cell and growth cone migrations in *C. elegans*. Cell 92, 785–795.

Stringham, E., Pujol, N., Vandekerckhove, J., Bogaert, T., 2002. *unc-53* controls longitudinal migration in *C. elegans*. Development 129, 3367–3379.

Struckhoff, E.C., Lundquist, E. a, 2003. The actin-binding protein UNC-115 is an effector of Rac signaling during axon pathfinding in *C. elegans*. Development 130, 693–704.

Sulston, J.E., 1983. Neuronal cell lineages in the nematode *Caenorhabditis elegans*. Cold Spring Harb. Symp. Quant. Biol. 48 Pt 2, 443–52.

Sulston, J.E., Schierenberg, E., White, J.G., Thomson, J.N., 1983. The embryonic cell lineage of the nematode *Caenorhabditis elegans*. Dev. Biol. 100, 64–119.

Sutherland, D.J., Pujic, Z., Goodhill, G.J., 2014. Calcium signaling in axon guidance. Trends Neurosci. 37, 424–432.

Swanson, J. a, Watts, C., 1995. Macropinocytosis. Trends Cell Biol. 5, 424–428.

Takeichi, M., 2007. The cadherin superfamily in neuronal connections and interactions. Nat. Rev. Neurosci. 8, 11–20.

Tamagnone, L., Artigiani, S., Chen, H., He, Z., Ming, G.L., Song, H.J., Chedotal, A., Winberg, M.L., Goodman, C.S., Poo, M.M., Tessier-Lavigne, M., Comoglio, P.M., 1999. Plexins are a large family of receptors for transmembrane, secreted, and GPI-anchored semaphorins in vertebrates. Cell 99, 71–80.

Tanabe, K., Takahashi, Y., Sato, Y., Kawakami, K., Takeichi, M., Nakagawa, S., 2006. Cadherin is required for dendritic morphogenesis and synaptic terminal organization of retinal horizontal cells. Development 133, 4085–4096.

Tear, G., Harris, R., Sutaria, S., Kilomanski, K., Goodman, C.S., Seeger, M. a., 1996. commissureless controls growth cone guidance across the CNS midline in *Drosophila* and encodes a novel membrane protein. Neuron 16, 501–514. d

Tessier-lavigne, A. M., Goodman, C. S. 1996. The molecular biology of axon guidance guidance. Science, 274 (5290), pp.1123–1133.

Timpl, R., Dziadek, M., Fujiwara, S., Nowack, H., Wick, G., 1983. Nidogen: a new, self-aggregating basement membrane protein. Eur. J. Biochem. 137, 455–465.

Tojima, T., 2012. Intracellular signaling and membrane trafficking control bidirectional growth cone guidance. Neurosci. Res. 73, 269–274.

Tojima, T., Akiyama, H., Itofusa, R., Li, Y., Katayama, H., Miyawaki, A., Kamiguchi, H., 2007. Attractive axon guidance involves asymmetric membrane transport and exocytosis in the growth cone. Nat. Neurosci. 10, 58–66.

Tojima, T., Hines, J.H., Henley, J.R., Kamiguchi, H., 2011. Second messengers and membrane trafficking direct and organize growth cone steering. Nat. Rev. Neurosci. 12, 191–203.

Tojima, T., Itofusa, R., Kamiguchi, H., 2014. Steering neuronal growth cones by shifting the imbalance between exocytosis and endocytosis. J. Neurosci. 34, 7165–78.

Tojima, T., Itofusa, R., Kamiguchi, H., 2010. Asymmetric clathrin-mediated endocytosis drives repulsive growth cone guidance. Neuron 66, 370–377.

Tojima, T., Kamiguchi, H., 2015. Exocytic and endocytic membrane trafficking in axon development. Dev. Growth Differ. 57(4): pp 291-304.

Trent, C., Tsung, N. & Horvitz, H. R., 1983. Egg-laying defective mutants of the nematode *Caenorhabditis elegans*. Genetics,104(4) pp.619–647

Trousse, F., Martí, E., Gruss, P., Torres, M., Bovolenta, P., 2001. Control of retinal ganglion cell axon growth: a new role for Sonic hedgehog. Development 128, 3927–3936.

Turney, S.G., Bridgman, P.C., 2005. Laminin stimulates and guides axonal outgrowth via growth cone myosin II activity. Nat. Neurosci. 8, 717–719.

Uemura, M. & Takeichi, M., 2006. αN-catenin deficiency causes defects in axon migration and nuclear organization in restricted regions of the mouse brain. Developmental Dynamics, 235(9), pp.2559–2566.

Vandenberg, P., Kern, a, Ries, a, Luckenbill-Edds, L., Mann, K., Kühn, K., 1991. Characterization of a type IV collagen major cell binding site with affinity to the alpha 1 beta 1 and the alpha 2 beta 1 integrins. J. Cell Biol. 113, 1475–1483.

Villarroel-Campos, D., Gastaldi, L., Conde, C., Caceres, A., Gonzalez-Billault, C., 2014. Rab-mediated trafficking role in neurite formation. J. Neurochem. 129, 240–248.

Wada, M., Nakanishi, H., Satoh, a, Hirano, H., Obaishi, H., Matsuura, Y., Takai, Y., 1997. Isolation and characterization of a GDP/DTP exchange protein specific for the Rab3 subfamily small G proteins. J. Biol. Chem. 272, 3875–3878.

Wadsworth, W.G., Bhatt, H., Hedgecock, E.M., 1996. Neuroglia and pioneer neurons express UNC-6 to provide global and local netrin cues for guiding migrations in *C. elegans*. Neuron 16, 35–46.

Wang, X., Kweon, J., Larson, S., Chen, L., 2005. A role for the *C. elegans* L1CAM homologue lad-1/sax-7 in maintaining tissue attachment. Dev. Biol. 284, 273–291.

Wang, X., Zhang, W., Cheever, T., Schwarz, V., Opperman, K., Hutter, H., Koepp, D., Chen, L., 2008. The *C. elegans* L1CAM homologue LAD-2 functions as a coreceptor in MAB-20/Sema2-mediated axon guidance. J. Cell Biol. 180, 233–246.

Ware, M., Dupé, V., Schubert, F.R., 2015. Evolutionary Conservation of the Early Axon Scaffold in the Vertebrate Brain. Dev. Dyn. doi: 10.1002/dvdy.24312.

Watari-Goshima, N., Ogura, K., Wolf, F.W., Goshima, Y., Garriga, G., 2007. *C. elegans* VAB-8 and UNC-73 regulate the SAX-3 receptor to direct cell and growth-cone migrations. Nat. Neurosci. 10, 169–176.

Whangbo, J., Kenyon, C. 1999. a Wnt signalling system that specifies two patterns of cell migration in *C. elegans*. Molecular Cell, 4(5): 851-8.

White, J. G., Southgate, E., Thomson, J. N., Brenner, S., 1986.The structure of thenervous system of the nematode *Caenorhabditis elegans*. Philos.Trans. R. Soc.Lond.B 314,1–340.

Wightman, B., Clark, S.G., Taskar, a M., Forrester, W.C., Maricq, a V, Bargmann, C.I., Garriga, G., 1996. The *C. elegans* gene vab-8 guides posteriorly directed axon outgrowth and cell migration. Development 122, 671–682.

Wilkinson DG, 2001. Multiple roles of EPH receptors and ephrins in neural development. Nat. Rev. Neurosci. 2, 155–64.

Wilson, S.W., Ross, L.S., Parrett, T., Easter, S.S., 1990. The development of a simple scaffold of axon tracts in the brain of the embryonic zebrafish, Brachydanio rerio. Development 108, 121–145.

Winberg, M.L., Noordermeer, J.N., Tamagnone, L., Comoglio, P.M., Spriggs, M.K., Tessier-Lavigne, M., Goodman, C.S., 1998. Plexin A is a neuronal semaphorin receptor that controls axon guidance. Cell 95, 903–916.

Winkle, C.C., McClain, L.M., Valtschanoff, J.G., Park, C.S., Maglione, C., Gupton, S.L., 2014. A novel netrin-1-sensitive mechanism promotes local SNARE-mediated exocytosis during axon branching. J. Cell Biol. 205, 217–232.

Wojtowicz, W.M., Flanagan, J.J., Millard, S.S., Zipursky, S.L., Clemens, J.C., 2004. Alternative splicing of *Drosophila* Dscam generates axon guidance receptors that exhibit isoform-specific homophilic binding. Cell 118, 619–633.

Wojtowicz, W.M., Wu, W., Andre, I., Qian, B., Baker, D., Zipursky, S.L., 2007. A Vast Repertoire of Dscam Binding Specificities Arises from Modular Interactions of Variable Ig Domains. Cell 130, 1134–1145.

Wolf, A.M., Lyuksyutova, A.I., Fenstermaker, A.G., Shafer, B., Lo, C.G., Zou, Y., 2008. Phosphatidylinositol-3-kinase-atypical protein kinase C signaling is required for Wnt attraction and anterior-posterior axon guidance. J. Neurosci. 28, 3456–3467.

Wolf, F.W., Hung, M.S., Wightman, B., Way, J., Garriga, G., 1998. *vab-8* is a key regulator of posteriorly directed migrations in *C. elegans* and encodes a novel protein with kinesin motor similarity. Neuron 20, 655–666.

Wong, J.T., Yu, W.T., O'Connor, T.P., 1997. Transmembrane grasshopper Semaphorin I promotes axon outgrowth in vivo. Development 124, 3597–3607.

Yamada, K.M., Spooner, B.S., Wessells, N.K., 1971. Ultrastructure and function of growth cones and axons of cultured nerve cells. J. Cell Biol. 49, 614–635.

Yang, L., Bashaw, G.J., 2006. Son of Sevenless Directly Links the Robo Receptor to Rac Activation to Control Axon Repulsion at the Midline. Neuron 52, 595–607.

Yang, L., Garbe, D.S., Bashaw, G.J., 2009. A frazzled/DCC-dependent transcriptional switch regulates midline axon guidance. Science 324, 944–947.

Yoshikawa, S., McKinnon, R.D., Kokel, M., Thomas, J.B., 2003. Wnt-mediated axon guidance via the *Drosophila* Derailed receptor. Nature 422, 583–588.

Yu, H.H., Araj, H.H., Ralls, S. a., Kolodkin, A.L., 1998. The transmembrane Semaphorin Sema I is required in *Drosophila* for embryonic motor and CNS axon guidance. Neuron 20, 207–220.

Yu, T.W., Hao, J.C., Lim, W., Tessier-Lavigne, M., Bargmann, C.I., 2002. Shared receptors in axon guidance: SAX-3/Robo signals via UNC-34/Enabled and a Netrin-independent UNC-40/DCC function. Nat. Neurosci. 5, 1147–1154.

Yurchenco, P.D., 2011. Basement membranes: Cell scaffoldings and signaling platforms. Cold Spring Harb. Perspect. Biol. 3, 1–27.

Zallen, J. a, Kirch, S. a, Bargmann, C.I., 1999. Genes required for axon pathfinding and extension in the *C. elegans* nerve ring. Development 126, 3679–3692.

Zallen, J., Yi, B. a, Bargmann, C.I., 1998. The conserved immunoglobulin superfamily member SAX-3/Robo direts multiple aspects of axon guidance in *C. elegans*. Cell 92, 217–227.

Zylbersztejn, K., Petkovic, M., Burgo, A., Deck, M., Garel, S., Marcos, S., Bloch-Gallego, E., Nothias, F., Serini, G., Bagnard, D., Binz, T., Galli, T., 2012. The vesicular SNARE Synaptobrevin is required for Semaphorin 3A axonal repulsion. J. Cell Biol. 196, 37–46.

Chapter 2.

PLR-1, a putative E3 ubiquitin ligase, controls cell polarity and axonal extensions in *C. elegans*

modified from

Jaffar M. Bhat, Jie Pan and Harald Hutter

PLR-1, a putative E3 ubiquitin ligase, controls cell polarity and axonal extensions in *C. elegans*

Developmental Biology (February 2015) Volume 398, Issue 1, pages 44-56.

Note: Refer to section 2.5 for author contributions

Abstract

During embryonic development neurons differentiate and extend axons and dendrites that have to reach their appropriate targets. In *C. elegans* the AVG neuron is the first neuron to extend an axon during the establishment of the ventral nerve cord, the major longitudinal axon tract in the animal. In genetic screens we isolated alleles of *plr-1,* which caused polarity reversals of the AVG neuron as well as outgrowth and navigation defects of the AVG axon. In addition *plr-1* mutants show outgrowth defects in several other classes of neurons as well as the posterior excretory canals. *plr-1* is predicted to encode a transmembrane E3 ubiquitin ligase and is widely expressed in the animal including the AVG neuron and the excretory cell. *plr-1* has recently been shown to negatively regulate Wnt signalling by removing Wnt receptors from the cell surface. We observed that mutations in a gene reducing Wnt signalling as well as mutations in *unc-53*/NAV2 and *unc-73*/Trio suppress the AVG polarity defects in *plr-1* mutants, but not the defects seen in other cells. This places *plr-1* in a Wnt regulation pathway, but also suggests that *plr-1* has Wnt independent functions and interacts with *unc-53* and *unc-73* to control cell polarity.

2.1. Introduction

The central nervous system consists of many neuronal circuits assembled in a precise manner. This is achieved by neuronal cell migrations and targeted outgrowth and navigation of individual neuronal processes (axons and dendrites). Navigation occurs through a complex environment during development by using conserved guidance cues and receptors (Goodman, 1996; Keynes and Cook, 1995; Tessier-Lavigne and Goodman, 1996) which is challenging due to the large number of neurons and potential navigational targets. The complexity of this navigation problem is reduced by the sequential outgrowth of axons. The first outgrowing axons are called 'pioneer' axons. These axons form a scaffold of axon tracts for later outgrowing 'follower' axons, which use these pre-established routes to extend along. Pioneer axons have been indentified in insects (Hidalgo and Brand, 1997; Klose and Bentley, 1989) and vertebrates (Chitnis and Kuwada, 1991; McConnell et al., 1989). In *C. elegans,* a single neuron, AVG, located at the anterior end of the ventral nerve cord (VNC) is the first neuron to send out an axon towards the posterior end of the body along the right side of the ventral nerve cord (Durbin, 1987). AVG is required for correct navigation of follower axons, because its removal leads to a disorganized ventral nerve cord with misguided axons (Durbin, 1987; Hutter, 2003).

C. elegans has a simple nervous system with axon tracts mainly running in parallel to the anterior-posterior (AP) and the dorso-ventral (DV) axis. Several guidance cues including UNC-6/netrin (Hedgecock et al., 1990; Ishii et al., 1992), SLT-1 (Hao et al., 2001) and the TGF-β/UNC-129 (Colavita et al., 1998) are known to guide the migration of cells and axons along the dorso-ventral axis. In contrast, few key players in the anterior-posterior migrations have been identified. UNC-53/NAV2, a cytoskeletal regulator has defects in both anterior and posterior axonal extensions and also shows guidance defects in many cell types (Stringham et al., 2002). VAB-8 is a cytoplasmic protein with kinesin-like motor domain and is required specifically for posterior-directed migrations (Wightman et al., 1996; Wolf et al., 1998). Wnts are known to control anterior-posterior polarity of neurons as well as certain cell migrations along the anterior-posterior axis (Hilliard and Bargmann, 2006; Pan et al., 2006). In contrast to many of the

genes implicated in dorso-ventral guidance, which act globally, the known genes acting in anterior-posterior migrations have a more limited role affecting only some migrations.

The guidance cues used by the ventral nerve cord poineer AVG are largely unknown (Hutter, 2003). Here we describe the roles of *plr-1* in axonal outgrowth and establishment of cell polarity. We isolated two alleles of *plr-1*, *hd128* and *hd129*, in genetic screens for AVG axon guidance defects. *plr-1* mutants show various defects in the outgrowth and navigation of the AVG axon including premature stop, navigation defects in the VNC and polarity reversal leading to an extension of the primary neurite in anterior rather than posterior direction. In addition *plr-1* mutants show defects in posterior extension of the AVK and CAN axons as well as posterior excretory canals, and migration and axonal navigation defects in HSN neurons. *plr-1* is predicted to encode an E3 ligase containing a transmembrane domain and a RING finger domain and is expressed in a variety of tissues including some cells affected in *plr-1* mutants. PLR-1 has recently been shown to remove Wnt receptors from the surface of the AVG neuron controlling polarity of the neuron (Moffat et al., 2014). Here we show that *plr-1* also interacts genetically with *unc-53*/NAV2 and *unc-73*/Trio in the context of regulating AVG polarity. In addition we demonstrate that reduced Wnt signalling restores AVG polarity, but does not rescue other defects seen in *plr-1* mutants, suggesting that *plr-1* has Wnt-independent functions as well.

2.2. Materials and methods

2.2.1. Nematode strains and alleles used

The following strains were used for phenotypic analysis: *hdIs51*[*odr-2::tdTomato*, *rol-6(su1006)*] X; *otIs182*[*inx-18::GFP*]; *hdIs29*[*odr-2::CFP,sra-6::DsRed2*] V; *zdIs13*[*tph-1::GFP*] IV; *gmIs18*[*ceh-23::GFP*]; *hdIs54*[*flp-1::GFP,sra-6::plum,pha-1(+)*]; *sIs10089*[*pgp-12::GFP,him-8*]; *rhIs5*[*glr-1::GFP,dpy-20(+)*] X; *zdIs5*[*mec-4::GFP]* I; *evIs111*[*rgef-1::GFP*] V; *hdIs22*[*unc-129::CFP, unc-47::DsRed2*] V; *hdEx556*[*Pplr-1::GFP, pha-1 (+)*]; *hdEx556*[*WRM0636cC10 (PLR-1 C-terminal GFP), pha-1 (+)*] *qpIs102*[*pexc-9::mCherry::chc-1*]; *qpIs95*[*pexc-9::mCherry::eea-1*] X; *qpIs99*[*pexc-9::mCherry::rab-5*] IV; *qpIs100*[*pexc-9::mCherry::rab-7*]; *qpIs98*[*pexc-9::mCherry::glo-1*];

qpIs101[*pexc-9::mCherry::rme-1*] X; *qpIs97*[*pexc-9::mCherry::rab-11*] V and *qpIs103*[*pexc-9::mCherry::GRIP*].

The following alleles were used for phenotypic analysis and genetic interaction studies: *plr-1(hd129)* III, *plr-1(hd128)* III, *plr-1(tm2975)* III, *mig-14(ga62)* II, *unc-53(n116)* II, *unc-73E(ev802)* I, *unc-73B(rh40)* I, *vab-8(e1017)* V, *sax-3(ky123)* X, *unc-6(ev400)* X, *unc-5(e53)* IV, *unc-40(e271)* I and *nid-1(cg119)* V. The strains were cultured and maintained at 20 ^{o}C under standard conditions (Brenner, 1974).

2.2.2. Mapping and gene identification

The *plr-1* alleles *hd128* and *hd129* were isolated after UV-TMP (*C. elegans* gene knockout consortium UBC) mutagenesis of *hdIs51*[*odr-2::tdTomato*] animals by the selection of F2 animals with AVG axon outgrowth defects in a non-clonal screen. The *tm2957* deletion allele was provided by the *C. elegans* Gene Knockout Consortium and National Bioresource project. We mapped both the *hd129* and *hd128* alleles to a 337.6 kb on Chromosome III between SNP-15 and pKP3074. Injection of Fosmids (Geneservices, Cambridge UK) into both alleles narrowed down the region to 34 kb region on the right arm of Chromosome III which only contains two genes, *plr-1(Y47D3B.11)* and *bed-2(Y447D3B.9).* These two genes are in opposite orientation. Fosmid WRM0636cC10 covers both the genes whereas Fosmid WRM0632aD04 covers only *plr-1* and a part of *bed-2*. Fosmids WRM0636cC10 (4.2 ng/ul) and WRM0632aD04 (5.2 ng/ul) along with *unc-122::*GFP (45 ng/ul) as a co-injection marker were injected into *hd129* animals for rescue. Fosmid WRM0636cC10 rescued the AVG defects of *hd-129* animals in two out of two lines and WRM0632aD04 rescued the AVG defects of *hd-129* animals in three out of three lines, thus identifying *plr-1*(*Y47D3B.11)* as a most-likely candidate. Sequencing the *plr-1*/*Y47D3B.11* coding region in *hd129* animals revealed a 159 bp deletion which completely removes exon 2 leading to a frameshift and premature stop codon. Sequencing of the *plr-1*/*Y47D3B.11* coding region in *hd128* animals revealed a 132bp in-frame deletion in exon 4. *tm2957* is a 239 bp deletion in the beginning of exon 4, which results in a frameshift and premature stop codon.

2.2.3. Expression constructs

The promoter reporter construct (*plr-1::GFP)* was generated by combining a 3906 bp upstream region of *plr-1* with GFP by using a PCR-based fusion method (Hobert, 2002). Transgenic lines were generated by injecting *plr-1*::GFP (25 ng/µl) along with *pha-1(+)* (pBX) (60 ng/µl) as a co-injection marker (Granato et al., 1994) in *pha-1(e2123ts)* animals. The translational reporter construct PLR-1::GFP was generated by tagging the C-terminus of PLR-1 with GFP in the Fosmid WRM0636cC10 by recombineering (Tursun et al., 2009). For all constructs, transgenic animals were generated as described (Mello et al., 1991).

To express *plr-1* specifically in the excretory cell, *pgp-12* promoter (Marcus-Gueret et al., 2012) and *plr-1* cDNA were cloned in to GFP vector pPD95.75 (Fire vector kit). This construct (15 ng/ul) was injected along with coninjection marker *unc-122::GFP* (45 ng/ul) into *plr-1* mutant animals and the animals from three independent transgenic lines were analysed for excretory canal defects.

2.2.4. Phenotypic analysis of neuronal and non-neuronal defects

Axonal defects were scored with a Zeiss Axiscope (40x objective) in adult animals expressing fluorescent markers in respective neurons. Animals were immobilised with 10 mM sodium azide in M9 buffer for 1hr and mounted on 3% agar pads before analysis. For excretory canal defects, adult animals expressing the *pgp-12::*GFP reporter were immobilised in the same way. Scoring and analysis of excretory canal defects was done according to (Marcus-Gueret et al., 2012).

2.2.5. Microscopy

Confocal images of mixed stage population of animals with respective fluorescent proteins were acquired on a Zeiss Axioplan II microscope (Carl-Zeiss AG, Germany) connected to a Quorum WaveFX spinning disc system (Quorum Technologies, Canada). Stacks of confocal images with 0.2 to 0.5 µm distance between focal planes were recorded. Image acquisition and analysis was carried out by using Volocity software (Perkin-Elmer, Waltham, MA). Images in the figures are maximum

intensity projections of all focal planes. Figures and GFP/Nomarski overlays were assembled with Adobe phoshop CS8.0 (Adobe, San Jose, CA, USA).

2.2.6. Genetic Interactions

To test genetic interactions between *plr-1* and potential interacting genes, phenotypes of both single and double mutants were examined. Two genes are thought to act in the same pathway if the penetrance of double mutant phenotype is similar to that of the strongest single mutant. χ^2 tests were used to determine statistical significance between double mutants and the strongest single mutant. For excretory canals, scoring and analysis was done according to (Marcus-Gueret et al., 2012). The posterior part of the body was divided into five regions (1-5) from the turning point of the anterior gonad arm to the tail as shown in Figure 2.9. The termination point of the canal was determined under the microscope using a GFP marker expressed in the canal. Phenotypes were grouped into two categories - wild type (scored as 5) and premature canal termination (scored as <5). Single mutants were compared with the wild type and double mutants were compared with the strongest single mutants, which was set as baseline for comparison while phenotypes showing further reduction in canal extensions were grouped together.

2.3. Results

2.3.1. *plr-1* mutant animals show polarity reversal and axon outgrowth defects in the ventral nerve cord pioneer AVG

Two alleles of *plr-1*, *hd128* and *hd129*, were isolated in genetic screens for AVG axon outgrowth defects. A third allele, *tm2957*, was kindly provided by the Mitani lab. The genetic screens were performed with a marker strain *(odr-2::tdTomato)* that allowed us to visualize the left and right VNC axon tracts in addition to the AVG axon in the right tract. This enabled us to detect navigation errors where the AVG axon crosses the ventral midline to extend in left axon tract referred to as cross-over defects. All three *plr-1* alleles showed cross-over defects with a similar penetrance of 15-18% (Figure 2.1G, Table 2.1). In a small number of animals, 3% in *plr-1(hd129),* the AVG axons left the

ventral cord (Figure 2.1H, Table 2.1). The most prominent AVG defect, found in more than half of the *plr-1(hd129)* mutant animals, is a premature stop of the AVG axon at various positions along the ventral cord (Figure 2.1C and D, Table 2.1). The penetrance of this defect ranged from 52% in *plr-1(hd129)* to 17% in *plr-1(hd128).* Overall *hd129* mutant animals displayed the most penetrant defects, *tm2957* mutants were less severely affected and *hd128* mutants showed the weakest defects (Table 2.1).

The AVG neuron normally extends a very short process anteriorly and a long process posteriorly (Figure 2.1A and B). The marker strain used for the initial analysis labels additional neurons in the head, preventing any analysis of AVG's anterior process. Analysis of the AVG defects with a marker strain that selectively labels AVG (*inx-18::*GFP) revealed that in a substantial fraction of *plr-1* mutant animals the AVG neuron had a long anterior and very short posterior process (Figure 2.1E and F, Table 2.1). Similar defects have been found by Moffat et al. (2014) and have been shown to be the result of a reversal of the anterior-posterior polarity of AVG (Moffat et al., 2014). In addition there are many animals, where the polarity of AVG is normal (defined as AVG having a very short anterior process and a long posterior process), but the AVG axon stops prematurely in the VNC (Figure 2.1C and D, Table 2.1).

2.3.2. *plr-1* mutant animals show cell migration, axon extension and axon guidance defects in a variety of neurons

Previous phenotypic analysis of *plr-1* mutants was limited to defects seen in AVG (Moffat et al., 2014). To determine whether *plr-1* mutants have defects in other neurons, we examined additional neurons using cell type-specific markers in the strongest allele, *hd129.* We found that *plr-1(hd129)* mutant animals had cell migration and axon navigation defects in HSN neurons (Figure 2.2A and B, Table 2.2). In 26% of *plr-1(hd129)* mutant animals, the HSN cell bodies were found at variable positions posterior to their normal location around the vulva (Table 2.2). In 48% of the animals, where the HSN cell bodies were correctly positioned and the HSN axons extended into the VNC, we found that HSN axons inappropriately crossed the ventral midline to extend in the contralateral axon tract (Figure 2.2A and B, Table 2.2).

Under normal conditions axons of the AVK neurons extend in the VNC all the way to the posterior end of the cord (Figure 2.2C and C'). However, in *plr-1(hd129)* animals we observed AVK axons frequently failing to reach their normal termination point (Figure 2.2D and D'). In most cases both AVK axons stop prematurely and in all cases the axons extend past the vulva, i.e. more than halfway towards the target (Table 2.2), suggesting that none of these defects are due to a reversal in the polarity of the neurons. CAN neurons have one anterior and one posterior processes of comparable length, extending from the cell body in a lateral position (Figure 2.2E). In *plr-1(hd129)* animals the posterior process often terminates short of its normal destination (Figure 2.2F, Table 2.2). As with AVK, the process always extends at least halfway to its target. In addition a fraction of animals display branching and/or navigation defects (Table 2.2). The anterior CAN process was unaffected in *plr-1* mutant animals.

Since processes from CAN neurons extend in close proximity to the excretory canals and studies suggested CAN neurons have a role in regulating the adjacent excretory canals (Hedgecock et al., 1987), we wanted to test whether excretory canals were also affected. The cell body of the excretory cell lies on the ventral side in the head region of the animal. The cell extends two shorter anterior and two longer posterior canals extending in lateral position all the way to the tail (Figure 2.2G and G'). We found that some *plr-1(hd129)* animals had excretory canals that terminated short of the normal position (Figure 2H and H', Table 2.2). Again the terminating points were all in the posterior half of the animal, indicating that the canals extend most of the distance. Anterior canals were not affected. Excretory canal defects are much less penetrant than CAN defects, suggesting that these defects in *plr-1* mutants are independent.

Using additional markers we found no significant defects in the migration of the Q neuroblasts, nor in the migration and axonal navigation of the touch receptor neurons, the GABAergic DD/VD and cholinergic DA/DB motor neuron axons, the PVP/PVQ axons in the VNC or the ASH dendrite and axon in the head (Table 2.3). We did observe mild navigation and premature stop defects in *glr-1*::GFP expressing interneurons, which normally extend in the right VNC tract (Table 2.3). Since navigation of these axons in part depends on the pioneer AVG, it is possible that these interneuron defects are secondary consequences of AVG defects. We found no polarity defects in neurons with

cell bodies close to AVG (RIF and RIG neurons) or in other neurons, whose polarity is affected by Wnt signalling (touch neurons), suggesting that the polarity defects in *plr-1* mutants are specific to AVG (Table 2.3). In summary, *plr-1* mutant animals are characterized by a polarity reversal defect of the AVG neuron and show a number of axonal extension and navigation defects in a small number of unrelated neurons located throughout the animal.

2.3.3. *plr-1* encodes a monomeric RING finger protein

We mapped *plr-1(hd129)* to a 337.6 kb interval on chromosome III using snip-SNP markers. Rescue experiments with genomic fosmid clones identified a single fosmid containing two genes (Figure 2.3A). Rescue experiments with individual genes revealed that *plr-1*/*Y47D3B.11* was the only gene able to rescue the AVG defects in *plr-1* mutants. Sequencing of *hd128* and *hd129* alleles identified mutations in *Y47D3B.11* (Figure 2.3B), confirming the identity of *plr-1*. The independently isolated *tm2957* allele showed similar AVG defects, further supporting the idea that *plr-1* is *Y47D3B.11.*

plr-1 encodes a protein with a predicted size of 487 amino acids. Its predicted domains include a signal peptide, a transmembrane domain, and a single RING finger domain (Figure 2.3C and D). It is classified as one of the 152 monomeric RING finger proteins in *C. elegans*. The presence of a signal peptide and transmembrane domain suggests that the protein enters the secretory pathway and is either located at the cell surface or in membrane-bound intracellular compartments that originate from the endoplasmic reticulum. Putative homologs of PLR-1 in mammals are RNF43 (Figure 2.3D) and ZNRF3 (Hao et al., 2012; Koo et al., 2012). All three proteins are similar in the N-terminal part up to and including the RING finger domain, but are divergent in the C-terminus with both RNF43 (784 amino acids) (Figure 2.3D) and ZNRF3 (913 amino acids) being substantially larger than PLR-1.

All three *plr-1* alleles are small deletions in the gene. *hd129* is a 159 bp deletion missing exon 2 and some flanking intronic sequences (Figure 2.3B). This deletion is expected to produce a frameshift and a stop codon truncating the protein after 79 amino acids (Figure 2.3C). *hd128* is a 132 bp in-frame deletion in exon 4, just C-terminal of the

transmembrane domain (Figure 2.3B and C). *tm2957* is a 239 bp deletion at the beginning of exon 4 resulting in a frameshift and truncation after 154 amino acids (Figure 2.3B and C). Based on the molecular nature of the alleles, *hd129* is expected to be the strongest loss-of-function allele, likely a null allele. *hd128* is expected to be the weakest allele. Consistent with our expectations, *hd129* showed the strongest defects, and *hd128* showed the weakest defects.

2.3.4. *plr-1* is widely expressed throughout development

To identify cells expressing *plr-1* we generated transgenic animals expressing green fluorescent protein (GFP) under the control of a 3.9 kb promoter fragment. *plr-1*::GFP expression became visible in late gastrulation stage embryos (Figure 2.4A and B). Strongest expression was detected in many cells in the tail region and by comma stage the most prominent expression was seen in body wall muscle cells (Figure 2.4C and D). In early larval stages expression was detectable in a number of different tissues including the major hypodermal cells, muscle and marginal cells of the pharynx, the intestine (strongest in the anteriormost and posteriormost cells) as well as the anal depressor and stomatointestinal muscle (Figure 2.4E and F). In the nervous system GFP expression was visible in a few neurons in head ganglia, many ventral cord motor neurons and several neurons in the tail ganglia including the PDA neuron (Figure 2.4E and F). Based on the lack of commissures the motor neurons are likely of the VA, VB, VC and/or AS class. Based on the number of cells the majority (or even all) of these classes express GFP. In general expression was strongest in the tail region throughout development. This also held true for the motor neurons in the ventral cord, where GFP was strongest in the posterior-most cells and barely detectable in anterior motor neurons. Expression is maintained throughout larval development. In later larval stages expression is also seen occasionally in the distal tip cell of the developing gonad, the vulva and uterine muscle cells and the VC4 and VC5 neurons flanking the vulva (Figure 2.4G and H). Expression in AVG, HSN or CAN neurons was not detectable with this reporter construct, but was detected in a previous study in HSN and CAN using a longer genomic construct (Moffat et al., 2014).

To determine the subcellular localization of PLR-1 we fused GFP to the C-terminus of the *plr-1* coding sequence in a fosmid containing the entire *plr-1* gene and surrounding genomic DNA. This construct was able to rescue the AVG defects, indicating that it is functional. PLR-1::GFP expression levels are variable, but generally fairly low. The GFP signal is concentrated in puncta spread throughout the cytoplasm mainly in the cell body, but also extends into neuronal processes. GFP expression is detectable in comma stage embryos (Figure 2.5A and B) with strongest expression in the tail region. The distinct subcellular localization makes it difficult to confirm cell identities, but overall expression is comparable to the *plr-1*::GFP promoter construct. Postembryonical GFP expression in the head region seems restricted to some neurons and the posterior region of the pharynx. Expression was not readily detectable in hypodermal or body wall muscle cells with this construct postembryonically. Expression of the PLR-1::GFP fusion protein, however, is detectable in the AVG neuron and also in the excretory cell (Figure 2.5D-G). This suggests that the promoter construct lacks some control elements. Since the GFP expression of the fusion protein is significantly lower than the expression of the promoter construct, it is possible that low levels of expression in tissues and cells expressing the *plr-1*::GFP transcriptional reporter remain undetectable.

The punctate expression of PLR-1::GFP fusion protein (Figure 2.5G) suggests that PLR-1 is present in some endocytotic compartments. Recently PLR-1 has been shown to colocalize with endosomal markers (Moffat et al., 2014), suggesting that PLR-1 indeed enters the secretory pathway. To characterize these PLR-1::GFP containing compartments in excretory cell which is much larger than AVG neuron, we tested if PLR-1 colocalizes with the known endocytotic compartment markers. We used the following markers provided by the Buechner lab: RME-1 (Recycling endosome marker), RAB-11 (Recycling endosome marker), CHC-1 (Clathrin heavy chain marker), RAB-5 (Early endosome marker), RAB-7 (Late endosome marker), GLO-1 (Lysosomal marker) and GRIP (Golgi marker) (Mattingly & Buechner, 2011). All these markers are fused with mCherry and driven under *exc-9* promoter which specifically expresses in the excretory cell (Mattingly & Buechner, 2011). Strains were made where each of these markers were combined with PLR-1::GFP containing strain, and later imaged under confocal microscope. We observed some colocalization of PLR-1 with clathrin heavy chain, golgi,

early endosomal and late endosomal markers (Figure 2.6). However we did not observe any colocalization of PLR-1::GFP with recycling endosomal and lysosomal markers (Figure 2.6). This suggests that some amount of PLR-1 is internalised from the cell membrane via clathrin mediated endocytosis to the endosomes. This also suggests that PLR-1 is not recycled via recycling endosomes to the plasma membrane after internalisation.

2.3.5. *mig-14*/Wntless mutants partially suppress the *plr-1* defects

PLR-1 and its vertebrate homologs RNF43 and ZNRF3 have been shown to downregulate Wnt receptors (Hao et al., 2012; Koo et al., 2012; Moffat et al., 2014). In *C. elegans* AVG polarity reversal defects have been linked to excessive Wnt signalling, since mutations in the Wnts *cwn-1* and *cwn-2* suppress the polarity defects in AVG (Moffat et al., 2014). Furthermore *plr-1* has been shown to reduce cell surface levels of Wnt receptors in AVG and ectopic expression of *plr-1* can block Wnt signalling (Moffat et al., 2014). We wanted to determine whether all defects seen in *plr-1* mutants can be suppressed by reducing Wnt signalling. *C. elegans* has five Wnt genes with overlapping functions (Pan et al., 2006; Yamamoto et al., 2011). Secretion of all Wnts requires the activity of the Wntless (*mig-14* in *C. elegans*) gene (Banziger et al., 2006; Yang et al., 2008). While a complete loss of function of *mig-14* is lethal due to the importance of Wnt signalling in early embryonic development, viable partial loss-of-function alleles exist (e.g. *ga62*). Those alleles are considered to have a reduced level of Wnt signalling (Eisenmann and Kim, 2000; Harris et al., 1996; Yang et al., 2008). We generated *mig-14(ga62); plr-1(hd129)* double mutants and evaluated the various defects seen in *plr-1* single mutants. We found that *mig-14(ga62)* was able to strongly suppress the polarity reversal, axonal stop and axonal navigation defects of AVG (Figure 2.7), confirming that these defects are due to abnormal Wnt signalling as previously observed (Moffat et al., 2014). In contrast, the premature termination defects of the AVK and CAN axons as well as the premature stop of the excretory canals were not effectively rescued (Figure 2.7). *mig-14(ga62)* mutants themselves have HSN migration defects, which makes it impossible to evaluate a potential rescue of the HSN defects in *plr-1*. Both *plr-1* animals and *mig-14; plr-1* animals show similar penetrant excretory canal defects, suggesting

that the two genes act in the same genetic pathway here (Figure 2.7). These data suggest that *plr-1* has both Wnt-dependent and Wnt-independent roles.

2.3.6. *unc-53* and *unc-73* mutants suppress AVG polarity reversal defect of *plr-1* mutants

UNC-53/NAV2 is a cytoskeleton regulator (Stringham and Schmidt, 2009) important for longitudinal migrations in *C. elegans* (Stringham et al., 2002). In *C. elegans*, *unc-53* mutant animals did not display AVG axon defects (Figure 2.8A), but have short posterior excretory canals similar to *plr-1* mutants. While testing genetic interactions of *plr-1* and *unc-53* in excretory canal extensions (see below) we found unexpectedly that the polarity reversal defects of AVG axon are completely suppressed in *unc-53; plr-1* animals (Figure 2.8A). We also observed that the majority of AVG axons in *unc-53; plr-1* animals terminate prematurely (Figure 2.8B), which suggests that *unc-53* also plays a role in the posterior extension of AVG axon. *unc-53* does not suppress the AVK, CAN, HSN and excretory canal defects found in *plr-1* mutants (Figure 2.8C), suggesting that interactions between *unc-53* and *plr-1* are limited to phenotypes related to AVG.

Mutations in *unc-73*/*Trio* encoding a Rac/Rho guanine nucleotide exchange factor (GEF) lead to a variety of axonal navigation defects including some premature stop defects of the AVG axon (Figure 2.8B). UNC-73/Trio has separate GEF domains for Rho and Rac and has different isoforms: UNC-73B interacts with Rac and UNC-73E interacts with Rho. We obtained isoform specific mutants affecting either of these domains and constructed double mutants with *plr-1*. We found a partial suppression of the *plr-1* AVG polarity reversal defects in *unc-73B(rh40); plr-1* and *unc-73E(ev802); plr-1* double mutants (Figure 2.8A). In both *unc-73; plr-1* double mutants the premature termination defect of the AVG axon were enhanced compared to *plr-1* single mutants (Figure 2.8B), suggesting that *unc-73* is acting independently of *plr-1* in the posterior extension of AVG axon.

VAB-8 is a cytosolic protein with a kinesin-like motor domain at the N-terminus promoting posterior cell migrations and axon guidance together with UNC-73 and UNC-53 (Marcus-Gueret et al., 2012; Wightman et al., 1996; Wolf et al., 1998). *vab-8* single

mutants show some premature termination of the AVG axon but do not display AVG polarity reversal defects. In *vab-8; plr-1* double mutants the AVG polarity reversal defects of *plr-1* are enhanced to 100% (Figure 2.8A) in striking contrast with the observations in *unc-53; plr-1* and *unc-73; plr-1* double mutants, suggesting that *vab-8* does not act in the same pathway as *unc-53* and *unc-73* in this context.

2.3.7. *plr-1* acts through a novel pathway to control posterior extension of excretory canals

The posterior extension of excretory canals is controlled by two distinct parallel pathways (Marcus-Gueret et al., 2012). In one pathway, VAB-8 interacts with the receptor SAX-3 and the RacGEF form of UNC-73 outside the excretory cell. In addition UNC-53 interacts with the RhoGEF form of UNC-73 and many components of cytoskeleton in the excretory cell itself. We wanted to test if *plr-1* acts in any of these two pathways. Given the expression of *plr-1* in excretory cell, one would expect *plr-1* to act in a cell autonomous manner possibly together with *unc-53*. To test this hypothesis, we chose components from both of these pathways for double mutant analysis with *plr-1*. In both *unc-53; plr-1* and *vab-8; plr-1* double mutants the excretory canal defects are stronger compared to the strongest single mutant (Figure 2.9). These data suggest that *plr-1* does not act in these pathways. We further tested the RacGEF and RhoGEF forms of UNC-73/Trio. In both *unc-73E(ev802); plr-1* and *unc-73 B(rh40); plr-1* double mutants the defects are stronger compared to the strongest single mutants (Figure 2.9), confirming the idea that *plr-1* acts through a novel parallel pathway to control the posterior extension of excretory canals. Given these observations we expressed PLR-1 specifically in excretory cell to determine whether PLR-1 is required in the excretory cell for proper excretory canal extensions. We examined the excretory canal defects in transgenic lines expressing a PLR-1 cDNA construct tagged with GFP specifically in excretory cell. We found that PLR-1 was able to rescue the excretory canal defects in three out of three independent transgenic lines (n >100). This strongly suggests that PLR-1 is required in the excretory cell for excretory canal extension and acts in a cell autonomous manner.

2.3.8. *plr-1* interacts with the *unc-73*/Trio for the correct navigation of AVG axon

In *plr-1* mutant animals the AVG axon crosses the midline and joins the contralateral tract in a significant fraction of animals (30%), suggesting a navigation defect likely due to a failure to respond to guidance cues. *sax-3/Robo*, *unc-6/Netrin* and *nid-1/Nidogen* mutants show similar midline crossing defects albeit with a lower penetrance (Hutter, 2003). To determine if *plr-1* genetically interacts with these genes for AVG axon navigation, double mutants were made with *plr-1*. In all cases we observed that the penetrance of AVG navigation defects in double mutants was not significantly different from *plr-1* single mutants (Figure 2.10), but also not significantly different from the sum of the two individual mutants. This suggests that *plr-1* does not act synergistically with any of these genes.

UNC-73/Trio mediates axonal responses to several guidance cues including Netrin and Slit (Watari-Goshima et al., 2007). We observed that *unc-73B(rh40)* which affects the RacGEF domain of UNC-73/Trio has midline crossing and premature termination defects of the AVG axon (Figure 2.10). AVG midline crossing defects are suppressed in *plr-1; unc-73B(rh40)* double mutants as compared to *plr-1* single mutants (Figure 2.10). *unc-73E(ev802)* mutants affecting the RhoGEF domain of UNC-73/Trio show only few midline crossing and no premature termination defects of the AVG axon. *plr-1; unc-73E(ev802)* double mutant are similar to *plr-1* single mutant (Figure 2.10), suggesting the interactions between *unc-73* and *plr-1* are limited to the RacGEF isoform of *unc-73*.

2.4. Discussion

2.4.1. *plr-1* affects multiple aspects of neuronal development

We identified alleles of *plr-1* in a forward genetic screen for outgrowth and navigation of the ventral nerve cord pioneer axon. *plr-1* mutant animals show a variety of defects including a polarity reversal of the AVG neuron, premature termination of axonal outgrowth and aberrant midline crossing of the AVG axon. While the polarity reversal

defects seem to be limited to AVG, we found outgrowth defects in additional axons as well as in non-neuronal processes such as the excretory canals. A common theme is that only posteriorly directed processes are affected and that processes can grow most of the distance and typically stop short at variable positions only in the posterior half of the animal. While individual aspects of the *plr-1* phenotype such as polarity reversals or axonal outgrowth defects are shared with other mutants, the combination of defects seen in *plr-1* mutants is rather unique and not found in other mutants so far.

2.4.2. *plr-1* encodes a putative E3 ligase

PLR-1 is predicted to be an E3 ligase. E3 ligases are part of the enzyme complex which transfers ubiquitin to substrate proteins in preparation for degradation by the proteosomal complex (Hershko and Ciechanover, 1982; Hershko et al., 2000). E3 ligases provide substrate specificity by bringing the target protein in contact with the E2 ubiquitin-conjugating enzyme. Ubiquitination by E3 ligases is also used to regulate receptor internalization from the cell surface and protein transport in endocytic compartments of the cell (d'Azzo et al., 2005; Hicke and Dunn, 2003). PLR-1 has a signal peptide and transmembrane domain, which suggests that it enters the secretory pathway. PLR-1 protein has been shown to localize to various endosomal compartments in particular early endosomes (Moffat et al., 2014). We found that some amount of PLR-1 enters the endosomal compartments via clathrin mediated endocytosis in the excretory cell. PLR-1 promotes endocytosis of Wnt receptors from the cell surface (Moffat et al., 2014). Similarly the vertebrate homologs RNF43 and ZNRF3 also induce the endocytosis of Wnt receptors such as frizzled and LRP6 (Hao et al., 2012; Koo et al., 2012). Both the ectodomain and the RING finger domain of RNF43 are necessary for the binding and internalization of Wnt receptor frizzled FZD5 (Koo et al., 2012). Similarly both the ectodomain and the RING finger domain of PLR-1 are required for this activity (Moffat et al., 2014). These data suggest that PLR-1 affects neuronal development indirectly by regulating the availability of Wnt receptors (and potentially other receptors) at the cell surface.

2.4.3. *plr-1* and Wnt signalling

The *C. elegans* genome encodes five Wnt genes (Herman et al., 1995; Maloof et al., 1999; Shackleford et al., 1993; Thorpe et al., 1997), which control a variety of developmental processes (Gleason and Eisenmann, 2010; Gleason et al., 2006; Goldstein et al., 2006; Green et al., 2008; Song et al., 2010). Several neuronal cell migrations are influenced by Wnts (Hilliard and Bargmann, 2006; Pan et al., 2006) and Wnts control the polarity of certain neurons, most notably ALM and PLM (Hilliard and Bargmann, 2006; Prasad and Clark, 2006). The ALM neurons have a short posterior neurite and a much longer anterior neurite (White et al., 1986). In animals with mutations in the Wnt genes *cwn-1* and *egl-20*, ALM sends out a long posterior process and a short anterior process, suggesting that its polarity is reversed (Hilliard and Bargmann, 2006). Strong overexpression of the Wnt *egl-20* or Frizzled receptor *lin-17* in ALM neurons causes similar polarity reversals (Hilliard and Bargmann, 2006). We observed polarity reversals of the AVG neuron, but not of ALM or PLM in *plr-1* mutant animals. *plr-1* induced AVG polarity reversal defects have been linked to excessive Wnt-signalling through the excessive presence of Wnt-receptors on the cell surface of AVG in *plr-1* mutants and *plr-1* has been shown to act cell-autonomously in AVG (Moffat et al., 2014). We found that mutations in *mig-14*/Wntless, a protein required for the secretion of Wnt proteins (Banziger et al., 2006; Yang et al., 2008) effectively suppresses AVG polarity reversal defects, confirming that these defects are indeed likely caused by too much Wnt signalling. Overall the phenotypic spectrum of *plr-1* mutants shows limited overlap with defects related to Wnt signaling. In particular, AVK, CAN and excretory canal outgrowth defects have not been reported to be linked to Wnt signalling. These defects are not effectively suppressed by reducing Wnt-signalling, suggesting that *plr-1* has additional roles unrelated to Wnt receptor presentation at the cell surface.

2.4.4. *unc-53*/NAV-2 and *unc-73*/Trio interact with *plr-1*

UNC-53 is a cytoskeletal regulator required for longitudinal migrations of cells and axons in *C. elegans* (Stringham et al., 2002; Stringham and Schmidt, 2009). Its mammalian homologs called navigators (NAV-1, NAV-2 and NAV-3) are also involved in axon guidance (Maes et al., 2002; Merrill et al., 2002). UNC-53/NAV-2 has been shown

to bind to ABI-1 (Abelson kinase interactor), a regulator of Arp2/3 which in turn nucleates actin filaments (Schmidt et al., 2009). Actin regulators such as Ena, WAVE complex, cofilin and profilin regulate neurite formation in mammalian neurons (Tahirovic and Bradke, 2009). UNC-73/Trio is a guanine nucleotide exchange factor (GEF) with separate Rac- and Rho-specific GEF domains. The GEF1 domain activates Rac proteins (MIG-2/RhoG and CED-10/Rac) whereas the GEF2 domain activates RHO-1/Rho (Kubiseski et al., 2003; Spencer et al., 2001; Steven et al., 1998; Wu et al., 2002), which in turn regulate the cytoskeleton and thus play role in cell migrations and axon guidance (Dyer et al., 2010; Spencer et al., 2001). In addition these Rho family GTPases are also involved in establishing polarity in *C. elegans* and mammals (Govek et al., 2005; Levy-Strumpf and Culotti, 2007; Quinn et al., 2008). *unc-53* genetically interacts with the RhoGEF form of *unc-73* along with other cytoskeletal components (Marcus-Gueret et al., 2012) to control posterior extension of excretory canals.

We found that *unc-53* mutants completely suppress the AVG polarity defect in *plr-1* mutants and that *unc-73* mutants partially suppress these defects. Alleles specific to both RacGEF and RhoGEF domains of UNC-73/Trio showed similar suppression, supporting the idea that both Rac and Rho specific effectors are involved in regulating AVG polarity. Since the polarity defects appear to be caused by ectopic Wnt signalling due to the presence of Wnt receptors on the surface of AVG, this suggests that *unc-53* and *unc-73* might negatively influence Wnt signalling. However, neither *unc-53* nor *unc-73* has been implicated in Wnt signalling, so it is currently unclear what the connection to Wnt signalling is. UNC-73/Trio together with VAB-8 has recently been shown to increase the cell surface availability of axon guidance receptors UNC-40/DCC and SAX-3/Robo in neurons (Levy-Strumpf and Culotti, 2007; Watari-Goshima et al., 2007). It is possible that UNC-73 promotes Wnt-receptor expression at the cell surface in AVG. A lack of UNC-73 could lead to reduced receptor presence at the cell surface counteracting effects of a lack of PLR-1, which would lead to increased receptor presence. If UNC-73 acts together with VAB-8 in this process, one would expect that mutations in *vab-8* also suppress *plr-1*-induced polarity defects. However, contrary to these expectations, we found that AVG polarity defects are enhanced in *vab-8; plr-1* double mutants, indicating that the interactions between *plr-1*, *unc-73* and *vab-8* are more complex in this situation.

plr-1 mutant animals show AVG axon navigation defects in the ventral nerve cord. Our genetic analysis indicated that the RacGEF form of *unc-73* suppresses AVG axon navigation defects, whereas the RhoGEF form of *unc-73* does not. This suggests that *plr-1* genetically interacts specifically with the RacGEF form of *unc-73* for the correct navigation of AVG axon. We found that *plr-1* does not act synergistically with *sax-3/Robo* (Slit receptor), *unc-6/Netrin* (guidance cue), *unc-5* (receptor for unc-6) and *nid-1/Nidogen* (basement membrane component) for AVG axon navigation.

plr-1 mutants have excretory canal outgrowth defects similar to *unc-53*, *unc-73* and *vab-8* mutants (Hedgecock et al., 1987; Stringham et al., 2002; Wightman et al., 1996). UNC-53 acts cell-autonomously together with the RhoGEF form of UNC-73 to control canal outgrowth. In a parallel pathway the RacGEF isoform of UNC-73 acts non-cell-autonomously. Our double mutant analysis indicates that *plr-1* does not act in either of these two pathways implicating a third yet unidentified pathway in this process. Our observation that PLR-1 acts in the excretory cell, suggests that PLR-1 like UNC-53 is required within the excretory cell for the posterior extension of canals but acts through a different genetic pathway. Interactions between PLR-1 and UNC-53 appear to be cell-type specific and different in AVG and the excretory cell adding an additional layer of complexity.

In summary, we have identified a putative E3 ligase, PLR-1, required for several aspect of nervous system development including cell polarity, axon extension and axon navigation in a subset of neurons in *C. elegans*. The cell polarity defects in *plr-1* mutants have recently been found to be secondary consequences of ectopic Wnt signalling and PLR-1 has been shown to remove Wnt receptors from the surface of the AVG neuron (Moffat et al., 2014). Our analysis confirmed that AVG-related defects are likely due to ectopic Wnt-signalling, but that additional defects found in *plr-1* mutants are unrelated to Wnt-signalling, suggesting that *plr-1* has Wnt-independent functions as well. Finally our data implicate *unc-53/NAV* and *unc-73/Trio* in regulating cell polarity together with *plr-1*.

2.5. Contributions

I, the first author of this study wrote the manuscript of the published paper together with the HH. The experiments were designed by HH and me. The project was initially started by the JP, who isolated alleles and identified the *plr-1*. The remaining experiments including the phenotypic characterization of the mutants, genetic interactions and cell specific rescue experiments were performed by me. I also analysed all the data and prepared the manuscript figures. I would also like to thank the Stringham, Hawkins and Buechner labs for strains and other reagents. Some of the nematode strains used in this work were provided by the *Caenorhabditis* Genetics Center, which is funded by the NIH National Center for Research Resources (NCRR). One *plr-1* allele was provided by the *C. elegans* National Bioresource Project (Japan). This work was supported by NSERC (9312498-2012) and CIHR (MOP 93719) grants to HH.

2.6. Figures

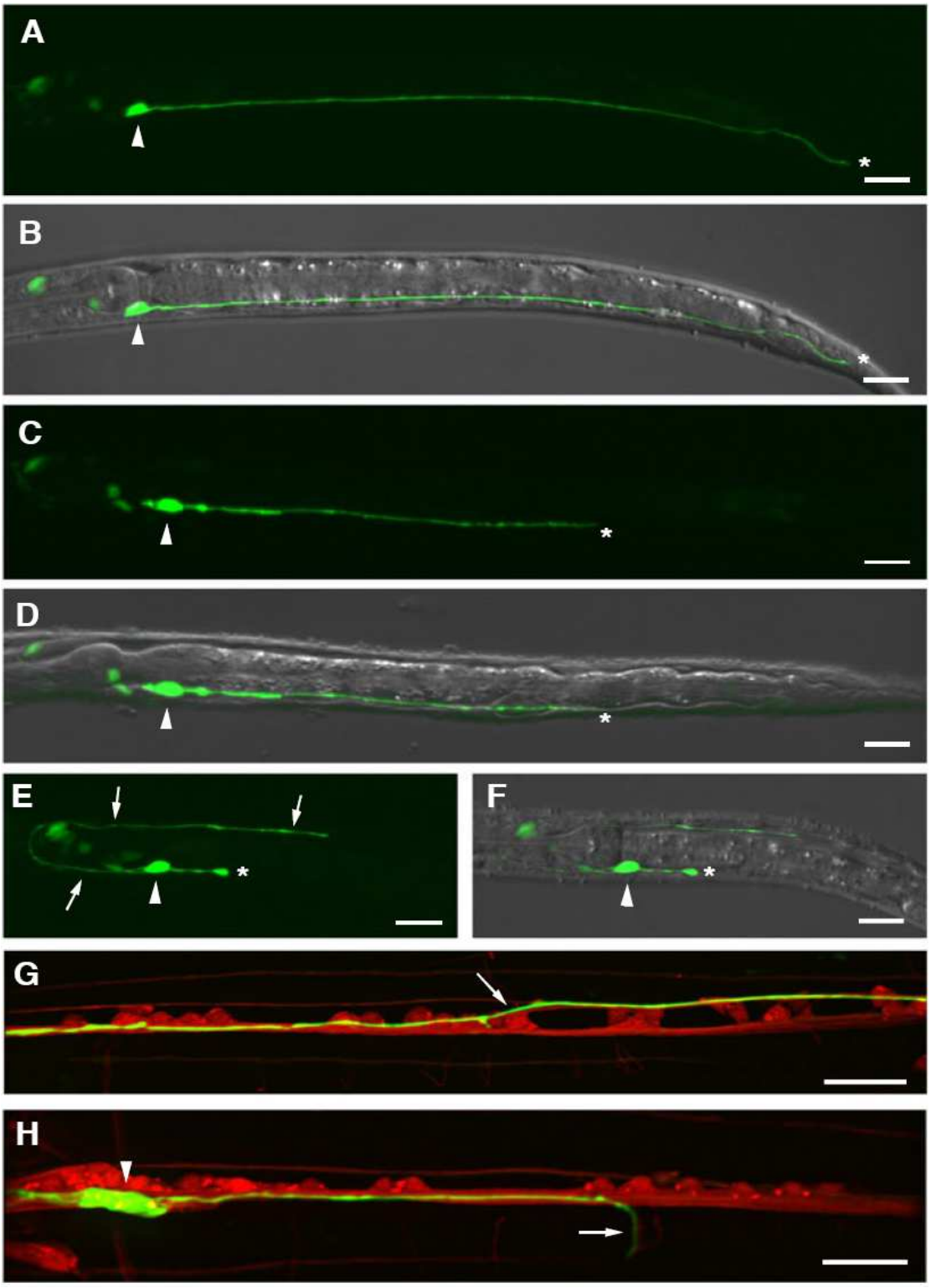

Figure 2.1 AVG defects in *plr-1(hd129)* mutant animals

(A, B) wild type L1, side view; the AVG cell body (arrow head) is located at the anterior end of the ventral nerve cord. The axon extends along the entire length of the animal on the ventral side and terminates in the tail region (asterisk). (C, D) In *plr-1*(*hd129*) mutant animals the AVG cell body is in its normal position (arrowhead), but the axon stops prematurely (asterisk). (E, F) In *plr-1*(*hd129*) mutant animals AVG sends out a short posterior process (asterisk) and a long anterior process that grows into the head (arrows), indicating a reversal of cell polarity. (G) In *plr-1*(*hd129*) mutant animals the AVG axon crosses the midline and joins the left ventral cord axon tract (arrow). (H) In some mutant animals the AVG axon leaves the ventral nerve cord (arrow). (A, C, E) GFP channel. (B, D, F) overlay of Nomarski and GFP channel. (G, H) overlay of GFP and DsRed channels. Scale bar: 20 µm. marker used: *otIs182* (*inx-18::GFP*) for AVG (green) and *evIs111* (*rgef-1::DsRed*) as panneuronal marker in panel G, H.

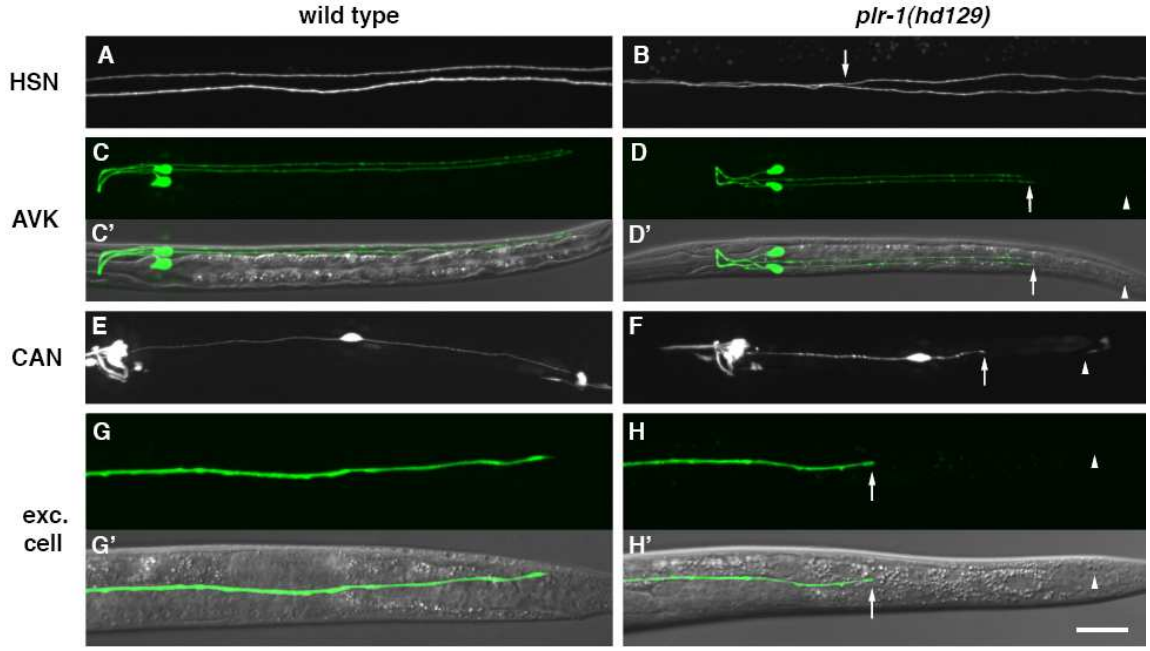

Figure 2.2 Other neuronal and non-neuronal defects of *plr-1(hd129)* mutant animals

Panels (A, C, C', E, G, G') are wild type and panels (B, D, D', F, H, H') are *plr-1(hd129).* In wild type animals HSN axons grow on both tracts of the ventral nerve cord and never cross the midline (A) but in *plr-1(hd129)* mutant animals HSN axons cross the midline as shown by arrow (B). In wild type animals AVK axons run on the contralateral sides of ventral nerve cord and terminate in the tail (C) and (C') whereas in *plr-1(hd129)* mutant animals AVK axons terminate prematurely past vulva (D) and (D'). In wild type animals CAN cell body is positioned laterally at the vulval region and sends out two processes in opposite directions. The posterior process terminates at the anus (E) whereas in *plr-1(hd129)* mutant animals CAN posterior process terminates prematurely between vulva and anus (F). In wild type animals excretory canal terminates at the anus (G) and (G') whereas in *plr-1(hd129)* mutant animals excretory canal terminates prematurely past vulva (H) and (H'). Arrow indicates the premature termination site and arrow head indicates the actual termination site. Fluorescent markers used: AVG marker *(odr-2::tdTomato),* AVK marker *(flp-1::GFP),* CAN marker *(pceh-23::GFP),* HSN marker *(tph-1::GFP)* and excretory canal marker *(pgp-12::GFP).* Scale bar: 20 µm.

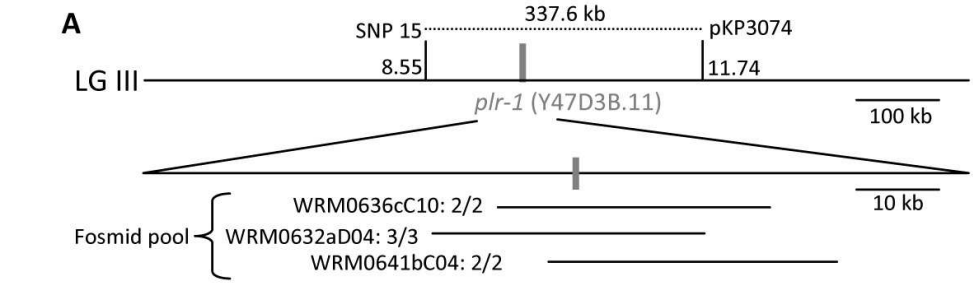

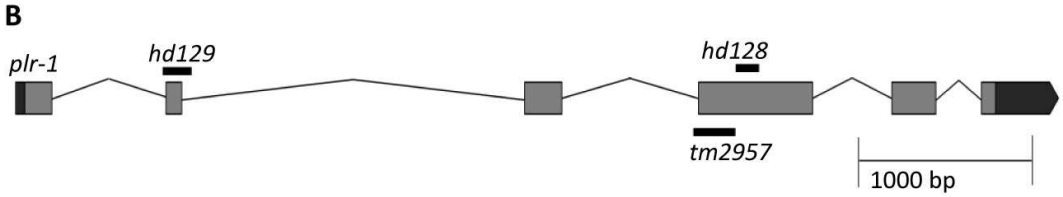

C

signal sequence

```
1    MRLLLFILLNTTLLSTNYVHARPSVSHTTLASQFKFAEKADIFVTHTNIN
                    hd129: deletion
51   EDRTQDEKTIKLSGTFSPVGSNYETGGDIVQVSSFRACDARRKGLDNTVF
101  EHVPVVFYDDVEKFLTGCVALDNQARFAEKSGAMALIVGPASRVERTTRP
                    tm2957: deletion
151  MMIGGSKIPVIVLDDEQTERLRSELRSASERGAVTKLRISFIDEKPTKVL
                                    hd128: inframe deletion
201  KLQVFRPTVLNITLLGLLIILIVFVSLLVVVKIRCQPTMHRELWLRALAR
          transmembrane region
251  TALTKMEIRSFQKEKNVEAGQKKKTSSTFARLKQHRSSSSRHSSYLAVFG
                                RING finger
301  SLTSVAQSSSHSAQERCVICLEEYEEGTELRVLFCGHEFHPKCVDPWLLS
351  KRRCPLCQFDVVYKHYPKVDSPEKLSGRSDDTTSLLPRTSPSEDLPSAPS
401  SRSTRLTRPYRTTHHLIPSSTRPSSHQRPSLQPTAPRTRSCPRRRQLRSR
451  NQIDFSIRIGGYSSDVSSSHAEQSRSFEIEPRTSQQL
```

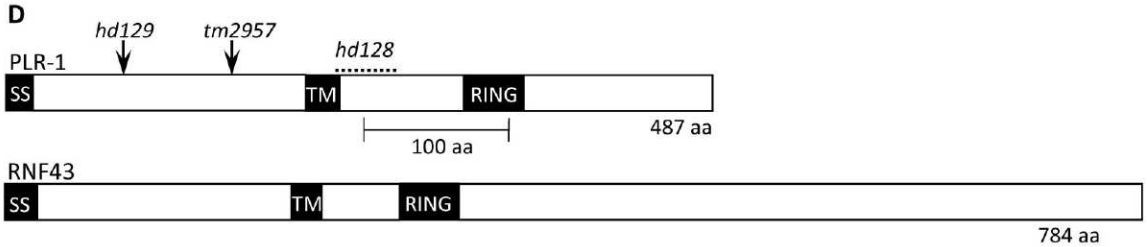

Figure 2.3 Molecular analysis of *plr-1*.

(A) Schematic drawing of the genomic region on the chromosome III (LG III) containing the *plr-1* gene. Numbers next to fosmid names (e.g. WRM0636cC10) indicate the fraction of transgenic lines rescuing the *plr-1* defects (e.g. 2/2) . “Fosmid pool” refers to a mixture of all the fosmids used for the initial resue. The only gene contained in all fosmids is Y47D3B.11 (B) Gene model for *plr-1* with exons shown by light gray shaded boxes. The black shaded boxes in the beginning and end represent the 5′ and 3′ UTRs respectively. The location of alleles used in this study is indicated by black bars. *hd129* is a 159 bp deletion removing whole exon 2 and adjoining parts of intron 1 and intron 2, which changes the reading frame and leads to the formation of stop codon. *tm2957* is a 239 bp deletion in the beginning of axon 4 which also changes the reading frame and leads to the formation of a stop codon. *hd128* is a 132 bp inframe deletion within axon 4. (C) PLR-1 amino acid sequence highlighting the signal sequence (SS), transmembrane (TM) and RING domains based on SMART analysis (http://smart.embl-heidelberg.de). Changes induced by *plr-1* mutations are also indicated. The *hd129* and *tm2957* deletions create frameshits and would lead to premature stop codons leading to truncated proteins of 79 aa and 154 aa respectively. (D) Domain structure of PLR-1 and vertebrate homologue RNF43. The positions of mutations are also indicated.

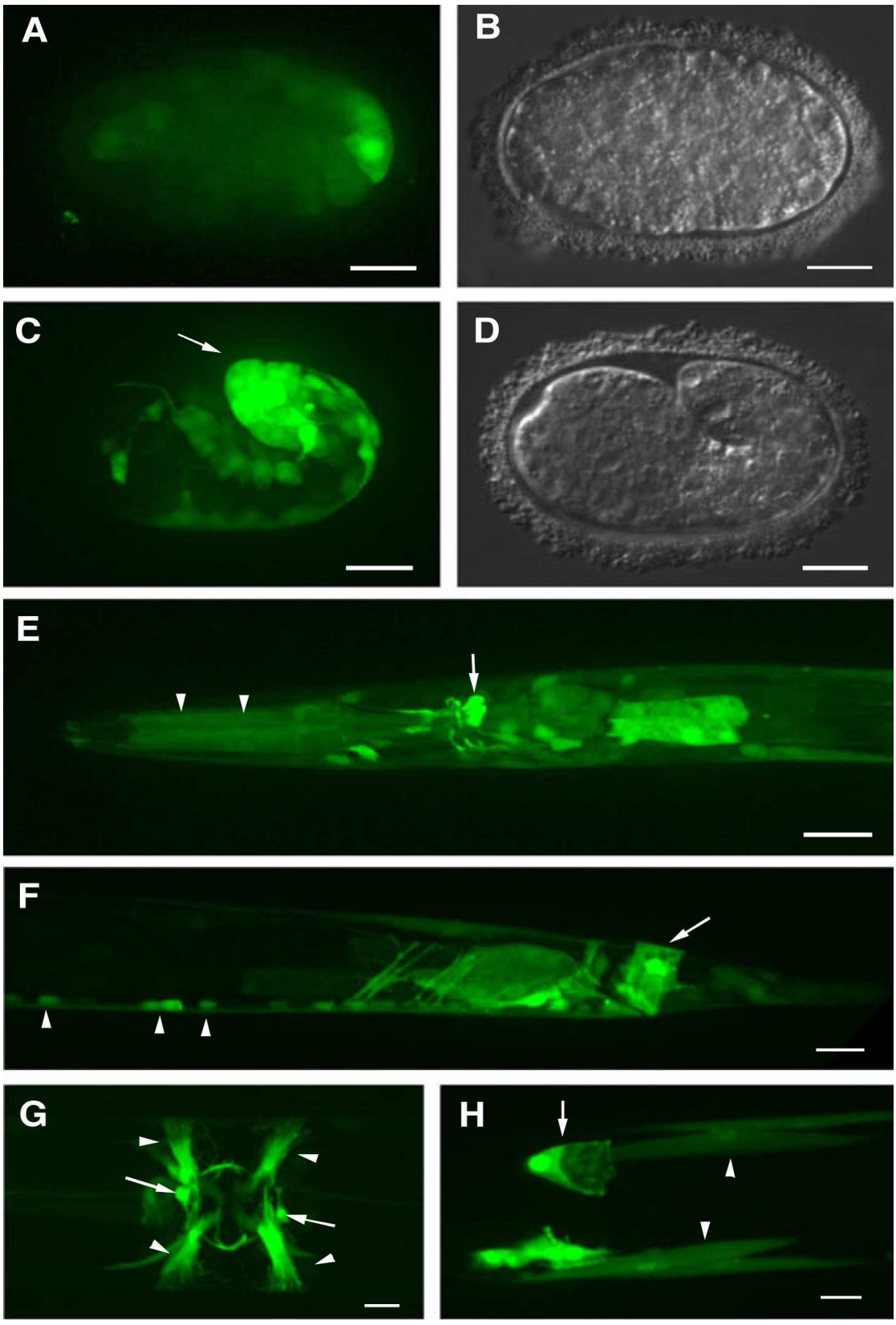
A
B
C
D
E
F
G
H

Figure 2.4 Expression pattern of a *plr-1*::GFP transcriptional reporter construct

(A, B) late gastrulation stage embryo. GFP is expressed in a large number of cells throughout the embryo. Posterior cells express GFP more strongly. (C, D) 1½ fold stage embryo. Expression is strongest in the tail region in hypodermal and muscle cells (arrow). (E) In larvae expression is seen in a few neurons in the head (arrow), the marginal cells in the pharynx (arrowheads) as well as hypodermal cells. (F) In the tail region of larvae expression is seen in motor neurons in the ventral nerve cord (arrowheads) and the anal depressor muscle (arrow). (G) In the vulva region expression is seen in the VC4 and VC5 neurons (arrows) and the vulva muscle cells (arrowheads). (H) Expression is also seen in the distal tip cells of the developing gonad (arrow) and body wall muscle cells (arrowheads). (B, D) are Nomarksi images, the other panels are fluorescent confocal images. Scale bars: 10 µm (A-D), 20 µm (E-H).

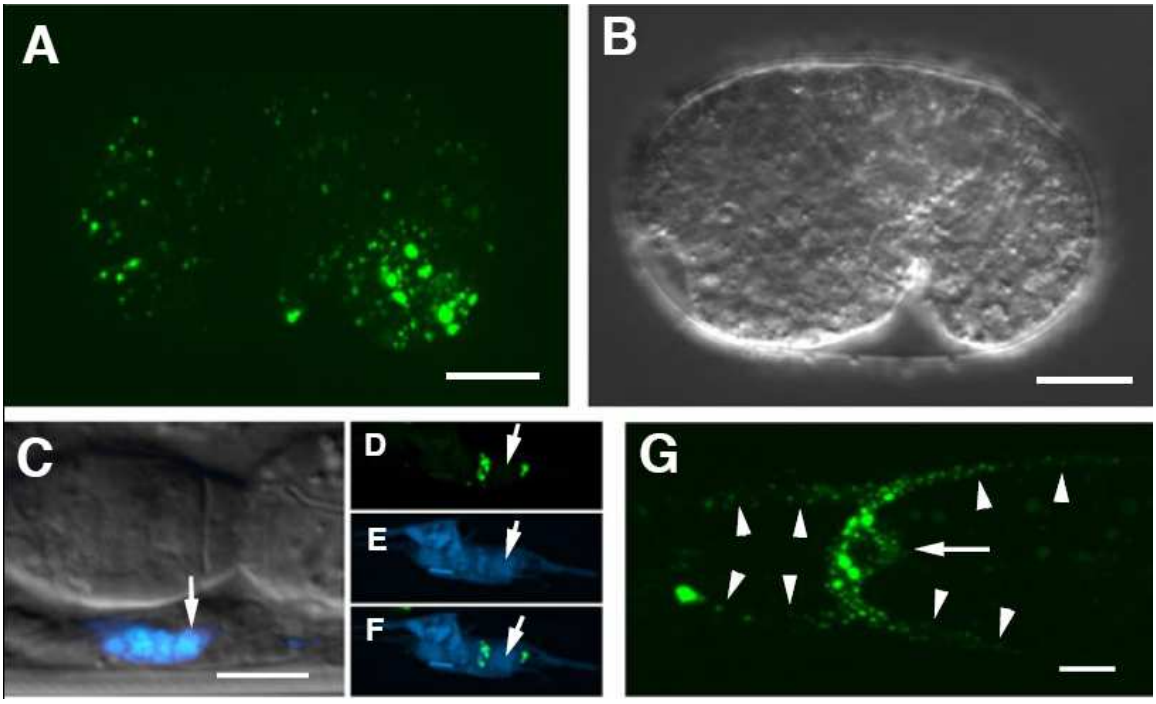

Figure 2.5 Expression pattern of a functional PLR-1::GFP protein fusion construct

(A, B) comma stage embryo. Expression is seen throughout the embryo with the strongest expression in the tail region. The PLR-1::GFP fusion protein is localized to variable-sized puncta throughout the cytoplasm. (C-F) In larval stages expression can be detected in the AVG neuron (arrowhead). (G) Expression is also seen in the excretory cell, where PLR-1::GFP puncta are concentrated in the cell body (arrow) and in anterior and posterior canal regions close to the cell body (arrowheads). (A, D, G), GFP channel, B Nomarksi, C close-up of the region, where the AVG cell body is located (overlay of Nomarksi and CFP channel, showing *odr-2::*CFP expression in RIF and AVG (arrow) cell bodies. (D-F) colocalization of PLR-1::GFP and *odr-2::*CFP in AVG (arrow). D, E single channel, F overlay. Scale bar: 10 µm.

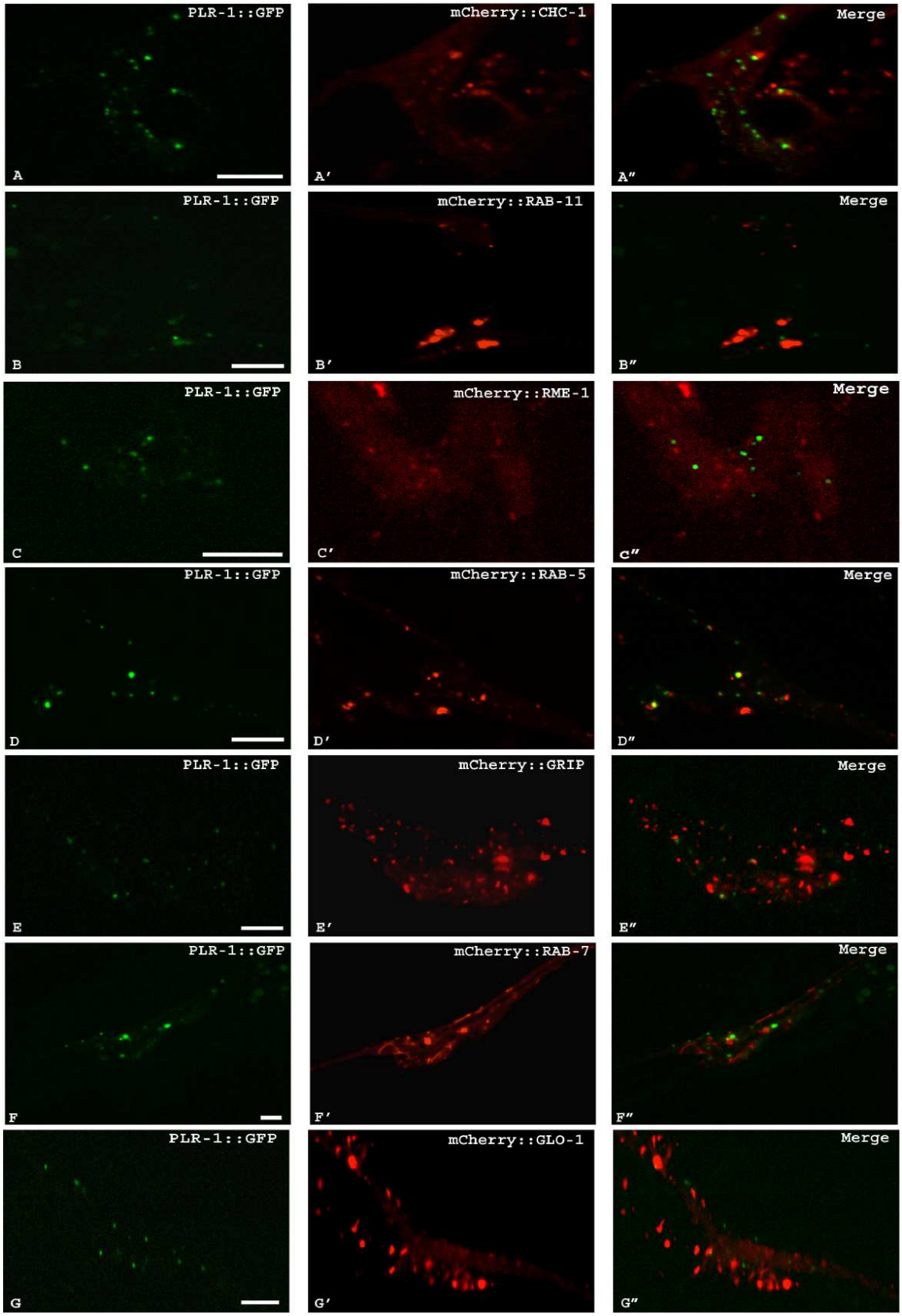
PLR-1::GFP
mCherry::CHC-1
Merge
A
A′
A″
PLR-1::GFP
mCherry::RAB-11
Merge
B
B′
B″
PLR-1::GFP
mCherry::RME-1
Merge
C
C′
C″
PLR-1::GFP
mCherry::RAB-5
Merge
D
D′
D″
PLR-1::GFP
mCherry::GRIP
Merge
E
E′
E″
PLR-1::GFP
mCherry::RAB-7
Merge
F
F′
F″
PLR-1::GFP
mCherry::GLO-1
Merge
G
G′
G″

Figure 2.6 Colocalisation of PLR-1 with various endocytotic pathway markers in excretory cell

Compound strains were made between PLR-1::GFP and each maker fused with mCherry labelling specific component of endocytotic pathway. Panel A, B, C, D, E, F and G are the fluorescent micrographs showing the expression of PLR-1::GFP in excretory cell in a region around cell body. Similarly panel A′, B′, C′, D′, E′, F′ and G′ are the fluorescent micrographs showing the expression of different endocytotic pathway markers fused with mCherry in the similar regions (example: A and A′ come from the same animal). Panels A″, B″, C″, D″, E″, F″ and G″ represent the merged fluorescent micrographs (example: A″ is the merged image of A and A′). Endocytotic markers used: CHC-1 (clathrin heavy chain), RAB-11 (recycling endosomes), RME-1 (recycling endosomes), RAB-5 (early endosomes), GRIP (golgi), RAB-7(late endosomes), and GLO-1 (lysosomes). Scale bar: 5µm.

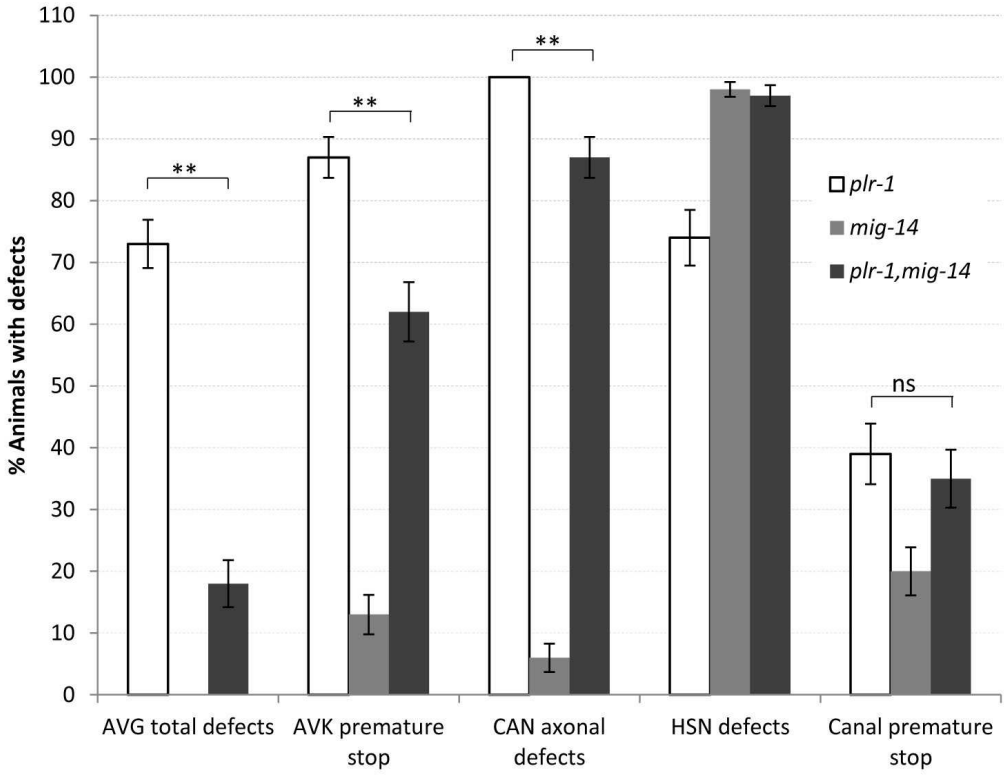

Figure 2.7 Suppression of AVG defects by *mig-14*

Columns are percentages of animals with defects (± standard error) with genotypes as indicated. Different types of defects are also indicated. For each strain $n > 100$ except *mig-14*; HSN (n =51) and *plr-1*; HSN (n=98) animals were analysed. χ^2 tests were used to determine whether double mutants are significantly different from the strongest single mutant (**: $p < 0.01$; ^{ns}: not significant). Mutant alleles used: *plr-1(hd129)* and *mig-14(ga62).* Fluorescent markers used: AVG marker *(odr-2::tdTomato),* AVK marker *(flp-1::*GFP*),* CAN marker *(ceh-23::* GFP*),* HSN marker *(tph-1::* GFP*)* and excretory canal marker *(pgp-12::* GFP*).*

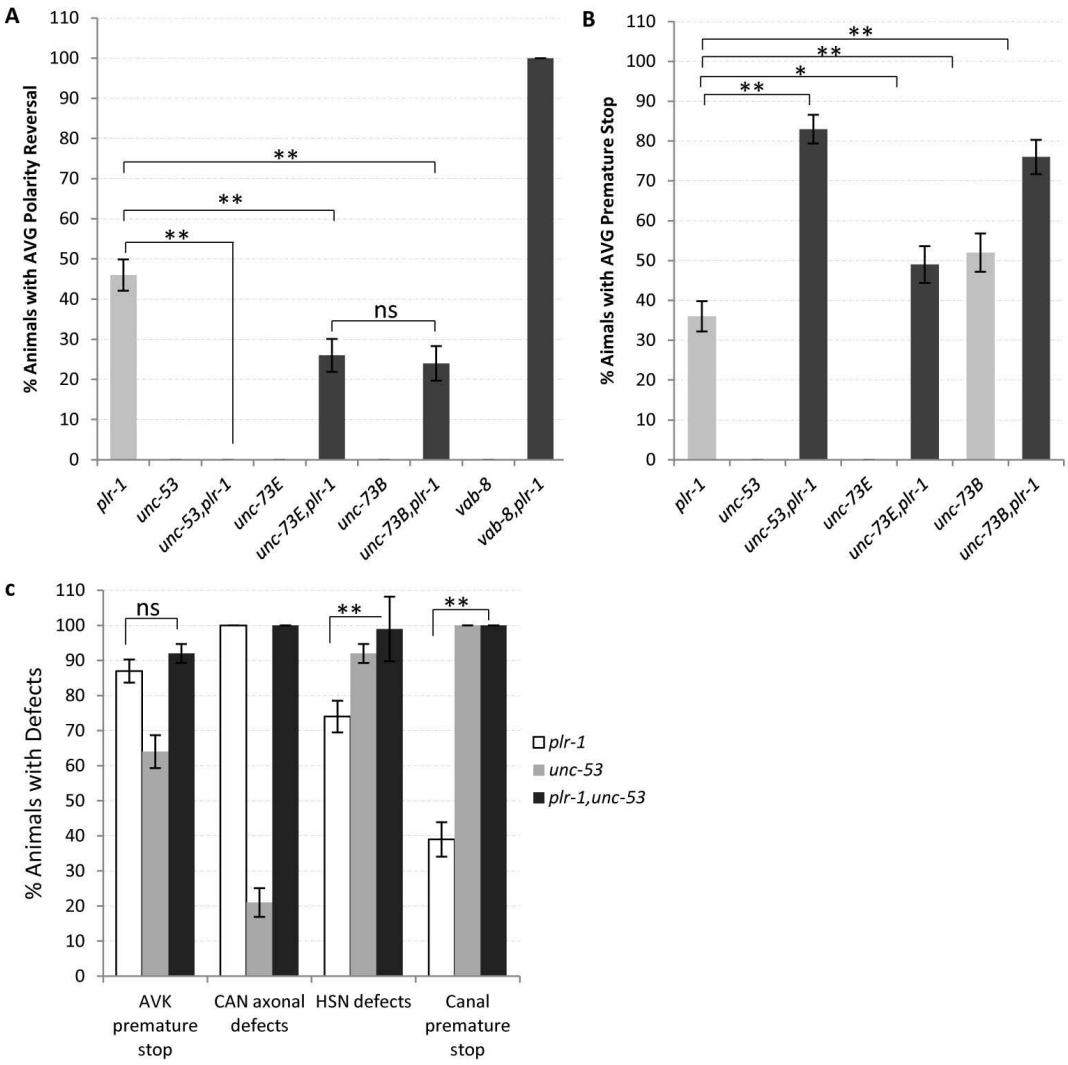

Figure 2.8 *plr-1* interacts genetically with *unc-53*, *unc-73* and *vab-8*

Columns represent percentage animals with (A) polarity reversal defects and (B) AVG premature stop defects (± standard error). (C) Shows the percentage of animals with indicated defects (± standard error) in other neuronal and non-neuronal cells. Genotypes are as indicated. For each strain $n \geq 100$ animals were analysed. $\chi 2$ tests were used to determine whether double mutants are significantly different from the stronger single mutant (*: $p < 0.05$; **: $p < 0.01$; ^{ns}: not significant). Mutant alleles used: *plr-1(hd129), unc-53(n116), unc-73E(ev802), unc-73B(rh40)* and *vab-8(e1017)*. Fluorescent markers used: AVG marker *(inx-18::GFP),* AVK marker *(flp-1::GFP),* CAN marker *(ceh-23::GFP),* HSN marker *(tph-1::GFP)* and excretory canal marker *(pgp-12::GFP)*.

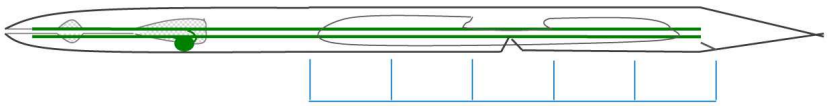

Genotype	Percentage EC termination					n	P Value	Versus
wt				3	97	210		
plr-1			6	18	76	204	< 0.01 **	*wt*
unc-53		31	69			212	< 0.01 **	*wt*
unc-53; plr-1		81	12			217	< 0.01 **	*unc-53*
vab-8		1	7	20	72	214	< 0.01 **	*wt*
vab-8; plr-1	1	16	22	27	34	207	< 0.01 **	*vab-8*
unc-73E				2	98	321	0.358 ns	*wt*
unc-73E; plr-1	1	5		2	92	230	< 0.01 **	*plr-1*
unc-73B	20	22	16	35	7	212	< 0.01 **	*wt*
unc-73B; plr-1	61	9	17	10	3	234	< 0.01 **	*unc-73B*

Figure 2.9 Genetic analysis of posterior excretory canal defects

For genetic interactions in excretory canals, scoring and analysis was done according to (Marcus-Gueret et al., 2012), also described in the materials and methods. Numbers in the boxes represent the percentage of excretory canal termination points in that region. Genotypes and the number of canals analysed are as indicated. χ^2 tests were used to determine statistical significance (**: $p < 0.01$; ^{ns}: not significant). Alleles used are: *plr-1(hd129), unc-53(n166), vab-8(e1017), unc-73E(ev802) and unc-73B(rh40).* Fluorescent marker used: *pgp-12::*GFP.

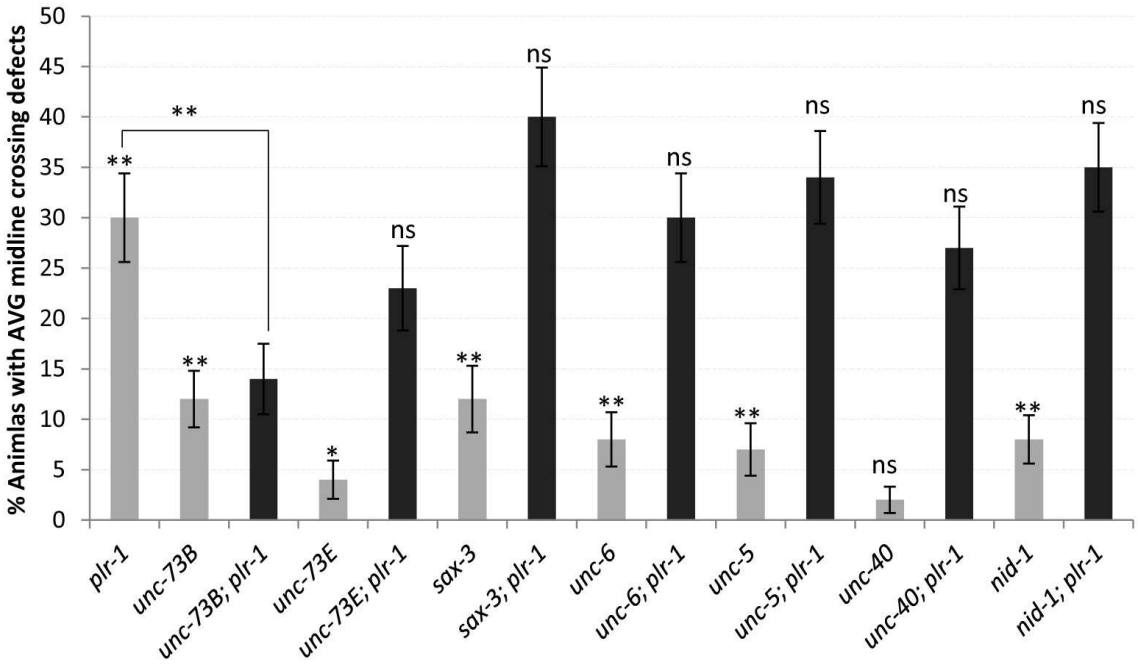

Figure 2.10 Genetic analysis of AVG midline crossing defects

For this analysis only those animals were counted in which the AVG axon extended beyond the vulva into the posterior half of the animal indicating normal polarity of AVG. Columns represent the percentage of animals with AVG midline crossing defects (± standard error) with different single mutants (light grey shaded) and *plr-1* double mutants (black shaded). For each strain $n \geq 100$ animals were analysed. χ^2 tests were used to establish statistical significance between the mutants. Single mutants were compared with wild type and double mutants were compared with *plr-1* single mutant (*: $p < 0.05$; **: $p < 0.01$; ^{ns}: not significant). Mutant alleles used: *plr-1(hd129), sax-3(ky123), unc-73E(ev802), unc-73B(rh40), ucn-6(ev400), unc-5(e53), unc-40(e271)* and *nid-1(cg119).* Fluorescent marker used: AVG marker (*odr-2::tdTomato)*.

2.7. Tables

Table 2.1 AVG defects in *plr-1* mutants (% animals with defects).

Phenotype	wild type	*plr-1(hd129)*	*plr-1(tm2957)*	*plr-1(hd128)*
marker: odr-2::tdTomato	*n*=117	*n*=139	*n*=69	*n*=135
premature stop[a]	0	52**	38**	17**
VNC cross-over[b]	0	18**	17**	15**
leaving VNC	0	3ns	3ns	0
no defect	100	27**	42**	68**
Marker inx-18::gfp	*n*=150	*n*=166	*n*=121	*n*=108
polarity reversal	0	46**	34**	7**
premature stop[c]	0	33**	21**	31**
leaving VNC	0	2ns	2ns	1ns
no defect	100	19**	43**	61**

[a] will include animals with polarity reversal.

[b] some animals have cross-over and premature stop defects.

[c] does not include animals with reversed polarity.

(**: $p < 0.01$; ns: not significant; $\chi 2$ test).

All mutant phenotypes are significantly different from wild type ($p<0.01$) except leaving VNC phenotype.

Table 2.2 Other neuronal defects in *plr-1(hd129)* mutant (% animals with defects)

Phenotype	wild type	*plr-1(hd129)*
HSN defects		
HSN migration defects[a]	5 (107)	26** (97)
HSN VNC cross-over defects[b]	16 (107)	48** (97)
CAN defects (posterior axons)		
premature stop[c]	0 (150)	82** (116)
navigation defect[d]	0 (150)	12** (116)
branching defect[e]	0 (150)	6** (116)
other defects		
premature stop of AVK axons[f]	0 (160)	87** (108)
premature stop of posterior excretory canals[g]	5 (104)	39** (103)

[a] at least one HSN neuron is located posterior to the vulva.

[b] only scored in animals without HSN migration defects.

[c] both posterior axons stop prematurely at variable positions.

[d] one axon makes a U-turn and grows anteriorly before stopping.

[e] one axon branches shortly before stopping prematurely.

[f] both AVK axons stop prematurely at variable positions posterior to the vulva.

[g] one or both excretory canals stop prematurely at variable positions posterior to the vulva.

Value in brackets indicates *n* (**: $p < 0.01$; χ^2 test).

Markers used: HSN *(tph-1::gfp)*, CAN *(ceh-23::gfp)*,AVK *(flp-1::gfp)* and excretory canal *(pgp-12::gfp)*

Table 2.3 Low penetrant neuronal defects in *plr-1(hd129)* mutant (% animals with defects)

Phenotype	wild type	*plr-1(hd129)*
Interneuron defects		
Premature stop	0 (101)	11** (131)
Navigation defect	0 (101)	5* (131)
Touch receptor neuron defects		
Ventral synapses missing	0 (110)	4* (92)
PLM premature stop	0 (110)	2^{ns} (92)
PVP and PVQ defects		
Navigation defects	7 (118)	8^{ns} (109)
Overextension	0 (118)	13** (109)
ASH neuron defects	0 (103)	0 (110)
RIF neuron defects	0 (103)	0 (111)
Motor neuron defects		
DD/VD	0 (110)	0 (72)
DA/DB	0 (85)	0 (105)
Commissures	0 (90)	0 (87)
Q neuroblast migration defects	0 (112)	0 (142)

Values in brackets indicate *n.*

(*: $p < 0.05$; **: $p < 0.01$; ^{ns}: not significant; χ^2 test).

Markers used: Interneuron *(glr-1::gfp),* Touch receptor *(mec-4::gfp),* PVP/PVQ/ ASH *(odr-2::cfp, sra-6::DsRed),* RIF *(odr-2::DsRed)*, DD/VD/commissures *(unc-47::DsRed-2),* DA/DB *(unc-129::cfp* and Q neuroblast migration *(F25B3.3::gfp).*

2.8. References

Banziger, C., Soldini, D., Schutt, C., Zipperlen, P., Hausmann, G., Basler, K., 2006. Wntless, a conserved membrane protein dedicated to the secretion of Wnt proteins from signaling cells. Cell 125, 509-522.

Brenner, S., 1974. The genetics of *Caenorhabditis elegans*. Genetics 77, 71-94.

Chitnis, A.B., Kuwada, J.Y., 1991. Elimination of a brain tract increases errors in pathfinding by follower growth cones in the zebrafish embryo. Neuron 7, 277-285.

Colavita, A., Krishna, S., Zheng, H., Padgett, R.W., Culotti, J.G., 1998. Pioneer axon guidance by UNC-129, a *C. elegans* TGF-beta. Science 281, 706-709.

d'Azzo, A., Bongiovanni, A., Nastasi, T., 2005. E3 ubiquitin ligases as regulators of membrane protein trafficking and degradation. Traffic 6, 429-441.

Durbin, R.M., 1987. Studies on the development and organisation of the nervous system of *Caenorhabditis elegans*. Cambridge, UK, p. 150.

Dyer, J.O., Demarco, R.S., Lundquist, E.A., 2010. Distinct roles of Rac GTPases and the UNC-73/Trio and PIX-1 Rac GTP exchange factors in neuroblast protrusion and migration in *C. elegans*. Small GTPases 1, 44-61.

Eisenmann, D.M., Kim, S.K., 2000. Protruding vulva mutants identify novel loci and Wnt signaling factors that function during *Caenorhabditis elegans* vulva development. Genetics 156, 1097-1116.

Gleason, J.E., Eisenmann, D.M., 2010. Wnt signaling controls the stem cell-like asymmetric division of the epithelial seam cells during *C. elegans* larval development. Dev Biol 348, 58-66.

Gleason, J.E., Szyleyko, E.A., Eisenmann, D.M., 2006. Multiple redundant Wnt signaling components function in two processes during *C. elegans* vulval development. Dev Biol 298, 442-457.

Goldstein, B., Takeshita, H., Mizumoto, K., Sawa, H., 2006. Wnt signals can function as positional cues in establishing cell polarity. Dev Cell 10, 391-396.

Goodman, C.S., 1996. Mechanisms and molecules that control growth cone guidance. Annu Rev Neurosci 19, 341-377.

Govek, E.E., Newey, S.E., Van Aelst, L., 2005. The role of the Rho GTPases in neuronal development. Genes Dev 19, 1-49.

Granato, M., Schnabel, H., Schnabel, R., 1994. *pha-1*, a selectable marker for gene transfer in *C. elegans*. Nucleic Acids Res 22, 1762-1763.

Green, J.L., Inoue, T., Sternberg, P.W., 2008. Opposing Wnt pathways orient cell polarity during organogenesis. Cell 134, 646-656.

Hao, H.X., Xie, Y., Zhang, Y., Charlat, O., Oster, E., Avello, M., Lei, H., Mickanin, C., Liu, D., Ruffner, H., Mao, X., Ma, Q., Zamponi, R., Bouwmeester, T., Finan, P.M., Kirschner, M.W., Porter, J.A., Serluca, F.C., Cong, F., 2012. ZNRF3 promotes Wnt receptor turnover in an R-spondin-sensitive manner. Nature 485, 195-200.

Hao, J.C., Yu, T.W., Fujisawa, K., Culotti, J.G., Gengyo-Ando, K., Mitani, S., Moulder, G., Barstead, R., Tessier-Lavigne, M., Bargmann, C.I., 2001. *C. elegans* slit acts in midline, dorsal-ventral, and anterior-posterior guidance via the SAX-3/Robo receptor. Neuron 32, 25-38.

Harris, J., Honigberg, L., Robinson, N., Kenyon, C., 1996. Neuronal cell migration in *C. elegans*: regulation of *Hox* gene expression and cell position. Development 122, 3117-3131.

Hedgecock, E.M., Culotti, J.G., Hall, D.H., 1990. The unc-5, *unc-6*, and *unc-40* genes guide circumferential migrations of pioneer axons and mesodermal cells on the epidermis in *C. elegans*. Neuron 4, 61-85.

Hedgecock, E.M., Culotti, J.G., Hall, D.H., Stern, B.D., 1987. Genetics of cell and axon migrations in *Caenorhabditis elegans*. Development 100, 365-382.

Herman, M.A., Vassilieva, L.L., Horvitz, H.R., Shaw, J.E., Herman, R.K., 1995. The *C. elegans* gene *lin-44*, which controls the polarity of certain asymmetric cell divisions, encodes a Wnt protein and acts cell nonautonomously. Cell 83, 101-110.

Hershko, A., Ciechanover, A., 1982. Mechanisms of intracellular protein breakdown. Annu Rev Biochem 51, 335-364.

Hershko, A., Ciechanover, A., Varshavsky, A., 2000. Basic Medical Research Award. The ubiquitin system. Nat Med 6, 1073-1081.

Hicke, L., Dunn, R., 2003. Regulation of membrane protein transport by ubiquitin and ubiquitin-binding proteins. Annu Rev Cell Dev Biol 19, 141-172.

Hidalgo, A., Brand, A.H., 1997. Targeted neuronal ablation: the role of pioneer neurons in guidance and fasciculation in the CNS of *Drosophila*. Development 124, 3253-3262.

Hilliard, M.A., Bargmann, C.I., 2006. Wnt signals and frizzled activity orient anterior-posterior axon outgrowth in *C. elegans*. Dev Cell 10, 379-390.

Hobert, O., 2002. PCR fusion-based approach to create reporter gene constructs for expression analysis in transgenic *C. elegans*. Biotechniques 32, 728-730.

Hutter, H., 2003. Extracellular cues and pioneers act together to guide axons in the ventral cord of *C. elegans*. Development 130, 5307-5318.

Ishii, N., Wadsworth, W.G., Stern, B.D., Culotti, J.G., Hedgecock, E.M., 1992. UNC-6, a laminin-related protein, guides cell and pioneer axon migrations in *C. elegans*. Neuron 9, 873-881.

Keynes, R., Cook, G.M., 1995. Axon guidance molecules. Cell 83, 161-169.

Klose, M., Bentley, D., 1989. Transient pioneer neurons are essential for formation of an embryonic peripheral nerve. Science 245, 982-984.

Koo, B.K., Spit, M., Jordens, I., Low, T.Y., Stange, D.E., van de Wetering, M., van Es, J.H., Mohammed, S., Heck, A.J., Maurice, M.M., Clevers, H., 2012. Tumour suppressor RNF43 is a stem-cell E3 ligase that induces endocytosis of Wnt receptors. Nature 488, 665-669.

Kubiseski, T.J., Culotti, J., Pawson, T., 2003. Functional analysis of the *Caenorhabditis elegans* UNC-73B PH domain demonstrates a role in activation of the Rac GTPase in vitro and axon guidance in vivo. Mol Cell Biol 23, 6823-6835.

Levy-Strumpf, N., Culotti, J.G., 2007. VAB-8, UNC-73 and MIG-2 regulate axon polarity and cell migration functions of UNC-40 in *C. elegans*. Nat Neurosci 10, 161-168.

Maes, T., Barcelo, A., Buesa, C., 2002. Neuron navigator: a human gene family with homology to *unc-53*, a cell guidance gene from *Caenorhabditis elegans*. Genomics 80, 21-30.

Maloof, J.N., Whangbo, J., Harris, J.M., Jongeward, G.D., Kenyon, C., 1999. A Wnt signaling pathway controls hox gene expression and neuroblast migration in *C. elegans.* Development 126, 37-49.

Marcus-Gueret, N., Schmidt, K.L., Stringham, E.G., 2012. Distinct cell guidance pathways controlled by the Rac and Rho GEF domains of UNC-73/TRIO in *Caenorhabditis elegans*. Genetics 190, 129-142.

Mattingly, B.C. & Buechner, M., 2011. The FGD homologue EXC-5 regulates apical trafficking in *C. elegans* tubules. *Developmental Biology*, 359(1), pp.59–72.

McConnell, S.K., Ghosh, A., Shatz, C.J., 1989. Subplate neurons pioneer the first axon pathway from the cerebral cortex. Science 245, 978-982.

Mello, C.C., Kramer, J.M., Stinchcomb, D., Ambros, V., 1991. Efficient gene transfer in *C.elegans*: extrachromosomal maintenance and integration of transforming sequences. Embo J 10, 3959-3970.

Merrill, R.A., Plum, L.A., Kaiser, M.E., Clagett-Dame, M., 2002. A mammalian homolog of *unc-53* is regulated by all-trans retinoic acid in neuroblastoma cells and embryos. Proc Natl Acad Sci U S A 99, 3422-3427.

Moffat, L.L., Robinson, R.E., Bakoulis, A., Clark, S.G., 2014. The conserved transmembrane RING finger protein PLR-1 downregulates Wnt signaling by reducing Frizzled, Ror and Ryk cell-surface levels in *C. elegans*. Development 141, 617-628.

Pan, C.L., Howell, J.E., Clark, S.G., Hilliard, M., Cordes, S., Bargmann, C.I., Garriga, G., 2006. Multiple Wnts and frizzled receptors regulate anteriorly directed cell and growth cone migrations in *Caenorhabditis elegans*. Dev Cell 10, 367-377.

Prasad, B.C., Clark, S.G., 2006. Wnt signaling establishes anteroposterior neuronal polarity and requires retromer in *C. elegans*. Development 133, 1757-1766.

Quinn, C.C., Pfeil, D.S., Wadsworth, W.G., 2008. CED-10/Rac1 mediates axon guidance by regulating the asymmetric distribution of MIG-10/lamellipodin. Curr Biol 18, 808-813.

Schmidt, K.L., Marcus-Gueret, N., Adeleye, A., Webber, J., Baillie, D., Stringham, E.G., 2009. The cell migration molecule UNC-53/NAV2 is linked to the ARP2/3 complex by ABI-1. Development 136, 563-574.

Shackleford, G.M., Shivakumar, S., Shiue, L., Mason, J., Kenyon, C., Varmus, H.E., 1993. Two wnt genes in *Caenorhabditis elegans*. Oncogene 8, 1857-1864.

Song, S., Zhang, B., Sun, H., Li, X., Xiang, Y., Liu, Z., Huang, X., Ding, M., 2010. A Wnt-Frz/Ror-Dsh pathway regulates neurite outgrowth in *Caenorhabditis elegans*. PLoS Genet 6.

Spencer, A.G., Orita, S., Malone, C.J., Han, M., 2001. A RHO GTPase-mediated pathway is required during P cell migration in *Caenorhabditis elegans*. Proc Natl Acad Sci U S A 98, 13132-13137.

Steven, R., Kubiseski, T.J., Zheng, H., Kulkarni, S., Mancillas, J., Ruiz Morales, A., Hogue, C.W., Pawson, T., Culotti, J., 1998. UNC-73 activates the Rac GTPase and is required for cell and growth cone migrations in *C. elegans*. Cell 92, 785-795.

Stringham, E., Pujol, N., Vandekerckhove, J., Bogaert, T., 2002. *unc-53* controls longitudinal migration in *C. elegans*. Development 129, 3367-3379.

Stringham, E.G., Schmidt, K.L., 2009. Navigating the cell: UNC-53 and the navigators, a family of cytoskeletal regulators with multiple roles in cell migration, outgrowth and trafficking. Cell Adh Migr 3, 342-346.

Tahirovic, S., Bradke, F., 2009. Neuronal polarity. Cold Spring Harb Perspect Biol 1, a001644.

Tessier-Lavigne, M., Goodman, C.S., 1996. The molecular biology of axon guidance. Science 274, 1123-1133.

Thorpe, C.J., Schlesinger, A., Carter, J.C., Bowerman, B., 1997. Wnt signaling polarizes an early *C. elegans* blastomere to distinguish endoderm from mesoderm. Cell 90, 695-705.

Tursun, B., Cochella, L., Carrera, I., Hobert, O., 2009. A toolkit and robust pipeline for the generation of fosmid-based reporter genes in *C. elegans*. PLoS One 4, e4625.

Watari-Goshima, N., Ogura, K., Wolf, F.W., Goshima, Y., Garriga, G., 2007. *C. elegans* VAB-8 and UNC-73 regulate the SAX-3 receptor to direct cell and growth-cone migrations. Nat Neurosci 10, 169-176.

White, J., Southgate, E., Thomson, J., Brenner, S., 1986. The structure of the nervous system of the nematode *Caenorhabditis elegans*. Phil. Trans. Royal Soc. London B. 314, 1-340.

Wightman, B., Clark, S.G., Taskar, A.M., Forrester, W.C., Maricq, A.V., Bargmann, C.I., Garriga, G., 1996. The *C. elegans* gene *vab-8* guides posteriorly directed axon outgrowth and cell migration. Development 122, 671-682.

Wolf, F.W., Hung, M.S., Wightman, B., Way, J., Garriga, G., 1998. *vab-8* is a key regulator of posteriorly directed migrations in *C. elegans* and encodes a novel protein with kinesin motor similarity. Neuron 20, 655-666.

Wu, Y.C., Cheng, T.W., Lee, M.C., Weng, N.Y., 2002. Distinct rac activation pathways control *Caenorhabditis elegans* cell migration and axon outgrowth. Dev Biol 250, 145-155.

Yamamoto, Y., Takeshita, H., Sawa, H., 2011. Multiple Wnts redundantly control polarity orientation in *Caenorhabditis elegans* epithelial stem cells. PLoS Genet 7, e1002308.

Yang, P.T., Lorenowicz, M.J., Silhankova, M., Coudreuse, D.Y., Betist, M.C., Korswagen, H.C., 2008. Wnt signaling requires retromer-dependent recycling of MIG-14/Wntless in Wnt-producing cells. Dev Cell 14, 140-147.

Chapter 3.

Identification of novel regulators of the AVG pioneer axon navigation in *C. elegans*

Abstract

Genetic screens are commonly used in model organisms to isolate mutants, which perturb a specific biological process. Once a mutant of interest is isolated, more mutants perturbing the same biological process can be isolated in modifier screens using existing mutants as a starting point. Enhancer screens in particular are powerful in identifying genes with redundant functions. In *C. elegans*, the AVG neuron pioneers the right axon tract of the ventral nerve cord and is important for its proper organisation. The molecular mechanism of AVG navigation is largely unknown as the known axon guidance mutants have only minimal AVG navigation defects. Moreover, direct screens have not yielded mutants with penetrant AVG navigation defects. We performed a semi-clonal enhancer screen in *nid-1*/Nidogen mutants, which have minimal AVG navigation defects and isolated 21 candidate mutants with penetrant AVG navigation defects. Out of these, the six mutants with the strongest AVG navigation defects were backcrossed and whole genome sequenced (WGS). The WGS revealed open reading frames with mutations in the candidate mutant strains. Some of these open reading frames represent genes with known roles in nervous system development. Complementation tests suggested that one of the candidate mutant, *hd148*, is an allele of *aex-3*. Further complementation tests, targeted mapping and detailed characterisation of the remaining candidate mutants will lead to the identication of genes involed in AVG navigation. Future detailed characterization of these genes will shed light on the molecular mechanism of AVG navigation.

3.1. Introduction

The model organism *Caenorhabditis elegans* is suitable for isolation and characterisation of new mutants mostly because of its hermaphroditic mode of life and short generation time. Genetic screens are designed to identify mutants that specifically disrupt the biological process of interest (Jorgensen & Mango, 2002). The first genetic screens in *C. elegans* were performed by Sydney Brenner where he isolated more than 500 mutants with visible phenotypes (Brenner, 1974). Since then genetic screens have been widely used to identify the genes associated with various biological processes. The common mutagenising agent used for this purpose is ethyl methanesulphonate (EMS) which induces mutations in the gametes (sperms and oocytes) of the wild type hermaphrodite. EMS usually induces point mutations which are mostly transitions where the original G:C pair is replaced by the A:T pair in the DNA. In *C. elegans*, the mutants isolated from the genetic screens are usually recessive and dominant mutations are rare (Jorgensen & Mango, 2002).

In simple forward genetic screens, which is the most common and straightforward method of identifying the genes, the parent hermaphrodite is mutagenised and then allowed to multiply for two generations. The F2 animals are picked on the basis of the phenotype of interest, mapped and further characterised in detail (Brenner, 1974). Once a gene or genes in a particular biological process defining a genetic pathway are identified, more genes are then identified by using modifier screens. These can be either suppressor or enhancer screens. The starting point for suppressor/enhancer screens is the mutant which perturbs a particular biological process. The second-site mutations either suppress or enhance the phenotype and thus identify genes that are involved in the same biological process. The suppressor screens are important and help in the identification of the key regulatory genes. However, enhancer screens are becoming more important than suppressor screens because they are generally more applicable and powerful and can uncover genes with redundant functions (Jorgensen & Mango, 2002).

In *C. elegans*, the VNC is the major longitudinal axon bundle which houses the essential components of the motor circuit (White et al., 1986). The formation of VNC starts in the embryo when AVG neuron extends an axon which pioneers the right axon tract (Durbin, 1987; also see chapter 1) and is required for its proper organization (Durbin, 1987; Hutter, 2003). The molecular mechanism of AVG axon navigation is largely unknown as the available axon guidance mutants do not display penetrant AVG axon guidance defects (Hutter, 2003). The earlier forward genetic screens performed in our laboratory only yielded alleles of *plr-1* (Bhat et al., 2015). RNAi for tested genes did not work in the AVG neuron even if we used the RNAi hypersensitive backgrounds (Calixto et al., 2010), hence limiting the scope of large scale genome-wide RNAi screen. Moreover, the earlier screens were performed in a non-clonal manner. In non-clonal screens a large number of mutagenised genomes can be screened quickly. However mutants with incompletely penetrant defects are difficult to find under these screening conditions. Furthermore, even a low background of animals with some AVG defects in the marker strain used for screening can make it difficult to identify novel mutations. I therefore chose to do a semi-clonal screen. While this increases the amount of time required for screening, it allows me to identify mutations with incompletely penetrant defects.

We performed a semi-clonal enhancer screen in a *nid-1*(*cg119*) mutant background. *cg119* is a molecular null allele, which delets 3133 nucleotides from 1499 to 4631. No *nid-1* transcripts are detected in the mutant animals (Kang and Kramer, 2000). In *C. elegans*, *nid-1* encodes the sole homolog of nidogen (enactin) (Kim and Wadsworth, 2000; Kang and Kramer, 2000). *nid-1* mutants show 10% AVG cross-over defects in the VNC (also see chapter 4; Table 4.1). This provides a sensitized background as a starting point for the enhancer screen. *In vitro* studies have demonstrated that Nidogens form a scaffold by connecting laminin with collagen IV, and integrate other basement proteins and were thought to stabilize the basement membrane (Fox et al., 1991; Mayer and Timpl., 1994; Kohfeldt et al., 1998). However, in both mammals and *C. elegans*, nidogen is not required for basement membrane assembly (Murshed et al., 2000; Kim and Wadsworth, 2000; Dong et al., 2002; Schymeinsky et al., 2002) and mutations in the *C. elegans nid-1* gene have no effect on collagen IV assembly (Kang & Kramer, 2000). Therefore, *nid-1* mutant animals are fertile

and viable and are well suited for a genetic screen. In *C. elegans*, NID-1 is a ubiquitous basement membrane protein but is more abundant in selected regions including the ventral and dorsal nerve cords between the muscles and neurons (Kang and Kramer, 2000; Kim and Wadsworth, 2000). In *nid-1* mutant animals, the guidance and positioning of many axons in the longitudinal axon tracts is affected. This in general is unlikely due to abnormal basement membrane as there are many axons which are guided normally (Kim and Wadsworth, 2000). The molecular mechanism of NID-1 mediated axon guidance is unknown. Nidogen has been shown to bind other basement membrane components such as collagen IV, laminin, perlecans and fibulins *in vitro* (Fox et al., 1991; Mayer and Timpl., 1994; Kohfeldt et al., 1998). The blocking of nidogen binding sites on laminin by antibodies leads to axon navigation defects (Bonner & O'Connor, 2001). However, there is no evidence of NID-1 binding to known guidance cues or receptors. Therefore, it is possible that NID-1 acts a cue itself and binds to some unknown receptor. The other possibility is that NID-1 can act indirectly by changing the responses of the known guidance cues and receptors. For example, the SDQR axon migrates from ventral to the sub-lateral dorsal region and from there takes an anterior turn (Kim et al., 1999). This switch from circumferential to longitudinal migration is controlled by NID-1 that changes the response of SDQR axon, which initially is repelled by UNC-6/Netrin to the sublateral dorsal region and then guided anteriorly by NID-1 and UNC-40/DCC (Kim & Wadsworth, 2000). Moreover, laminin-1, a basement membrane protein which binds to nidogen (Fox et al., 1991; Mayer and Timpl., 1994; Yurchenco, 2011) has been shown to convert the Netrin-1 mediated attraction of growth cones into repulsion in cell culture (Höpker et al., 1999). Therefore, in this genetic screen we expect to identify genes which either act redundantly with *nid-1* or whose response is modified in the sensitized genetic background. The major goal of this screen is to identify and characterize genes regulating AVG axon navigation.

3.2. Materials and methods

3.2.1. Marker strain

The transgenic strain *hdIs51*[*odr-2::tdTomato, rol-6(su1006)*] X with the *nid-1(cg119)* V mutation was used for the enhancer screen. The *hdIs51*[*odr-2::tdTomato*] marker strain (Figure 3.1) driving the expression of *tdTomato* (red marker) under the *odr-2* promoter was made by Jie Pan in our laboratory. In *C. elegans odr-2* encodes for the Ly-6 (leukocyte antigen-6) related protein required for the olfaction and is expressed in sensory neurons, interneurons and motor neurons with axonal enrichment (Chou et al., 2001). In *hdIs51* transgenic animals, many cell bodies and axons in the head region as well as nerve ring are labelled. However, in the ventral nerve cord only AVG and the two PVP neurons are labelled which makes visible simultaneously both the right and the left axon tracts of ventral nerve cord (Figure 3.1). This enabled us to score guidance defects where the AVG axon, which is normally present in the right axon tract, by mistake crosses and extends into the left axon tract. These defects are referred to as AVG axon cross-over (AVG CO).

3.2.2. F2 semi-clonal enhancer screen

A standard EMS protocol (Brenner, 1974) with some modification at the level of mutant selection was followed for the mutagenesis. L4 worms were treated with EMS (50 mM) for 1 hr and after a recovery time of about 4 hrs to overnight, young healthy adults (P0 generation) were picked and cultured on 60 mm x 15 mm NGM plates, with 9 P0 animals on each plate and 30 plates total for two generations. From these plates individual F2 worms were transferred onto separate 60 mm x 15 mm NGM plates for selfing. Plates with a sufficient (> 100) number of animals were screened for AVG cross-over defects under a fluorescence dissecting microscope (LEICA MZ12). The plates where a significant (> 10) number of worms showed AVG cross-over phenotype were further examined. The AVG cross-over phenotype was confirmed and quantified by high magnification fluorescence microscopy (Zeiss Axiscope) under a 40x objective in adult animals. After screening 2400 haploid genomes, 21 candidate mutants with penetrant AVG cross-over defects were isolated. The six selected candidate mutants were four

times backcrossed (4x) with *nid-1(cg119)* males to get rid of the unwanted background mutations.

3.2.3. DNA prepration and Whole Genome Sequencing (WGS)

The WGS was done in Dr. Don Moerman laboratory at UBC according to (Thompson et al., 2013), the protocol is briefly as follows: animals were cultured in 150 mm petri plates containing NGM medium seeded with *E. coli* χ 1666. The starved plates were washed with M9/Triton X-100 buffer and pelleted in sterile 15 ml centrifuge tubes, which were frozen at - 80 ℃. Later on genomic DNA was isolated from these thawed worm pellets by using the PureGene Genomic DNA Tissue Kit (Qiagen catalog number 158622), which was followed by a supplementary Qiagen protocol. The quantity and the quality of the DNA were determined by using nanodrop and electrophoresis respectively. For DNA library prepration a modified version of the Illumina sequencing protocol was used. 100µl microTube containing 3ug of genomic DNA in 85ul of 1x TE buffer were sonicated by Covaris to yiled 200-400 bp fragments. NEBNext end repair module was used to end-repair the sheared DNA. Agencourt AMPure XP beads were used to purify the end product. To generate 3' adenine overhangs, DNA products were incubated with 0.4mM dATP, 10mM MgCl2, and AmpliTaq DNA Polymerase kit. The beads already present in the reaction were used to purify the product, which was followed by pre-annealed genomic DNA Illumina adapters containing 5' thymine overhangs. After purifying the products with 1x binding buffer and removing the solution from the beads, the adapter-ligated products were PCR-amplified with Kapa Hifi DNA Polymerase using Illumina's paired end genomic DNA. The 300-400 bp fragments of DNA were excised from the 6% polyacrylamide gels and purified with 0.9x Agencourt AMPure beads. DNA quality and quantity was assessed by using Agilent HS series assay and dsDNA HS Qubit assay. Sequencing was done on HiSeq following manufacturer's instructions. Raw sequencing data for all the six candidate mutant strains was generated by extracting the sequences form the resulting image files by using manufactures software. Custom Perl scripts were used to convert sequences passing the Illumina quality filter into fastq format and demultiplexed, allowing a single base change with respect to the known barcodes used in each lane. Sequene coverage was between 24-fold and 48-fold. After comparing the sequences with the reference genome (WS230) and subtraction of

common SNPs found in more than one of the six strains (likely background mutations), lists of unique mutation in the coding part of the genome were generated for each candidate strain.

3.3. Results and discussion

3.3.1. Candidate mutants show highly penetrant AVG navigation defects

In wild type, the AVG axon extends into the right axon tract from the anterior side, terminates in the tail region and never crosses the ventral midline (Figure 3.1). In the candidate mutant animals the AVG axon makes mistakes and crosses the midline and extends into the left axon tract. By performing a F2 semi-clonal enhancer screens in a *nid-1; hdIs51* background, we isolated 21 candidate mutants with penetrant AVG cross-over defects. The *nid-1* single mutants display 10% AVG cross-over defects. The penetrance of defects in the candidate mutants is enhanced with some candidates displaying more that 50% AVG cross-over defects. The detailed phenotypic characterisation of the candidate mutants prior to outcrossing is presented in table 3.1. Apart from the AVG cross-over defects, the candidate mutants were superficially characterised for visible phenotypes. The most common phenotypes shown by the candidate mutants are mild uncoordinated (Unc) and mild dumpy (Dpy) (Table 3.1) (Brenner, 1974). In addition some candidate mutants also had egg-laying (Egl) defects and a protruding vulva. For example, the most severe phenotypes are shown by the candidate mutants *hd144*, *hd145*, *hd147*, which are Unc and Egl with protruding vulva (Table 3.1). These defects are most likely independent from the AVG cross-over defects. Uncoordinated behaviour is the impairment in the movement of the animal and is mostly associated with the mutations in the genes, which regulate the development and function of the nervous system (Brenner, 1974; Hedgecock et al., 1990; Ishii et al., 1992; Leung-Hagesteijn et al., 1992; Chan et al., 1996). The egg-laying defect is the inability of the animals to lay eggs which instead are retained inside the body of an organism. The egg laying behaviour is controlled by the coordination between hermaphrodite specific neurons, which comprise of two HSN motor neurons and six VCs (VC 1-6) neurons with the vulval muscles. Any disruption in this circuitry leads to the egg-laying defects (Trent

et al., 1983; Desai et al., 1988; Schafer, 2005). Therefore, it is possible that these mutants represent the genes with pleiotropic functions and are likely involved in the multiple genetic pathways. The other candidate mutants are mild Unc Dpy *(hd136* and *hd142),* mild Unc (*hd140*, *hd151* and *hd153),* or mild Dpy (*hd139, hd143, hd149, hd150, hd154* and *hd155*). Many *dpy* genes are present in *C. elegans*, which mostly affect cuticular development or structure (Brenner, 1974; von Mende et al., 1988; Johnstone et al., 1992). It is possible that some of these non-neuronal phenotypes, e.g. Dpy, are due to additional background mutations and might disappear after outcrossing. A few of the candidate mutants (*hd137, hd138, hd146, hd152*) are wild type which suggests that some amount of miswiring in the nervous system can be tolerated. Although the screen was not baised towards any behavioral or visible plate phenotype, we may have missed slow growing, strong Unc and embryonic lethat mutants.

3.3.2. Sequencing revealed the open reading frames with mutations in the candidates

Six candidate mutants (allele names: *hd141, hd142, hd144, hd148, hd152, hd153*) with highly penetrant AVG cross-over defects were chosen for further analysis (Table 3.2). To get rid of the unwanted background mutations, these six candidate mutants were backcrossed four times (4x) with *nid-1* males and the mutants were recovered on the basis of the AVG cross-over phenotype (Table 3.2). *nid-1* males were used for backcrossing because all the candidates were isolated in a *nid-1* mutant background. After backcrossing the entire genome of the six candidate strains was sequenced (WGS) which is a quick way of identifying all mutations present in the strains (Zuryn et al., 2010; Doitsidou et al., 2010). This revealed gene with changes in their open reading frames (ORFs) and their chromosomal location in the candidate mutant strains. Moreover, the positions and the types of the nucleotide changes as well as the corresponding amino acid changes are also revealed. The results are presented in separate tables for each candidate mutant strain, *hd141* (Table 3.3), *hd142* (Table 3.5), *hd144* (Table 3.4), *hd148* (Table 3.7), *hd152* (Table 3.6) and *hd153* (Table 3.8). Each strain has some open reading frames with changes linked to the X-chromosome. This is because the marker *hdIs51* used for the screen is located on the X-chromosome and as a consequence mutations on the X-chromosome are not efficiently outcrossed. To

determine wether the candidate mutation is present on the X-chromosome or not, we crossed these six strains with *nid-1* males and analysed the phenotype of F1 males. *C. elegans* is a diploid (2n) organism and the difference between hermaphrodites and males lies in the number of sex chromosomes. Hermaphrodites have two sex chromosomes (XX) and males have only one sex chromosome (XO). Therefore, mutations in recessive genes which are recessive which are X-linked show the phenotype in F1 males but not in F1 hermaphrodites. The F1 males of only one candidate *(hd148)* showed AVG cross-over phenotype similar to that of the parent mutant, suggesting that *hd148* is located on the X-chromosome (Table 3.9). For other mutants, F1 male AVG cross-over defects are below 10% similar to that of *nid-1* mutants, suggesting that the causative mutation is not linked to the X-chromosome (Table 3.9). This result was surprising *hd153*, which displays only few open reading frames with changes on the X-chromosome and has no candidates outside the X-chromosome (Table 3.9). It is possible that *hd153* is a deletion or a point mutation in some regulatory element outside the coding part of the gene. The genome sequence data will be re-examined for such changes in *hd153*.

3.4. Future directions

The WGS revealed the list of the open reading frames with changes for each candidate mutant as mentioned above. The next step is to identify the mutation causing the phenotype for each candidate. The list of mutations includes a few genes with known roles in axon guidance or nervous system development or development in general (Table 3.10). For example, the WGS of the candidate mutant *hd148* revealed 10 ORFs with changes (Table 3.7) linked to the X-chromosome (Table 3.9). Among these, *aex-3* and *sax-1* are involved in synaptic transmission (Iwasaki et al., 1997) and axonal outgrowth (Zallen et al. 2000) respectively (Table 3.10). This indicates that there is a possibility that one of these two genes could turn out to be the *hd148* candidate gene. To confirm this we carried out a complementation test. In a complementation test the candidate mutant and the tester mutant are crossed and the phenotype of the F1 heterozygote is analysed. If the phenotype of the F1 heterozygote is similar to the candidate or the tester mutant, the two mutations in question do not complement each

other, meaning that they are the same gene. However, if the phenotype of the F1 heterozygote is wild type, the two mutations in question complement each other, meaning that they are not alleles of the same gene (Brenner, 1974). We did a complementation test of the *hd148* candidate mutant against *aex-3* and *sax-1*. We found that *hd148* did not complement *aex-3*, suggesting that *hd148* is an allele of *aex-3*. Moreover, *hd148* did complement *sax-1* excluding the latter as the possible candidate. Known alleles of *aex-3* (*n2166, sa5, js815*) (Thomas, 1990; Iwasaki et al., 1997; Mahoney et al., 2006) also displayed the AVG cross-over defects in the *nid-1* mutant background (see also chapter 4; Table 4.1) and an *aex-3* containing fosmid rescued the AVG cross-over defects in the mutant background. This further proved beyond any doubt that *hd148* is an allele of *aex-3*. AEX-3, which is a guanine nucleotide exchange factor (GEF) for RAB-3 GTPase, is discussed in chapter 4. Similarly some of the other candidates also have mutations in genes with known roles in nervous system or general development (Table 3.10). For example, the candidate *hd141* revealed a change in *lam-1*, *hd142* in *unc-105* and *ram-2* and *hd152* in *cdh-4.* In *C. elegans*, CDH-4 is a FAT-like cadherin which is involved in many aspects of development including axon fasciculation (Schmitz et al., 2008). *lam-1* encodes for the single β chain of laminin (Hutter et al., 2000) which is a basement membrane component and laminin in general is required during development (Huang et al., 2003; Kramer, 2005). *unc-105* encodes for a putative mechanosensory membrane channel, which interacts with the type IV collagen (LET-2) in the extracellular matrix underneath the muscles (Liu et al., 1996) and LET-2 is required during embryogenesis (Sibley et al., 1994). *ram-2* encodes for a cuticular collagen which affects ray cell migration and embryonic viability (www.wormbase.org). There is a possibility that some of these are the potential phenotype causing mutations. To determine whether this is the case a similar strategy for what we used for *hd148* would be followed. First we will do complementation tests with known mutants e.g. the candidate *hd152* will be tested against the *cdh-4* gene. If *hd152* indeed turns out to be an allele of *cdh-4* in the complementation test, the next step would be to test the known alleles of *cdh-4* (Schmitz et al., 2008) for AVG cross-over defects. This would be followed by testing the *chd-4* containing fosmid for the rescue of AVG cross-over defects in the *cdh-4* mutant background. This will lead to the quick identification of the phenotype causing mutations. The candidates that will complement the tester mutants will not be alleles of known genes and the ones (*hd144* and *hd153)*, which did not

display any gene with known roles in nervous system development (Table 3.10), could be novel regulators of AVG axon navigation. For them, since we know the chromosome location of the phenotype causing gene, targeted mapping using single nucleotide polymorphism (snip-SNP) markers will be carried out to narrow down the location of the gene. Fosmids containing the genes with changes in that region will be tested for the AVG cross-over rescue. This would lead to the identification of the genes which will be further analysed for expression pattern, protein localisation, genetic interactions and detailed phenotypic characterisation by using neuron specific markers.

3.5. Summary

We have carried out an enhancer screen for AVG axon guidance defects and have isolated 21 candidates with AVG CO defects. Out of these we have selected six candidates with highly penetrant defects for further characterisation. All the six candidates were backcrossed four times (4x) and whole genome sequenced. *hd148* turned out to be an allele of *aex-3* and was characterised in detail (see chapter 4). The future work would be characterising in detail the other candidates which would uncover more genes that mediate AVG navigation. This would shed light on the molecular mechanism and genetic pathways of AVG axon navigation.

3.6. Contributions

I performed the enhancer screen and was initially helped by the summer student Keri Ozsumanogiu. All the mutants were isolated by me. The screen was designed by me and HH. DNA library prepration and whole genome sequencing for all the six backcrossed mutant strains were done in Dr. Don Moerman's laboratory at UBC. I would like to thank Vinci Au for the sequencing and Stephane Flibotte for analysing the sequence data. This work was supported by CIHR grant (MOP 93719) to HH.

3.7. Figures

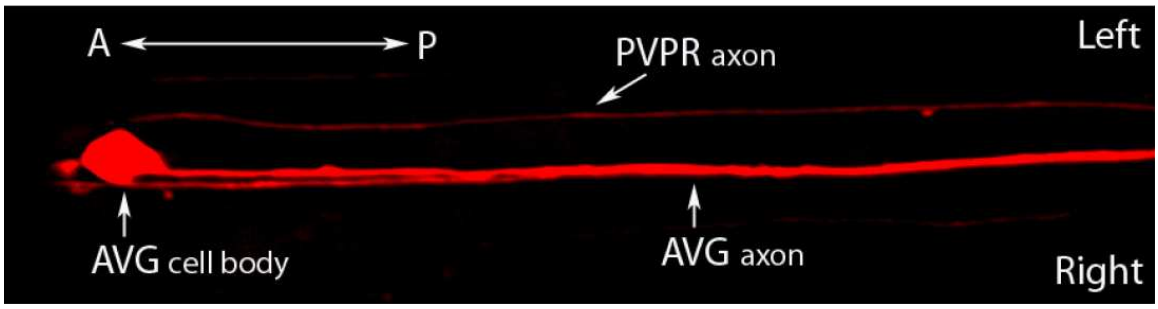

Figure 3.1 Marker strain used for the genetic screen

hdIs51 is a transgenic strain that labels both axon tracts of the VNC. The AVG cell body is present at the anterior side and extends an axon into the right axon tract of VNC. The PVPR neuron extends an axon into the left axon tract from the posterior side. Left and right sides are also indicated. Double headed arrow indicates anterior A: posterior P axis.

3.8. Tables

Table 3.1 List of isolated candidate mutants

Candidate	Strain name	Allele name	% AVG CO	Visible/Plate phenotypes
1a	VH2463	*hd135*	31 (101)	mild Dpy
1b	VH2464	*hd136*	36 (58)	mild Unc Dpy
8	VH2465	*hd137*	34 (64)	wild type
10a	VH2466	*hd138*	29 (104)	wild type
10b	VH2467	*hd139*	35 (101)	mild Dpy
1.1f	VH2468	*hd140*	27 (84)	some animals are mild Unc
1.1h	VH2469	*hd141*	42 (57)	wild type
9.1d	VH2470	*hd142*	45 (99)	mild Unc Dpy
9.1e	VH2471	*hd143*	31 (64)	some animals are mild Dpy
10.1b	VH2472	*hd144*	57 (122)	Unc, Egl with protruding vulva
10.1e	VH2473	*hd145*	45 (64)	Unc, Egl with protruding vulva
10.1f	VH2474	*hd146*	37 (75)	wild type
10.1i	VH2475	*hd147*	54 (72)	Unc, Egl with protruding vulva
10.1j	VH2476	*hd148*	57 (217)	Egl, lethargic and slow moving
18c	VH2477	*hd149*	30 (61)	mild Dpy
21f	VH2478	*hd150*	24 (37)	mild Dpy
22a	VH2479	*hd151*	41 (56)	mild Unc
22d	VH2480	*hd152*	50 (105)	wild type
22g	VH2481	*hd153*	48 (42)	mild Unc
28c	VH2482	*hd154*	27 (44)	mild Dpy
28j	VH2483	*hd155*	24 (41)	mild Dpy

The right column represents the candidate names initially assigned to the each isolated mutant. Numerical value represents the original P0 plate. The alphabets represent the candidates picked from the same P0 plate. For example, 10.1(b, e, f, i, j) means that all these F2's come from the same P0 plate i.e. 10.1. Later on each candidate mutant was assigned strain and allele names. The %age of animals with AVG CO and roughly description of the visible phenotype for each candidate mutant is also shown. The values in the brackets indicate *n*. Unc: Uncoordinated, Dpy: Dumpy, Egl: egg-laying defect, CO: cross-over.

Table 3.2 List of backcrossed mutants

Strain	Allele	% AVG CO (4x)
VH2496	*hd141*	50 (102)
VH2498	*hd142*	52 (124)
VH2497	*hd144*	52 (122)
VH2500	*hd148*	56 (97)
VH2499	*hd152*	46 (102)
VH2501	*hd153*	41 (105)

The six candidate mutants with highly penetrant AVG CO (cross-over) defects were selected and backcrossed four times. Strain and allele names along with the % AVG CO defects after four times (4x) backcrossing are shown. The values within the brackets indicate the *n*.

Table 3.3 Whole genome sequencing of *hd141*

Chromosome No.	Nucleotide position	Nucleotide change		Gene/ORF name	Amino acid change	
I	3939262	G	A	lrp-2	T	I
IV	5173419	G	A	lam-1	D	N
IV	8482896	G	A	spp-8	M	I
IV	10794059	G	A	pept-2	S	N
IV	11290532	G	A	F54D1.6	D	N
IV	12357782	G	A	sec-24.2	A	V
IV	13507717	G	A	seld-1	G	E
IV	17481322	G	A	4R79.2	T	M
X	644358	C	T	ifc-2	R	H
X	1976284	C	T	F52D2.6	L	F
X	2032211	C	A	Y102A11A.6	Affects_Splicing	
X	4703355	C	T	aqp-8	G	D
X	5176973	C	T	T03G11.3	Q	*

The strain name is VH2496. The table shows all the open reading frames (ORF) with changes and their chromosome location in the *hd141* candidate mutant background revealed by the whole genome sequencing. The positions and the types of nucleotide changes along with the amino acid changes are also indicated.

Table 3.4 Whole genome sequencing of *hd144*

Chromosome No.	Nucleotide position	Nucleotide change		Gene/ORF name	Amino acid change	
IV	1986704	C	T	Y76B12C.6	H	Y
IV	2247438	C	G	M70.1	N	K
IV	2355183	G	T	Y38F2AR.6	V	F
IV	4912491	C	T	Y9C9A.17	R	K
IV	6807952	G	A	C17H12.10	R	Q
IV	7485959	G	A	his-61	L	F
IV	10389771	G	A	spe-26	P	L
IV	13326246	G	T	fat-2	V	F
IV	17283720	C	G	nra-1	V	L
V	20325878	C	T	Y38H6A.1	P	S
X	177621	T	C	T08D2.4	Affects_Splicing	
X	1554233	G	C	K06A9.1	G	A
X	1559016	A	C	K06A9.1	K	Q
X	1559019	T	C	K06A9.1	S	P
X	7295190	C	G	Iron-7	T	S
X	8420155	T	A	tag-123	T	S
X	8421690	T	A	tag-123	N	Y

The strain name is VH2497. The table shows all the open reading frames (ORF) with changes and their chromosome location in the *hd144* candidate mutant background revealed by whole genome sequencing. The positions and the types of nucleotide changes along with the amino acid changes are also indicated.

Table 3.5 Whole genome sequencing of *hd142*

Chromosome No.	Nucleotide position	Nucleotide change		Gene/ORF name	Amino acid change	
I	47542	A	G	Y48G1C.12	D	G
I	515106	C	T	acs-13	G	R
I	645541	C	T	Y65B4A.2	A	V
I	1737844	G	A	Y71G12B.11	D	N
II	3074536	C	T	Y25C1A.8	D	N
II	3336311	T	C	F14D2.19	I	V
II	3503393	C	T	Y49F6B.2	A	V
II	3583360	C	T	srh-59	S	F
II	3764542	C	T	srx-112	M	I
II	4124480	G	A	rhgf-2	D	N
II	4220852	T	A	F31D5.1	S	T
II	4402886	C	T	mlt-7	T	I
II	4754715	C	T	C27D9.1	A	V
II	5253654	C	T	frpr-4	M	I
II	5968634	G	A	B0034.4	P	S
II	6442875	C	T	cutl-16	L	F
II	7063593	C	T	acs-6	H	Y
II	7103810	C	T	farl-11	R	H
II	7532210	G	A	wrt-1	E	K
II	7536342	G	A	ZK1290.13	M	I
II	8017787	T	A	zyg-11	N	K
II	8018507	G	A	zyg-11	D	N
II	8102824	G	A	sfxn-5	P	S
II	8116882	C	T	unc-105	P	S
II	8363082	C	T	M195.2	L	F
II	8468936	G	A	M05D6.2	M	I
II	8715526	A	T	T01B7.13	Y	F
II	8930096	G	A	mrpl-50	A	T
II	9327122	G	A	eat-3	D	N
II	9401873	G	A	Y51B9A.6	H	Y
II	10478738	G	A	clec-59	S	F
II	11015970	T	C	ram-2	T	A
II	11971925	G	A	mex-1	A	T

II	12406236	G	A	sre-30	L	F
II	12406278	G	A	sre-30	H	Y
II	12459474	G	T	sre-38	Q	H
II	12522943	C	A	ceh-99	A	E
II	12536744	T	A	F49C5.3	Y	N
II	12536853	C	T	F49C5.3	S	L
II	12538409	T	C	F49C5.3	W	R
II	13628124	C	T	gst-17	E	K
II	14498126	G	A	dhs-8	G	E
IV	1246225	G	A	clec-165	S	F
IV	3433398	C	T	C04C3.7	W	*
IV	3957814	C	T	clec-74	A	V
IV	7482538	C	T	rod-1	L	F
IV	8739980	C	T	mrps-33	G	E
IV	9708785	C	T	ant-1.3	A	T
IV	13265247	T	A	unc-26	Q	H
IV	16930938	C	T	Y116A8C.49	G	R
X	3032987	G	A	clec-265	G	R
X	4514324	C	T	spr-3	T	M
X	6282301	G	A	T07H6.4	L	F
X	6452223	G	A	nas-33	P	S
X	7336541	G	A	atg-11	A	T
X	8731699	A	T	M02D8.6	D	E
X	9553652	G	A	F49E2.5	E	K
X	9764266	G	A	T09B9.2	A	V

The strain name is VH2498. The table shows all the open reading frames (ORF) with changes and their chromosome location in the *hd142* candidate mutant background revealed by whole genome sequencing. The positions and the types of nucleotide changes along with the amino acid changes are also indicated.

Table 3.6 Whole genome sequencing of *hd152*

Chromosome No.	Nucleotide position	Nucleotide change		Gene/ORF name	Amino acid change	
III	4074005	G	A	unc-79	G	R
III	4531259	G	A	cdh-4	S	N
III	4810327	A	T	C38D4.7	S	T
III	5271346	G	A	ztf-8	P	S
III	6211891	G	A	C23G10.1	V	M
III	7336627	A	T	gsp-2	D	V
III	8889012	G	A	ZK637.14	S	L
III	9141340	G	A	eat-4	V	M
III	10372386	G	A	tbc-8	D	N
III	10788105	G	A	ptr-19	E	K
X	2570136	T	G	F52H2.7	H	P
X	4204688	C	T	F20B6.9	G	S
X	6334695	G	A	col-171	G	E
X	10987449	G	A	ver-4	G	R
X	11418174	G	A	F46C3.2	T	I

The strain name is VH2499. The table shows all the open reading frames (ORF) with changes and their chromosome location in the *hd152* candidate mutant background revealed by whole genome sequencing. The positions and the types of nucleotide changes along with the amino acid changes are also indicated.

Table 3.7 Whole genome sequencing of *hd148*

Chromosome No.	Nucleotide position	Nucleotide change		Gene/ORF name	Amino acid change	
IV	4003544	C	T	F47C12.1	P	L
IV	4502788	C	T	gbb-2	G	S
IV	5355738	C	T	Y4C6B.1	S	F
IV	7796017	C	T	sgo-1	V	I
IV	10218417	C	T	qns-1	E	K
IV	13779133	G	A	gly-10	R	K
IV	14697610	C	T	haf-8	M	I
IV	15308937	C	T	Y73F8A.11	A	V
IV	15504136	C	T	acr-24	T	I
V	2296468	C	T	nhr-226	S	F
V	12912297	A	T	nid-1	Q	H
X	462682	C	T	aagr-4	P	S
X	757939	C	T	aex-3	Affects_Splicing	
X	1559138	C	A	K06A9.1	T	K
X	2569429	C	T	F52H2.7	Affects_Splicing	
X	3648102	G	A	sax-1	R	C
X	4832017	A	T	R08E3.1	R	S
X	5359446	C	T	chtl-1	D	N
X	12993097	T	G	F11C1.5	L	V
X	13245461	G	A	hpl-1	G	R
X	13404610	G	A	F02C12.1	A	T

The strain name is VH2500. The table shows all the open reading frames (ORF) with changes and their chromosome location in the *hd148* candidate mutant background revealed by whole genome sequencing. The positions and the types of nucleotide changes along with the amino acid changes are also indicated.

Table 3.8 Whole genome sequencing of *hd153*

Chromosome No.	Nucleotide position	Nucleotide change		Gene/ORF name	Amino acid change	
X	558265	G	A	nas-38	A	T
X	1547984	G	A	K06A9.1	D	N
X	1673061	C	T	tbx-31	G	S
X	3065152	G	A	ceh-30	A	T
X	3891360	G	A	F47F2.1	G	E
X	5785799	T	A	tag-257	F	Y
X	5785800	T	G	tag-257	F	L
X	8797073	G	A	R04E5.7	P	S
X	9407264	C	A	fln-2	Y	*

The strain name is VH2501. The table shows all the open reading frames (ORF) with changes and their chromosome location in the *hd153* candidate mutant background revealed by whole genome sequencing. The positions and the types of nucleotide changes along with the amino acid changes are also indicated.

Table 3.9 % AVG cross-over defects in F1 males

Strain	Allele	% AVG CO
VH2496	*hd141*	3 (33)
VH2497	*hd144*	0 (30)
VH2498	*hd142*	7 (28)
VH2499	*hd152*	3 (37)
VH2500	*hd148*	48 (63)
VH2501	*hd153*	8 (103)

To determine whether the candidate mutant is linked to the X-chromosome or not, the candidate mutants were crossed with the *nid-1* males and the F1 males were analysed for the AVG cross-over (CO) phenotype. The strain names, allele names and the % AVG CO defects are shown. The values within brackets indicate *n.*

Table 3.10 List of genes with known roles in axon guidance or nervous system development

Candidate mutant	No. of ORFs with changes	Genes with known roles in axon guidance/nervous system development	Amino acid changes	
hd141	7	*lam-1* (laminin β)	D	N
hd142	47	*unc-105* *ram-2*	P T	S A
hd144	9	none		
hd148	10	*aex-3* *sax-1*	Affects_ Splicing R	 C
hd152	10	*cdh-4*	S	N
hd153	9	none		

The six selected candidate mutants along with the number of open reading frames (ORF) with changes are shown. Among these genes, the ones with known roles in axon guidance or nervous system or general development along with the amino acid changes are also shown.

3.9. References

Bhat, J.M., Pan, J., Hutter, H., 2015. PLR-1, a putative E3 ubiquitin ligase, controls cell polarity and axonal extensions in *C. elegans*. Dev. Biol. 398, 44–56.

Bonner, J., O'Connor, T.P., 2001. The permissive cue laminin is essential for growth cone turning in vivo. J. Neurosci. 21, 9782–9791.

Brenner, S., 1974. The genetics of *Caenorhabditis elegans*. Genetics. 77, 71–94.

Calixto, A., Chelur, D., Topalidou, I., Chen, X., Chalfie, M., 2010. Enhanced neuronal RNAi in *C. elegans* using SID-1. Nat. Methods 7, 554–559.

Chan, S.S.Y., Zheng, H., Su, M.W., Wilk, R., Killeen, M.T., Hedgecock, E.M., Culotti, J.G., 1996. UNC-40, a *C. elegans* homolog of DCC (Deleted in Colorectal Cancer), is required in motile cells responding to UNC-6 netrin cues. Cell 87, 187–195.

Chou, J.H., Bargmann, C.I., Sengupta, P., 2001. The *Caenorhabditis elegans odr-2* gene encodes a novel Ly-6-related protein required for olfaction. Genetics 157, 211–224.

Desai, C., Garriga, G., McIntire, S.L., Horvitz, H.R., 1988. A genetic pathway for the development of the *Caenorhabditis elegans* HSN motor neurons. Nature 336, 638–646.

Doitsidou, M., Poole, R.J., Sarin, S., Bigelow, H., Hobert, O., 2010. *C. elegans* mutant identification with a one-step whole-genome-sequencing and SNP mapping strategy. PLoS One 5, 1–7.

Dong, L., Chen, Y., Lewis, M., Hsieh, J.-C., Reing, J., Chaillet, J.R., Howell, C.Y., Melhem, M., Inoue, S., Kuszak, J.R., DeGeest, K., Chung, A.E., 2002. Neurologic defects and selective disruption of basement membranes in mice lacking entactin-1/nidogen-1. Lab. Invest. 82, 1617–1630.

Durbin, R.M., 1987. Studies on the development and organisation of the nervous system of *Caenorhabditis elegans*. Cambridge, UK, p. 150.

Fox, J.W., Mayer, U., Nischt, R., Aumailley, M., Reinhardt, D., Wiedemann, H., Mann, K., Timpl, R., Krieg, T., Engel, J., 1991. Recombinant nidogen consists of three globular domains and mediates binding of laminin to collagen type IV. EMBO J. 10, 3137–3146.

Hedgecock, E.M., Culotti, J.G., Hall, D.H., 1990. The *unc-5*, *unc-6*, and *unc-40* genes guide circumferential migrations of pioneer axons and mesodermal cells on the epidermis in *C. elegans*. Neuron 4, 61–85.

Höpker, V.H., Shewan, D., Tessier-Lavigne, M., Poo, M., Holt, C., 1999. Growth-cone attraction to netrin-1 is converted to repulsion by laminin-1. Nature 401, 69–73.

Huang, C.-C., Hall, D.H., Hedgecock, E.M., Kao, G., Karantza, V., Vogel, B.E., Hutter, H., Chisholm, A.D., Yurchenco, P.D., Wadsworth, W.G., 2003. Laminin alpha subunits and their role in *C. elegans* development. Development 130, 3343–3358.

Hutter, H., 2003. Extracellular cues and pioneers act together to guide axons in the ventral cord of *C. elegans*. Development 130, 5307–5318.

Hutter, H., Vogel, B.E., Plenefisch, J.D., Norris, C.R., Proenca, R.B., Spieth, J., Guo, C., Mastwal, S., Zhu, X., Scheel, J., Hedgecock, E.M., 2000. Conservation and novelty in the evolution of cell adhesion and extracellular matrix genes. Science 287, 989–994.

Ishii, N., Wadsworth, W.G., Stern, B.D., Culotti, J.G., Hedgecock, E.M., 1992. UNC-6, a laminin-related protein, guides cell and pioneer axon migrations in *C. elegans*. Neuron 9, 873–881.

Iwasaki, K., Staunton, J., Saifee, O., Nonet, M., Thomas, J.H., 1997. *aex-3* encodes a novel regulator of presynaptic activity in *C. elegans*. Neuron 18, 613–622.

Johnstone, I.L., Shafi, Y., Barry, J.D., 1992. Molecular analysis of mutations in the *Caenorhabditis elegans* collagen gene *dpy-7*. EMBO J. 11, 3857–3863.

Jorgensen, E.M., Mango, S.E., 2002. The art and design of genetic screens: *caenorhabditis elegans*. Nat. Rev. Genet. 3, 356–369.

Kang, S.H., Kramer, J.M., 2000. Nidogen is nonessential and not required for normal type IV collagen localization in *Caenorhabditis elegans*. Mol. Biol. Cell 11, 3911–3923.

Kim, S., Ren, X.C., Fox, E., Wadsworth, W.G., 1999. SDQR migrations in *Caenorhabditis elegans* are controlled by multiple guidance cues and changing responses to netrin UNC-6. Development 126, 3881–3890.

Kim, S., Wadsworth, W.G., 2000. Positioning of longitudinal nerves in *C. elegans* by nidogen. Science 288, 150–154.

Kohfeldt, E., Sasaki, T., Göhring, W., Timpl, R., 1998. Nidogen-2: a new basement membrane protein with diverse binding properties. J. Mol. Biol. 282, 99–109.

Kramer, J.M., 2005. Basement membranes. WormBook 1–15.

Leung-Hagesteijn, C., Spence, a. M., Stern, B.D., Zhou, Y., Su, M.W., Hedgecock, E.M., Culotti, J.G., 1992. UNC-5, a transmembrane protein with immunoglobulin and thrombospondin type 1 domains, guides cell and pioneer axon migrations in *C. elegans*. Cell 71, 289–299.

Liu, J., Schrank, B., Waterston, R.H., 1996. Interaction between a putative mechanosensory membrane channel and a collagen. Science 273, 361–364.

Mahoney, T.R., Liu, Q., Itoh, T., Luo, S., Hadwiger, G., Vincent, R., Wang, Z.-W., Fukuda, M., Nonet, M.L., 2006. Regulation of synaptic transmission by RAB-3 and RAB-27 in *Caenorhabditis elegans*. Mol. Biol. Cell 17, 2617–25.

Mayer, U., Timpl, R., 1994. Nidogen, a versatile binding protein of basement membranes. In Extracellular Matrix Assembly and Structure (Yurchenco, P. D., Birk, D. & Mecham, R. P., eds), pp. 389-416,Academic Press, Orlando, FL.

Murshed, M., Smyth, N., Miosge, N., Karolat, J., Krieg, T., Paulsson, M., Nischt, R., 2000. The absence of nidogen 1 does not affect murine basement membrane formation. Mol. Cell. Biol. 20, 7007–7012.

Schafer, W.R., 2005. Egg-laying. WormBook 1–7. doi:10.1895/wormbook.1.38.1

Schmitz, C., Wacker, I., Hutter, H., 2008. The Fat-like cadherin CDH-4 controls axon fasciculation, cell migration and hypodermis and pharynx development in *Caenorhabditis elegans*. Dev. Biol. 316, 249–259.

Schymeinsky, J., Nedbal, S., Miosge, N., Poschl, E., Rao, C., Beier, D.R., Skarnes, W.C., Timpl, R., Bader, B.L., 2002. Gene structure and functional analysis of the mouse *nidogen-2* gene: *nidogen-2* is not essential for basement membrane formation in mice. Mol Cell Biol 22, 6820–6830.

Sibley, M.H., Graham, P.L., von Mende, N., Kramer, J.M., 1994. Mutations in the alpha 2(IV) basement membrane collagen gene of *Caenorhabditis elegans* produce phenotypes of differing severities. EMBO J. 13, 3278–3285.

Thomas, J.H., 1990. Genetic analysis of defecation in *Caenorhabditis elegans*. Genetics 124, 855–872.

Thompson, O., Edgley, M., Strasbourger, P., Flibotte, S., Ewing, B., Adair, R., Au, V., Chaudhry, I., Fernando, L., Hutter, H., Kieffer, A., Lau, J., Lee, N., Miller, A., Raymant, G., Shen, B., Shendure, J., Taylor, J., Turner, E.H., Hillier, L.W., Moerman, D.G., Waterston, R.H., 2013. The million mutation project: a new approach to genetics in *Caenorhabditis elegans*. Genome Res. 23, 1749–62.

Trent, C., Tsung, N. & Horvitz, H. R., 1983. Egg-laying defective mutants of the nematode *Caenorhabditis elegans*. Genetics,104(4) pp.619–647.

Von Mende, N., Bird, D.M., Albert, P.S., Riddle, D.L., 1988. Dpy-13: a Nematode Collagen Gene That Affects Body Shape. Cell 55, 567–576.

White, J. G., Southgate, E., Thomson, J. N., Brenner, S., 1986.The structure of the nervous system of the nematode *Caenorhabditis elegans*. Philos.Trans.R.Soc.Lond. B 314, 1–340.

Yurchenco, P.D., 2011. Basement membranes: Cell scaffoldings and signaling platforms. Cold Spring Harb. Perspect. Biol. 3, 1–27.

Zallen, J. a, Peckol, E.L., Tobin, D.M., Bargmann, C.I., 2000. Neuronal cell shape and neurite initiation are regulated by the Ndr kinase SAX-1, a member of the *Orb6*/COT-1/warts serine/threonine kinase family. Mol. Biol. Cell 11, 3177–3190.

Zuryn, S., Le Gras, S., Jamet, K., Jarriault, S., 2010. A strategy for direct mapping and identification of mutations by whole-genome sequencing. Genetics 186, 427–430.

Chapter 4.

A novel role for AEX-3, a guanine nucleotide exchange factor (GEF) for the RAB-3 GTPase, in axon navigation in *C. elegans*

Jaffar M. Bhat and Harald Hutter

Abstract

Nervous system development is a highly regulated process that involves precise and accurate axon tract formation. This is achieved by the proper navigation of early outgrowing axons (pioneers), allowing the late outgrowing axons (followers) to extend unerringly in the embryo. In *Caenorhabditis elegans*, the AVG axon pioneers the right axon tract and is required for the proper guidance of follower axons and hence organisation of ventral nerve cord. We isolated an allele of *aex-3* in an enhancer screening for AVG axon guidance defects in a *nid-1/*Nidogen mutant background. *aex-3* mutant animals show highly penetrant AVG axon guidance defects which are dependent on a mutation in *nid-1*/Nidogen, a basement membrane component. We also observed AVG pioneer dependent and independent follower axon guidance defects in *aex-3; nid-1* mutant animals. AEX-3 is a GDP/GTP exchange factor homologue for RAB-3 GTPase and is expressed in nearly all the neurons, including the ventral nerve cord axons. Our genetic interaction data suggests that *aex-3* and *rab-3* act in the same genetic pathway, suggesting that AEX-3 likely activates RAB-3 GTPase in the context of AVG axon navigation. Moreover, we also observed that *aex-3* acts in the same genetic pathway with *unc-64*/Syntaxin, *unc-31*/CAPS and *ida-1*/IA-2, known players of vesicular release and exocytosis. Finally, our genetic interaction data suggests that *aex-3* and the *unc-5* Netrin receptor act in the same genetic pathway. This indicates that AEX-3 might regulate the trafficking of Netrin receptor UNC-5 to the growth cone and/or its insertion into the membrane at the growth cone to mediate the proper guidance of AVG axon.

4.1. Introduction

Precise assembly of neuronal networks is a hallmark of a functional nervous system. Building these networks begins with early outgrowing axons from neurons called “pioneers”. Pioneer neurons form the initial axon scaffold used by the later outgrowing “follower” axons to extend upon. Pioneers provide guidance cues and substrate for the follower axons to navigate properly. This sequential outgrowth of axons simplifies the problem of axonal pathfinding by allowing the majority of axons to extend along preexisting pathways rather than having to navigate exclusively on their own. Pioneer axons have been identified in many organisms. In grasshopper embryos, a pair of neurons (Ti) arise at the tips of the limb bud to extend axons towards the central nervous system. Follower (SGO) axons cannot extend further upon ablation of these pioneers (Klose & Bentley, 1989). Similarly the *Drosophila* ventral nerve cord (VNC) is pioneered by four axons forming longitudinal tracts. Ablation of these pioneers leads to defects in the navigation of follower axons (Hidalgo & Brand, 1997). The thalamus of the mouse cerebral cortex is first invaded by short-lived subplate neurons, guiding later outgrowing cortical axons to their target (McConnell et al., 1989). However, pioneer neurons are not always required for the guidance of follower axons (Chitnis & Kuwada, 1991) and in some cases are dispensable for this purpose (Cornel and Holt, 1992; Eisen et al., 1989; Keshishian and Bentley., 1983).

The *C. elegans* nervous system is arranged along two body axis, anterior-posterior (AP) and dorso-ventral (DV) axes (White et al., 1986). The ventral nerve cord, which runs in the AP direction, is the major longitudinal bundle and is divided into right and left axon tracts. The right axon tract contains most of the axons (around 50), whereas only four axons form the left axon tract in the adult animal. The right side of the VNC harbours the main components of the circuit controlling the movement of the animal. This is where command interneurons connect to motor neurons, which in turn connect to nearby ventral or faraway dorsal muscles. The corresponding synapses between inter- and motor neurons can only be established between neurites in immediate contact. Even a local disorganization, i.e. axons in the “wrong neigbourhood” will disrupt the circuitry (White et al., 1976). Interneuron or motorneuron axons crossing

into the left axon tract will not be able to establish the correct synaptic connections, unless their synaptic partners happen to join them.

As in other animals, pioneers play an important role in *C. elegans* (Durbin, PhD Thesis, University of Cambridge, 1987; Garriga et al., 1993). The AVG neuron extends the first axon and pioneers the right VNC axon tract followed by motor neuron (DD/VD and DA/DB) and interneuron axons in a defined order (Durbin, PhD Thesis, University of Cambridge, 1987). Removal of the AVG axon early in development does not prevent the outgrowth of follower axons. The ventral nerve cord still forms, but is disorganised with axons crossing between right and left tracts (Durbin, PhD Thesis, University of Cambridge, 1987; Hutter, 2003). This suggests that AVG pioneer is important for the correct organisation of the ventral nerve cord. The left axon tract is pioneered by the PVPR axon from the posterior end and is closely followed by PVQL axon (Durbin, 1987). The pioneer follower relationship is more tight here. The left axon tract fails to form in the absence of the PVPR axon (Durbin, 1987; Garriga et al., 1993), suggesting that no other neuron can pioneer this axon tract. Under such circumstances the follower axons extend in the already established right axon tract (Durbin, PhD Thesis, University of Cambridge, 1987; Garriga et al., 1993). This is further supported by two independent investigations where in mutant animals with misguided PVPR also have PVQL axon following along the pioneer (Steimel et al., 2010; Unsoeld et al., 2013).

In addition to pioneers, extracellular guidance cues actively mediate outgrowth and navigation of axons and pioneers exclusively dependent on these guidance cues. The homologs of these guidance genes have been identified and their role characterised in detail. UNC-6 (Netrin in vertebrates) is a laminin-like secreted protein forming a gradient along the dorso-ventral axis and is an essential cue for axons and cells migrating in dorso-ventral direction (Hedgecock et al., 1990; Ishii et al., 1992; Wadsworth et al., 1996; Wadsworth, 2002). Cells and axons expressing the receptor UNC-40 (DCC in vertebrates) are attracted by UNC-6, whereas those expressing both UNC-40 and UNC-5 receptors are repelled, illustrating that the response to a guidance cue can depend on the receptors expressed by the neuron (Hedgecock et al., 1990; Ishii et al., 1992; Leung-Hagesteijn et al., 1992; Chan et al., 1996). UNC-129, a member of TGF-β family, also affects dorso-ventral migrations by promoting UNC-40 + UNC-5

signalling (Colavita et al., 1998); MacNeil et al., 2009). Dorsally expressed SLT-1/Slit repels axonal growth cones expressing the corrsponding SAX-3 receptors towards the ventral side (Zallen et al., 1998). Finally, NID-1/Nidogen, a basement membrane protein, positions axons in the sublateral and ventral nerve cords (Kim & Wadsworth, 2000).

Mutants for all the major guidance cues and receptors are available in *C. elegans* and none of them substantially affects AVG axon navigation (Hutter, 2003). Moreover, direct genetic screens for mutants affecting AVG navigation have yielded only a few new genes (Bhat et al., 2015; Moffat et al., 2014). This emphasized the need for other strategies like modifier screens to uncover AVG axon guidance genes. A good starting point for enhancer screens are *nid-1* mutants, which have minimal AVG axon guidance defects, but are otherwise healthy. We isolated an allele of *aex-3* in an enhancer screens for AVG axon guidance defects in a *nid-1*(*cg119*) mutant background. We used the deletion allele *cg119* of *nid-1*, which is a molecular null with no protein detected in the mutant animals (Kang and Kramer, 2000). *aex-3* mutant animals display highly penetrant AVG axon guidance defects which are dependent on *nid-1*. AEX-3, the homologue of the vertebrate MAP kinase-activating death domain protein (MADD), is a guanine nucleotide exchange factor (GEF) for Rab3 and Rab27 GTPases and is expressed in nervous system (Iwasaki et al., 1997; Mahoney et al., 2006). GEFs activate Rab proteins by promoting the exchange of GDP with GTP, which control various aspects of vesicle trafficking in a cell (Wada et al., 1997; Zerial and McBride, 2001; Hutagalung and Novick, 2011). Our genetic interaction data suggests that AEX-3 activates Rab3, but not Rab27. AEX-3 is known to interact with multiple proteins and thereby regulates multiple pathways (Iwasaki et al., 1997; Iwasaki and Toyonaga, 2000; Mahoney et al., 2006). We found that *aex-3* acts with *unc-64*/Syntaxin, *unc-31*/CAPS and *ida-1*/IA-2, the known players of vesicular exocytosis in the same genetic pathway (Saifee et al., 1998; Speese et al., 2007; Cai et al., 2004; Wit et al., 2006; Hammarlund et al., 2008). In addition, we found that both *unc-6*/Netrin and its receptor *unc-5* have *nid-1* dependent AVG navigation defects. Genetic interaction data suggests that *aex-3* and *unc-5* are in the same genetic pathway, suggesting that AEX-3 regulates the trafficking of the Netrin receptor UNC-5 to the growth cone and/or its insertion into the membrane at the growth cone.

4.2. Materials and methods

4.2.1. Nematode strains and alleles used

The following strains were used for phenotypic analysis: *hdIs51*[*odr-2::tdTomato, rol-6(su1006)*] X; *zdIs13*[*tph-1::GFP*] IV; *hdIs54*[*flp-1::GFP,sra-6::plum, pha-1(+)*]; *rhIs4*[*glr-1::GFP,dpy-20(+)*] III; *hdIs24*[*unc-129::CFP, unc-47::DsRed2]; hdIs36*[*rgef-1::DsRed2*]*;* and *leIs1722*[*WO5H121::GFP, unc-119(+)*].

The following alleles were used for complementation: *aex-3*(*n2166*) X, *aex-3*(*sa5*) X and *sax-1(ky211)* X.

The following alleles were used for phenotypic analysis and genetic interaction studies: *aex-3*(*hd148*) X*, aex-3*(*n2166*) X*, aex-3*(*sa5*) X, *aex-3*(*js815*) X, *rab-3*(*js49*) II, *aex-6*(*sa24*) I, *cab-1*(*tg49*) X, *unc-31*(*e169*) IV, *unc-64*(*e264*) III, *unc-104*(*e1265*) II, *unc-10*(*md1117*) X, *unc-6*(*ev400*) X, *unc-5*(*e53*) IV, *unc-40*(*e271*) I, *ida-1*(*ok409*) III and *nid-1*(*cg119*) V. The strains were cultured and maintained at 20 ^{o}C under standard conditions (Brenner 1974).

4.2.2. Isolation of *hd148* allele of *aex-3*

The *hd148* mutation*,* an allele of *aex-3* was isolated after EMS mutagenesis of *nid-1*; *hdIs51*[*odr-2::tdTomato, rol-6*(*su1006*)] animals in F2 semi-clonal screen for axon guidance defects in the ventral nerve cord pioneer AVG. Briefly, after EMS treatment, the healthy adult animals were transferred to 60 mm x 15 mm seeded plates with each plate having 9 animals (P0 generation) and 30 plates in total. After selfing for two generations, F2 animals were picked and transferred onto separate 60 mm x 15 mm seeded plates. Plates with sufficient (> 100) number of animals after selfing were analysed under dissecting fluorescence microscope (LEICA MZ12) for AVG cross-over defects. Plates where a significant number of animals (> 10) showed AVG axon cross-over defects were isolated and further analysed under high resolution fluorescence microscope (Zeiss Axiscope-40x objective). By using this strategy and screening 2400 haploid genomes, we were able to isolate 21 candidate mutants. The *hd148* mutant was backcrossed four times (4x), and whole genome sequenced to get the list of open

reading frames (ORFs) with changes in the mutant strain. The *hd148* mutation was linked to the X-chromosome simply by crossing it with *nid-1* males and then counting the phenotype of F1 males. *aex-3* was picked as the potential candidate as the known phenotypes (egg-laying and body movement) of *aex-3* matched with the isolated mutant. Complementation test was done to confirm that *hd148* is the allele of *aex-3*.

4.2.3. Fosmid rescue and expression constructs

The *aex-3*-containing fosmid (WRM0629dA08) was injected (1 ng/µl) into *nid-1* mutant animals along with a coinjection marker *myo-2::GFP* (5 ng/µl) and filler DNA pBluescript KS (-) (94 ng/µl) to create a stable transgenic line. *nid-1* males with the *hdEx602* [*WRM0629dA08, (aex-3), myo-2::GFP*] extrachromosomal array were then crossed with *aex-3(hd148); nid-1* mutant animals, and mutant animals with an *hdEx602* array were analyzed for the AVG axon cross-over defects. We injected more than 600 adult animals, obtained around 60 F1s and out of these only one stable transgenic line. The same problem was encountered earlier by other groups who worked with the *aex-3* gene (Iwasaki et al., 1997; Iwasaki and Toyonaga, 2000).

To express *aex-3* specifically in AVG the neuron, *lin-11* promoter fragment (B. G. Unpublished data - personnel communication) and *aex-3* cDNA were cloned into GFP vector pPD95.75 (Fire vector kit). This construct (5-15 ng/µl) was injected along with coinjection marker *unc-122::GFP* (45 ng/µl) into *nid-1* mutant animals. The *nid-1* males with an extra-chromosomal array were then crossed with *aex-3(hd148); nid-1* mutant animals and the animals from three independent transgenic lines were analysed for AVG axon cross-over defects. Transgenic lines for fosmid as well as the expression vector were generated as described (Mello et al., 1991).

4.2.4. Construction of triple mutants and genetic Interactions

Triple mutants were constructed according to (Iwasaki et al., 1997). *unc-31*; *aex-3*; *nid-1* triple mutant was generated by crossing *unc-31/*+; *nid-1/*+ males with *aex-3* hermaphrodites. From F1 triple heterozygous, F2 Aex progeny was picked and from these F3 Unc progeny were picked which were genotyped for the *nid-1* deletion. *unc-64*;

aex-3; *nid-1*, *unc-5*; *aex-3*; *nid-1*, *ida-1*; *aex-3*; *nid-1* and *rab-3*; *aex-3*; *nid-1* triple mutants were constructed in the same way. *rab-3 (js49)* is a point mutation and was confirmed by sequencing a PCR fragment from the triple mutant. The following forward 5′ CCAGCAGACAATACTTCGCC 3′ and reverse 5′ CTCCTTGGCTGATGTTCG 3′ primers were used to amplify 610 bp fragment by Phusion PCR from *rab-3* genomic sequence including the change (G to A) in the *rab-3(js49)* mutant. Forward primer 5′ CCAGCAGACAATACTTCGCC 3′ was also used for the sequencing of 610 bp PCR fragment to confirm the *rab-3* mutation. Similarly for all the triple mutants, *aex-3(hd148)* which is a point mutation (G to A) in the 5′ splice donor of 6th intron, was also confirmed by sequencing. The forward 5′ AGCACTTTTATACCCACTGG 3′ and reverse primer 5′ CTGGACAATGATGCTTTATTCAG 3′ primers were used to amplify 529 bp fragment by Phusion PCR from *aex-3* genomic sequence including the change (G to A) in *aex-3(hd148)* mutant. Forward primer 5′ AGCACTTTTATACCCACTGG 3′ was also used for the sequencing of 529 bp PCR fragment to confirm the *aex-3* mutation.

To test genetic interactions between *aex-3* and other known interacting genes in *nid-1* background, phenotypes of both double and triple mutants were examined. Two genes are thought to act in the same pathway if the penetrance of double mutant phenotype is similar to that of the strongest single mutant. χ^2 tests were used to determine statistical significance between double mutants and the strongest single mutant.

4.2.5. Phenotypic analysis of neuronal defects

Axonal defects were scored with a Zeiss Axiscope (40x objective) in adult animals expressing fluorescent markers in respective neurons. Animals were immobilised with 10 mM sodium azide in M9 buffer for 1hr and mounted on 3% agar pads before analysis.

4.2.6. Microscopy

Confocal images of mixed stage population of animals with respective fluorescent proteins were acquired on a Zeiss Axioplan II microscope (Carl-Zeiss AG,

Germany) connected to a Quorum WaveFX spinning disc system (Quorum Technologies, Canada). Stacks of confocal images with 0.2 to 0.5 µm distance between focal planes were recorded. Image acquisition and analysis was carried out by using Volocity software (Perkin-Elmer, Waltham, MA). Images in the figures are maximum intensity projections of all focal planes. Figures were assembled with Adobe Photoshop CS8.0 (Adobe, San Jose, CA, USA).

4.3. Results

4.3.1. Identification of a novel allele of *aex-3*

The molecular basis for AVG axon guidance is largely unknown. We isolated *hd148,* an allele of *aex-3* in an enhancer screen for AVG axon guidance defects in a *nid-1* mutant background. *hd148* is a recessive mutation and the axon cross-over defects it displays are dependent on a mutation in *nid-1* (Table 4.1). We used a marker strain *hdIs51*[*odr-2::tdTomato*] which labels the AVG and PVP neurons to visualise both right and left axon tracts of ventral nerve cord simultaneously. This enabled us to score guidance defects where the AVG axon, which is present on the right axon tract in wild type, by mistake crosses and extends into the left axon tract. The whole genome sequencing of the *hd148* mutant strain after backcrossing four times (4x) revealed a short list of open reading frames (21) with changes, mostly located on Chromosome IV and X. We mapped the *hd148* mutation on chromosome X by crossing it with *nid-1* males and scoring F1 males for the AVG axon cross-over defects. Among the list of open reading frames (now reduced to 10) with changes, *aex-3* and *sax-1* were picked as possible candidates. Previously isolated *aex-3* mutant animals have locomotion and egg-laying defects (Thomas, 1990; Iwasaki et al., 1997; Mahoney et al., 2006) similar to defects seen in *hd148*. We tested two known alleles (*n2166* and *sa5*) of *aex-3* for complementation (Thomas, 1990; Iwasaki et al., 1997), both of which gave us the same results. *aex-3* did not complement *hd148* for AVG axon cross-over defects, slow movement and egg-laying (Egl) phenotypes seen in *hd148*; *nid-1* mutant animals, suggesting that *hd148* is an allele of *aex-3*. Moreover, these known alleles of *aex-3*, *n2166*, *sa5* and *js815* (Thomas, 1990; Iwasaki et al., 1997; Mahoney et al., 2006),

showed AVG axon cross-over defects in a *nid-1* mutant background (Table 4.1). *hd148* is a point mutation (G to A) in the splice donor at the beginning of 6th intron of *aex-3*, which would result in the early truncation of the protein after 388 of 1409 amino acids, if intron 6 is not spliced out. As revealed by whole genome sequencing the *hd148*-containing strain also carries a misssense mutation in *sax-1*, a gene closely linked to *aex-3*. *sax-1* is required for neurite initiation and outgrowth in sensory neurons (Zallen et al., 2000). However, *sax-1(ky211)* did complement *hd148* in a *nid-1* mutant background for AVG axon cross-over, slow movement and egl phenotypes suggesting that the mutation in *sax-1* does not contribute to the navigation defects seen in our isolate. In addition a fosmid containing the *aex-3* gene (WRM0629dA08) rescued the AVG axon cross-over defects of *aex-3(hd148); nid-1(cg119)* mutant animals. The rescuing line shows only 24% animals with AVG axon cross-over defects which are significantly less as compared to the 56% defects shown by the *aex-3; nid-1* mutant animals (Figure 4.1). Taken together, these data suggest that *hd148* is an allele of *aex-3*.

4.3.2. *aex-3* mutant animals show *nid-1*-dependent AVG axon navigation defects

In wild type animals the AVG axon pioneers the right axon tract of the ventral nerve cord from the anterior side extending straight to the tail where it terminates (Durbin, 1987) (Figure 4.2A, C and E). In 56% of *aex-3(hd148); nid-1* mutant animals the AVG axon crosses the ventral midline from right to left, referred to as AVG cross-over (AVG CO) defects. These cross-overs can occur anywhere along the anterior-posterior axis (Figure 4.2B, D and F), but occur more frequently in the anterior half of the animal. After crossing the AVG axon remains in the left axon tract in the majority of the animals. However, in 19% of the mutant animals the AVG axon crosses back into the right axon tract. AVG cross-over defects in *aex-3* are almost completely dependent on *nid-1*, as *aex-3*(*hd148*) on its own has only 4% defects (Table 4.1), whereas *nid-1* single mutant animals have around 10% AVG cross-over defects (Table 4.1). Three other alleles (*n2116*, *sa5*, *js815*) of *aex-3* (Thomas, 1990; Iwasaki et al., 1997; Mahoney et al., 2006) show *nid-1* dependent AVG cross-over defects with a penetrance similar to *hd148* (Table 4.1). Defects are somewhat higher in *hd148*, but not significantly different from the other alleles except for *js815*, which has the least penetrant defects (Table 4.1). The

molecular nature of the *hd148* allele - expected to lead to an early truncation of the protein - matches well with the strong defects it shows and suggests that it is a strong loss-of-function allele.

4.3.3. Follower axon navigation is disrupted in *aex-3; nid-1* mutant animals

Laser ablations of the AVG neuron early in development leads to the formation of disorganised ventral nerve cord with axons switching between the right and left axon tracts (Durbin, 1987; Hutter, 2003). Among the follower neurons, the command interneurons and motor neurons (DD/VD and DA/DB) are largely affected (Durbin, 1987; Hutter, 2003). We wanted to test whether follower axons are also affected and evaluated *aex-3*(*hd148)*; *nid-1(cg119)* mutant animals with neuron-specific markers for follower defects. Command interneurons initially exit the nerve ring in two fascicles one on each on the right and left side. Immediately after the nerve ring exit, the left side fascicle crosses and extends into the right axon tract and both fascicles follows the AVG axon (Figure 4.3E). In *aex-3*; *nid-1* double mutants, 49% of animals show cross-over defects where interneuron axons cross from the right to the left side of the VNC (Figure 4.3F; Table 4.2). Among these, 35% are AVG dependent, i.e. interneurons cross the midline at the same position where the AVG axon crosses, as evident from the merged images of the AVG neuron and interneurons (Figure 4.3F, F' and F''; Table 4.2). In the remaining 14% animals, interneuron axons cross independently of the AVG axon (Table 4.2). This suggests that while the majority of the interneuron cross-over defects are likely secondary consequences of AVG defects, some of the defects are likely primary defects in interneurons themselves.

The two AVK neurons also send axons into the VNC from the nerve ring. However in this case one of them extends in the left tract, whereas the other one extends on the right side (Figure 4.3A). In *aex-3*; *nid-1* double mutant animals we observed that both AVKR/L axons frequently cross the ventral midline with equal penetrance (Figure 4.3B; Table 4.2). However we did not observe any correlation between the AVG and AVK axon cross-overs, suggesting that these defects are likely independent. In some mutant animals, AVK axons terminate prematurely, but this is not

significantly different from *nid-1* single mutants (Table 4.2). HSNs are a pair of ipsilateral neurons which are born in the tail during embryogenesis and migrate towards the midbody, where each neuron extends an axon on either side of the ventral midline towards the nerve ring (Garriga et al., 1993) (Figure 4.3C). *nid-1* single mutants have highly penetrant HSN cross-over defects which are not enhanced in *aex-3*; *nid-1* double mutant animals (Figure 4.3D; Table 4.2). However in *aex-3*; *nid-1* double mutant animals some HSN neurons fail to migrate properly, defects not seen in *nid-1* single mutants (Table 4.2).

In summary, among the follower axons, command interneurons and AVKs have significant guidance defects in *aex-3*; *nid-1* whereas HSN guidance defects are not enhanced in the double mutant animals. The interneurons seem to follow AVG pioneer strictly as more mutant animals have AVG dependent interneuron axon cross-over defects. All the above data suggests that *aex-3* is required for the proper navigation of the follower neurons in *nid-1* dependent manner.

4.3.4. *aex-3; nid-1* mutant animals show motor neuron axon navigation defects

The ventral nerve cord in *C. elegans* contains essential components of the motor circuit (White et al., 1986). DD/VD GABAergic motor neuron cell bodies are located along the ventral midline and send out processes in the right axon tract that branch and extend a commissure to the dorsal side (Figure 4.4A, C and E). In *aex-3; nid-1* double mutants, 28% of the animals show DD/VD axon guidance defects, where motor neuron axons cross from the right to the left tract of the ventral nerve cord (Figure 4.4B; Table 4.2). These defects are mostly dependent on AVG, since DD/VD axons cross together with the AVG axon. This suggests that these defects are likely the secondary consequences of the misguided AVG pioneer. In addition in 36% of *aex-3; nid-1* mutant animals some DD/VD axons grow in the left rather than the right axon tract, which makes the ventral nerve cord symmetrical in appearance (symmetric VNC) (Figure 4.4B and D; Table 4.2). DD/VD commissures individually (as pioneers) navigate towards the dorsal side, where they extend to form the dorsal nerve cord (DNC) (Figure 4.4E and G). About 65% of *nid-1* single mutants have commissural defects, where some commissures

(5 out of 19 per animal) fail to reach the dorsal cord leading to gaps (DNC gaps, Table 4.2). We observed that in *aex-3*; *nid-1* double mutant animals these defects are enhanced to 100% with every animal showing commissural defects (7 out of 19 per animals fail to reach the dorsal side) and gaps in the DNC (Figure 4.4F and H; Table 4.2). This suggests that *aex-3* is required independently of *nid-1* in the guidance of commissures and the proper formation of dorsal nerve cord.

We also analysed DA/DB cholinergic motor neurons in *aex-3*; *nid-1* double mutant animals. DA/DB motor neuron cell bodies are also located along the ventral midline. They send their dendrites into the right axon tract of the VNC and axons towards the dorsal nerve cord (Figure 4.4I, K and M). We found that in 29% of the *aex-3*; *nid-1* double mutant animals DA/DB motor dendrites cross from the right to the left axon tract of the VNC (Figure 4.4J; Table 4.2). These defects are mostly dependent on AVG, as cross-overs occur together with the AVG axon, again suggesting that these are secondary defects. In addition some DA/DB motor neurons extend dendrites into the left axon tract so that VNC appears symmetric (symmetric ventral nerve cord) (Figure 4.4L; Table 4.2). We observed very few DA/DB commissural defects (Figure 4.4N) and no DNC gaps in *aex-3; nid-1* double mutant animals, suggesting that commisural defects are neuron-specific.

We used a pan-neuronal marker to assess the overall state of the nervous system as well as selected neurons with axons outside the VNC. We did not observe guidance defects in touch receptor axons, other longitudinal axons and neuronal processes in the head region. The nervous system by and large seems intact. Defects in *aex-3; nid-1* mutant animals are largely confined to the VNC and some commissural axons.

In summary we have observed that *aex-3*; *nid-1* mutant animals have VNC cross-over, symmetric VNC and commissural defects in both classes of motor neurons (DD/VD and DA/DB). Both types of motor neurons depend on AVG for navigation. DD/VD motor neurons have more severe commissural defects than DA/DB motor neurons and as a result we see an incomplete DNC in case of DD/VD motor neurons. Taken together, the above data suggests that *aex-3* is required for the proper placement

and navigation of DD/VD GABAergic and DA/DB cholinergic motor neurons in a *nid-1* dependent manner.

4.3.5. AEX-3 activates the RAB-3 GTPase in the context of AVG navigation

AEX-3 is a guanine nucleotide exchange factor and regulates the activity of the RAB-3 and AEX-6/Rab27 GTPases (Mahoney et al., 2006). Guanine nucleotide exchange factors (GEF) activate GTPases by promoting the exchange of GDP to GTP (Wada et al., 1997). Both RAB-3 and AEX-6/Rab-27 bind to synaptic vesicle precursors in their GTP form and regulate trafficking of these vesicles (Nonet et al., 1997; Mahoney et al., 2006). In wild type, RAB-3 and AEX-6/Rab27 are localised to axons and enriched in synaptic regions, whereas in *aex-3* mutant animals RAB-3 as well as AEX-6/Rab27 are mislocalised to the cell body (Iwasaki and Toyonaga, 2000; Mahoney et al., 2006). Even though both RAB-3 and AEX-6/Rab27 are activated by AEX-3, they act through different downstream effectors (Mahoney et al., 2006). To test whether AEX-3 regulates RAB-3 or AEX-6/Rab27 (or both) in the context of AVG axon navigation we constructed *rab-3*; *nid-1* and *aex-6*; *nid-1* double mutants in the putative null alleles and evaluated them for AVG axon cross-over defects. *rab-3*; *nid-1* mutant animals show AVG axon cross-over defects with a penetrance similar to *aex-3; nid-1*, whereas *aex-6*; *nid-1* double mutants do not (Figure 4.5). *rab-3* single mutants have weakly penetrant AVG axon cross-over defects and *aex-6* single mutants do not have any such defects (Figure 4.5). The penetrance of AVG axon cross-over defects in *aex-3*; *rab-3*; *nid-1* triple mutant animals is not significantly different from *aex-3*; *nid-1* double mutants (Figure 4.5), suggesting that *aex-3* and *rab-3* are in the same genetic pathway. This indicates that AEX-3 likely activates RAB-3, but not AEX-6/Rab27 in the context of AVG navigation.

The pleiotropic behavioural defects shown by *aex-3* mutant animals indicate that AEX-3 regulates multiple pathways with a common synaptic transmission defect. AEX-3 physically interacts with CAB-1 to regulate defecation, a pathway distinct from the *rab-3* pathway (Iwasaki & Toyonaga, 2000). We tested *cab-1*; *nid-1* double mutant animals for AVG axon cross-over defects and observed only a mild enhancement of the defects

(Figure 4.5), suggesting that CAB-1 does not have a major role in the context of AVG navigation.

Since RAB-3 is associated with synaptic vesicle precursors which are transported by the UNC-104/Kinesin-3 motor in *C. elegans*, we wanted to test if UNC-104 plays any role here (Hall and Hedgecock, 1991; Nonet et al., 1997). AVG axon cross-over defects are enhanced in *unc-104*; *nid-1* double mutant animals compared to either single mutant, but these defects are less penetrant compared to the *aex-3*; *nid-1* or *rab-3*; *nid-1* double mutants (Figure 4.5). This suggests that AEX-3 could be involved in transport of vesicles in outgrowing axons in part mediated through UNC-104.

UNC-10/Rim is a RAB-3 effector molecule, which interacts with RAB-3 during priming of synaptic vesicles prior to their release at the synapse (Koushika et al., 2001). *unc-10* single mutants have no AVG axon cross-over defects, and *nid-1* defects are not enhanced in *unc-10; nid-1* double mutants (Figure 4.5), indicating that UNC-10/Rim is not involved in the navigation of the AVG axon. This may be not surprising, since there are no synapses at that stage of pioneer axon outgrowth.

Given the reason that AEX-3 regulates RAB-3 in the context of AVG navigation, one would expect AEX-3 to act in a cell autonomous manner. To determine whether AEX-3 is required within the AVG neuron for its axon navigation, we expressed AEX-3 cDNA construct tagged with GFP specifically in the AVG neuron. We observed that AEX-3 cDNA was able to rescue the AVG axon cross-over defects in all the three independent transgenic lines (n > 100) (Figure 4.6). The transgenic line #1 has (18%), line #2 (16%) and line #3 (13%) AVG axon cross-over defects which are significantly less as compared to the 56% AVG axon cross-over defects in *aex-3; nid-1* double mutant animals (Figure 4.6). This suggests that AEX-3 is required in the AVG neuron for its axon navigation and thus acts in a cell autonomous manner.

In summary, the above data suggests that AEX-3 regulates RAB-3 but not AEX-6/Rab27 in the context of AVG navigation and potentially is involved in vesicle transport that in part depends on UNC-104. Moreover, this pathway is distinct from *cab-1* and *unc-10/*Rim pathways as neither of these have AVG axon cross-over defects in a *nid-1* background.

4.3.6. *aex-3*, *unc-31*/CAPS, *ida-1*/IA-2 and *unc-64*/Syntaxin act in the same genetic pathway

aex-3 genetically interacts with *unc-31* and *unc-64* for the dauer formation constitutive (Daf- c) phenotype (Iwasaki et al., 1997). UNC-31 is the nematode homolog of CAPS (Ca^{2+}-dependent secretion activator) and is required for secretion of dense core vesicles (Livingstone, 1991; Walent et al., 1992; Speese et al., 2007). *unc-64* encodes the nematode homolog of Syntaxin, a SNARE component involved in the fusion or docking of synaptic vesicles and dense core vesicles (Saifee et al., 1998; Wit et al., 2006; Hammarlund et al., 2008). Recently it has been shown that Syntaxin1 binds to the guidance receptor DCC in the growth cone, where it is required for the chemo-attraction of migrating axons to the guidance cue Netrin (Cotrufo et al., 2012). We wanted to test if *unc-31* and *unc-64* mutants also have AVG axon guidance defects like *aex-3*. Neither *unc-31* nor *unc-64* single mutants have AVG axon cross-over defects, but both mutants enhance AVG axon cross-over defects of *nid-1* mutants (Figure 4.7). Both *unc-31; nid-1* and *unc-64; nid-1* double mutants have defects that are significantly less penetrant than defects in *aex-3; nid-1* double mutants. However, both *unc-31; aex-3; nid-1* and *unc-64; aex-3; nid-1* triple mutants are not significantly different from defects in *aex-3; nid-1* double mutants, suggesting that both genes act in the same pathway as *aex-3*.

unc-31 has been shown to interact with *ida-1* for dense core vesicle exocytosis (Cai et al., 2004), therefore, we wanted to test whether *ida-1* is also involved in AVG navigation. *ida-1* single mutants do not display AVG axon cross-over defects, however, *ida-1*; *nid-1* double mutant animals have AVG axon-cross over defects with a penetrance close to *aex-3*; *nid-1* double mutants (Figure 4.7). Defects in *ida-1*; *aex-3*; *nid-1* triple mutant are not enhanced compared to *aex-3*; *nid-1* double mutants (Figure 4.7), again suggesting that these genes act together in the same pathway. In summary, all the above data suggests that *aex-3* acts along with *unc-31, unc-64* and *ida-1*, known players of vesicle exocytosis through the same genetic pathway for the proper navigation of AVG axon in *nid-1* dependent manner.

4.3.7. AEX-3 might regulate the trafficking of Netrin receptor UNC-5

Since Syntaxin1 (UNC-64) has recently been directly implicated in Netrin-1 mediated axonal navigation (Cotrufo et al., 2012), we wanted to test if UNC-6/Netrin is involved in AVG axon navigation. *unc-6* mutant animals have only weakly penetrant AVG axon cross-over defects similar to *nid-1* mutant animals (Figure 4.8). AVG axon-cross-over defects are significantly enhanced in *unc-6*; *nid-1* double mutants, however not as much as in *aex-3; nid-1* double mutants (Figure 4.8). The enhancement of AVG cross-over defects in the *unc-6; nid-1* double mutant suggests that *unc-6* indeed plays a role in the navigation of the AVG axon. Two receptors, UNC-40/DCC and UNC-5, mediate responses to UNC-6/Netrin in *C. elegans* (Hedgecock et al., 1990; Ishii et al., 1992; Leung-Hagesteijn et al., 1992; Chan et al., 1996). *unc-5* mutants have mild AVG axon cross-over defects, whereas *unc-40* has none (Figure 4.8). *unc-5; nid-1* double mutant animals have penetrant AVG axon cross-over defects comparable to *aex-3; nid-1* (Figure 4.8). They are not further enhanced in *unc-5; aex-3; nid-1* triple mutants (Figure 4.8). In contrast *unc-40* does not enhance *nid-1* defects (Figure 4.8). This suggests that UNC-5, but not UNC-40 is required for the navigation of the AVG axon. In summary, the above data suggest that AEX-3 might regulate the trafficking of the UNC-5 receptor to the AVG growth cone.

4.4. Discussion

4.4.1. Ventral cord axon guidance requires *aex-3* in a Nidogen dependent manner

The AVG axon pioneers the right axon tract of the ventral nerve cord in *C. elegans* and is critical for the navigation of follower axons (Durbin, 1987; Hutter, 2003). The molecular basis for AVG navigation is largely unknown as the available axon guidance mutants have weakly penetrant AVG guidance defects (Hutter, 2003). Moreover, simple screens have not yielded new mutants with penetrant AVG navigation defects except the alleles of *plr-1* (Bhat et al., 2015; Moffat et al., 2014). We isolated an allele of *aex-3* in an enhancer screen for AVG axon guidance defects in a *nid-1* mutant background. In *C. elegans*, *nid-1* encodes the sole homolog of nidogen (entactin), a

basement membrane component. *nid-1* is required for the correct positioning of longitudinal axons and proper organisation of the presynaptic zones which is in accordance with the NID-1 being localised to ventral nerve cord close to the site of synapses formation (Kim and Wadsworth, 2000; Ackley et al., 2003). NID-1 affects the guidance of many neurons, most notably the command interneurons, motor neurons and HSN neurons (Kim & Wadsworth, 2000). However, NID-1 is not required for the basement membrane assembly and the guidance defects in *nid-1* mutants are not due to abnormal basement membrane per se (Kim & Wadsworth, 2000). Therefore, *nid-1* mutant animals are viable and healthy. *nid-1* mutant animals have weakly penetrant AVG axon cross-over defects, which are substantially enhanced in *aex-3*; *nid-1* double mutants. Moreover, known alleles (*n2166*, *sa5* and *js815*) of *aex-3* also showed AVG axon cross-over defects in *nid-1* background, suggesting that *aex-3* is required for axon navigation in *nid-1* dependent manner. AEX-3 is the nematode homolog of the Rab3/Rab27 GDP/GTP exchange factor (GEF) and is expressed in most neurons, including the ventral nerve cord axons (Iwasaki et al., 1997). AEX-3 activates the RAB-3 and AEX-6/Rab27 GTPases through distinct pathways to regulate synaptic vesicle transport and exocytosis (Mahoney et al., 2006). Since *aex-3* and *nid-1* are not obviously in a common pathway the synergistic effects on axon pathfinding are likely due to functional redundancy of different pathways.

AVG pioneer navigation defects are expected to have secondary consequences on follower navigation (Hutter, 2003). We found navigation defects in several classes of VNC follower neurons (command interneurons, motor neurons, AVK and HSN neurons) in *aex-3; nid-1* mutant animals. In many cases (command interneurons, DD/VD and DA/DB motor neurons) these axons followed the misguided poineer, suggesting that the defects are indeed secondary. However, in some cases follower defects (AVK, HSN and motor neuron commissures) were not correlated with pioneer defects, raising the possibility that primary defects are not limited to AVG. For example we found no correlation between AVK and AVG defects, indicating that AVK defects are not secondary consequences of AVG defects, at the same time indicating that AVK navigation is independent of the pioneer. This is consistent with earlier studies, where defects in AVK axon navigation in the left axon tract were also independent of pioneer defects (Steimel et al., 2010; Unsoeld et al., 2013). The idea that *aex-3* defects are not

limited to the VNC pioneer is strengthened by the observation of synergistic effects in *aex-3; nid-1* double mutants in commissural navigation, which is completely independent of AVG navigation. On the other hand visualization of the entire nervous system suggests that the overall structure of the nervous system is intact in *aex-3; nid-1* mutant animals and that the defects are largely limited to the VNC and commissures.

We did not observe any misplacement of neuronal cell bodies (with one exception see below), indicating that neuronal cell migration is not affected in *aex-3; nid-1* double mutants. However, in a small fraction (16%) of animals HSN neurons fail to reach their normal position at the vulva. HSN migration is controlled by Wnt signalling and both *egl-20*/Wnt and *mig-1*/Frizzled mutants display similar but more penetrant HSN defects (Pan et al., 2006). Mutations in other Wnts or Frizzled receptors do not cause these defects, but enhance HSN migration defects of *egl-20* and *mig-1*, suggesting a partially redundant function for Wnts and their receptors in this process (Pan et al. 2006). *aex-3* so far has not been linked to Wnt signalling. However, LIN-44/Wnt has been proposed to control sorting of pre-synaptic RAB-3 to axons and precludes its entry into the dendrite (Poon et al., 2008). This raises the possibility that HSN migration defects in *aex-3(hd148); nid-1* mutant animals could be a secondary consequence of a mislocalization of RAB-3.

4.4.2. AEX-3 and its interacting partners in AVG axon navigation

AEX-3 activates RAB-3 and AEX-6/Rab27 to regulate synaptic transmission (Mahoney et al., 2006) and physically interacts with CAB-1 to control the defecation motor program (Iwasaki & Toyonaga, 2000). Moreover, *aex-3* genetically interacts with *unc-31* and *unc-64* in the context of dauer formation (Iwasaki et al., 1997). All this indicates that AEX-3 regulates multiple processes through different downstream effectors. We found that *rab-3* but not *aex-6*/Rab27 mutant animals have AVG axon cross-over defects in a *nid-1* mutant background. Our genetic interaction data suggests that *aex-3* and *rab-3* act in the same genetic pathway. This suggests that AEX-3 activates RAB-3 but not AEX-6/Rab27 in the context of AVG axon navigation. Activated RAB-3 binds to synaptic precursor vesicles (Mahoney et al., 2006), which are transported from the cell body to synapses by the Kinesin-3 motor UNC-104 (Hall &

Hedgecock, 1991). Besides this, UNC-104 also transports dense core vesicle precursors to their release sites in the neurons (Jacob and Kaplan, 2003; Zahn et al., 2004). We observed some AVG axon cross-over defects in *unc-104; nid-1* mutant animals, but significantly less compared to either *aex-3; nid-1* or *rab-3; nid-1* mutant animals. This suggests that *aex-3* might be involved in vesicle transport in the context of axonal navigation, but that these vesicles are not exclusively transported by UNC-104. There is a possibility that some of the vesicles either move independent of motor proteins or alternately some other motor proteins are also involved. The *C. elegans* genome encodes for 21 kinesins, mostly involved in transport, spindle movement and chromosome segregation (Siddiqui, 2002). UNC-116/KIF5 is the kinesin heavy chain anterograde motor protein involved in the transport of synaptic vesicle components and glutamate receptors (Patel et al., 1993; Sakamoto et al., 2005; Hoerndli et al., 2013). VAB-8, an atypical kinase which controls the posteriorly directed cell migrations and axon outgrowth, also has been shown to regulate the levels of axon guidance receptors UNC-40/DCC and SAX-3/Robo in neurons (Wightman et al., 1996; Wolf et al., 1998; Levy-Strumpf and Culotti, 2007; Watari-Goshima et al., 2007). Moreover, the actin based minus-end-directed motor Myosin V1 transports both denritic as well as axonal surface proteins (Lewis et al., 2011). Therefore, it is possible that any motor protein/s present in the *C. elegans* can regulate the vesicular transport individually or in cooperation with UNC-104 for the proper AVG axon navigation, thus making it difficult to test the individual motor proteins. Upon reaching the synapses vesicles are made competent for fusion by the Rab3 effector molecule UNC-10/ Rim (Koushika et al., 2001). We did not observe AVG axon cross-over defects in the *unc-10; nid-1* mutant animals, suggesting that *unc-10*/Rim and by inference synaptic vesicle release is not involved in AVG axon navigation. Since the AVG axon extends before synapses are formed, this is not unexpected and indicates that the role of *aex-3* and *rab-3* here is independent of synaptic vesicle release.

Both *unc-31* and *ida-1,* which are required for dense core vesicle release (Cai et al., 2004; Speese et al., 2007), have AVG axon cross-over defects in a *nid-1* mutant background. Both genes as well as UNC-64/Syntaxin, a component of the SNARE complex required for synaptic vesicle release and dense core vesicle release (Saifee et al., 1998; Wit et al., 2006; Hammarlund et al., 2008), act in the same pathway as *aex-3*.

Since neither mature synaptic vesicles nor mature dense core vesicles are expected to be found in neurons at the beginning of axonal outgrowth, it seems more likely that these proteins during AVG axon outgrowth are involved in the release of some precursor vesicles in the growth cone. Since both *unc-31; nid-1* and *unc-64; nid-1* double mutants have less penetrant AVG defects than *aex-3; nid-1* double mutants, it is possible that two different populations of vesicles are involved. Alternatively *unc-31* and *unc-64* might have a partially redundant role in the release of a single type of precursor vesicle. It has been shown that mature synaptic vesicles from vertebrate cultured neurons are different both in function and composition than the vesicles found in growth cones. The SNARE complex proteins are present in both, but are regulated differently (Igarashi et al., 1997). The SNARE complex proteins and Rab3a appear early in the growth cone (Igarashi et al., 1997). Taken together with our genetic interaction data, it seems that the vesicular events happening in the growth cone are mediated by the RAB-3 activation and vesicle fusion with the growth cone membrane in the context of AVG axon navigation.

Vesicles in neurons carry specific molecules e.g. synaptic vesicles are loaded with neurotransmitters whereas dense core vesicles with neuropeptides and accessory proteins which are exocytosed at the neuronal terminals (Südhof, 1995; Kantardzhieva et al., 2012; Wilhelm et al., 2014). Besides this, vesicles can also supply and renew the membrane for the advancing growth cone which spans axon behind (Owen Lockerbie et al., 1991; Igarashi et al., 1996; Pfenninger, 2009). There are at least two possible functions for vesicles in the growth cone in the context of axon navigation. First they can deliver molecules essential for navigation, such as receptors for guidance molecules, to the membrane of the growth cone. We found that UNC-5, one of the receptors for the guidance cue UNC-6/Netrin, acts in the same pathway as AEX-3 for AVG axon navigation. This raises the possibility that AEX-3 is involved in the transport of vesicles carrying UNC-5 to the growth cone. An UNC-5::GFP reporter appears in punctate form in growth cones and axons, suggesting that it is localised to vesicles (Ogura and Goshima, 2006; Norris et al., 2014). UNC-51, a serine/threonine kinase and UNC-14, a RUN (RPIP8, UNC-14, and NESCA) domain-containing protein (Ogura et al., 1994; Ogura et al., 1997) have been proposed to co-operate with an unknown motor protein to regulate the formation, processing and transport of UNC-5 containing vesicles (Ogura & Goshima, 2006). VAB-8L, an atypical kinase with N-terminal motor domain (Wolf et al.

1998) physically interacts with UNC-51(Lai & Garriga, 2004) and has been shown to regulate the surface expression of SAX-3/Robo, UNC-40/DCC and possibly UNC-5 receptors (Watari-Goshima et al., 2007; Levy-Strumpf and Culotti, 2007). Therefore, it is possible that AEX-3 activates RAB-3 which in turn recruits VAB-8L to the vesicles carrying UNC-5 that are transported to the growth cone. However, it needs to be tested whether *vab-8* has *nid-1* dependent AVG axon cross-over defects and acts with *aex-3* through the same genetic pathway.

A second possible role of vesicles in axon guidance arises from the observation that Syntaxin1 associates with DCC (another Netrin receptor) at the growth cone. This interaction is required for UNC-6/Netrin dependent migration of axons (Cotrufo et al., 2012). Localized insertion of membrane at sites of activation of guidance receptors is thought to be the key function of this interaction (Tojima et al., 2011; Tojima and Kamiguchi, 2015). This raises the possibility that *aex-3* is involved in the localized insertion of membrane in the growth in response to activation of UNC-5. Distinguishing between these two models would require *in vivo* observations of growth cones, which unfortunately is not possible for AVG.

In summary, we are proposing a novel role for AEX-3 in axon guidance during the nervous system development in *C. elegans*. We found that AEX-3 is required for axon guidance in pioneer neurons during nervous system development in *C. elegans*. *aex-3* genetically interacts with *rab-3*, several genes controlling vesicle release in neurons and the axon guidance receptor *unc-5* (Figure 4.9). *aex-3* is likely involved in transport and/or release of vesicles at the growth cone. It could control delivery and insertion of UNC-5 protein into the membrane of the growth cone or be involved in targeted insertion of membrane after receptor activation. Given the evolutionary conservation of all genes we found to be involved in this process, it seems likely that AEX-3 and RAB-3 homologues (Iwasaki et al., 1997; Schievella et al., 1997; Wada et al., 1997) have a similar role in the mammalian nervous system.

4.5. Contributions

The experiments were designed by me and HH. I, the first author of this study performed all the experiments and analysed the data. The *aex-3* cDNA was kindly provided by Dr. Erik Jorgensen, *lin-11* promoter by Dr. Bhagwati Gupta and UNC-5::GFP strain by Dr. Erik A. Lundquist. The *aex-3* mutant strain was whole genome sequenced in Dr. Don Moerman's laboratory at UBC. I would like to thank Vinci Au for the sequencing and Stephane Flibotte for analysing the sequence data. Some of the strains used in this study were provided by CGC, which is funded by the NIH National Center for Research Resources (NCRR). This work was supported by CIHR grant (MOP 93719) to HH.

4.6. Figures

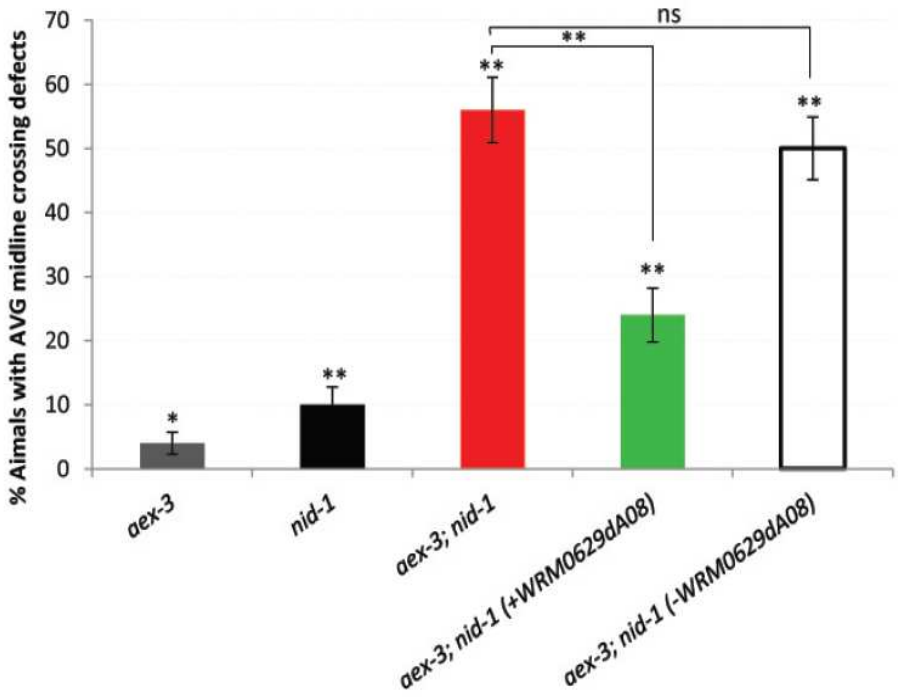

Figure 4.1 AVG cross-over defects are rescued by *aex-3* containing fosmid

Columns are percentages of animals with AVG midline crossing defects (± standard error) with genotypes as indicated. The transgenic animals with an extrachromosomal array (+WRM0629dA08) (green bar) and non-transgenic animals without an extrachromosomal array (-WRM0629dA08) (white bar) from the same strain were counted for the AVG axon cross-over defects. AVG CO defects are significantly rescued by the *aex-3* containg fosmid in transgenic animals whereas these defects are not rescued in non-transgenic animals. For each strain $n >$ 100 except *aex-3; nid-1* ($n = 97$) animals were analysed. χ^2 tests were used to establish statistical significance between the mutants. Single mutants were compared with wild type, *aex-3; nid-1* double mutant with *nid-1* single mutant and *aex-3; nid-1* (+/-WRM0629dA08) with *aex-3*; *nid-1* double mutant (*: $p < 0.05$; **: $p < 0.01$; ^{ns}: not significant). Mutant alleles used: *aex-3(hd148)* and *nid-1(cg119).* Fluorescent marker used: AVG marker (*odr-2::tdTomato*).

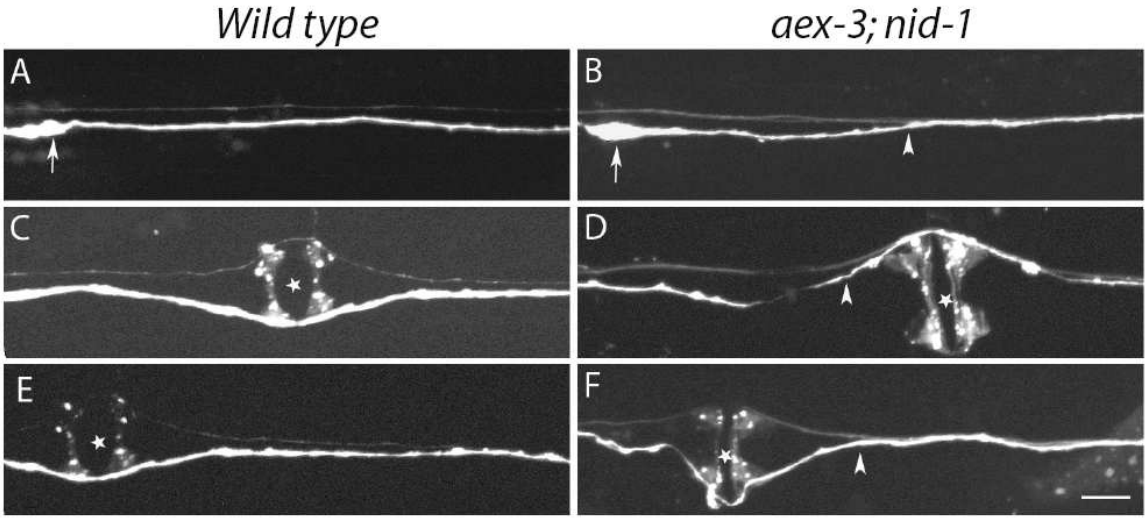

Figure 4.2 AVG cross-over defects in *aex-3(hd148)*; *nid-1* mutant animals

(A, C, E) wild type; (B, D, F) *aex-3(hd148)*; *nid-1*. (A, C, E) In wild type animals AVG cell body (arrow) is located on the anterior side which extends an axon on the right side of the ventral nerve cord (VNC) that never crosses the ventral midline. In majority of the *aex-3(hd148); nid-1* mutant animals AVG axon crosses the ventral midline at the anterior half (B) and (D) and in some animals at the posterior half of the animal's body (F), and joins the left axon tract of the VNC. The AVG axon stays mostly on the left side of VNC after crossing the midline but in some animals it switches back to the right side of VNC. Arrows indicates the position of AVG cell body, arrow heads indicates the position of AVG axon cross-over and the asterisks marks the vulva position. Marker used: (*odr-2::tdTomato*). Scale bar: 10µm.

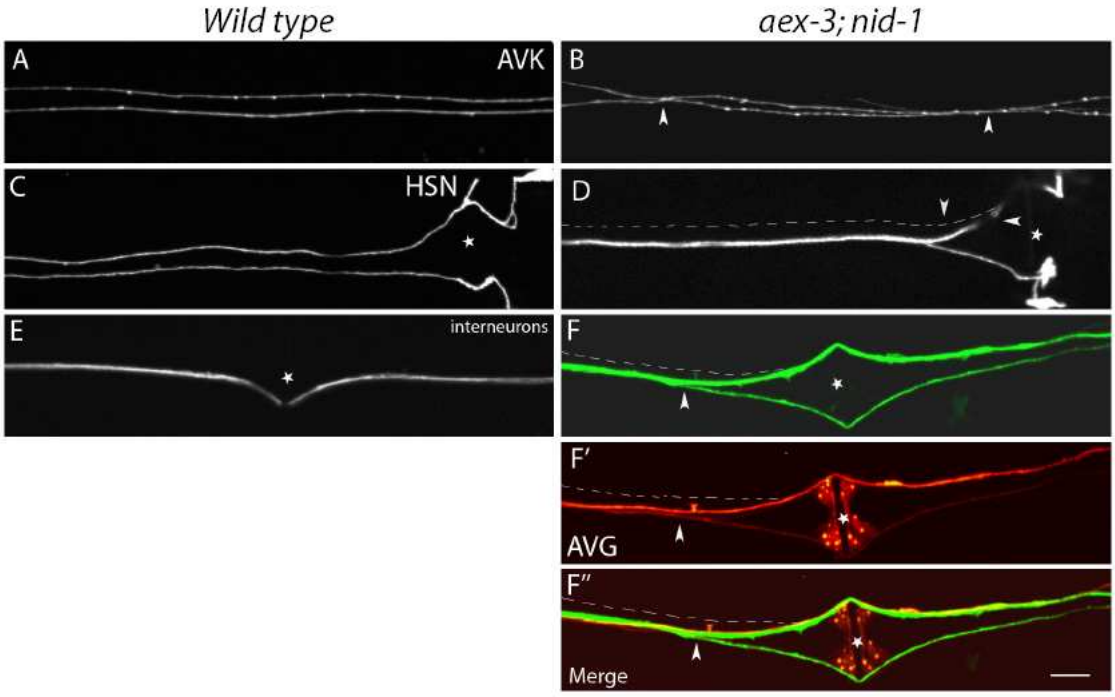

Figure 4.3 Interneuron, AVK and HSN axon defects in *aex-3(hd148); nid-1* mutant animals

(A, C, E) wild type; (B, D, F, F′, F″) *aex-3*(*hd148*); *nid-1*. (A) In wild type animals AVK axons extend in both ventral nerve cord axon tracts and never make mistakes. (B) In *aex-3*(*hd148*); *nid-1* mutant animals AVK axons frequently cross the ventral midline (arrow head). (C) In wild type animals HSN axons are ipsilateral and extend axons in both ventral nerve cord axon tracts on their respective sides. (D) In majority of the *aex-3*(*hd148*); *nid-1* mutant animals the left side HSN axon crosses the ventral midline and joins the right axon tract (arrow head). (E) In wild type animals command interneurons extend into the right axon tract of the ventral nerve cord. (F, F′) In *aex-3*(*hd148*); *nid-1* mutant animals the command interneurons make mistakes along with the AVG pioneer by crossing (arrow head) from right side and extend into the left axon tract of VNC at the same position. F″ is the merged image of F and F′. Asterisks marks the vulva position. The dashed lines (white) mark the normal axon trajectories. Markers used: Interneuron marker (*glr-1::GFP*), AVK marker (*flp-1::*GFP) and HSN marker (*tph-1::* GFP). Scale bar: 10µm.

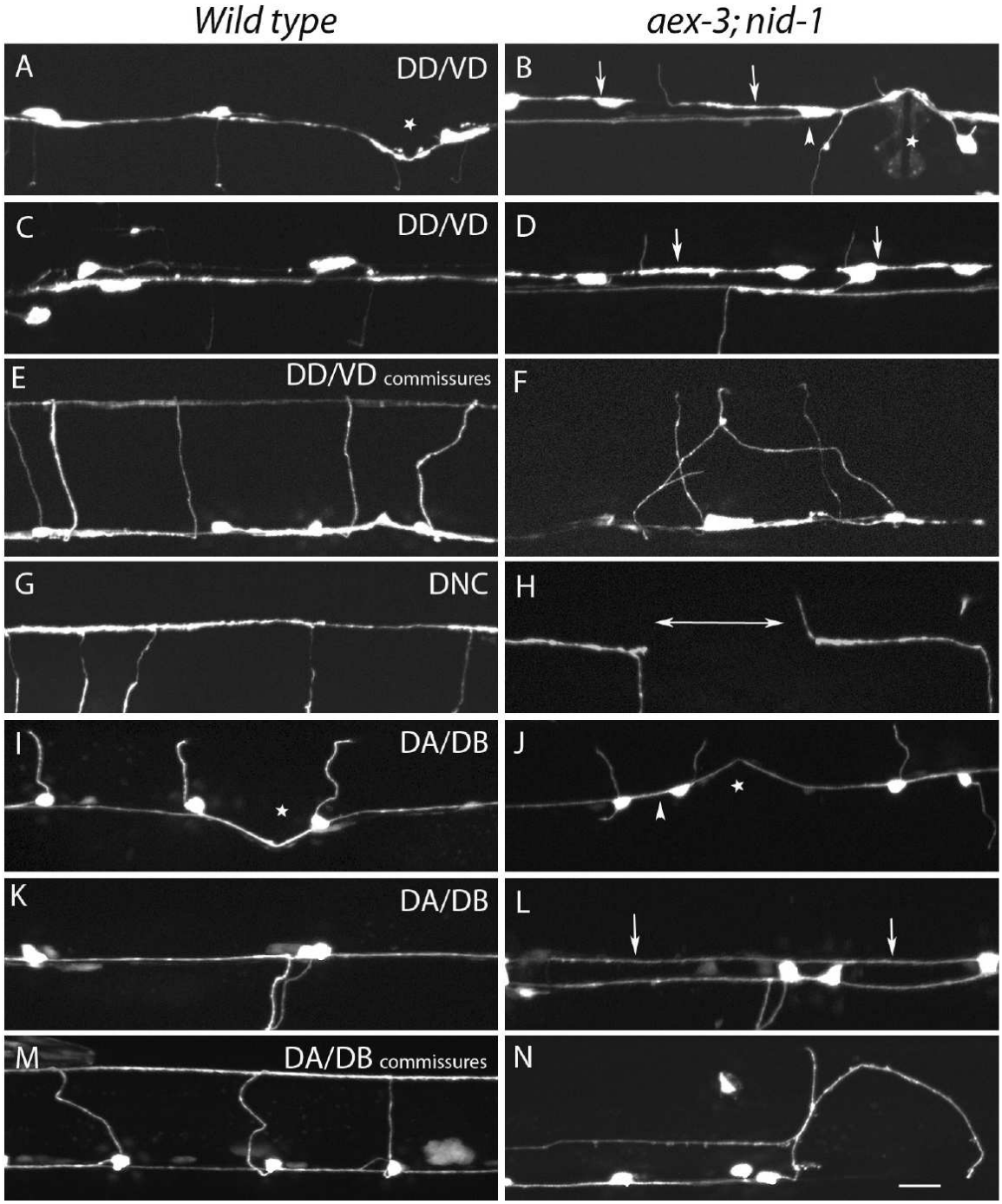
Wild type
aex-3; nid-1
A
DD/VD
B
C
DD/VD
D
E
DD/VD commissures
F
G
DNC
H
I
DA/DB
J
K
DA/DB
L
M
DA/DB commissures
N

Figure 4.4 DD/VD and DA/DB motor neuron defects in *aex-3*(*hd148*); *nid-1* mutant animals

(A, C, E, G, I, K, M) wild type; (B, D, F, H, J, L, N) *aex-3*(*hd148*); *nid-1*. (A, C, E, G) In wild type animals DD/VD motor neurons extend axons towards the anterior end in the right axon tract that branch and extend commissures towards the dorsal side to form the dorsal nerve cord (DNC). In *aex-3*(*hd148*); *nid-1* mutant animals motor neuron axons either cross (arrow head) the ventral midline and extend into the left axon tract (B) or wrongly invade the left axon tract (arrow) (B, D). The DD/VD commissures are severely affected (F) with some of them not making it to the dorsal side, resulting in the formation of incomplete DNC (H) (arrow with two heads). (I, K, M) In wild type animals, DA/DB motor neurons extend dendrites to the right axon tract and commissures which directly arise from the cell body towards the dorsal cord. (J, L, N) In *aex-3*(*hd148*); *nid-1* mutant animals DA/DB dendrites cross the ventral midline (arrow head) and extend into the left axon tract (J) or wrongly invade the left axon tract (arrow) (L) and have mild commissural navigation defects (N). Asterisks mark the vulva position. Markers used: DD/VD/Commissures (*unc-47::DsRed2*) DA/DB/Commissures (*unc-129::CFP*). Scale bar: 10µm.

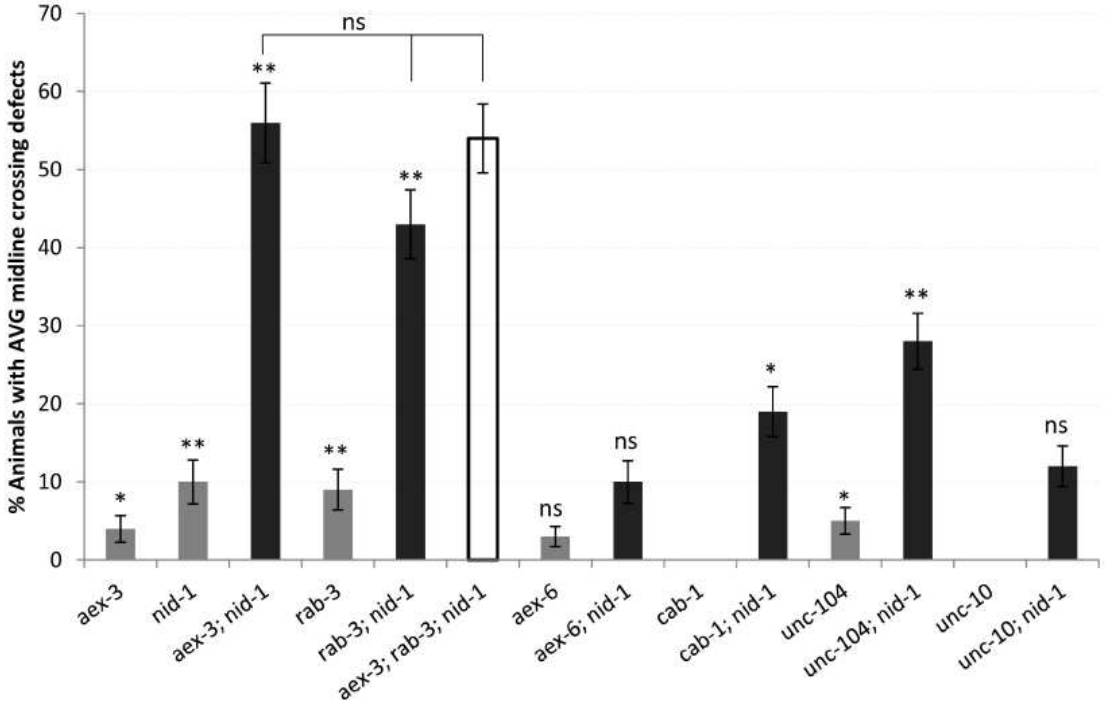

Figure 4.5 *aex-3* and *rab-3* act through the same genetic pathway for AVG axon navigation

Columns are percentages of animals with AVG midline crossing defects (± standard error) with genotypes as indicated. In the bar diagram the single mutants are represented by light grey shaded bars, the double mutants by black shaded bars and the triple mutant by a white bar. For each strain $n > 100$ except *aex-3; nid-1* ($n = 97$) animals were analysed. χ^2 tests were used to establish statistical significance between the mutants. Single mutants were compared with wild type, double mutants with *nid-1* single mutant and the triple mutant with *aex-3*; *nid-1* double mutant (*: $p < 0.05$; **: $p < 0.01$; ^{ns}: not significant). Mutant alleles used: *aex-3(hd148)*, *nid-1(cg119)*, *rab-3(js49)*, *aex-6(sa24), cab-1(tg49, unc-104(e1265)* and *unc-10(md1117).* Fluorescent marker used: AVG marker (*odr-2::tdTomato*).

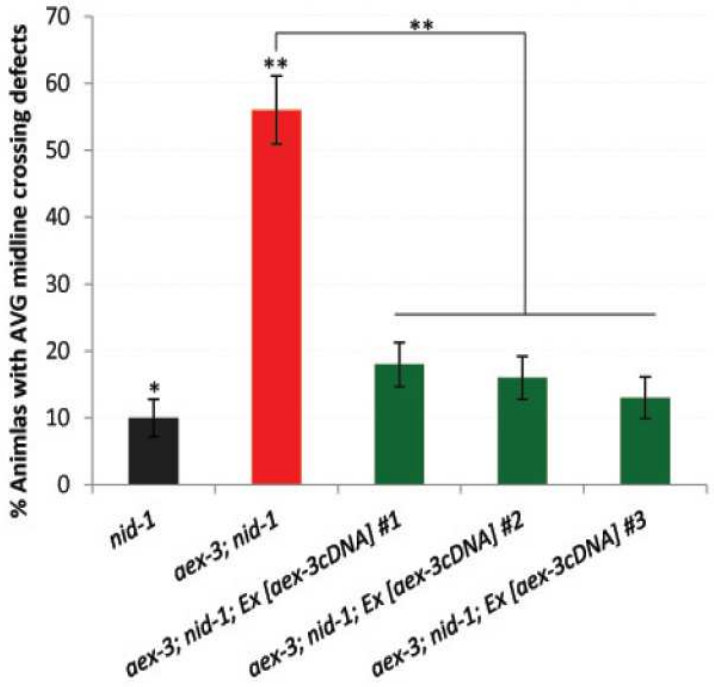

Figure 4.6 *aex-3* functions cell autonomously for the AVG axon navigation

Columns are percentages of animals with AVG midline crossing defects (± standard error) with genotypes as indicated. The transgenic animals from three independent lines (#1, #2 and #3) expressing *aex-3*cDNA in the AVG neuron were analysed for AVG axon cross-over defects. AVG CO defects are significantly rescued by the *aex-3*cDNA in all the three transgenic lines. For each strain $n > 100$ except *aex-3; nid-1* ($n = 97$) animals were analysed. χ^2 tests were used to establish statistical significance between the mutants. *nid-1* is compared with wild type, *aex-3; nid-1* double mutant with *nid-1* single mutant and *aex-3; nid-1; Ex[aex-3cDNA*] #1, #2 and #3 with *aex-3*; *nid-1* double mutant (*: $p < 0.05$; **: $p < 0.01$). Mutant alleles used: *aex-3(hd148)* and *nid-1(cg119.* Fluorescent marker used: AVG marker (*odr-2::tdTomato*).

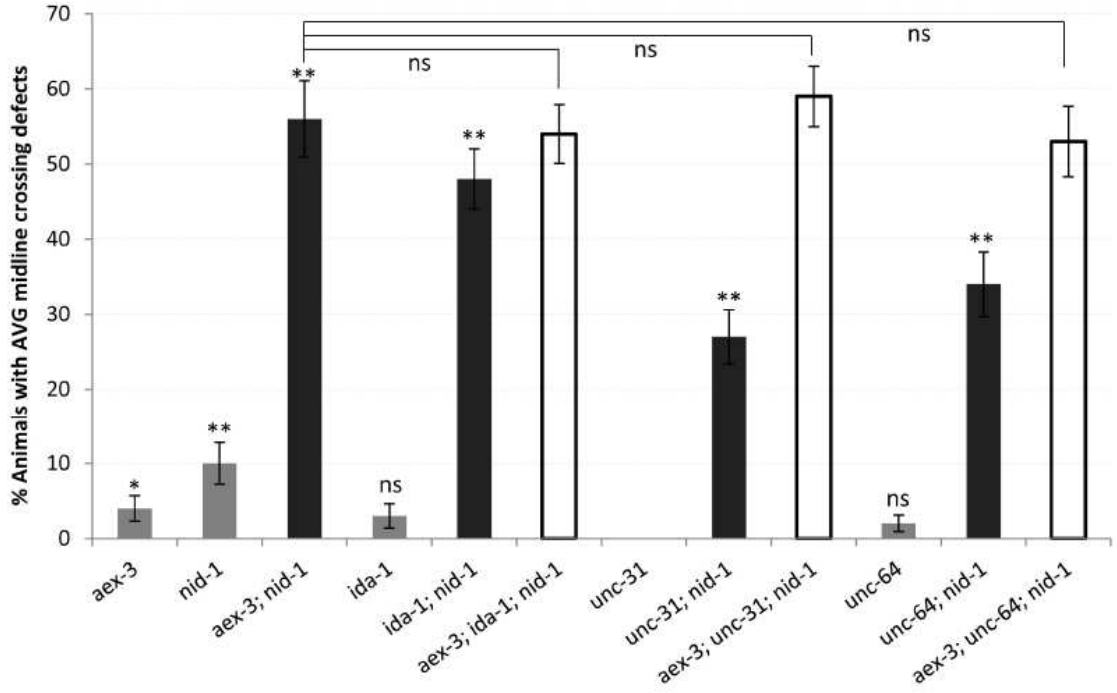

Figure 4.7 *aex-3*, *ida-1, unc-31* and *unc-64* act through the same genetic pathway for AVG axon navigation

Columns are percentages of animals with AVG midline crossing defects (± standard error) with genotypes as indicated. In the bar diagram the single mutants are represented by light grey shaded bars, the double mutants by black shaded bars and the triple mutants by white bars. For each strain $n > 100$ except *aex-3; nid-1* ($n = 97$) animals were analysed. χ^2 tests were used to establish statistical significance between the mutants. Single mutants were compared with wild type, double mutants with *nid-1* single mutant and the triple mutants with *aex-3*; *nid-1* double mutant (*: $p < 0.05$; **: $p < 0.01$; ^{ns}: not significant). Mutant alleles used: *aex-3(hd148)*, *nid-1(cg119)*, *ida-1(ok409)*, *unc-31(e169)* and *unc-64(e264)*. Fluorescent marker used: AVG marker *(odr-2::tdTomato)*.

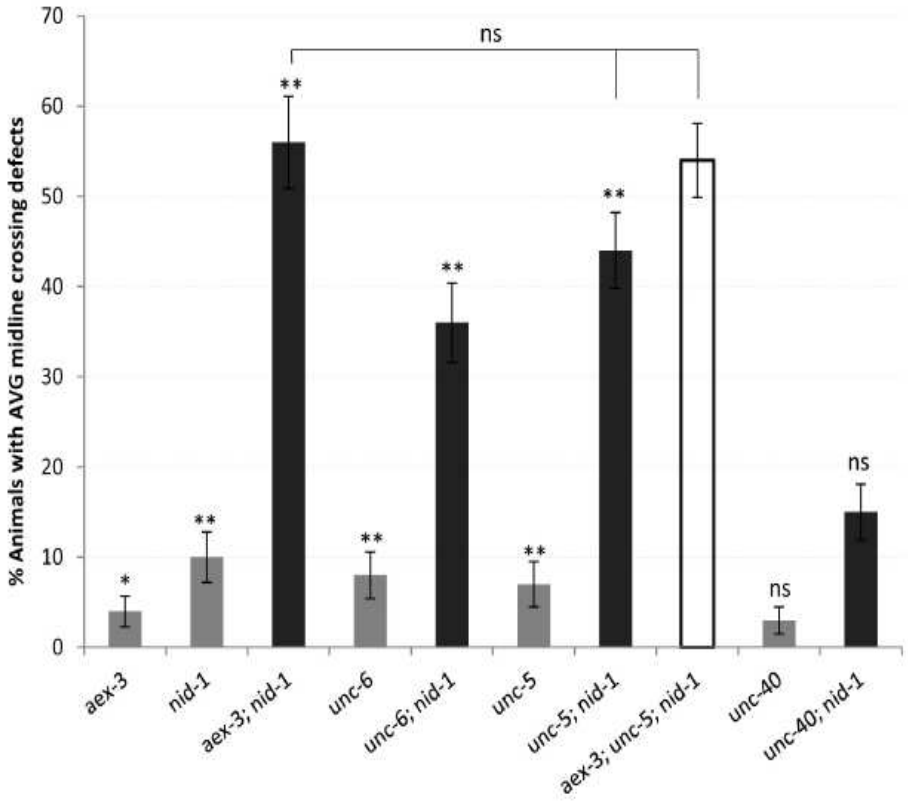

Figure 4.8 *aex-3* and *unc-5* act through the same genetic pathway for AVG axon navigation

Columns are percentages of animals with AVG midline crossing defects (± standard error) with genotypes as indicated. In the bar diagram the single mutants are represented by light grey shaded bars, the double mutants by black shaded bars and the triple mutant by white bar. For each strain $n > 100$ except *aex-3; nid-1* ($n = 97$) animals were analysed. χ^2 tests were used to establish statistical significance between the mutants. Single mutants were compared with wild type, double mutants with *nid-1* single mutant and the triple mutant with *aex-3*; *nid-1* double mutant (*: $p < 0.05$; **: $p < 0.01$; ^{ns}: not significant). Mutant alleles used: *aex-3(hd148)*, *nid-1(cg119)*, *unc-6(ev400), unc-40(e271)* and *unc-5(e53).* Fluorescent marker used: AVG marker *(odr-2::tdTomato)*.

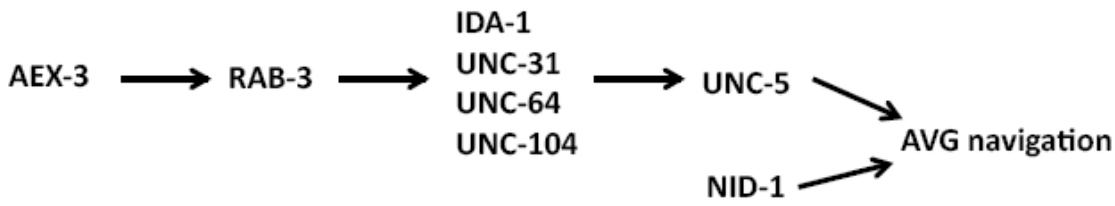

Figure 4.9 The *aex-3* pathway in AVG axon navigation

The figure describes the observed genetic interactions in the context of the known molecular functions of the proteins involved (e.g. *aex-3* is upstream of *rab-3* because it is known to activate *rab-3*).

4.7. Tables

Table 4.1 AVG cross-over defects in *aex-3* mutants with and without *nid-1* (% animals with defects)

Genotype	AVG CO	*n*
aex-3(hd148)	4*	104
aex-3(hd148);nid-1	56**	97
aex-3(n2166)	3ns	74
aex-3(n2166);nid-1	46**	112
aex-3(sa5)	3ns	95
aex-3(sa5);nid-1	43**	130
aex-3(js815)	4*	121
aex-3(js815);nid-1	39**	112
nid-1(cg119)	10**	118
Wildtype	0	117

marker used: *hdIs51[odr-2::tdTomato].*
n = number of animals.
CO: cross-over.
(For statistical significance single mutants were compared with wild type and double mutants with *nid-1* single mutant; *: $p < 0.05$; **: $p < 0.01$; ns: not significant; χ^2 test).

Table 4.2 Other neuronal defects in *nid-1* single and *aex-3(hd148)*; *nid-1* double mutants (% animals with defects).

Phenotype	*nid-1*	*aex-3(hd148)*; *nid-1*
Interneuron cross-over defects		
AVGdependent[a]	6 (114)	35** (104)
AVGindependent[b]	0 (114)	14** (104)
AVK defects		
VNC cross-over	18 (115)	49** (109)
Premature stop	12 (115)	22[ns] (109)
Leaving VNC	1 (115)	3[ns] (109)
HSN neurons		
VNC cross-over	58 (103)	68[ns] (109)
Undermigration & VNC cross-over	3 (103)	16** (109)
motor neuron defects		
DD/VD		
VNC cross-over[c]	8 (133)	28** (123)
Symmetrical VNC	0 (133)	36** (123)
Commissural defects	65 (133)[d]	100** (123)[e]
DNC gaps	85 (53)	100* (26)
DA/DB		
VNC cross-over[f]	8 (110)	29** (103)
Symmetrical VNC	0 (110)	20** (103)
Commissural defects	0 (110)	18** (103)

[a] means where interneurons either have cross-over defects at the same or different position where AVG has cross-over defects, in a dependent manner.

[b] means interneurons have cross-over defects but the AVG is wild type in these animals. [c] & [f] both DD/VD and DA/DB axons cross at the same position where AVG axon crosses.

In each animal on an average 14[e] and 12[f] commissures make it to the dorsal nerve cord (DNC).

Values in brackets indicate *n*

Markers used: Interneuron *(glr-1::GFP),* AVK *(flp-1::GFP),* HSN *(tph-1::GFP),* DD/VD/Commissures *(unc-47::DsRed-2)* and DA/DB *(unc-129::CFP)*

(For statistical significance *aex-3*; *nid-1* double mutants are compared with *nid-1* single mutant; *: $p < 0.05$; **: $p < 0.01$; [ns]: not significant; χ^2 test).

4.8. References:

Ackley, B.D., Kang, S.H., Crew, J.R., Suh, C., Jin, Y., Kramer, J.M., 2003. The basement membrane components nidogen and type XVIII collagen regulate organization of neuromuscular junctions in *Caenorhabditis elegans*. J. Neurosci. 23, 3577–3587.

Bhat, J.M., Pan, J., Hutter, H., 2015. PLR-1, a putative E3 ubiquitin ligase, controls cell polarity and axonal extensions in *C. elegans*. Dev. Biol. 398, 44–56.

Brenner, S., 1974. The genetics of *Caenorhabditis elegans*. Genetics 77, 71–94.

Cai, T., Fukushige, T., Notkins, A.L., Krause, M., 2004. Insulinoma-Associated Protein IA-2, a Vesicle Transmembrane Protein, Genetically Interacts with UNC-31/CAPS and Affects Neurosecretion in *Caenorhabditis elegans*. J. Neurosci. 24, 3115–3124.

Chan, S.S.Y., Zheng, H., Su, M.W., Wilk, R., Killeen, M.T., Hedgecock, E.M., Culotti, J.G., 1996. UNC-40, a *C. elegans* homolog of DCC (Deleted in Colorectal Cancer), is required in motile cells responding to UNC-6 netrin cues. Cell 87, 187–195.

Chitnis, a. B., Kuwada, J.Y., 1991. Elimination of a brain tract increases errors in pathfinding by follower growth cones in the zebrafish embryo. Neuron 7, 277–285.

Colavita, a, Krishna, S., Zheng, H., Padgett, R.W., Culotti, J.G., 1998. Pioneer axon guidance by UNC-129, a *C. elegans* TGF-beta. Science 281, 706–709.

Cornel, E., Holt, C., 1992. Precocious pathfinding: Retinal axons can navigate in an axonless brain. Neuron 9, 1001–1011.

Cotrufo, T., Andrés, R.M., Ros, O., Pérez-Brangulí, F., Muhaisen, A., Fuschini, G., Martínez, R., Pascual, M., Comella, J.X., Soriano, E., 2012. Syntaxin 1 is required for DCC/Netrin-1-dependent chemoattraction of migrating neurons from the lower rhombic lip. Eur. J. Neurosci. 36, 3152–3164.

Darchen, F., Senyshyn, J., Brondyk, W.H., Taatjes, D.J., Holz, R.W., Henry, J.P., Denizot, J.P., Macara, I.G., 1995. The GTPase Rab3a is associated with large dense core vesicles in bovine chromaffin cells and rat PC12 cells. J. Cell Sci. 108 (Pt 4), 1639–1649.

Durbin, R.M., 1987. Studies on the Development and Organisation of the Nervous System of *Caenorhabditis elegans*. Ph.D.dissertation,University of Cambridge, England.

Eisen, J.S., Pike, S.H., Debu, B., 1989. The growth cones of identified motoneurons in embryonic zebrafish select appropriate pathways in the absence of specific cellular interactions. Neuron 2, 1097–1104.

Fischer von Mollard, G., Mignery, G. a, Baumert, M., Perin, M.S., Hanson, T.J., Burger, P.M., Jahn, R., Südhof, T.C., 1990. rab3 is a small GTP-binding protein exclusively localized to synaptic vesicles. Proc. Natl. Acad. Sci. U. S. A. 87, 1988–1992.

Fischer von Mollard, G., Südhof, T.C., Jahn, R., 1991. A small GTP-binding protein dissociates from synaptic vesicles during exocytosis. Nature 349, 79–81.

Garriga, G., Desai, C., Horvitz, H.R., 1993. Cell interactions control the direction of outgrowth, branching and fasciculation of the HSN axons of Caenorhabditis *elegans*. Development 117, 1071–1087.

Hall, D.H., Hedgecock, E.M., 1991. Kinesin-related gene *unc-104* is required for axonal transport of synaptic vesicles in *C. elegans*. Cell 65, 837–847.

Hammarlund, M., Watanabe, S., Schuske, K., Jorgensen, E.M., 2008. CAPS and syntaxin dock dense core vesicles to the plasma membrane in neurons. J. Cell Biol. 180, 483–491.

Hedgecock, E.M., Culotti, J.G., Hall, D.H., 1990. The *unc-5*, *unc-6*, and *unc-40* genes guide circumferential migrations of pioneer axons and mesodermal cells on the epidermis in *C. elegans*. Neuron 4, 61–85.

Hidalgo, a, Brand, a H., 1997. Targeted neuronal ablation: the role of pioneer neurons in guidance and fasciculation in the CNS of *Drosophila*. Development 124, 3253–3262.

Hoerndli, F.J., Maxfield, D. a., Brockie, P.J., Mellem, J.E., Jensen, E., Wang, R., Madsen, D.M., Maricq, A. V., 2013. Kinesin-1 regulates synaptic strength by mediating the delivery, removal, and redistribution of AMPA receptors. Neuron 80, 1421–1437.

Hutagalung, A.H., Novick, P.J., 2011. Role of Rab GTPases in membrane traffic and cell physiology. Physiol. Rev. 91, 119–49.

Hutter, H., 2003. Extracellular cues and pioneers act together to guide axons in the ventral cord of *C. elegans*. Development 130, 5307–5318.

Igarashi, M., Tagaya, M., Komiya, Y., 1997. The soluble N-ethylmaleimide-sensitive factor attached protein receptor complex in growth cones: molecular aspects of the axon terminal development. J. Neurosci. 17, 1460–1470.

Igarashi, M., Terakawa, S., Ide, C., Iomiya, Y., 1996. 1224 A t-Snare is involved in axonal growth: Botulinum neurotoxin C1 induces growth cone collapse. Neurosci. Res. 25, S134.

Ishii, N., Wadsworth, W.G., Stern, B.D., Culotti, J.G., Hedgecock, E.M., 1992. UNC-6, a laminin-related protein, guides cell and pioneer axon migrations in *C. elegans*. Neuron 9, 873–881.

Iwasaki, K., Staunton, J., Saifee, O., Nonet, M., Thomas, J.H., 1997. *aex-3* encodes a novel regulator of presynaptic activity in *C. elegans*. Neuron 18, 613–622.

Iwasaki, K., Toyonaga, R., 2000. The Rab3 GDP/GTP exchange factor homolog AEX-3 has a dual function in synaptic transmission. EMBO J. 19, 4806–4816.

Jacob, T.C., Kaplan, J.M., 2003. The EGL-21 carboxypeptidase E facilitates acetylcholine release at *Caenorhabditis elegans* neuromuscular junctions. J. Neurosci. 23, 2122–2130.

Kantardzhieva, a., Peppi, M., Lane, W.S., Sewell, W.F., 2012. Protein composition of immunoprecipitated synaptic ribbons. J. Proteome Res. 11, 1163–1174.

Keshishian, H., Bentley, D., 1983. Embryogenesis of peripheral nerve pathways in grasshopper legs. II. The major nerve routes. Dev. Biol. 96, 103–15.

Kim, S., Wadsworth, W.G., 2000. Positioning of longitudinal nerves in *C. elegans* by nidogen. Science 288, 150–154.

Klose, M., Bentley, D., 1989. Transient pioneer neurons are essential for formation of an embryonic peripheral nerve. Science 245, 982–984.

Koushika, S.P., Richmond, J.E., Hadwiger, G., Weimer, R.M., Jorgensen, E.M., Nonet, M.L., 2001. A post-docking role for active zone protein Rim. Nat. Neurosci. 4, 997–1005.

Lai, T., Garriga, G., 2004. The conserved kinase UNC-51 acts with VAB-8 and UNC-14 to regulate axon outgrowth in *C. elegans*. Development 131, 5991–6000.

Leung-Hagesteijn, C., Spence, a. M., Stern, B.D., Zhou, Y., Su, M.W., Hedgecock, E.M., Culotti, J.G., 1992. UNC-5, a transmembrane protein with immunoglobulin and thrombospondin type 1 domains, guides cell and pioneer axon migrations in *C. elegans*. Cell 71, 289–299.

Levy-Strumpf, N., Culotti, J.G., 2007. VAB-8, UNC-73 and MIG-2 regulate axon polarity and cell migration functions of UNC-40 in *C. elegans*. Nat. Neurosci. 10, 161–168.

Lewis, T.L., Mao, T., Arnold, D.B., 2011. A role for Myosin VI in the localization of axonal proteins. PLoS Biol. 9 (3) :e1001021.

Livingstone D (1991) Studies on the unc-31 gene of *Caenorhabditis elegans.* PhD thesis, University of Cambridge.

MacNeil, L.T., Hardy, W.R., Pawson, T., Wrana, J.L., Culotti, J.G., 2009. UNC-129 regulates the balance between UNC-40 dependent and independent UNC-5 signaling pathways. Nat. Neurosci. 12, 150–155.

Mahoney, T.R., Liu, Q., Itoh, T., Luo, S., Hadwiger, G., Vincent, R., Wang, Z.-W., Fukuda, M., Nonet, M.L., 2006. Regulation of synaptic transmission by RAB-3 and RAB-27 in *Caenorhabditis elegans*. Mol. Biol. Cell 17, 2617–25.

McConnell, S.K., Ghosh, a, Shatz, C.J., 1989. Subplate neurons pioneer the first axon pathway from the cerebral cortex. Science 245, 978–982.

Mello, C.C., Kramer, J.M., Stinchcomb, D., Ambros, V., 1991. Efficient gene transfer in *C.elegans*: extrachromosomal maintenance and integration of transforming sequences. EMBO J. 10, 3959–70.

Moffat, L.L., Robinson, R.E., Bakoulis, A., Clark, S.G., 2014. The conserved transmembrane RING finger protein PLR-1 downregulates Wnt signaling by reducing Frizzled, Ror and Ryk cell-surface levels in *C. elegans*. Development 141, 617–28.

Nonet, M.L., Staunton, J.E., Kilgard, M.P., Fergestad, T., Hartwieg, E., Horvitz, H.R., Jorgensen, E.M., Meyer, B.J., 1997. Caenorhabditis elegans *rab-3* mutant synapses exhibit impaired function and are partially depleted of vesicles. J. Neurosci. 17, 8061–8073.

Norris, a. D., Sundararajan, L., Morgan, D.E., Roberts, Z.J., Lundquist, E. a., 2014. The UNC-6/Netrin receptors UNC-40/DCC and UNC-5 inhibit growth cone filopodial protrusion via UNC-73/Trio, Rac-like GTPases and UNC-33/CRMP. Development 141, 4395–4405.

Ogura, K.-I., Goshima, Y., 2006. The autophagy-related kinase UNC-51 and its binding partner UNC-14 regulate the subcellular localization of the Netrin receptor UNC-5 in *Caenorhabditis elegans*. Development 133, 3441–3450.

Ogura, K.I., Shirakawa, M., Barnes, T.M., Hekimi, S., Ohshima, Y., 1997. The UNC-14 protein required for axonal elongation and guidance in *Caenorhabditis elegans* interacts with the serine/threonine kinase UNC-51. Genes Dev. 11, 1801–1811.

Ogura, K.I., Wicky, C., Magnenat, L., Tobler, H., Mori, I., Müller, F., Ohshima, Y., 1994. *Caenorhabditis elegans unc-51* gene required for axonal elongation encodes a novel serine/threonine kinase. Genes Dev. 8, 2389–2400.

Owen Lockerbie, R., Miller, V.E., Pfenninger, K.H., 1991. Regulated plasmalemmal expansion in nerve growth cones. J. Cell Biol. 112, 1215–1227.

Pan, C.L., Howell, J.E., Clark, S.G., Hilliard, M., Cordes, S., Bargmann, C.I., Garriga, G., 2006. Multiple Wnts and Frizzled receptors regulate anteriorly directed cell and growth cone migrations in *Caenorhabditis elegans*. Dev. Cell 10, 367–377.

Patel, N., Thierry-Mieg, D., Mancillas, J.R., 1993. Cloning by insertional mutagenesis of a cDNA encoding *Caenorhabditis elegans* kinesin heavy chain. Proc. Natl. Acad. Sci. U. S. A. 90, 9181–9185.

Pfenninger, K.H., 2009. Plasma membrane expansion: a neuron's Herculean task. Nat. Rev. Neurosci. 10, 251–261.

Poon, V.Y., Klassen, M.P., Shen, K., 2008. UNC-6/netrin and its receptor UNC-5 locally exclude presynaptic components from dendrites. Nature 455, 669–73.

Saifee, O., Wei, L., Nonet, M.L., 1998. The *Caenorhabditis elegans unc-64* locus encodes a syntaxin that interacts genetically with synaptobrevin. Mol. Biol. Cell 9, 1235–1252.

Sakamoto, R., Byrd, D.T., Brown, H.M., Hisamoto, N., Matsumoto, K., Jin, Y., 2005. The *Caenorhabditis elegans* UNC-14 RUN domain protein binds to the kinesin-1 and UNC-16 complex and regulates synaptic vesicle localization. Mol. Biol. Cell 16, 483–496.

Schievella, a R., Chen, J.H., Graham, J.R., Lin, L.L., 1997. MADD, a novel death domain protein that interacts with the type 1 tumor necrosis factor receptor and activates mitogen-activated protein kinase. J. Biol. Chem. 272, 12069–12075.

Siddiqui, S.S., 2002. Metazoan motor models: kinesin superfamily in *C. elegans*. Traffic 3, 20–28.

Speese, S., Petrie, M., Schuske, K., Ailion, M., Ann, K., Iwasaki, K., Jorgensen, E.M., Martin, T.F.J., 2007. UNC-31 (CAPS) is required for dense-core vesicle but not synaptic vesicle exocytosis in *Caenorhabditis elegans*. J. Neurosci. 27, 6150–6162.

Steimel, A., Wong, L., Najarro, E.H., Ackley, B.D., Garriga, G., Hutter, H., 2010. The Flamingo ortholog FMI-1 controls pioneer-dependent navigation of follower axons in *C. elegans*. Development 137, 3663–3673.

Südhof, T.C., 1995. The synaptic vesicle cycle: a cascade of protein-protein interactions. Nature. 375 (6533), 645-53.

Thomas, J.H., 1990. Genetic analysis of defecation in *Caenorhabditis elegans*. Genetics 124, 855–872.

Tojima, T., Hines, J.H., Henley, J.R., Kamiguchi, H., 2011. Second messengers and membrane trafficking direct and organize growth cone steering. Nat. Rev. Neurosci. 12, 191–203.

Tojima, T., Kamiguchi, H., 2015. Exocytic and endocytic membrane trafficking in axon development. Dev. Growth Differ. 57 (4), 291- 304.

Unsoeld, T., Park, J.O., Hutter, H., 2013. Discoidin domain receptors guide axons along longitudinal tracts in *C. elegans*. Dev. Biol. 374, 142–152.

Wada, M., Nakanishi, H., Satoh, a, Hirano, H., Obaishi, H., Matsuura, Y., Takai, Y., 1997. Isolation and characterization of a GDP/DTP exchange protein specific for the Rab3 subfamily small G proteins. J. Biol. Chem. 272, 3875–3878.

Wadsworth, W.G., 2002. Moving around in a worm: Netrin UNC-6 and circumferential axon guidance in *C. elegans*. Trends Neurosci. 25, 423–429.

Wadsworth, W.G., Bhatt, H., Hedgecock, E.M., 1996. Neuroglia and pioneer neurons express UNC-6 to provide global and local netrin cues for guiding migrations in *C. elegans*. Neuron 16, 35–46.

Walent, J.H., Porter, B.W., Martin, T.F., 1992. A novel 145 kd brain cytosolic protein reconstitutes Ca(2+)-regulated secretion in permeable neuroendocrine cells. Cell 70, 765–775.

Watari-Goshima, N., Ogura, K., Wolf, F.W., Goshima, Y., Garriga, G., 2007. *C. elegans* VAB-8 and UNC-73 regulate the SAX-3 receptor to direct cell and growth-cone migrations. Nat. Neurosci. 10, 169–176.

White, J. G., Southgate, E., Thomson, J. N., Brenner, S., 1976.The structure of the ventral cord of *Caenorhabditis elegans*. Philos.Trans.R.Soc.Lond. B 275, 327–348.

White, J. G., Southgate, E., Thomson, J. N., Brenner, S., 1986.The structure of the nervous system of the nematode *Caenorhabditis elegans*. Philos. Trans. R. Soc.Lond. B 314, 1–340.

Wightman, B., Clark, S.G., Taskar, a M., Forrester, W.C., Maricq, a V, Bargmann, C.I., Garriga, G., 1996. The *C. elegans* gene *vab-8* guides posteriorly directed axon outgrowth and cell migration. Development 122, 671–682.

Wilhelm, B.G., Mandad, S., Truckenbrodt, S., Kröhnert, K., Schäfer, C., Rammner, B., Koo, S.J., Claßen, G. a, Krauss, M., Haucke, V., Urlaub, H., Rizzoli, S.O., 2014. Composition of isolated synaptic boutons reveals the amounts of vesicle trafficking proteins. Science 344, 1023–8.

Wit, H. De, Cornelisse, L.N., Toonen, R.F.G., Verhage, M., 2006. Docking of Secretory Vesicles Is Syntaxin Dependent. PLoS One 1, e126.

Wolf, F.W., Hung, M.S., Wightman, B., Way, J., Garriga, G., 1998. *vab-8* is a key regulator of posteriorly directed migrations in *C. elegans* and encodes a novel protein with kinesin motor similarity. Neuron 20, 655–666.

Zahn, T.R., Angleson, J.K., MacMorris, M. a., Domke, E., Hutton, J.F., Schwartz, C., Hutton, J.C., 2004. Dense core vesicle dynamics in *Caenorhabditis elegans* neurons and the role of kinesin UNC-104. Traffic 5, 544–559.

Zallen, J. a, Peckol, E.L., Tobin, D.M., Bargmann, C.I., 2000. Neuronal cell shape and neurite initiation are regulated by the Ndr kinase SAX-1, a member of the *Orb6*/COT-1/warts serine/threonine kinase family. Mol. Biol. Cell 11, 3177–3190.

Zallen, J., Yi, B. a, Bargmann, C.I., 1998. The conserved immunoglobulin superfamily member SAX-3/Robo direts multiple aspects of axon guidance in *C. elegans*. Cell 92, 217–227.

Zerial, M., McBride, H., 2001. Rab proteins as membrane organizers. Nat. Rev. Mol. Cell Biol. 2, 107–17.

Chapter 5. Summary and conclusions

In *C. elegans* the ventral nerve cord (VNC) is the major longitudinal axon bundle that houses the essential components of the motor circuit (White et al., 1986). The formation of the VNC starts in the embryo when the AVG neuron extends an axon which pioneers the right axon tract of the VNC (Durbin, 1987). Laser ablation of the AVG neuron early during the development leads to the formation of a disorganised VNC with misguided axons. This suggests that the AVG neuron plays a critical role for the proper establishment of the VNC (Durbin, 1987; Hutter, 2003). The molecular mechanism of AVG axon navigation is largely unknown. The major axon guidance mutants do not display penetrant AVG axon guidance defects (Hutter, 2003). Therefore, the genes which control the AVG axon navigation remain to be identified. The major goal of this study was to identify the novel regulators of AVG axon navigation.

We identified alleles of *plr-1* gene in a forward genetic screen for the AVG axon guidance and outgrowth defects (Bhat et al., 2015). *plr-1* mutant animals display a variety of defects including polarity reversal of the AVG neuron, premature termination of outgrowth and midline crossing of the AVG axon. The broad phenotypic spectrum suggests that *plr-1* is involved in many developmental processes which is in consistent with its wide expression during embryogenesis. The polarity reversal defects are unique to the AVG neuron whereas the outgrowth and guidance defects are shared with a group of unrelated neuronal and non-neuronal cells. The premature terminations of outgrowth defects are restricted to the posterior half of trajectory for all the affected axons and excretory canals. This suggests that initially the axons as well as excretory canals respond to the guidance cues but as the outgrowth progresses, they stop responding to the cues. Alternately, the supply of materials required for the continuous growth of axons decrease as the growth cone moves faraway from the cell body (Owen Lockerbie et al., 1991; Igarashi et al., 1996; Pfenninger, 2009). The nervous system by and large is intact

as we did not observe defects in several other neuronal markers tested, suggesting that *plr-1* does not act globally.

PLR-1 is predicted to encode a transmembrane E3 ubiquitin ligase with a signal peptide and a single RING finger domain. E3 ligases are a part of enzyme complex which transfers ubiquitin to the substrate proteins meant for degradation by proteosomal complex and can also internalise membrane proteins (receptors) from the cell surface (Hershko et al., 2000; d'Azzo et al., 2005; Lecker et al., 2006). PLR-1 and its vertebrate homologues RNF43 and ZNRF3 downregulate Wnt signalling by removing Wnt receptors from the cell surface (Koo et al., 2012; Hao et al., 2012; Moffat et al., 2014). In *plr-1* mutant animals the ectopic Wnt signalling leads to the polarity reversal of the AVG neuron which is suppressed by the Wnts *cwn-1* and *cwn-2* and frizzled *mom-5* in *C. elegans* (Moffat et al., 2014). Moreover, the overexpression of the frizzled MOM-5 leads to the polarity reversal defects of AVG neuron in wild type. This suggests that the inappropriate activation by the Wnts CWN-1 and CWN-2 through the frizzled MOM-5 causes the ectopic Wnt signalling (Moffat et al., 2014). We have shown that compromising genetically Wnt signalling in *plr-1* mutant animals rescues the polarity reversal defects of AVG neuron. This suggests that indeed polarity reversal defects of *plr-1* arise inpart due to ectopic Wnt signalling. However, we have also observed that *plr-1* defects outside AVG (AVK axon, CAN axon and excretory canal outgrowth and HSN migration and navigation defects) are either partially or are not rescued at all. This suggests that *plr-1* has both Wnt dependent and independent functions.

Our genetic interaction data suggests that *plr-1*, *unc-53* and *unc-73* together regulate the polarity of AVG neuron. The evidence for this comes from the observations that a mutation in *unc-53*/NAV2, which is a cytoskeleton regulator required for cell and axon migrations (Stringham et al., 2002), completely suppress the polarity reversal defects of the AVG neuron. The polarity reversal defects of *plr-1* mutants are also partially suppressed by a mutations in *unc-73,* a Rho/Rac guanine nucleotide exchange factor (GEF) involved in the cell migrations and axon guidance (Spencer et al., 2001; Dyer et al., 2010). This suggests that UNC-53 and UNC-73 might negatively regulate the Wnt signalling. However, both UNC-53 and UNC-73 have not been linked to the Wnt signalling, so it remains to be established what the connection is here. It is possible that

UNC-73 and UNC-53 regulate the surface expression of Wnt receptors in the AVG neuron. UNC-73B/Rac GEF along with VAB-8L regulate the cell surface availability of the axon guidance receptors UNC-40/DCC, UNC-5 and SAX-3/Robo in the neurons (Watari-Goshima et al., 2007; Levy-Strumpf and Culotti, 2007). VAB-8L is a cytoplasmic protein with N-terminal kinesin like motor domain (Wolf et al., 1998) which physically interacts with UNC-73B and has been proposed to regulate the trafficking of guidance receptors (Watari-Goshima et al., 2007). Moreover, VAB-8L physically interacts with UNC-51, a serine/threonine kinase (Ogura et al., 1994; Lai and Garriga, 2004), which together with UNC-14 regulates the subcellular localisation of the UNC-5 (Netrin receptor) in neurons (Ogura & Goshima, 2006). The absence of UNC-73 simply would reduce the Wnt receptor surface levels which inturn would counter the effects of lack of PLR-1. In this situation one would expect that a mutation in *vab-8* to suppress the polarity reversal defects of *plr-1* mutants. However, in contrast to this *vab-8* strongly enhanced the polarity reversal defects of *plr-1*. This suggests that *unc-73* and *vab-8* function independently and that the interaction between these two genes is more complex in the context of AVG polarity.

The suppression of polarity reversal defects of the *plr-1* mutants also suggests that *unc-53* and *unc-73* act downstream of *plr-1* for the AVG neuron polarity. The guidance cues and other downstream signalling molecules have been shown to regulate the polarized growth of neurons (Tahirovic and Bradke, 2009; Ou and Shen, 2011). In *C. elegans* the HSN, AVM and PVM neurons extend axons ventrally which turn anteriorly and extend into the ventral nerve cord (White et al., 1986; Desai et al., 1988; Garriga et al., 1993). From different studies a conceptual model has emerged which explains the dorsal-ventral polarisation and the initial outgrowth of these neurons. UNC-6/Netrin and SLT-1/slit1 gradients lead to the asymmetric distribution of UNC-40/DCC which inturn activates the UNC-34/Ena (actin regulator) and accumulates PI(3,4)P2 on the ventral side. The PI(3,4)P2 inturn recruits the MIG-10/Lamellipodin which binds to the CED-10/Rac. UNC-34, MIG-10 and CED-10 are the downstream effectors which collectively reorganise the cytoskeleton and mediate the polarized growth of these neurons (Adler et al., 2006; Quinn et al., 2008, 2006; Ou and Shen, 2011). It is possible that PLR-1 downregulates the Wnt receptors in a manner which generates the asymmetric distribution and enrichment of these receptors to the position where axonal outgrowth

initiates. This would lead to the localised Wnt activity and the directional axon outgrowth. The lack of PLR-1 would lead to the uniform distribution of these receptors and thus interfere with the initial polarisation. This inturn would lead to Wnt signalling all over the cell and somehow randomize the polarity of the AVG neuron in an UNC-53 and UNC-73 dependent manner. Indeed, colocalisation experiments have suggested that PLR-1 and frizzled are present in the endosomes but not on the plasmamembrane (Moffat et al., 2014), akin to vertebrate homologues (Hao et al., 2012; Koo et al., 2012). However, these colocalisation experiments were done in touch receptor neurons (ALM and PLM) in *C. elegans* which are different from the AVG neuron (Moffat et al., 2014). The Wnt receptor LIN-17 is asymmetrically distributed in the PLM neuron with lower surface levels in the anterior process and higher surface levels in the posterior process (Hilliard & Bargmann, 2006). Moreover, LIN-17 is detected on the surface of posterior process but not on anterior processes, when coexpressed with PLR-1 (Moffat et al., 2014). It would be interesting to see whether other downstream effectors which interact with UNC-73 and UNC-53 can suppress the polarity reversal defects of *plr-1* mutants animals.

While the polarity reversal defects of *plr-1* mutants are unique, the outgrowth defects particularly in the posterior region are shared with other known mutants. The mutations in the *unc-53/NAV-2* (cytoskeleton regulator), *abi-1* (Abelson kinase interactor), *unc-73* (Rho-Rac GEF), *vab-8* (atypical kinase) and many other cytoskeleton regulators lead to the posterior truncation of axons and excretory canals (Wolf et al., 1998; Steven et al., 1998; Wightman et al., 1996; Wu et al., 2002; Stringham et al., 2002; Kubiseski et al., 2003; Schmidt et al., 2009; Marcus-Gueret et al., 2012; McShea et al., 2013). We found that *plr-1* has excretory canal and axon outgrowth defects in the posterior region. The posterior extension of excretory canals is controlled by two distinct parallel guidance pathways. UNC-53 acts cell autonomously together with Rho-GEF form of UNC-73 and many other components of cytoskeleton to control the outgrowth of excretory canals. In a parallel pathway Rac-GEF form of UNC-73 acts cell non-autonomously together with VAB-8 (Marcus-Gueret et al., 2012). We found that PLR-1 acts cell autonomously through a third yet unidentified genetic pathway for the posterior outgrowth of excretory canals. Moreover, we also found that *plr-1* does not act with either *unc-53* or *unc-73* in the same genetic pathway for the posterior extension of the

AVG axon. Therefore, it is possible that PLR-1 downregulates some unknown receptor/s, which functions independent of UNC-53 and UNC-73 and is required for the posterior extension of axons. It would be interesting to further characterize the molecular mechanism of the posterior extension of the axons and excretory canals. Since PLR-1 downregulates the Wnt signalling (Moffat et al., 2014) and Wnts in general control the polarity (Pan et al., 2006) but are not required for the posterior extension of neurons. It is possible that *plr-1* has two separate genetic activities, one required for the AVG neuron polarity (Wnt-dependent) and the other required for the posterior extension of axons and excretory canals (Wnt-independent).

plr-1 mutant animals also display AVG midline crossing (AVG cross-over) defects which are suppressed by the RacGEF form of UNC-73/Trio but not by the RhoGEF form of UNC-73/Trio. This suggests that *plr-1* genetically interacts with the RacGEF form of *unc-73*, a downstream component of signalling pathway, for the correct navigation of AVG axon. The axon guidance mutants *sax-3*/Robo (Slit receptor), *unc-6*/Netrin, *unc-5*(Netrin receptor) and *nid-1* (basement membrane component) also display low penetrant AVG midline crossing defects (Hutter, 2003). However, the double mutant analysis suggested that *plr-1* does not act synergistically with the *sax-3*/Robo, *unc-6*/Netrin, *unc-5*/Netrin receptor and *nid-1*/Nidogen for AVG axon navigation. This suggests that AVG axon navigation is controlled by multiple genetic pathways and that PLR-1 does not regulate the above mentioned guidance cues and receptors.

Simple genetic screens have not yielded mutants with highly penetrant AVG axon navigation defects except for *plr-1* (Moffat et al., 2014; Bhat et al., 2015). This emphasizes the need of using other strategies like modifier screens to uncover the AVG axon guidance genes. We performed an enhancer screen in a *nid-1* mutant background for AVG axon guidance defects and isolated several candidate mutants including an allele of *aex-3.* In *C. elegans nid-1* encodes the sole homologue of Nidogen, a basement membrane component (Kang and Kramer, 2000 Kim and Wadsworth, 2000) which has low penetrant AVG axon cross-over (AVG CO) defects (Hutter, 2003) which are substantially enhanced in *aex-3* mutant animals. The AVG axon pioneers the right axon tract of the VNC and is closely followed by the command interneurons and motor neurons (follower neurons) (Durbin, 1987). The ablation or removal of the AVG neuron

leads the guidance defects in the follower neurons (Durbin, 1987; Hutter, 2003). We observed that in *aex-3; nid-1* double mutant animals the command interneuron and motor neurons (DD/VD and DA/DB) follow the misguided AVG pioneer and cross the ventral midline at the same position where the AVG axon crosses. This suggests that the follower neuron guidance defects are likely secondary consequences of the misguided AVG pioneer. However, the motor neuron (DD/VD and DA/DB) commissure guidance defects, symmetric ventral nerve cord defects, AVK and HSN axon guidance defects we observed in *aex-3; nid-1* mutant animals are AVG pioneer independent, suggesting that *aex-3* also has primary defects outside AVG. In general the axons in the VNC are affected and the rest of the nervous system is intact, as we did not observe any defects outside the VNC. Taken together, the mutations in *aex-3* lead to the primary as well secondary guidance defects in the VNC axons, which are dependent on a mutation in *nid-1*. While the secondary guidance defects are due to the misguided AVG pioneer, the primary defects point out the direct role of AEX-3 in the affected neurons. As the *aex-3* and *nid-1* are in different pathways, the synergistic effects on axon guidance are due the functional redundancy of two separate genetic pathways.

AEX-3 is a GDP/GTP exchange factor for RAB-3 and AEX-6/Rab27 GTPases which are involved in the synaptic vesicle precursor trafficking and thus mediate synaptic transmission (Iwasaki et al., 1997; Mahoney et al., 2006). Our genetic interaction data suggests that AEX-3 regulates RAB-3 and not the AEX-6/Rab27 in the context of AVG navigation. RAB-3 is associated with synaptic vesicle precursors which are transported by the kinesin 3 (UNC-104) motor proteins in *C. elegans* (Hall and Hedgecock, 1991; Nonet et al., 1997). Besides this, UNC-104 is also required for the dense core vesicle transport in *C. elegans* (Jacob and Kaplan, 2003; Zahn et al., 2004). We found that UNC-104 motor protein inpart mediates the transport of vesicles but is not exclusively required in the context of AVG axon navigation. The *C. elegans* genome codes for 21 kinesins (Siddiqui, 2002) with some of them having well documented role in transport e.g. UNC-116/KIF5, a kinesin heavy chain anterograde motor in synaptic vesicle components and glutamate receptors (Patel et al., 1993; Sakamoto et al., 2005; Hoerndli et al., 2013) and VAB-8 in guidance receptors (Levy-Strumpf and Culotti, 2007; Watari-Goshima et al., 2007). It is possible that some other motor protein/s act in parallel to UNC-104 in the context of AVG navigation. Once the synaptic vesicles arrive at

synapses, they are primed by RAB-3 interacting protein and effector molecule UNC-10/Rim (Koushika et al., 2001). We found that vesicle priming and UNC-10/Rim are not involved in the AVG axon navigation. This indicates that vesicular transport events happening in the growth cone are different from that of the neuron terminals.

We also found that UNC-31/CAPS and IDA-1/IA-2 required for dense core vesicle release (Cai et al., 2004; Speese et al., 2007) and UNC-64/Syntaxin, a SNARE component involved in the synaptic vesicle and dense core vesicle release (Saifee et al., 1998; Wit et al., 2006; Hammarlund et al., 2008) have *nid-1* dependent AVG axon cross-over defects, suggesting their role in the context of AVG navigation. Our genetic interaction data suggests that *aex-3* acts along with *unc-31*/CAPS, *ida-1*/IA-2 and *unc-64*/Syntaxin in the same genetic pathway for the AVG axon navigation. The AVG neuron extends an axon when there are no other axons and synapses present in *C. elegans* embryo. This limits the scope of mature synaptic vesicles and dense core vesicles being present at that stage of development. There is a possibility that some kind of precursor vesicle is present in the growth cone which uses the components from both synaptic vesicles as well as from dense core vesicles for the release. It has been shown in vertebrate cultured neurons that growth cone vesicles or particles differ with mature synaptic vesicles both in composition and regulation (Igarashi et al., 1997). The molecular players first to appear in growth cone vesicles are Rab3a and SNARE components (Igarashi et al., 1997). Taken together with our genetic interaction data, it seems that the vesicular events happening in the growth cone are mediated by the RAB-3 activation and vesicle fusion with the growth cone membrane in the context of AVG axon navigation.

The likely function of vesicles in the growth cone would be to deliver receptors for guidance cues in the growth cone. We found that *unc-6*/Netrin and its receptor *unc-5* but not *unc-40* mutant animals display *nid-1* dependent AVG axon cross-over defects. This suggests that UNC-6/Netrin likely acts through the receptor UNC-5 in the context of AVG navigation. Moreover, our genetic interaction data suggests that *unc-5* and *aex-3* are in the same genetic pathway. This indicates that AEX-3 might regulate the trafficking of UNC-5 to the growth cone. UNC-5::GFP appears to be localised in small vesicles which are transported by UNC-51 and UNC-14 by cooperating with an unknown motor protein

(Ogura and Goshima, 2006; Norris et al., 2014). As mentioned earlier, VAB-8L, an atypical kinase with N-terminal motor domain (Wolf et al., 1998) physically interacts with UNC-51 (Lai & Garriga, 2004) and has been shown to regulate the surface expression of SAX-3/Robo, UNC-40/DCC and possibly UNC-5 receptors (Watari-Goshima et al., 2007; Levy-Strumpf and Culotti, 2007). Therefore, it is possible that AEX-3 activates RAB-3 which in turn recruits VAB-8L to the vesicles carrying UNC-5 that are transported to the growth cone. However, it needs to be tested whether *vab-8* has *nid-1* dependent AVG axon cross-over defects and acts with *aex-3* through the same genetic pathway. The UNC-5 signalling can control the AVG axon navigation either by activating downstream effectors or by inserting the membrane at the site of receptor activation. It has been shown that UNC-40/DCC co-associates with the Syntaxin in Netrin dependent manner and guides the sensory neurons in vertebrates (Cotrufo et al., 2011). The membrane insertion at the growth cone surface has been proposed a mechanism for the growth cone attraction (Tojima et al., 2011; Tojima and Kamiguchi, 2015). Therefore, it is plausible that UNC-5 acts through the same mechanism by recruiting the membrane at the growth cone surface for the proper guidance of AVG axon. Testing these models would require *in vivo* observations of the AVG axon growth cone which at present is a real challenge.

In summary, we have identified and characterised PLR-1 a putative E3 ubiquitin ligase, required for AVG neuron polarity, extension and navigation. PLR-1 is also required for the navigation and extension of a small group of unrelated neurons as well as the posterior extension of excretory canals. PLR-1 has both Wnt dependent and independent functions and regulates the polarity of AVG neuron along with UNC-53/NAV2 and UNC-73/Trio. We have also performed an enhancer screen to identify regulators of AVG axon navigation and have isolated several candidate mutants with penetrant AVG axon cross-over defects, including an allele of *aex-3*. *aex-3* mutant animals apart from AVG axon cross-over defects also show pioneer dependent and independent follower neuron defects in the VNC which are dependent on *nid-1* mutation. Our genetic interaction data suggests that *aex-3* activates the *rab-3* and also acts along with *unc-31*/CAPS, *ida-1*/IA-2 and *unc-64*/Syntaxin in the same genetic pathway for the AVG axon navigation. Finally, our data suggests that AEX-3 might regulate the

trafficking of the Netrin receptor UNC-5 to the growth cone and this signalling can mediate the proper guidance of AVG axon.

5.1. References:

Adler, C.E., Fetter, R.D., Bargmann, C.I., 2006. UNC-6/Netrin induces neuronal asymmetry and defines the site of axon formation. Nat. Neurosci. 9, 511–518.

Bhat, J.M., Pan, J., Hutter, H., 2015. PLR-1, a putative E3 ubiquitin ligase, controls cell polarity and axonal extensions in *C. elegans*. Dev. Biol. 398, 44–56.

Cai, T., Fukushige, T., Notkins, A.L., Krause, M., 2004. Insulinoma-Associated Protein IA-2, a Vesicle Transmembrane Protein, Genetically Interacts with UNC-31/CAPS and Affects Neurosecretion in *Caenorhabditis elegans*. J. Neurosci. 24, 3115–3124.

Cotrufo, T., Perez-Branguli, F., Muhaisen, a., Ros, O., Andres, R., Baeriswyl, T., Fuschini, G., Tarrago, T., Pascual, M., Urena, J., Blasi, J., Giralt, E., Stoeckli, E.T., Soriano, E., 2011. A Signaling Mechanism Coupling Netrin-1/Deleted in Colorectal Cancer Chemoattraction to SNARE-Mediated Exocytosis in Axonal Growth Cones. J. Neurosci. 31, 14463–14480.

d'Azzo, A., Bongiovanni, A., Nastasi, T., 2005. E3 ubiquitin ligases as regulators of membrane protein trafficking and degradation. Traffic 6, 429–441.

Desai, C., Garriga, G., McIntire, S.L., Horvitz, H.R., 1988. A genetic pathway for the development of the *Caenorhabditis elegans* HSN motor neurons. Nature 336, 638–646.

Durbin, R.M., 1987. Studies on the Development and Organisation of the Nervous System of *Caenorhabditis elegans*. Ph.D.dissertation, University of Cambridge, England.

Dyer, J.O., Demarco, R.S., Lundquist, E. a, 2010. Distinct roles of Rac GTPases and the UNC-73/Trio and PIX-1 Rac GTP exchange factors in neuroblast protrusion and migration in *C. elegans.* Small GTPases 1, 44–61.

Garriga, G., Desai, C., Horvitz, H.R., 1993. Cell interactions control the direction of outgrowth, branching and fasciculation of the HSN axons of *Caenorhabditis elegans*. Development 117, 1071–1087.

Hall, D.H., Hedgecock, E.M., 1991. Kinesin-related gene *unc-104* is required for axonal transport of synaptic vesicles in *C. elegans*. Cell 65, 837–847.

Hammarlund, M., Watanabe, S., Schuske, K., Jorgensen, E.M., 2008. CAPS and syntaxin dock dense core vesicles to the plasma membrane in neurons. J. Cell Biol. 180, 483–491.

Hao, H.-X., Xie, Y., Zhang, Y., Charlat, O., Oster, E., Avello, M., Lei, H., Mickanin, C., Liu, D., Ruffner, H., Mao, X., Ma, Q., Zamponi, R., Bouwmeester, T., Finan, P.M., Kirschner, M.W., Porter, J. a., Serluca, F.C., Cong, F., 2012. ZNRF3 promotes Wnt receptor turnover in an R-spondin-sensitive manner. Nature 485, 195–200.

Hershko, a, Ciechanover, a, Varshavsky, a, 2000. Basic Medical Research Award. The ubiquitin system. Nat. Med. 6, 1073–1081.

Hilliard, M. a., Bargmann, C.I., 2006. Wnt signals and Frizzled activity orient anterior-posterior axon outgrowth in *C. elegans*. Dev. Cell 10, 379–390.

Hoerndli, F.J., Maxfield, D. a., Brockie, P.J., Mellem, J.E., Jensen, E., Wang, R., Madsen, D.M., Maricq, A. V., 2013. Kinesin-1 regulates synaptic strength by mediating the delivery, removal, and redistribution of AMPA receptors. Neuron 80, 1421–1437.

Hutter, H., 2003. Extracellular cues and pioneers act together to guide axons in the ventral cord of *C. elegans*. Development 130, 5307–5318.

Igarashi, M., Tagaya, M., Komiya, Y., 1997. The soluble N-ethylmaleimide-sensitive factor attached protein receptor complex in growth cones: molecular aspects of the axon terminal development. J. Neurosci. 17, 1460–1470.

Igarashi, M., Terakawa, S., Ide, C., Iomiya, Y., 1996. 1224 A t-Snare is involved in axonal growth: Botulinum neurotoxin C1 induces growth cone collapse. Neurosci. Res. 25, S134.

Iwasaki, K., Staunton, J., Saifee, O., Nonet, M., Thomas, J.H., 1997. *aex-3* encodes a novel regulator of presynaptic activity in *C. elegans*. Neuron 18, 613–622.

Jacob, T.C., Kaplan, J.M., 2003. The EGL-21 carboxypeptidase E facilitates acetylcholine release at Caenorhabditis elegans neuromuscular junctions. J. Neurosci. 23, 2122–2130.

Kang, S.H., Kramer, J.M., 2000. Nidogen is nonessential and not required for normal type IV collagen localization in *Caenorhabditis elegans*. Mol. Biol. Cell 11, 3911–3923.

Kim, S., Wadsworth, W.G., 2000. Positioning of longitudinal nerves in *C. elegans* by nidogen. Science 288, 150–154.

Koo, B.-K., Spit, M., Jordens, I., Low, T.Y., Stange, D.E., van de Wetering, M., van Es, J.H., Mohammed, S., Heck, A.J.R., Maurice, M.M., Clevers, H., 2012. Tumour suppressor RNF43 is a stem-cell E3 ligase that induces endocytosis of Wnt receptors. Nature 488, 665–669.

Koushika, S.P., Richmond, J.E., Hadwiger, G., Weimer, R.M., Jorgensen, E.M., Nonet, M.L., 2001. A post-docking role for active zone protein Rim. Nat. Neurosci. 4, 997–1005.

Kubiseski, T.J., Culotti, J., Pawson, T., 2003. Functional analysis of the *Caenorhabditis elegans* UNC-73B PH domain demonstrates a role in activation of the Rac GTPase in vitro and axon guidance in vivo. Mol. Cell. Biol. 23, 6823–6835.

Lai, T., Garriga, G., 2004. The conserved kinase UNC-51 acts with VAB-8 and UNC-14 to regulate axon outgrowth in *C. elegans*. Development 131, 5991–6000.

Lecker, S.H., Goldberg, A.L., Mitch, W.E., 2006. Protein degradation by the ubiquitin-proteasome pathway in normal and disease states. J. Am. Soc. Nephrol. 17, 1807–1819.

Levy-Strumpf, N., Culotti, J.G., 2007. VAB-8, UNC-73 and MIG-2 regulate axon polarity and cell migration functions of UNC-40 in *C. elegans*. Nat. Neurosci. 10, 161–168.

Mahoney, T.R. et al., 2006. Regulation of synaptic transmission by RAB-3 and RAB-27 in *Caenorhabditis elegans*. Molecular biology of the cell, 17(6), pp.2617–25.

Marcus-Gueret, N., Schmidt, K.L., Stringham, E.G., 2012. Distinct cell guidance pathways controlled by the Rac and Rho GEF domains of UNC-73/TRIO in *Caenorhabditis elegans*. Genetics 190, 129–142.

McShea, M. a., Schmidt, K.L., Dubuke, M.L., Baldiga, C.E., Sullender, M.E., Reis, A.L., Zhang, S., O'Toole, S.M., Jeffers, M.C., Warden, R.M., Kenney, A.H., Gosselin, J., Kuhlwein, M., Hashmi, S.K., Stringham, E.G., Ryder, E.F., 2013. Abelson interactor-1 (ABI-1) interacts with MRL adaptor protein MIG-10 and is required in guided cell migrations and process outgrowth in *C. elegans*. Dev. Biol. 373, 1–13.

Moffat, L.L., Robinson, R.E., Bakoulis, A., Clark, S.G., 2014. The conserved transmembrane RING finger protein PLR-1 downregulates Wnt signaling by reducing Frizzled, Ror and Ryk cell-surface levels in *C. elegans*. Development 141, 617–28.

Nonet, M.L., Staunton, J.E., Kilgard, M.P., Fergestad, T., Hartwieg, E., Horvitz, H.R., Jorgensen, E.M., Meyer, B.J., 1997. *Caenorhabditis elegans rab-3* mutant synapses exhibit impaired function and are partially depleted of vesicles. J. Neurosci. 17, 8061–8073.

Norris, a. D., Sundararajan, L., Morgan, D.E., Roberts, Z.J., Lundquist, E. a., 2014. The UNC-6/Netrin receptors UNC-40/DCC and UNC-5 inhibit growth cone filopodial protrusion via UNC-73/Trio, Rac-like GTPases and UNC-33/CRMP. Development 141, 4395–4405.

Ogura, K.-I., Goshima, Y., 2006. The autophagy-related kinase UNC-51 and its binding partner UNC-14 regulate the subcellular localization of the Netrin receptor UNC-5 in *Caenorhabditis elegans*. Development 133, 3441–3450.

Ogura, K.I., Wicky, C., Magnenat, L., Tobler, H., Mori, I., Müller, F., Ohshima, Y., 1994. *Caenorhabditis elegans unc-51* gene required for axonal elongation encodes a novel serine/threonine kinase. Genes Dev. 8, 2389–2400.

Ou, C.Y., Shen, K., 2011. Neuronal polarity in *C. elegans*. Dev. Neurobiol. 71, 554–566.

Owen Lockerbie, R., Miller, V.E., Pfenninger, K.H., 1991. Regulated plasmalemmal expansion in nerve growth cones. J. Cell Biol. 112, 1215–1227.

Pan, C.L., Howell, J.E., Clark, S.G., Hilliard, M., Cordes, S., Bargmann, C.I., Garriga, G., 2006. Multiple Wnts and Frizzled receptors regulate anteriorly directed cell and growth cone migrations in *Caenorhabditis elegans*. Dev. Cell 10, 367–377.

Patel, N., Thierry-Mieg, D., Mancillas, J.R., 1993. Cloning by insertional mutagenesis of a cDNA encoding Caenorhabditis elegans kinesin heavy chain. Proc. Natl. Acad. Sci. U. S. A. 90, 9181–9185.

Pfenninger, K.H., 2009. Plasma membrane expansion: a neuron's Herculean task. Nat. Rev. Neurosci. 10, 251–261.

Quinn, C.C., Pfeil, D.S., Chen, E., Stovall, E.L., Harden, M. V., Gavin, M.K., Forrester, W.C., Ryder, E.F., Soto, M.C., Wadsworth, W.G., 2006. UNC-6/Netrin and SLT-1/Slit Guidance Cues Orient Axon Outgrowth Mediated by MIG-10/RIAM/Lamellipodin. Curr. Biol. 16, 845–853.

Quinn, C.C., Pfeil, D.S., Wadsworth, W.G., 2008. CED-10/Rac1 Mediates Axon Guidance by Regulating the Asymmetric Distribution of MIG-10/Lamellipodin. Curr. Biol. 18, 808–813.

Saifee, O., Wei, L., Nonet, M.L., 1998. The *Caenorhabditis elegans unc-64* locus encodes a syntaxin that interacts genetically with synaptobrevin. Mol. Biol. Cell 9, 1235–1252.

Sakamoto, R., Byrd, D.T., Brown, H.M., Hisamoto, N., Matsumoto, K., Jin, Y., 2005. The *Caenorhabditis elegans* UNC-14 RUN domain protein binds to the kinesin-1 and UNC-16 complex and regulates synaptic vesicle localization. Mol. Biol. Cell 16, 483–496.

Schmidt, K.L., Marcus-Gueret, N., Adeleye, A., Webber, J., Baillie, D., Stringham, E.G., 2009. The cell migration molecule UNC-53/NAV2 is linked to the ARP2/3 complex by ABI-1. Development 136, 563–574.

Siddiqui, S.S., 2002. Metazoan motor models: kinesin superfamily in *C. elegans*. Traffic 3, 20–28.

Speese, S., Petrie, M., Schuske, K., Ailion, M., Ann, K., Iwasaki, K., Jorgensen, E.M., Martin, T.F.J., 2007. UNC-31 (CAPS) is required for dense-core vesicle but not synaptic vesicle exocytosis in *Caenorhabditis elegans*. J. Neurosci. 27, 6150–6162.

Spencer, a G., Orita, S., Malone, C.J., Han, M., 2001. A RHO GTPase-mediated pathway is required during P cell migration in *Caenorhabditis elegans*. Proc. Natl. Acad. Sci. U. S. A. 98, 13132–13137.

Steven, R., Kubiseski, T.J., Zheng, H., Kulkarni, S., Mancillas, J., Morales, A.R., Hogue, C.W. V, Pawson, T., Culotti, J., 1998. UNC-73 activates the Rac GTPase and is required for cell and growth cone migrations in *C. elegans*. Cell 92, 785–795.

Stringham, E., Pujol, N., Vandekerckhove, J., Bogaert, T., 2002. *unc-53* controls longitudinal migration in *C. elegans*. Development 129, 3367–3379.

Tahirovic S, Bradke F. 2009. Neuronal Polarity. Cold Spring Harbor Perspectives in Biology1. Available at:http://cshperspectives.cshlp.org/content/1/3/a001644.

Tojima, T., Hines, J.H., Henley, J.R., Kamiguchi, H., 2011. Second messengers and membrane trafficking direct and organize growth cone steering. Nat. Rev. Neurosci. 12, 191–203.

Tojima, T., Kamiguchi, H., 2015. Exocytic and endocytic membrane trafficking in axon development. Dev. Growth Differ. 57(4), pp 291-304.

Watari-Goshima, N., Ogura, K., Wolf, F.W., Goshima, Y., Garriga, G., 2007. *C. elegans* VAB-8 and UNC-73 regulate the SAX-3 receptor to direct cell and growth-cone migrations. Nat. Neurosci. 10, 169–176.

Wightman, B., Clark, S.G., Taskar, a M., Forrester, W.C., Maricq, a V, Bargmann, C.I., Garriga, G., 1996. The C. *elegans gene vab-8* guides posteriorly directed axon outgrowth and cell migration. Development 122, 671–682.

White, J. G., Southgate, E., Thomson, J. N., Brenner, S., 1986.The structure of the nervous system of the nematode *Caenorhabditis elegans*. Philos. Trans. R. Soc.Lond.B 314,1–340.

Wit, H. De, Cornelisse, L.N., Toonen, R.F.G., Verhage, M., 2006. Docking of Secretory Vesicles Is Syntaxin Dependent. PLoS One 1, e126.

Wolf, F.W., Hung, M.S., Wightman, B., Way, J., Garriga, G., 1998. *vab-8* is a key regulator of posteriorly directed migrations in *C. elegans* and encodes a novel protein with kinesin motor similarity. Neuron 20, 655–666.

Wu, Y.-C., Cheng, T.-W., Lee, M.-C., Weng, N.-Y., 2002. Distinct rac activation pathways control *Caenorhabditis elegans* cell migration and axon outgrowth. Dev. Biol. 250, 145–155.

Zahn, T.R., Angleson, J.K., MacMorris, M. a., Domke, E., Hutton, J.F., Schwartz, C., Hutton, J.C., 2004. Dense core vesicle dynamics in *Caenorhabditis elegans* neurons and the role of kinesin UNC-104. Traffic 5, 544–559.

Appendix. Behavioral assays

Genotype	Pharyngeal pumping[a]	Swimming[b]	Embryonic lethality[c]
Wild type	208 (10)	212 (10)	0.6 (9)
plr-1(hd129)	193 (10)	161 (10)	0.4^{ns} (9)

[a] pharyngeal pumping rate (Average number of counts per minute).

[b] Swimming rate (Average number of body bends per minute).

[c] % Average embryonic lethality (progeny from nine animal was analyzed)

Values in brackets indicate *n* which indicates the number of animals analyzed

(^{ns}: not significant; χ^2 test).